

---

## Master thesis : Neuromodulation of calcium-based plasticity rules

**Auteur** : Ponnet, Juliette

**Promoteur(s)** : Drion, Guillaume

**Faculté** : Faculté des Sciences appliquées

**Diplôme** : Master en ingénieur civil biomédical, à finalité spécialisée

**Année académique** : 2021-2022

**URI/URL** : <http://hdl.handle.net/2268.2/14570>

---

### *Avertissement à l'attention des usagers :*

*Tous les documents placés en accès ouvert sur le site le site MatheO sont protégés par le droit d'auteur. Conformément aux principes énoncés par la "Budapest Open Access Initiative"(BOAI, 2002), l'utilisateur du site peut lire, télécharger, copier, transmettre, imprimer, chercher ou faire un lien vers le texte intégral de ces documents, les disséquer pour les indexer, s'en servir de données pour un logiciel, ou s'en servir à toute autre fin légale (ou prévue par la réglementation relative au droit d'auteur). Toute utilisation du document à des fins commerciales est strictement interdite.*

*Par ailleurs, l'utilisateur s'engage à respecter les droits moraux de l'auteur, principalement le droit à l'intégrité de l'oeuvre et le droit de paternité et ce dans toute utilisation que l'utilisateur entreprend. Ainsi, à titre d'exemple, lorsqu'il reproduira un document par extrait ou dans son intégralité, l'utilisateur citera de manière complète les sources telles que mentionnées ci-dessus. Toute utilisation non explicitement autorisée ci-avant (telle que par exemple, la modification du document ou son résumé) nécessite l'autorisation préalable et expresse des auteurs ou de leurs ayants droit.*

---

UNIVERSITY OF LIÈGE  
FACULTY OF APPLIED SCIENCES



---

# Neuromodulation of calcium-based plasticity rules

---

*Master thesis realized with the aim of obtaining the degree of Master in  
Biomedical Engineering*

*Juliette Ponnet*

PROMOTOR: DRION Guillaume

JURY MEMBERS: DRION Guillaume  
PHILIPS Christophe  
SACRÉ Pierre  
SEUTIN Vincent

ACADEMIC YEAR 2021 - 2022



# Neuromodulation of calcium-based plasticity rules.

Juliette Ponnet

*Supervisor:* G. Drion

Master in Biomedical Engineering, University of Liège

Academic year 2021-2022

## Abstract

In the age of navigation systems, online reminders, and calendars, there is little room left for our memory capacity. Once disconnected from these tools, we constantly check our pockets and wonder: *how do I get to that friend's house again?* Due to this more-than-connected world, it sometimes becomes difficult to even take the time to sleep. However, many people know that sleep is one of the keys to our well-being. But what if sleep was actually our secret memory weapon?

During learning, neurons are able to rewire their neuronal connection to encode and store information, a property known as synaptic plasticity. While during wakefulness thalamic neurons are activated according to tonic firing pattern to process information, during sleep there is a change in neuronal firing pattern and these neurons are bursting. Experimental studies provide evidence of the link between this switch in brain neuronal patterns and the memory function of sleep. It has been shown that during sleep following learning, neurons in specific areas of the brain are activated. This activity remodels the neuronal connections (*i.e.*, synaptic plasticity) that mediate the formation and storage of memories. Despite ample evidence pointing to the role of sleep in memory consolidation, the detailed cellular mechanisms remain to be understood.

Different approaches can be taken to understand how sleep shapes our memories. In this thesis, we apply a computational approach to model the evolution of the synaptic strength. These synaptic plasticity rules are divided into two categories: *phenomenological* models and *biological* models. We focus on biological rules that are based on calcium dynamics (*i.e.*, calcium-based plasticity rules) to predict the direction of the synaptic plasticity (*i.e.*, strengthening or weakening of neuronal connections). While these models accurately describe the dynamics of neuronal components during wakefulness, they are not adapted to changes in neuronal firing patterns that take place during the switch from wake to sleep state as shown by [Jacquerie et al., 2022]. They observed that, no matter how important a piece of information is received during the day (important vs irrelevant), it is consolidated in the same way during sleep. They named this phenomenon, which is inconsistent with memory consolidation, the "*homeostatic reset*".

Since we want to observe a behavior that is consistent with memory consolidation during sleep (*i.e.*, memorization of important information and forgetting of irrelevant ones), this thesis aims at adapting the calcium-based plasticity rules to bypass this "*homeostatic reset*". With this aim in mind, we ask whether, during sleep, neuromodulators could act as regulators of synaptic plasticity and affect the different signaling cascades linked to it to allow the consolidation of important information. To this end, we conduct a literature review detailing the role of principal neuromodulators on synaptic plasticity and related signaling cascades. Then, based on these biological facts, we suggest modification of computational biological plasticity rules that are inconsistent regarding memory consolidation due to the "*homeostatic reset*". While the outcomes are convincing, they prove to be fragile and artificial. Finally, insights are given regarding another approach that would instead benefit from the "*homeostatic reset*" rather than trying to overcome it.

# Acknowledgements


I would like to sincerely express my gratefulness to my promoter, Guillaume Drion, for his time and guidance. His creativity and experience have been of great benefit to me during the development of this thesis. I would also like to acknowledge Mr. Pierre Sacré who has also been very helpful and available during the whole semester. I want to express my heartfelt recognition to Kathleen Jacquerie and Caroline Minne, who have supervised, advised, and encouraged me throughout this journey. They gave me the opportunity to work on a subject that I find fascinating and collaborating with them was a real pleasure.

This work would not have been successful without the contribution of my colleagues Nora B., Nora S., and Pauline G. Special thanks to them for the warmth of their presence, the hours spent together, and the many coffees we had. No one could have understood my concerns better than them and I honestly want to express my deepest gratitude for their support.

I would like to warmly thank my family for backing me up and always encouraging me so that I could accomplish all the objectives I aimed for. Finally, I owe a special mention to Thomas, Pauline, Myriam, Maud, and all my dearest friends for always caring for me in times of crisis throughout my years of study. I will never be grateful enough for the luck I had to cross the road of all these extraordinary persons.

Liège, June 9<sup>th</sup>, 2022

Juliette Ponnet

A handwritten signature in black ink, consisting of a stylized, cursive script that appears to read 'Juliette Ponnet'. The signature is written over a horizontal line.

# Contents

<b>1</b>	<b>Introduction</b>	<b>1</b>
1.1	Motivation . . . . .	1
1.2	Structure . . . . .	2
<b>I</b>	<b>Background</b>	<b>4</b>
<b>2</b>	<b>Elements of neurophysiology</b>	<b>5</b>
2.1	Neurons . . . . .	5
2.1.1	Morphology . . . . .	5
2.1.2	Membrane excitability . . . . .	5
2.1.3	Synaptic transmission . . . . .	6
2.2	Neuromodulators . . . . .	6
2.2.1	Most common neuromodulators involved in the wake-sleep cycle and synaptic plasticity . . . . .	8
2.2.2	Other chemicals regulating sleep and synaptic plasticity . . . . .	10
2.3	From wakefulness to sleep . . . . .	12
2.3.1	Sleep macrostructure . . . . .	12
2.3.2	Neurobiology of sleep . . . . .	12
2.3.3	Electroencephalogram and thalamocortical cellular signatures . . . . .	13
2.4	Synaptic plasticity . . . . .	14
2.4.1	Role of calcium in N-methyl-D-aspartate (NMDA)R-based long-term synaptic plasticity . . . . .	15
2.4.2	Other long-term plasticity mechanisms . . . . .	16
2.5	Summary . . . . .	19
<b>3</b>	<b>Calcium-based plasticity rules</b>	<b>20</b>
3.1	Calcium-dependent synaptic plasticity rule with a continuous function of the calcium concentration [Shouval et al., 2002] . . . . .	21
3.2	Calcium-dependent synaptic plasticity rule with potentiation and depression thresholds [Graupner et al., 2016] . . . . .	23
3.3	Equivalence between the continuous-calcium dependency model and the two thresholds-calcium dependency model . . . . .	24
3.3.1	Construction of a model equivalent to model 2 written in the format of model 1	24
3.3.2	Similarities between the models . . . . .	26
3.4	Summary . . . . .	27

<b>II</b>	<b>Neuromodulation of synaptic plasticity from a biological perspective</b>	<b>28</b>
<b>4</b>	<b>Review of neuromodulators influence on synaptic plasticity and their activity during sleep</b>	<b>29</b>
4.1	Acetylcholine . . . . .	29
4.2	Noradrenaline . . . . .	35
4.3	Serotonin . . . . .	39
4.4	Dopamine . . . . .	44
4.5	Histamine . . . . .	48
4.6	Brain-Derived Neurotrophic Factor (BDNF) . . . . .	51
4.7	Summary . . . . .	55
<b>III</b>	<b>Computational Study</b>	<b>56</b>
<b>5</b>	<b>Homeostatic reset: development of the analytical prediction</b>	<b>57</b>
5.1	The explanation for <i>soft-based</i> models . . . . .	58
5.1.1	Analytical demonstration of the convergence value . . . . .	59
5.1.2	Comparison of the equation obtained to compute the convergence value with the one given by [Graupner and Brunel, 2012] . . . . .	60
5.1.3	Numerical simulation against analytical prediction . . . . .	61
5.1.4	Validity of the equation predicting the convergence value during sleep . . . . .	62
5.2	The explanation for <i>hard-bounds</i> models . . . . .	64
5.2.1	Analytical demonstration of the slope value . . . . .	64
5.2.2	Numerical simulation against analytical prediction . . . . .	65
5.3	Summary . . . . .	68
<b>6</b>	<b>Homeostatic reset disabling: neuromodulation of calcium-based synaptic rules during sleep in <i>bursting</i> mode</b>	<b>69</b>
6.1	Hand-tuned calcium-based synaptic rules . . . . .	70
6.1.1	Modification of potentiation threshold $\theta_p$ . . . . .	70
6.1.2	Modification of the potentiation level $\Omega^p$ to make it weight-dependent . . . . .	71
6.1.3	Modification of the convergence speed in depression $1/\tau_d$ to make it weight-dependent . . . . .	74
6.1.4	Modification of the maximal calcium influx to make it weight-dependent . . . . .	75
6.2	Implementation of [González-Rueda et al., 2018] phenomenological Up state-mediated plasticity rule in calcium-based plasticity rules . . . . .	77
6.2.1	Translation of the Up state-mediated plasticity rule into a calcium-based plasticity rule . . . . .	77
6.2.2	Evolution of synaptic weights during sleep using algorithm 1 . . . . .	79
6.2.3	Change of the original 3-points Spike Timing-Dependent Plasticity (STDP) curve . . . . .	82
6.3	Summary and conclusion . . . . .	88
<b>IV</b>	<b>Conclusion and Perspectives</b>	<b>90</b>
<b>7</b>	<b>Conclusion and Perspectives</b>	<b>91</b>
7.1	Thesis summary . . . . .	91
7.2	Perspectives . . . . .	92

7.2.1	Presence of variability in cortical network . . . . .	92
7.2.2	Taking advantage of the homeostatic reset: the AMPAfication . . . . .	94
<b>V</b>	<b>Appendix</b>	<b>97</b>
	<b>Appendices</b>	<b>A1</b>
<b>A</b>	<b>Elements of neurophysiology</b>	<b>A1</b>
A.1	Thalamocortical neurons: EEG and cellular signatures . . . . .	A1
A.2	Others sleep concepts . . . . .	A1
<b>B</b>	<b>Neurons models description</b>	<b>A3</b>
B.1	Conductance-based modeling . . . . .	A3
B.2	[Drion et al., 2018] . . . . .	A4
<b>C</b>	<b>Cortical network</b>	<b>A6</b>
C.1	Connection between cells . . . . .	A6
C.2	Burst pattern . . . . .	A7
<b>D</b>	<b>Synaptic plasticity models description</b>	<b>A8</b>
D.1	Model 1: soft-bounds and hard-bounds parameters . . . . .	A8
D.2	Model 2: soft-bounds parameters . . . . .	A10
D.3	Model 3: soft-bounds and hard-bounds parameters . . . . .	A10
D.4	Up state-mediated plasticity rule from [González-Rueda et al., 2018] . . . . .	A11
<b>E</b>	<b>Supplementary results</b>	<b>A12</b>
E.1	[González-Rueda et al., 2018] into calcium-based rule: change of the original 3-points STDP curve . . . . .	A12
E.1.1	Original STDP curve . . . . .	A12
E.1.2	Extension or retraction of the <i>no-change</i> 10ms window . . . . .	A13
E.1.3	Modification of the <i>no-change</i> window into a potentiation window . . . . .	A13
E.1.4	Translation of [González-Rueda et al., 2018] phenomenological plasticity rule in a calcium-based plasticity rule by changes in parameterization only . . . . .	A14
	<b>Bibliography</b>	<b>A27</b>



# Acronyms

**5HT** serotonin. 6, 39, 40, 43

**AC** Adenylate Cyclase. 7, 33, 35, 40, 43, 44, 47

**ACh** acetylcholine. 6, 30

**AMPA**  $\alpha$ -amino-3-hydroxy-5-methyl-4-isoxazolepropionic acid receptor. 9, 14–17, 30–32, 35, 37–40, 42–46, 50, 52, 53, 57

**ASCHY** Active Systems Consolidation Hypothesis. 33, 34, 74

**BDNF** Brain-Derived Neurotrophic Factor. 7, 10, 47, 51–54, 71

**CaM** calmodulin. 15–17, 30, 35

**CaMKII**  $Ca^{2+}$ /Calmodulin-dependent Protein Kinase II. 16, 17, 40, 45–47, 51, 53

**cAMP** Cyclic Adenosine Monophosphate. 16–18, 33, 34, 40, 45, 52

**DA** dopamine. 6, 46, 47

**DAG** diacylglycerol. 16, 18

**EC** endocannabinoids. 7, 10, 18

**EEG** electroencephalogram. 13, 14

**EPSP** Excitatory Postsynaptic Potential. 5, 7, 14, 30, 48, 52, 82

**ERK** Extracellular-signal-Regulated Kinase. 30, 35, 51

**GABA**  $\gamma$ -Aminobutyric acid. 7, 9, 12

**GLUT** glutamate. 7, 17, 18

**HA** histamine. 7, 48

**IEGs** Immediate Early Genes. 34, 38, 69

inositol triphosphate. 16, 18

**IPSP** Inhibitory Postsynaptic Potential. 5

**LTD** Long-Term Depression. 14–18, 23, 29–32, 34–46, 48–53, 71, 77, 79, 80, 83, 85

**LTP** Long-Term Potentiation. 14–18, 23, 29, 30, 32, 34, 35, 37, 39, 40, 42, 44–46, 48–53, 70, 71, 77, 78, 85

**MAPK** ras–Mitogen-Activated Protein Kinase. 10, 16, 18, 40, 45

**mRNA** messenger ribonucleic acid. 51, 54

**mTOR** mammalian Target Of Rapamycin. 30, 35

**NA** noradrenaline. 6, 38, 39, 43

**NMDA** N-methyl-D-aspartate. iii, 9, 15, 17, 18, 21, 23, 24, 30–33, 35–37, 40, 42, 44–46, 48–53, 70, 71, 75, 78, 85

**NMOD** neuromodulators. 6, 7

**NREM** Non-Rapid Eye Movements. 12, 33, 34, 38, 39, 43, 47, 54, 69, 71, 76

**PI3K** Phosphatidylinositol 3-Kinase. 10, 40

**PKA** Protein kinase A. 16–18, 33–35, 37, 40, 43–45, 70

**PKC** Protein kinase C. 30, 41, 45

**PLC** Phospholipase C. 7, 10, 16, 31, 33, 35, 51

**PP1** Protein Phosphatase 1. 16, 45

**REM** Rapid Eye Movements. 12, 33, 34, 38, 39, 43, 47, 50, 54, 69, 70

**SHY** Synaptic Homeostasis Hypothesis. 33, 34, 47, 69–71, 77, A11

**SK** small conductance calcium-activated potassium. 30, 32, 35, 37

**STDP** Spike Timing-Dependent Plasticity. iv, 20, 35, 36, 77, 79–83, 85–87

**SWRs** Sharp-Wave Ripples. 33, 38, 47

**SWS** Slow-Wave Sleep. 12, 47, 70, 77, 80, 81

**TrkB** Tropomyosin-Related Kinase Receptors of subtype B. 10, 51–54

**VDCC** Voltage-Dependent Calcium Channel. 16, 23, 51, 53, 70, 75

# Chapter 1

## Introduction

### 1.1 Motivation

Nowadays, a great deal of effort is devoted by researchers to understand the link between sleep and memory. On one side, memory is stored thanks to the ability of neurons to constantly remodel their neuronal connections and thus change the efficiency of information transmission at the synapse, a process called synaptic plasticity. On the other side, scientists have speculated that some memory functions require us to be asleep. Indeed, during sleep, we can observe a change in neuronal firing patterns that would be responsible for the encoding and/or consolidation of memory. However, no clear-cut explanations have yet been established. Indeed, conducting an experimental study to understand some cellular mechanisms on asleep subjects (*i.e.*, not awake nor anesthetized) is a difficult task to carry out. To overcome these limitations, an alternative is to conduct a computational study. In this sense, computational modeling of the brain during sleep can complement experimental evidence and perhaps get the chance to underlie the mechanisms behind memory consolidation during sleep.

In 2002, [Shouval et al., 2002] pioneered neuroplasticity modeling. Based on biological evidence, he established a rule with mathematical equations that is able to model the evolution of synaptic strength (*i.e.*, the connectivity between neurons, the efficiency of information transmission between them) as a function of calcium dynamics resulting from neuronal activity. Calcium is a key player in synaptic plasticity: typically, the induction of synaptic plasticity depends on the influx of calcium into the neuron arising from the surrounding neuronal activity.

Recently, [Jacquerie et al., 2022] used these calcium-based plasticity rules to underlie the mechanisms behind memory consolidation during sleep. However, while these models accurately describe the dynamics of neuronal components during wakefulness (on tonic patterns), they are not adapted to the change in neuronal firing pattern that takes place during the transition from wake to sleep state. Using these rules on bursting patterns led to the convergence of any synaptic strength (strong or weak) towards the same basal value meaning that every information learned during the day would be memorized in the same way during subsequent sleep. They named this process the *homeostatic reset*.

This thesis aims at adapting the calcium-based plasticity rules to make them consistent with memory consolidation (*i.e.*, strengthening or maintaining strong synapses and weakening weak synapses). With this aim in mind, we asked whether, during sleep, neuromodulators could act as regulators of synaptic plasticity mechanisms and allow the consolidation of important information. To this end, we attempted to address the following key motivational points:

- *What are the well-established notions regarding neuronal processes and the contributions of neu-*

*ronal synapses in information transmission and memory?* (CHAPTER 2) *How can this synaptic plasticity be modeled based on experimental data?* (CHAPTER 3)

- *How do neuromodulators affect synaptic plasticity in distinct brain regions, and more specifically in the hippocampus and cortex? Do they affect the mechanisms of synaptic plasticity during sleep?* (CHAPTER 4)
- *What is the homeostatic reset associated with modeling of plasticity during sleep? How can this phenomenon, which is inconsistent with memory consolidation, be demonstrated analytically?* (CHAPTER 5) *Can the role of neuromodulators on synaptic plasticity be used to modify these plasticity models and overcome this homeostatic reset?* (CHAPTER 6)

## 1.2 Structure

To embark on this journey into computational neuroscience, this thesis is divided into 4 main parts:

**Part I** covers the basic elements of neurophysiology: the neurons morphology, the neuromodulators and other chemicals regulating sleep and their principal features (*i.e.* targeting receptors, origin, behavioral and functional effects), how these neuromodulators trigger the switch between wakefulness to sleep, what is the impact of this switch on brain signals and finally how the connection between two neurons is strengthened or weakened in response to a specific neuronal activity (*i.e.*, synaptic plasticity) (CHAPTER 2).

Afterward, two computational modeling rules of synaptic plasticity are presented. In this thesis, we focus on calcium-based plasticity rules that are known to be more complex but more accurate than phenomenological rules. Finally, we explain how [Jacquerie et al., 2022] managed to derive a more intuitive rule based on the two models described (CHAPTER 3).

**Part II** summarizes all the literature we have found concerning the effects of neuromodulators on synaptic plasticity. Some information is also given about their effect on sleep. The following neuromodulators are investigated: acetylcholine, noradrenaline, serotonin, dopamine, histamine, and brain-derived neurotrophic factor (CHAPTER 4). This section is very useful to better understand the interplay of neuromodulators in the brain and justify the computational experiments we conduct afterward.

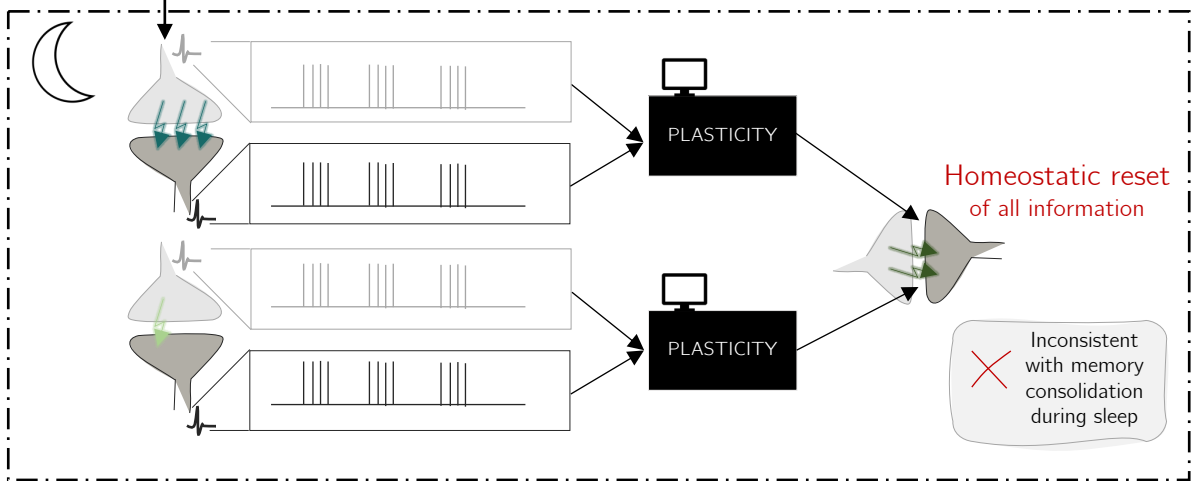
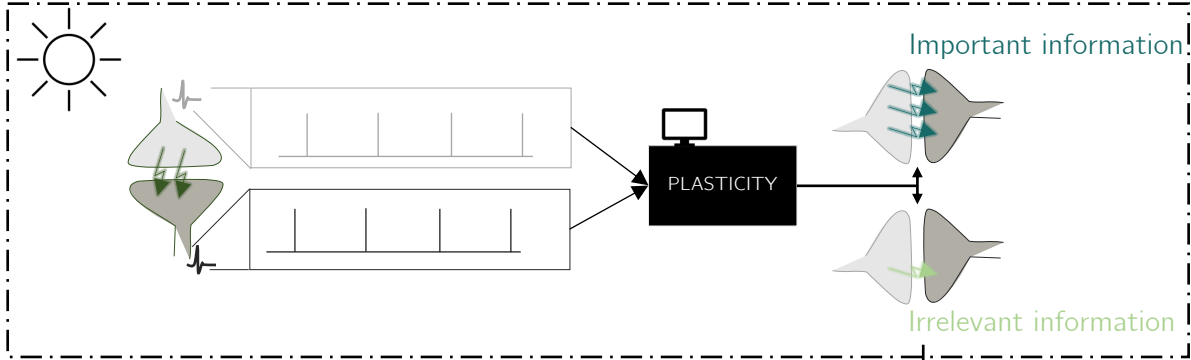
**Part III** introduces the problematic of this thesis by explaining the phenomenon of homeostatic reset observed by [Jacquerie et al., 2022]. From this explanation is derived an analytical prediction allowing to formalize this behavior which is not consistent with memory consolidation during sleep (CHAPTER 5). Then, the computational calcium-based rule that models synaptic plasticity is modified in order to obtain results consistent with memory storage. For each of these changes, a discussion is made with respect to the possible role of neuromodulators reviewed in part III. Finally, the phenomenological rule proposed by [González-Rueda et al., 2018] is translated into a calcium-based plasticity rule (CHAPTER 6).

**Part IV** encapsulates all of the topics that have been discussed throughout this thesis and respond to the key motivational points raised above. Supplementary results demonstrating the robustness of the homeostatic reset are shown and an approach taking advantage of this robust phenomenon is presented as an alternative.

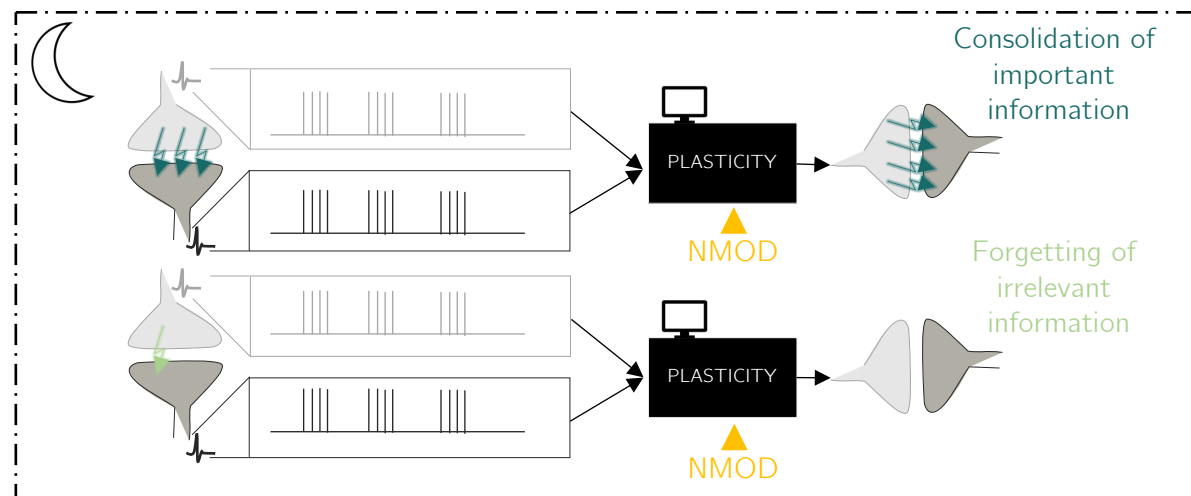
# Motivation and the scope of this thesis

## Problematic

[Jacquerie-Minne, 2022, in progress]



## Aims



Part I

Background

# Chapter 2

## Elements of neurophysiology

### 2.1 Neurons

A neuron is a nerve cell sending, receiving, and transmitting signals from and to the nervous system. The brain is composed of roughly 85 billion of these cells [Williams and Herrup, 1988] and, altogether, they are responsible for coordinating all the essential human functions [Bear et al., 2016].

#### 2.1.1 Morphology

This functional unit has all sorts of morphologies but overall, they share common characteristics [Purves, 2004]. Neurons are made up of three principal regions: the dendrites, the axon, and the soma (see Figure 2.1A).

- The dendrites, resembling the branching of a tree, are responsible for capturing incoming signals. The electrochemical signals picked up by the dendritic spines cause electrical activity changes processed in the soma.
- The soma contains common elements between a nerve cell and other types of cells, naming the nucleus and organelles. It is connected to the axon by the axon hillock which is the usual active synaptic inputs summation site of all Excitatory Postsynaptic Potential (EPSP)s and Inhibitory Postsynaptic Potential (IPSP)s.
- The axon enables the efficient transmission of the action potential down to the axon terminals causing the transmission of the information to the postsynaptic neuron. This transmission occurs almost instantaneously or by the release of chemical messengers, known as neurotransmitters, into the synaptic cleft to interact with the postsynaptic neuron.

#### 2.1.2 Membrane excitability

The plasma membrane is an important site of dynamic interaction between cells. It separates the extracellular matrix from the inside of a cell and allows, via membrane proteins that cross the membrane, the transfer of different molecules in and out of the cell. In neurons, we are referring specifically to sodium ( $Na^+$ ), chlorine ( $Cl^-$ ), calcium ( $Ca^{2+}$ ), and potassium ( $K^+$ ). These ions, being by definition charged, define an electrochemical equilibrium known as the Nernst potential. The transport phenomena and the relative permeability of the membrane generate a concentration gradient of these ions inside and outside the cell leading to a potential difference of the order of -70[mV] named membrane potential  $V_m$  [Purves, 2004].

An action potential (Figure 2.1A) is a localized and transient variation of the membrane potential: upon threshold (or suprathreshold) stimulation (*i.e.*, stimulus exceeding the triggering threshold at the axon hillock), the membrane potential, initially at its resting potential, moves towards 0V (depolarization) which results in a polarity reversal and a peak. Then, there is repolarization of the membrane with even a hyperpolarization and finally a return to rest. The cause of such an action potential is the change in membrane permeability [Purves, 2004, Bear et al., 2016].

### 2.1.3 Synaptic transmission

To transmit information, the communicating neurons must be close to each other and form a junction, known as a synapse, between an axon terminal of the presynaptic neuron and a dendrite of the postsynaptic neuron. This communication is carried out using chemical signals or using ion flows, resulting in two types of synapses: chemical (Figure 2.1B) and electrical synapses [Heidelberger et al., 2014].

- In chemical synapses, neurotransmitters/neuromodulators (NMOD) initially stored in synaptic vesicles are released in the synaptic cleft following the elevation of cytosolic calcium concentration due to the arrival of an action potential. In the synaptic cleft, neurotransmitters bind to receptors localized on the membrane of the postsynaptic neuron, causing the opening or closing of these channels. This induces depolarization (resp. hyperpolarization) of the postsynaptic membrane and the generation of an excitatory postsynaptic potential EPSP (resp. inhibitory postsynaptic potential IPSP) increasing (resp. decreasing) the likelihood of exceeding the triggering action potential threshold in the postsynaptic cell. Finally, neurotransmitters are washed out from the synaptic cleft by either diffusion, re-uptake, or enzymatic hydrolysis [Heidelberger et al., 2014].
- In electrical synapses, presynaptic and postsynaptic neurons are directly connected via intracellular channels allowing direct cell-cell transfer of ions named gap junction, and the signals are therefore instantaneously transmitted [Heidelberger et al., 2014].

## 2.2 Neuromodulators

The same chemicals released by a neuron can act as a neurotransmitter or as a neuromodulator. Due to the discrepancy in existing definitions and for the sake of clarity in this thesis, the definitions given in [Hoyle, 1985] are used:

- Neurotransmitter – A natural neuroactive substance that is released at a synapse and alters the ion permeability of the postsynaptic membrane.
- Neuromodulator – A natural neuroactive substance that is released in the general vicinity of a group of synapses and affects synaptic transmission by either pre- or postsynaptic action, or both.

According to this definition, a chemical is called a neuromodulator rather than a neurotransmitter when it affects (modulates) the communication and the transmission of information between neurons, shaping the strength between these two. More specifically, neuromodulators can affect a whole population of neurons. They have numerous functions, each resulting from specific interaction on dedicated receptors throughout the brain.

This section reviews the global implications, the target receptors, and specific brain areas producing these neuromodulators for acetylcholine (ACh), dopamine (DA), noradrenaline (NA), serotonin



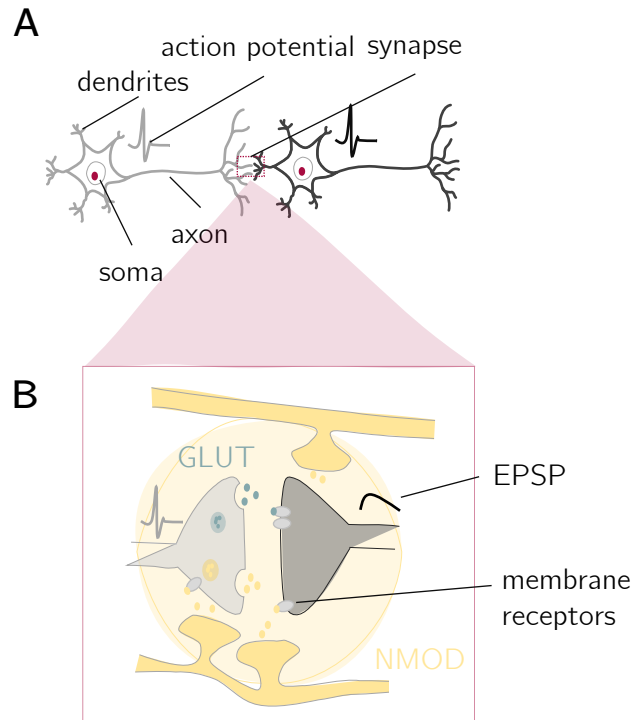


Figure 2.1: *Elements of neurophysiology: neurons and transmission of the information at an excitatory synapse.* **A.** A presynaptic neuron (gray) communicates with a postsynaptic neuron (black) via the propagation of an action potential down the axon. The soma processes all synaptic inputs and trigger an action potential if the threshold is reached. **B.** A chemical synapse enables this synaptic transmission by the release of glutamate (GLUT) and other NMODs binding to receptors located on the postsynaptic membrane. This results in membrane potential change (EPSP) in the postsynaptic dendrites (inspired from [Graupner, 2017]).

(5HT), histamine (HA), glutamate (GLUT),  $\gamma$ -Aminobutyric acid (GABA), endocannabinoids (EC), and Brain-Derived Neurotrophic Factor (BDNF). A summary table covering the secretion region, global effects, receptors names, and types can be found on Figure 2.2.

Before this, it is important to recall the two main classes of existing receptors: ionotropic and metabotropic receptors.

- Ionotropic receptors are ion channels that bind chemicals at their extracellular domain enabling the transfer of ions.
- Metabotropic receptors, upon chemicals bindings, utilize so-called G-proteins (also called guanine nucleotide-binding proteins) to affect other channels or signaling pathways [Gu, 2002]. The signal is triggered indirectly through a cascade of various messengers. These G-proteins are classified into four main families according to their signal transduction:  $G_{i/o}$ ,  $G_q$ ,  $G_s$ , and  $G_{12/13}$  [The Nature Reviews Drug Discovery GPCR Questionnaire Participants. and Ellis, 2004].
  - ❖  $G_{i/o}$  proteins inhibit Adenylate Cyclase (AC)
  - ❖  $G_s$  proteins activate AC
  - ❖  $G_q$  proteins activate Phospholipase C (PLC)
  - ❖  $G_{12/13}$  proteins activate the Rho family of GTPases

## 2.2.1 Most common neuromodulators involved in the wake-sleep cycle and synaptic plasticity

### Acetylcholine

Acetylcholine regulates sensory processing, attention, learning, arousal, memory, mood, synaptic plasticity, and many more behaviors [Gu, 2002, Atherton et al., 2015].

Neurons secreting acetylcholine are called cholinergic neurons. The main areas in the brain where these neurons are found are the basal forebrain in the nucleus basalis of Meyner and the brainstem [Gu, 2002].

Acetylcholine acts on both ionotropic receptors, named nicotinic acetylcholine receptors due to their sensitivity to nicotine, and metabotropic receptors, named muscarinic acetylcholine receptors due to their sensitivity to the muscarine. There exist at least two subtypes of nAChRs and five subtypes of mAChRs conventionally denoted  $M_1 - M_5$ .  $M_1, M_3, M_5$  are mostly bound to G proteins of class  $G_q$  while  $M_2, M_4$  are mostly bound to  $G_{i/o}$  but exceptions arise.  $M_1$  and  $M_2$  receptors are the most studied in the cortex [Gu, 2002].

### Dopamine

Dopamine is known as the pleasure neuromodulator and its level is commonly increased in a reward-motivated manner. It mediates cognitive, emotive, motor, and endocrine functions and is also involved in addiction. Many common diseases, such as schizophrenia, Parkinson's disease, and Alzheimer's disease, are due to a dysfunction in the secretion and diffusion of dopamine in the central nervous system [Gu, 2002].

Neurons secreting dopamine are called dopaminergic neurons. The main area in the brain where these neurons are found is the midbrain, in the substantia nigra and the ventral tegmental area [Gu, 2002].

Dopamine only binds to metabotropic receptors known as dopaminergic receptors. There are five subtypes, designated  $D_1$  through  $D_5$ .  $D_1$  and  $D_5$  are coupled to  $G_s$  proteins while  $D_2, D_3, D_4$  are coupled to the G protein  $G_{i/o}$  [Gu, 2002].

### Noradrenaline

Noradrenaline is also sometimes named norepinephrine. Noradrenaline levels are high during a stressful situation to increase arousal and alertness and promote vigilance. It also has a role in the formation and retrieval of memory, processing of hunger and satiety, and attention [Gu, 2002].

Neurons secreting noradrenaline are called noradrenergic neurons. The main area in the brain where these neurons are found is the brainstem, and more specifically in the locus coeruleus located in the pons and medulla [Gu, 2002].

Noradrenaline only binds to metabotropic receptors known as adrenergic receptors. There are at least five subtypes, designated by  $\alpha_1, \alpha_2, \beta_1, \beta_2$  and  $\beta_3$ .  $\alpha_1$  are coupled to the G protein  $G_q$  whereas  $\alpha_2$  are coupled to the G protein  $G_{i/o}$  and  $\beta_1, \beta_2$  and  $\beta_3$  are coupled to  $G_s$  proteins [Gu, 2002].

### Serotonin

Serotonin is a neuromodulator that mainly modulates mood and impulse. It is also implicated in the regulation of memory, learning, sleep, pain, appetite, and many more processes [Gu, 2002].

Neurons secreting serotonin are called serotonergic neurons. The main area in the brain where these neurons are found is the brainstem, and more specifically in the raphe nuclei.

Serotonin binds to ionotropic and metabotropic receptors. There is only one family of ionotropic receptors designated by  $5HT_3$  and which is a ligand-gated  $Na^+$  and  $K^+$  cation channel. There are at least six families of metabotropic receptors named  $5HT_1$ ,  $5HT_2$ ,  $5HT_4$ ,  $5HT_5$ ,  $5HT_6$  and  $5HT_7$ .  $5HT_4$ ,  $5HT_6$  and  $5HT_7$  are coupled to the G protein  $G_s$ ,  $5HT_1$  and  $5HT_5$  are coupled to the G protein  $G_{i/o}$  and  $5HT_2$  are coupled to  $G_q$ .  $5HT_1$ ,  $5HT_2$  and  $5HT_5$  is further classified resulting in a total of 14 different types of receptors [Gu, 2002].

## Histamine

Histamine is an early-stage development neuromodulator. It is involved in sleep regulation, arousal, motor activity, learning, stress, aggression, pain, self-stimulation, reinforcement, and other physiological functions [Gu, 2002].

Neurons secreting serotonin are called histaminergic neurons. The main area in the brain where these neurons are found is the hypothalamus, in the tuberomammillary nucleus [Gu, 2002].

Histamine binds only to metabotropic receptors. There are four known receptors named  $H_1, H_2, H_3$  and  $H_4$ .  $H_2$  are coupled to the G protein  $G_s$ ,  $H_3$  and  $H_4$  are coupled to the G protein  $G_{i/o}$  and  $H_1$  are coupled to  $G_q$ .

## Glutamate

Glutamate, already mentioned in the previous section, is the major and most common excitatory neurotransmitter in the central nervous system and, together with GABA, they maintain homeostasis within the brain. It also has a main role as a neuromodulator in the regulation of learning and memory. It is also involved in the sensation of pain [Peng et al., 2011] and mediates the wake-sleep cycle [Watson et al., 2011].

Neurons secreting glutamate are everywhere in the brain. Specifically, the excitatory role of glutamate is predominant in the cortical activity of pyramidal cells [Della Sala, 2021].

Glutamate interacts with ionotropic and metabotropic receptors. Ionotropic receptors subtypes are the  $\alpha$ -amino-3-hydroxy-5-methyl-4-isoxazolepropionic acid receptor (AMPA) receptor (AMPA) and the NMDA receptor (NMDAR) but also the kainate receptors. Metabotropic receptors come in various subtypes ranging from  $mGluR_1$  to  $mGluR_8$  [Willard and Koochekpour, 2013].  $mGluR_2$ ,  $mGluR_3$ ,  $mGluR_4$ ,  $mGluR_6$ ,  $mGluR_7$  and  $mGluR_8$  are coupled to the G protein  $G_{i/o}$  and  $mGluR_1$  and  $mGluR_5$  are coupled to  $G_q$ .

## GABA

GABA, whose precursor is glutamate, is the main inhibitory neurotransmitter throughout the brain and it counterbalances the effect of glutamate to maintain homeostasis by reducing neuronal excitability. As a neuromodulator, it is mainly involved in the regulation of vigilance, anxiety, and memory processes [Gasbarri and Pompili, 2014].

There exist two types of neurons producing GABA (*i.e.*, GABAergic neurons): interneurons (acting locally) and large neurons (projecting to other brain areas). Among the latter, we find Purkinje cells in the cerebellum or medium spiny neurons in the striatum [Caputi et al., 2013].

GABA interacts with the two kinds of receptor families named  $GABA_A$  for the ionotropic receptors and  $GABA_B$  for the metabotropic receptors.  $GABA_B$  receptors are mainly coupled to G proteins  $G_{i/o}$  [Chebib and Johnston, 1999].

## 2.2.2 Other chemicals regulating sleep and synaptic plasticity

### Endocannabinoids

Endocannabinoids are cannabinoid molecules that are naturally expressed inside our organism (endogenous cannabinoids). This neurotransmitter is part of the crucial endocannabinoid system (ECS) which comprises cannabinoid receptors, endocannabinoids, and proteins and enzymes. This system is crucial for the development of the brain and synapses. It promotes homeostasis within the whole body [De Petrocellis and Di Marzo, 2009]. Endocannabinoids play a role in nociception, appetite, pain, motor activity, neuroendocrine regulation, immune function, mood, learning, and also in neuronal development [Fernández-Ruiz et al., 1999, Aizpurua-Olaizola et al., 2017]. Due to its predominant role in the proper functioning of the brain, the disturbance of the endocannabinoid system has an impact on several neurodegenerative and convulsive diseases [Iannotti et al., 2016].

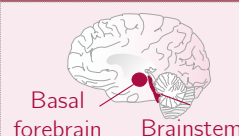
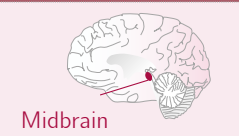


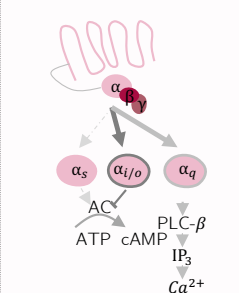
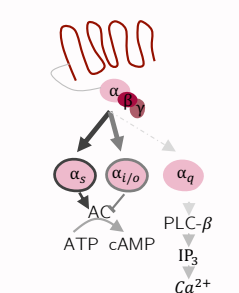
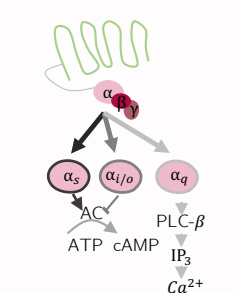
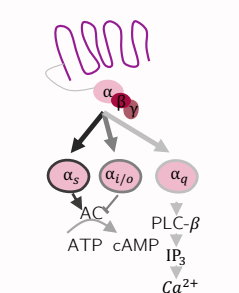
Endocannabinoids are produced all over the brain and anandamide and 2-arachidonoylglycerol are the best-known endocannabinoids [De Petrocellis and Di Marzo, 2009].

Endocannabinoids are the endogenous ligands of cannabinoid receptors. These receptors belong to the metabotropic family and are subdivided into two families:  $CB_1$  and  $CB_2$  both binding to G proteins  $G_{i/o}$  [Piscitelli, 2015].  $CB_1$  is predominant in the central nervous system compared to  $CB_2$ , the latter being mostly expressed in non-neuronal cells [Ofek et al., 2011].

### Brain-Derived Neurotrophic Factor (BDNF)

BDNF is a chemical known for its predominant role in early brain development and survival of neuronal populations [Barde et al., 1982, Huang and Reichardt, 2001, Acheson et al., 1995, Cabelli et al., 1995], thus it is not considered in the proper sense as a neuromodulator. However, in a more mature brain and depending on the context, it also plays a role as (reviewed by [Binder and Scharfman, 2004]) a modulator of pain [Malcangio and Lessmann, 2003], synaptic transmission [Schinder and Poo, 2000], neurogenesis [Pencea et al., 2001], learning and memory [Yamada and Nabeshima, 2003], and epileptogenesis [Jankowsky and Patterson, 2001].

It is distributed throughout the central nervous system and binds to Tropomyosin-Related Kinase Receptors of subtype B (TrkB). This receptor is not a G-coupled receptor but upon activation, it also leads to a variety of intracellular signaling cascades [Binder and Scharfman, 2004]). Activation of TrkB triggers several signaling cascade among which the ras–Mitogen-Activated Protein Kinase (MAPK) pathway, the Phosphatidylinositol 3-Kinase (PI3K)–Akt pathway, or the PLC $\gamma$ – $Ca^{2+}$  pathway [Leal et al., 2017].

	Acetylcholine (ACh)	Dopamine (DA)	Noradrenaline (NA)	Serotonin (5HT)
Region	 Basal forebrain    Brainstem	 Midbrain	 Brainstem	 Brainstem
Global effect	<ul style="list-style-type: none"> <li>Sensory processing</li> <li>Attention</li> <li>Learning</li> <li>Arousal</li> <li>Memory</li> <li>Mood</li> <li>Synaptic plasticity</li> <li>....</li> </ul>	<ul style="list-style-type: none"> <li>Pleasure</li> <li>Reward</li> <li>Cognitive functions</li> <li>Emotion</li> <li>Motor</li> <li>Endocrine</li> <li>Addiction</li> <li>....</li> </ul>	<ul style="list-style-type: none"> <li>Stress</li> <li>Arousal</li> <li>Alertness</li> <li>Vigilance</li> <li>Memory</li> <li>Hunger</li> <li>Satiety</li> <li>Attention</li> <li>....</li> </ul>	<ul style="list-style-type: none"> <li>Mood</li> <li>Impulse</li> <li>Memory</li> <li>Learning</li> <li>Sleep</li> <li>Pain</li> <li>Appetite</li> <li>....</li> </ul>
Receptors	<ul style="list-style-type: none"> <li><math>M_{2,4}</math></li> <li><math>M_{1,3,5}</math></li> </ul>	<ul style="list-style-type: none"> <li><math>D_{1,5}</math></li> <li><math>D_{2,3,4}</math></li> </ul>	<ul style="list-style-type: none"> <li><math>\beta_{1,2,3}</math></li> <li><math>\alpha_2</math></li> <li><math>\alpha_1</math></li> </ul>	<ul style="list-style-type: none"> <li><math>5HT_{4,6,7}</math></li> <li><math>5HT_{1,5}</math></li> <li><math>5HT_2</math></li> </ul>
G-coupled proteins				

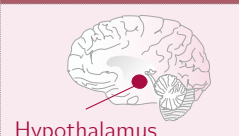



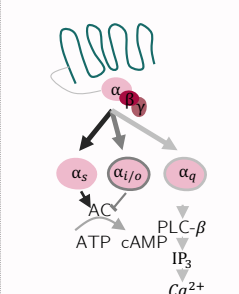
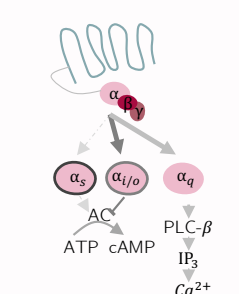
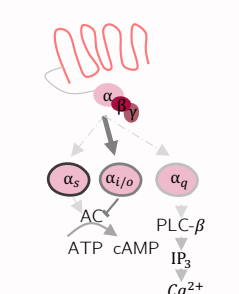
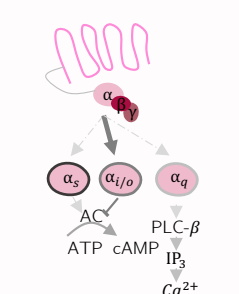
	Histamine (HA)	Glutamate (GLUT)	GABA	Endocannabinoids (EC)
Region	 Hypothalamus			
Global effect	<ul style="list-style-type: none"> <li>Development</li> <li>Sleep</li> <li>Arousal</li> <li>Motor</li> <li>Stress</li> <li>Learning</li> <li>Aggression</li> <li>Pain</li> <li>Stimulation</li> <li>....</li> </ul>	<ul style="list-style-type: none"> <li>Excitatory</li> <li>Homeostasis</li> <li>Learning</li> <li>Memory</li> <li>Pain</li> <li>Sleep</li> <li>....</li> </ul>	<ul style="list-style-type: none"> <li>Inhibitory</li> <li>Homeostasis</li> <li>Vigilance</li> <li>Anxiety</li> <li>Memory</li> <li>....</li> </ul>	<ul style="list-style-type: none"> <li>Homeostasis</li> <li>Nociception</li> <li>Appetite</li> <li>Pain</li> <li>Motor</li> <li>Endocrine</li> <li>Immunity</li> <li>Mood</li> <li>Development</li> <li>....</li> </ul>
Receptors	<ul style="list-style-type: none"> <li><math>H_2</math></li> <li><math>H_{3,4}</math></li> <li><math>H_1</math></li> </ul>	<ul style="list-style-type: none"> <li><math>mGluR_{2,3,4,6,7,8}</math></li> <li><math>mGluR_{1,5}</math></li> </ul>	<ul style="list-style-type: none"> <li><math>GABA_B</math></li> </ul>	<ul style="list-style-type: none"> <li><math>CB_{1,2}</math></li> </ul>
G-coupled proteins				

Figure 2.2: Summary table of neuromodulators regulating sleep. The secretion regions, global effects, receptors names, and types are detailed for some neuromodulators. Note that only metabotropic receptors are summarized. The signaling cascades triggered upon  $G_s$ - (black bolted arrays),  $G_{i/o}$ - (grey bolted arrays) or  $G_q$ - (light grey bolted arrays) coupled receptors activation are also developed. Dashed light grey arrays are non-triggered cascades. Brain with red lines means that the specific neuromodulator is secreted everywhere in the brain.

## 2.3 From wakefulness to sleep

### 2.3.1 Sleep macrostructure

Sleep is divided into two distinct periods: Non-Rapid Eye Movements (NREM) sleep and Rapid Eye Movements (REM) sleep. NREM sleep is divided into three stages defined by the deepness of sleep and brain wave patterns. Stage 1 is the lightest stage of sleep and is characterized by waves of 8-12Hz (called alpha brain waves). During Stage 2, brain waves slow down with the intermittent onset of K-complexes and spindles. The deepest stage of sleep is characterized by slow oscillations below 4Hz of UP and DOWN states named Slow-Wave Sleep (SWS) (can also be called delta waves). At the macro level, REM sleep is characterized by hippocampal theta rhythms, fast movements of the eyes, irregular breathing patterns, and wake-like signals [Fernandez and Luthi, 2019]. All the rhythms are depicted on Figure 2.3.

Generally speaking, a typical night of sleep goes as follows: an NREM-REM cycle lasts about ninety minutes and there are about four to five NREM-REM cycles in one night. Overnight, REM sleep time increases with each cycle while stage 3 NREM sleep time is longer at the beginning and shorten throughout the night (see Figure 2.3). It is assumed that this NREM-REM cycling has memory and cellular functions [Langille, 2019].

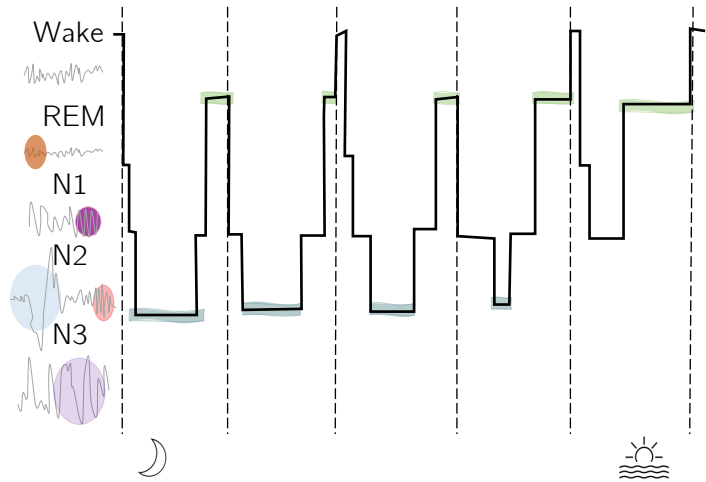


Figure 2.3: *Hypnogram of sleep stages.* Along the y-axis (resp. x-axis) are the sleep stages (resp. NREM-REM cycles throughout one night). From wake to very light sleep (N1) characterized by alpha waves (dark purple), then to light sleep (N2) characterized by K-complexes (blue) and spindles (pink), then to deep sleep (N3) characterized by delta waves (light purple) and lastly to REM characterized by theta rhythms (orange).

### 2.3.2 Neurobiology of sleep

Three main structures are involved in the generation of wakefulness and sleep: the basal forebrain, the hypothalamus, and the brainstem [Berry, 2012, Saper et al., 2010].

During the day, wakefulness is maintained by the secretion of neuromodulators from these structures (see Figure 2.4A). Noradrenaline is secreted from the locus cerebellum (LC) of the brainstem, histamine from the tuberomammillary nucleus (TMN) of the hypothalamus, serotonin from the dorsal raphe nuclei (DRN) of the brainstem, and adrenaline from the cholinergic nuclei of the brainstem. The structures are then responsible for the projection of the neuromodulators, acting as mediators, to large cortical territories. When active, the nuclei DRN, LC, and TMN send inhibitory projection to the sleep-promoting area ventrolateral preoptic nucleus (VLPO) [Berry, 2012, Saper et al., 2010].

During sleep initiation, VLPO in the hypothalamus secretes GABA, the most common inhibitory neurotransmitter (see Figure 2.4B). This leads to the inhibition of all nuclei of the ascending system responsible for maintaining wakefulness [Berry, 2012, Saper et al., 2010].

The transition between wake and sleep, known as the flip-flop switch model of sleep [Berry, 2012], is

due to the mutually inhibitory process between the arousal activating system and the sleep-promoting system. It is essential to mention the major role of the factor involved in this switch from wakefulness to sleep, orexin (also known as hypocretin). Orexin, secreted in the lateral hypothalamic area (LH), is active during wake and innervates all the nuclei of this network, as well as the cerebral cortex thus reinforcing the impact of this arousal system to promote wakefulness and inhibit VLPO. Upon sleep, VLPO takes the lead and inhibits the arousal activating system as well as orexin. Therefore, orexin acts as a stabilizer for transitions between wake and sleep [Berry, 2012, Saper et al., 2010].

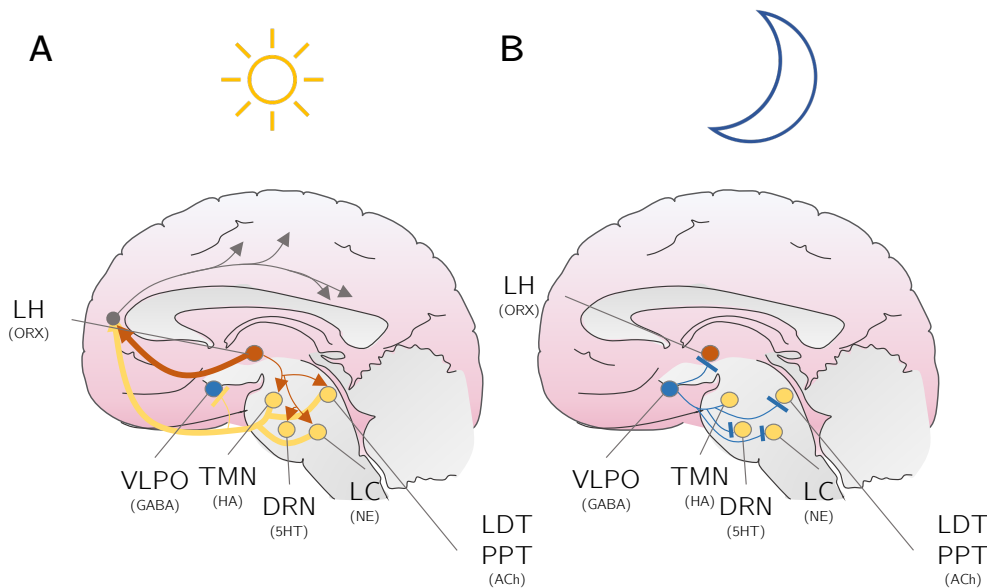


Figure 2.4: *Neurobiology of wake and sleep.* **A.** Orexin (ORX) secreted by the lateral hypothalamus (LH, orange) innervates the ascending arousal systems (yellow) and the cortex (grey arrays). In turn, the ascending arousal systems innervate the cortex and inhibit the ventrolateral preoptic area (VLPO, blue). **B.** The VLPO inhibits the lateral hypothalamus and the ascending arousal systems. LC = locus coeruleus; LDT = lateral dorsal tegmental; PPT = pedunculopontine tegmental; TMN = tuberomammillary nucleus; DRN = dorsal raphe nucleus. Adapted from [Berry, 2012].

### 2.3.3 Electroencephalogram and thalamocortical cellular signatures

An action potential is a key feature of every neuron comprising the brain but the way it is generated and its subsequent firing pattern may differ from one type of neuron to the other as well as from one state to the other. Because of the predominant role of the thalamus in the processing and transmission of sensory and motor information [Huguenard and McCormick, 2007], as well as its ability to regulate sleep patterns [Jan et al., 2009], thalamocortical neuron behavior during wakefulness and sleep is of particular interest for this work.

To fulfill its function, the thalamus relies on the *relay nucleus* that transmits information to the cortex and to the *thalamic reticular nucleus* through excitatory connections and it relies on the *thalamic reticular nucleus* that transmits information back to the *relay nuclei* through inhibitory connections. The cortex also innervates the two nuclei with excitatory connections (Figure 2.5B) [Zagha and McCormick, 2014]. Thalamocortical neurons reveal different behaviors depending on the state of an individual due to these excitatory and inhibitory connections. During wakefulness, at the scalp level, fast and low amplitude activity (Figure 2.5A) is observed on the electroencephalogram

(EEG) signal and neurons are firing in a tonic mode (Figure 2.5C). Upon sleep, the activity is a slow with a high amplitude signal (Figure 2.5A) because of the switch from a tonic to a bursting activity at the cellular level. A bursting pattern is represented by a succession of action potentials discharging at a high frequency, followed by a period of silence (Figure 2.5C) [McCormick and Bal, 1997].

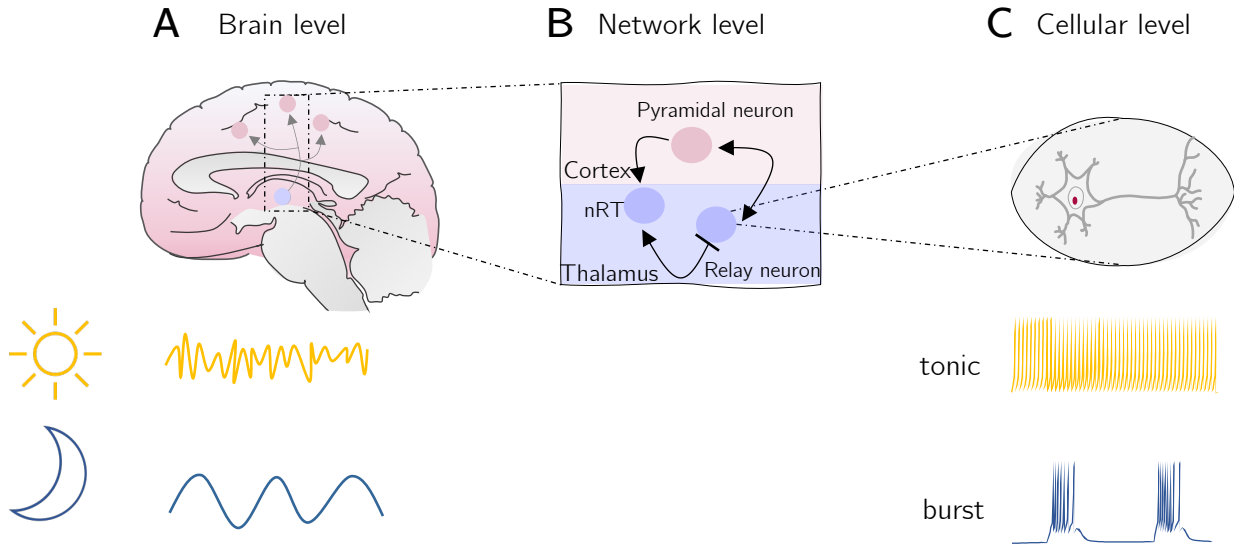


Figure 2.5: *EEG and cellular signatures of thalamocortical neurons during wakefulness and sleep.* **A.** At the brain level, during wakefulness, EEG signal is low and fast while during sleep, it is high and slow **B.** At the network level, relay neurons are linked through excitatory connections to the thalamic reticular nucleus (nRT) and to pyramidal neurons of the cortex and receive excitatory (resp. inhibitory) feedback connections from the cortex (resp. nRT). The cortex also innervates nRT with excitatory connections. **C.** At the cellular level, there is a switch from a tonic activity during wakefulness to a bursting activity upon sleep. Adapted from [Zagha and McCormick, 2014].

## 2.4 Synaptic plasticity

*"Brains comprise well-defined circuits that are nonetheless modifiable by experience, a property critical for learning. This property is often attributed to the ability of neurons to modify their connections with other cells through a mechanism called synaptic plasticity. It exploits the correlation level in the activity of neighboring neurons"* [Jacquerie et al., 2022].

At the synapses, plasticity results in either the reinforcement or the weakening of the strength between two neurons. This effect is measured by EPSPs amplitude changes due to modification of presynaptic neurotransmitters release and/or changes in the cell-intrinsic properties of the postsynaptic neuron [Heidelberger et al., 2014]. Synaptic plasticity occurs at different timescales ranging from minutes (*i.e.*, short-term plasticity) to hours and days (*i.e.*, long-term plasticity). While short-term plasticity has as a main consequence a change in the probability of neurotransmitters released by the presynaptic neurons [Yang and Calakos, 2013], long-term plasticity has, in addition, long-lasting effects on the postsynaptic neuron such as changes in volume and number of dendritic spines [Segal, 2005], changes in AMPA receptors number, changes in receptor conductance and gene expression [Purves, 2004]. In this research, we rather focus on long-term plasticity.

Long-Term Potentiation (LTP) defines the long-lasting strengthening of synapses and Long-Term Depression (LTD) defines the long-lasting weakening of synapses. LTP is further sub-classified into



two groups: when the effects of reinforcement are expressed between one and two hours, it is referred to as early-phase LTP (E-LTP) and if this effect persists, it is referred to as late-phase LTP (L-LTP) [Citri and Malenka, 2008]. Conversely, it is not as evident whether long-term depression may be classified in such away. The early phase of plasticity is transformed into the late phase when new proteins and ribonucleic acid messengers (mRNAs) are synthesized to support the maintenance of plastic changes [Bliss and Cooke, 2011].

Long-term synaptic plasticity appears in various forms. The most well-known process involves the activation of NMDA receptors but other processes are possible, some recognized and others still under investigation. A detailed description of the role of calcium in NMDAR-based long-term synaptic plasticity is provided first, followed by a brief explanation of other less common mechanisms.

### 2.4.1 Role of calcium in NMDAR-based long-term synaptic plasticity

As the main objective of this thesis is to highlight the impact of neuromodulators on synaptic plasticity by using synaptic computational models based on calcium dynamics, it is important to review in detail the major role played by calcium in this phenomenon.

NMDAR-based plasticity at the postsynaptic site relies on the interaction between glutamate, glutamate receptors AMPARs, NMDARs and the subsequent influx of calcium in the postsynaptic neuron (Figure 2.6A). AMPA receptors open when glutamate binds to them. Following their respective concentration gradient, sodium ( $Na^+$ ) ions flow inwards with a greater flux than the potassium ( $K^+$ ) flowing outwards, thus changing the charge balance in and out of the cell and increasing membrane potential. To be activated, NMDAR receptors not only need to be bound to glutamate, but they must also release a magnesium ( $Mg^{2+}$ ) ion occupying the gateway of the pore.  $Mg^{2+}$  binding to the channel is voltage-dependent and the more depolarized the membrane is, the more poorly the binding is held. Once the  $Mg^{2+}$  ion is released, the receptor is permeable to  $Na^+$ ,  $K^+$  ions, and, most importantly, to calcium ( $Ca^{2+}$ ) ions [Purves, 2004].

Upon stimulation, an action potential propagates down the axon of the presynaptic neuron and causes the release of specific neurotransmitters. As the studied synapse are excitatory, glutamate is found among the released neurotransmitters and is the key player in synaptic plasticity as it binds to AMPA and NMDA receptors. These receptors are co-existing at the same synapse and mediate the influx of calcium into the postsynaptic neuron. Under basal conditions, AMPARs are closed and magnesium ions block NMDARs. Once activated by glutamate, AMPAR is permeable to sodium and potassium, thus depolarizing the inner side of the post synapse. After this voltage shift,  $Mg^{2+}$  ions are repelled from the NMDA receptors, and due to this phenomenon and the activation by glutamate, these channels are activated and allow a calcium influx. NMDAR thus acts as a coincidence signal as it requires a presynaptic activity (*i.e.*, glutamate release) and a postsynaptic activity (*i.e.*, depolarization to remove  $Mg^{2+}$  block). The difference in cytosolic calcium leads the direction of the synaptic changes towards either synaptic strength weakening (long-term depression, LTD) or synaptic strength reinforcement (LTP). Following the transient rise in cytosolic calcium, calmodulin is activated (Figure 2.6B) and, depending on the level of  $Ca^{2+}$  concentration, this  $Ca^{2+}$ /calmodulin (CaM) complex triggers activation of either kinase or phosphatase signaling cascades. The  $Ca^{2+}$ /calmodulin-dependent protein kinase II (CAMKII) senses a brief and transient elevated increase in calcium level (Figure 2.6C.1) whereas the phosphatase calcineurin rather reads a prolonged and sustained intermediate level of calcium (Figure 2.6C.2), giving plastic changes in different ways [Purves, 2004]:

- LTP relies on the direct  $Ca^{2+}$ /Calmodulin-dependent Protein Kinase II (CaMKII)-mediated phosphorylation and is expressed by the increase of AMPA receptors efficiency and by the number of AMPA receptors on the membrane surface. The calcium/calmodulin complex also directly activates Cyclic Adenosine Monophosphate (cAMP) and Protein kinase A (PKA) which results in a CaMKII activity increase from cyclic-AMP and PKA-directed inhibition of the Protein Phosphatase 1 (PP1). Enhancement of the conductance of AMPA receptors is the result of its phosphorylation by activated CaMKII. The mechanism behind the exocytosis of AMPAR remains unclear and may vary from one condition to the other. Some particular mechanisms, involving the contribution of neuromodulators, are described in detail later (see chapter 4) [Derkach et al., 1999].
- LTD relies on a protein signaling cascade governing the calcineurin-mediated CaMKII dephosphorylation. Calcineurin is a phosphatase activated by the calcium/calmodulin complex and activates itself PP1 by dephosphorylating inhibitor 1. Once activated, PP1 dephosphorylates CaMKII resulting in opposite outcomes regarding CaMKII-mediated LTP [Mulkey et al., 1994].

cAMP and PKA, activated by  $Ca^{2+}$ /CaM complex, are also major players in the maintenance of long-term plasticity by triggering a signaling pathway involved in the transcription of new genes and, through the mediation of MAPK, the initiation of local translation of existing transcripts (Figure 2.6D). In these newly synthesized proteins, we find proteins that are involved in the trafficking of AMPA receptors and growth factors that enable alterations in the structure of the synapse to enforce long-term changes in synaptic strength [Bliss and Cooke, 2011].

## 2.4.2 Other long-term plasticity mechanisms

### mGluR-dependent LTD

At certain locations in the brain including the hippocampus, activation of metabotropic glutamate receptors (mGluR) trigger another form of LTD independent of extracellular calcium (Figure 2.7). When glutamate binds to group 1 mGluR located at the postsynaptic membrane, the lipid phosphoinositide ( $PIP_2$ ) is hydrolyzed by PLC resulting in the production of diacylglycerol (DAG) and inositol triphosphate ( $IP_3$ ) (Figure 2.7A) [Bliss and Cooke, 2011, Citri and Malenka, 2008].  $IP_3$  activation increases the intracellular  $Ca^{2+}$  cation concentration from intracellular stores (Figure 2.7B.2) while DAG activates protein kinase C (PKC) which is thought to be involved in the release of endocannabinoids driving a form of presynaptic LTD (Figure 2.7B.1) [Ohno-Shosaku et al., 2005, Valentinova and Mamei, 2016]. The MAPK signaling pathway is also thought to be important for mGluR LTD (Figure 2.7C).

### Presynaptic long-term plasticity

Presynaptic plasticity is a type of plasticity expressed by changes in the probability of neurotransmitters (*i.e.*, glutamate) released at the presynapse (Figure 2.8) [Yang and Calakos, 2013]. The increase or decrease of the probability of glutamate release favors LTP or LTD respectively. This form of presynaptic plasticity is induced presynaptically (autocrine communication) or postsynaptically (paracrine communication) using a retrograde signaling mechanism. In both cases, the increase in intracellular calcium in the neuron by Voltage-Dependent Calcium Channel (VDCC) is also involved in the increase in probability of neurotransmitters release.

When induced presynaptically, presynaptic plasticity is due to the activation of certain glutamatergic receptors on the membrane of the presynaptic neuron by the binding of glutamate that is released from the same neuron. In this case, the activation of  $mGluR_{2,3}$  inhibits the cAMP/PKA pathway

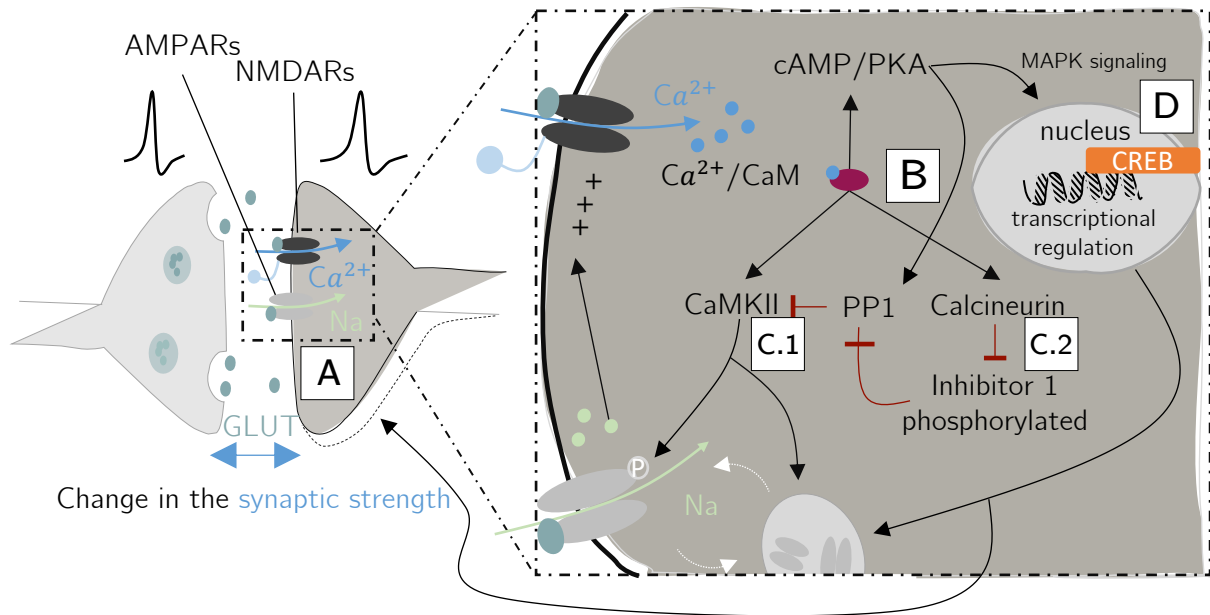


Figure 2.6: *Molecular mechanisms of NMDAR-based long-term synaptic plasticity.* **A.** The presynaptic neuron (grey) releases glutamate (GLUT) upon stimulation. GLUT binds to AMPARs and NMDARs. Activation of AMPARs triggers the influx of  $Na^{2+}$  into the postsynaptic cell (black), depolarization, and removal of  $Mg^{2+}$  block located on the NMDARs such that  $Ca^{2+}$  enters the postsynaptic neuron and binds to CaM. **B.** The  $Ca^{2+}$ /CaM complex activates kinases (CaMKII), phosphatases (calcineurin) as well as PKA via cAMP activation. **C.**  $Ca^{2+}$  transients determine the polarity of the induced early-phase plasticity: high and brief  $Ca^{2+}$  transients induce LTP via CaMKII expressed by phosphorylation and exocytosis of AMPARs enhancing their conductance (**C.1**), low and prolonged  $Ca^{2+}$  transients induce LTD via calcineurin expressed by dephosphorylation and endocytosis of AMPARs decreasing their conductance (**C.2**). **D.** Activation of cAMP-dependent signaling cascade and PKA contributes to late-phase plasticity requiring synthesis of new proteins through novel gene transcription or initiation of local translation of existing transcripts located in dendritic storage sites. This form of plasticity results in the growth of dendritic spines (dotted line). Adapted from [Bliss and Cooke, 2011].

and decreases the release of neurotransmitters (Figure 2.8A.1). Conversely, the activation of presynaptic NMDARs activates the cAMP/PKA pathway and increases the release of neurotransmitters (Figure 2.8A.2).

When induced postsynaptically, presynaptic plasticity is due to a retrograde signaling. Among the possible signaling is the mGluR- and  $CB_1$ - dependent LTD explained more in detail here-above (Figure 2.7B.1). Another mechanism involves nitric oxide (NO) that notify the presynaptic terminal that a coincidence has happened to induce LTD or LTP (Figure 2.8B) [Gage et al., 1997, Stanton et al., 2003, Huang, 1997]. For more detailed information about this topic, you may refer to [Meunier et al., 2017b].

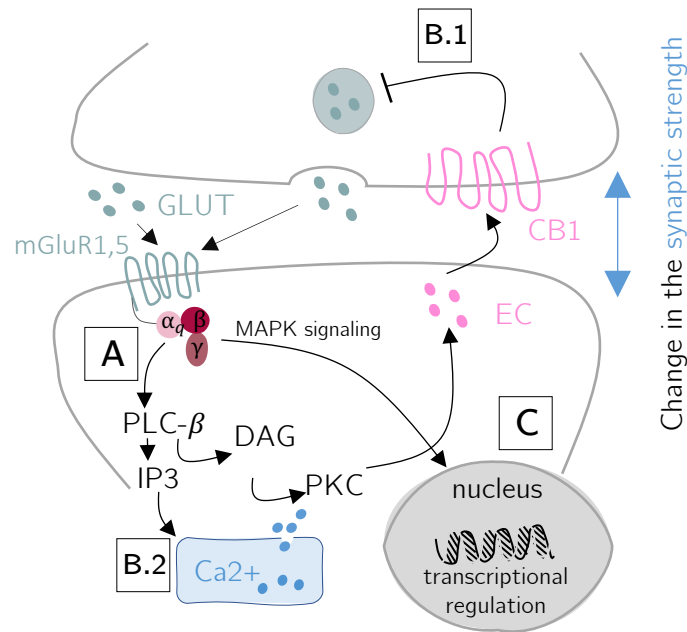


Figure 2.7: *Molecular mechanisms of mGluR-dependent LTD.* **A.** GLUT binds to  $mGluR_{1,5}$  and activates  $PLC - \beta$  resulting into the production of DAG and  $IP_3$ . PKC is activated by DAG and decreases the probability of neurotransmitters release by the presynaptic neuron via the intermediate of EC acting on  $CB_1$  receptors (**B.1**).  $IP_3$  increases the release of intracellular  $Ca^{2+}$  from internal stores (**B.2**). **C.** By acting on MAPK signaling,  $mGluR_{1,5}$  activation regulates transcriptional processes. Adapted from [Bliss and Cooke, 2011].

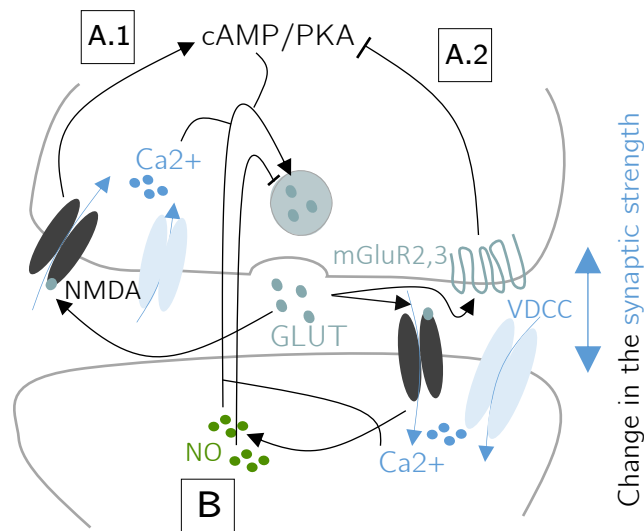
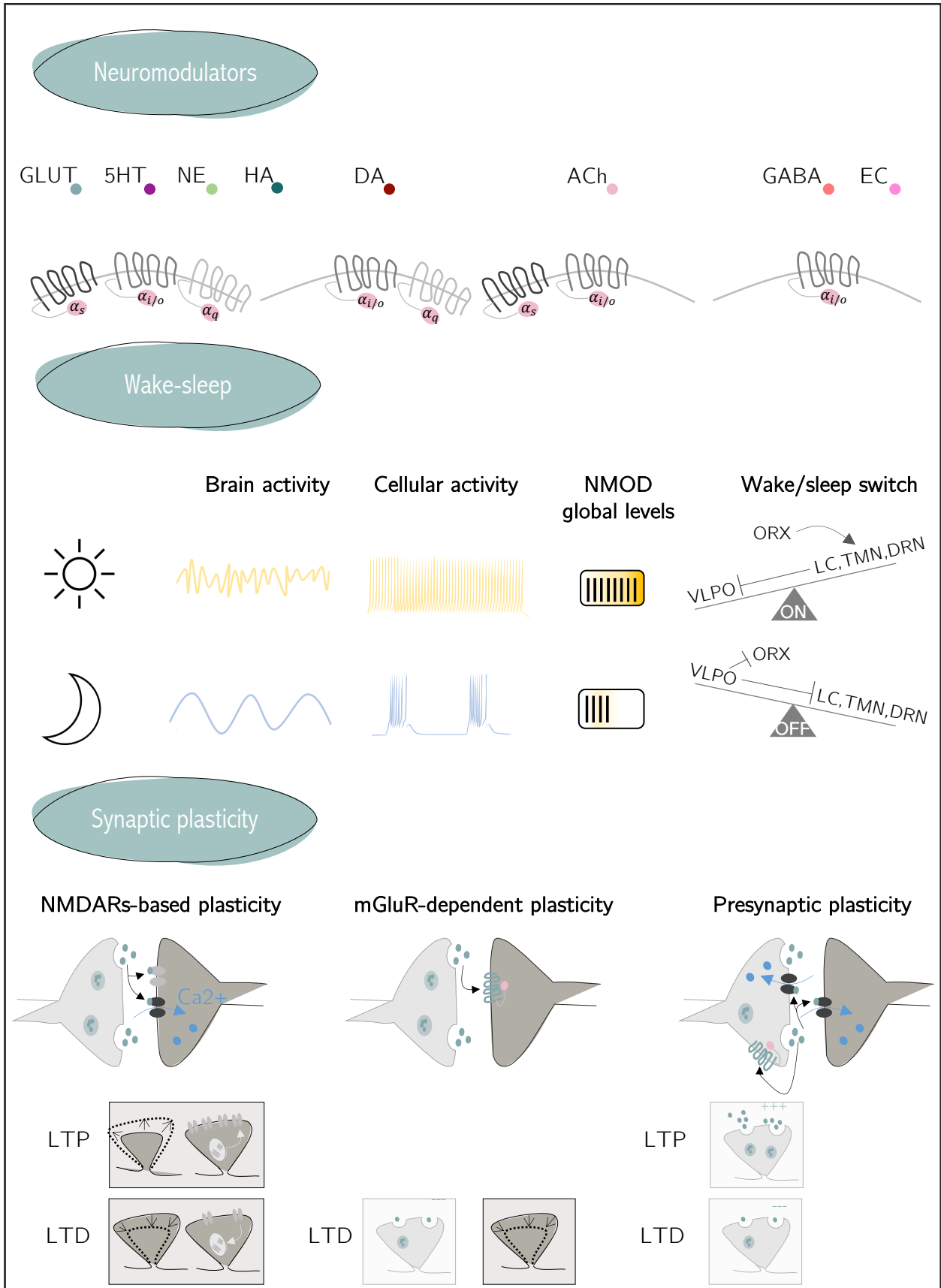


Figure 2.8: *Molecular mechanisms of presynaptic long-term plasticity.* **A.** Presynaptic plasticity induced presynaptically. Glutamate (GLUT) binding to NMDARs triggers the activation of cAMP/PKA pathway and induces LTP (**A.1**). GLUT binding to  $mGluR_{2,3}$  triggers the inhibition of cAMP/PKA pathway and induces LTD (**A.2**). **B.** Presynaptic plasticity induced postsynaptically. GLUT binding to NMDARs triggers the activation of a molecular mechanism involving nitric oxide (NO) to induce bidirectional plasticity. In both case, calcium ( $Ca^{2+}$ ) favors LTP. Adapted from [Bliss and Cooke, 2011].

## 2.5 Summary

### Elements of neurophysiology



## Chapter 3

# Calcium-based plasticity rules

Synaptic plasticity can be modeled mathematically by expressing the temporal evolution of the synaptic strength, encapsulated in the parameter  $w$ , between two neurons as ordinary differential equations. Synaptic plasticity rules are represented by a black box that takes as input the neuronal activity of the pre- and post- synaptic neurons (Figure 3.1A). These rules are divided into two categories: *phenomenological* models and *biological* models [Jacquerie et al., 2022].

*Biological* rules model the cellular and/or molecular phenomena that occur during synaptic change. They describe only the calcium dynamics or they go into more details and describe the signaling cascade triggered by the entry of calcium into the postsynaptic neuron, the latter yielding more complex mechanisms. Therefore, the input of the black box is the calcium influx resulting from the neuronal activity (Figure 3.1B).

*Phenomenological* rules are based on a fit to experimental data of neuron spiking activity following the STDP protocol. This protocol consists in 60 pair pulses of the presynaptic and postsynaptic neurons at a fixed frequency of 1 Hz for various time lag  $\Delta t$  between the presynaptic and postsynaptic spikes [Bi and Poo, 1998], Therefore, the input of the black box is the spike times resulting from the neuronal activity (Figure 3.1C).

In this project, we focus on biophysical models and more specifically on models describing the calcium dynamics, hence the name "*calcium-based plasticity rules*".

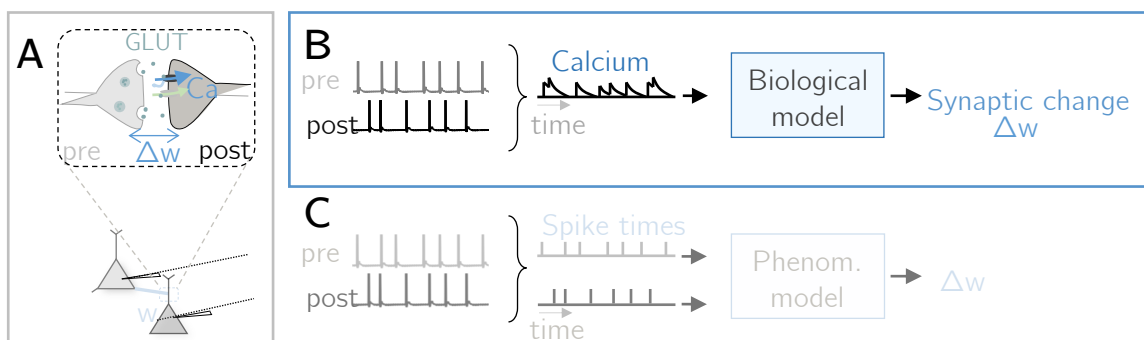


Figure 3.1: *Black box: computational modeling of synaptic plasticity.* **A.** A presynaptic neuron (grey) is connected to a postsynaptic neuron (black) with a certain weight ( $w$ ). **B.** Biological rules take as input the calcium influx and give as output a synaptic change ( $\Delta w$ ). **C.** Phenomenological rules take as input the spikes times and give as output a synaptic change ( $\Delta w$ ). Adapted from [Jacquerie et al., 2022].

### 3.1 Calcium-dependent synaptic plasticity rule with a continuous function of the calcium concentration [Shouval et al., 2002]

[Shouval et al., 2002] pioneered calcium-based synaptic plasticity rules. Considering that a low concentration of calcium does not impact the synaptic strength, medium concentration leads to depression and a high concentration of calcium leads to potentiation [Yang et al., 1999], they presented a mathematical model of bidirectional NMDAR-dependent synaptic plasticity named **model 1** in this thesis for clarity. The evolution of the synaptic strength  $w$  follows a sigmoidal shape as function of the calcium level (Figure 3.2). Based on biological facts, they established the potentiation process faster than the depression process. Furthermore, this model can reproduce different plasticity induction protocols including presynaptic frequency-response synaptic plasticity whose qualitative curve shape is supported experimentally by [Sjöström et al., 2001]. In his work, he showed that potentiation increases with firing frequencies in the cortex (for more information about the frequency-response curve of synaptic plasticity and [Sjöström et al., 2001] protocol go to subsection 3.3.1). The temporal evolution of synaptic strength established by [Shouval et al., 2002] is based on two main assumptions:

- (i) The calcium is the primary signal for synaptic plasticity. Different calcium levels trigger different forms of synaptic plasticity
- (ii) The dominant source of calcium influx to the postsynaptic cell is through NMDARs

According to the first assumption, [Shouval et al., 2002] modeled the evolution of the synaptic strength as a sigmoid function of calcium concentration  $\Omega([Ca])$  weighted by a time-constant  $\tau_w$ :

$$\tau_w \dot{w} = \Omega([Ca]) \quad (3.1)$$

To avoid a physiologically impossible state where synaptic weights evolve linearly with time for a sustained level of calcium, it is important to bound this equation such that the weights can not exceed a maximal and minimal limit that are respectively set at 1 and 0 ( $w = 1$  if  $w \geq 1$  and  $w = 0$  if  $w \leq 0$ ). In this thesis, the models using such bounding-depend synaptic weight will be referred to as *hard-bound* models.

[Shouval et al., 2002] provided another way to overcome this limitation by adding a calcium-dependent weight decay term using the following formula:

$$\tau_w([Ca]) \dot{w} = \Omega([Ca]) - w \quad (3.2)$$

$$\Omega([Ca]) = 0.25 - 0.25 \frac{\exp(\beta_1 ([Ca] - \alpha_1))}{1 + \exp(\beta_1 ([Ca] - \alpha_1))} + \frac{\exp(\beta_2 ([Ca] - \alpha_2))}{1 + \exp(\beta_2 ([Ca] - \alpha_2))} \quad (3.3)$$

$$\tau_w([Ca]) = P_4 + \frac{P_1}{P_2 + [Ca]^{P_3}} \quad (3.4)$$

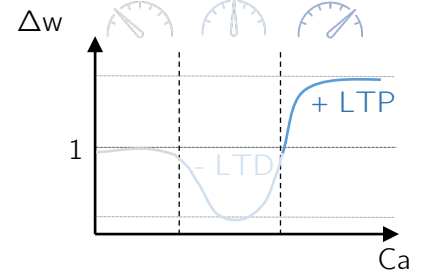


Figure 3.2: **Model 1: Continuous-calcium dependency rule.** The synaptic rule follows a sigmoidal shape as function of the calcium level with potentiation faster than depression. Adapted from [Jacquerie et al., 2022].

all the parameter values can be found in Appendix section D.1.

$\Omega([Ca])$  is a double-shaped sigmoid function and enables a depression at intermediate calcium concentration and potentiation at high calcium concentration (Figure 3.3) while  $\tau([Ca])$  is a decreasing function enabling a faster potentiation then depression.

Intuitively Equation 3.2 means that, for an infinite period of time, the weight  $w$  converges towards  $\Omega([Ca])$ . For a sustained level of calcium, when we integrate in the limit  $t \rightarrow \infty$ , we get the following:

$$w(t) = w_0 e^{-\frac{t}{\tau_w([Ca])}} + \Omega([Ca]) \xrightarrow{t \rightarrow \infty} \Omega([Ca]) \quad (3.5)$$

From this result, it is therefore interesting to better understand how the doubled-shaped sigmoid is constructed (see Figure 3.3) and what is the meaning of each parameter. Equation 3.3 can be rewritten in a more generalized format [Jacquerie et al., 2022]:

$$\Omega([Ca]) = a_0 - m_1 \frac{\exp(b_1 ([Ca] - a_1))}{1 + \exp(b_1 ([Ca] - a_1))} + m_2 \frac{\exp(b_2 ([Ca] - a_2))}{1 + \exp(b_2 ([Ca] - a_2))} \quad (3.6)$$

where

- $a_0 > 0$  is the ordinate at low concentration of calcium (*i.e.*, the value towards which  $w$  converges to when the calcium is in the region considered as not impacting synaptic weight)
- $a_0 - m_1$  with  $m_1 > 0$  is the ordinate at medium concentration of calcium (*i.e.*, the value towards which  $w$  converges to when the calcium is in the region considered as depression)
- $m_2 > 0$  is the ordinate at high concentration of calcium (*i.e.*, the value towards which  $w$  converges to when the calcium is in the region considered as potentiation)
- $a_1 > 0$  is the abscissa where the ordinate is  $\frac{a_0}{2}$  dictating the place along the x-axis where the first sigmoid is decreasing (*i.e.*, the concentration of calcium defining the lower bound of the region considered as depressing synaptic weight),  $b_1 > 0$  defines the slope of this decrease
- $a_2 > 0$  is the abscissa where the ordinate is  $\frac{m_2}{2}$  dictating the place along the x-axis where the second sigmoid is increasing (*i.e.*, the concentration of calcium defining the higher bound of the region considered as potentiated synaptic weight),  $b_2 > 0$  defines the slope of this increase

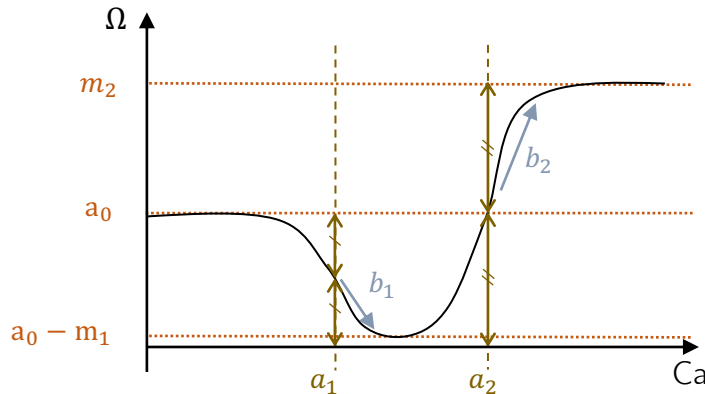


Figure 3.3: *Doubled-shaped sigmoid in function of calcium  $\Omega([Ca])$ .* Continuous function referring to Equation 3.6. Adapted from [Jacquerie et al., 2022].



In this thesis, the models using such weight decay terms is referred to as *soft-bound* models. According to the second assumption, the differential equation governing calcium dynamics is written by:

$$[Ca\dot{(t)}] = I_{NMDA}(t) - \left(\frac{1}{\tau_{Ca}}\right) [Ca(t)]$$

where  $I_{NMDA}$  is the voltage-dependent current flow through the ion channel and  $\tau_{Ca}$  is a time constant associated to calcium decay.

**Hard-bound models** "In hard-bound condition, the equation  $\tau_w dw/dt = \Omega$  means that the synaptic change evolves with a given velocity." [Jacquerie et al., 2022]  
**Soft-bound models** "In soft-bound condition, the rule corresponds to a standard first-order differential equation  $\tau_w dw/dt = \Omega - w$  such as the weight evolves towards its steady-state value  $\Omega$  with a time-constant of  $\tau_w$ ." [Jacquerie et al., 2022]

### 3.2 Calcium-dependent synaptic plasticity rule with potentiation and depression thresholds [Graupner et al., 2016]

[Graupner et al., 2016] came up with a new calcium-based synaptic plasticity rule relying on a simplification of [Shouval et al., 2002] work named **model 2** in this thesis for clarity. Instead of having a synaptic rule that follows a sigmoidal shape depending on the calcium level, they decided to introduce the concept of depression threshold ( $\theta_d$ ) and potentiation threshold ( $\theta_p$ ) (see Figure 3.4) by implementing in a schematic fashion "two opposing calcium-triggered pathways mediating the increase of synaptic strength (LTP; i.e., protein kinase cascades) and the decrease of synaptic strength (LTD; i.e., protein phosphatase cascades or G-protein cascades)" [Graupner and Brunel, 2012]. Following the bi-directional plasticity implemented by the continuous-calcium dependency rule [Shouval et al., 2002], they imposed that  $\theta_d < \theta_p$  such that when the concentration of calcium is below the depression threshold there is no synaptic change ( $[Ca] < \theta_d$ ), when the calcium concentration is higher than the threshold of depression but lower than the one of potentiation there is depression ( $[Ca] > \theta_d$  and  $[Ca] < \theta_p$ ) and when the concentration of calcium is higher than the threshold of potentiation there is potentiation ( $[Ca] > \theta_p$ ).

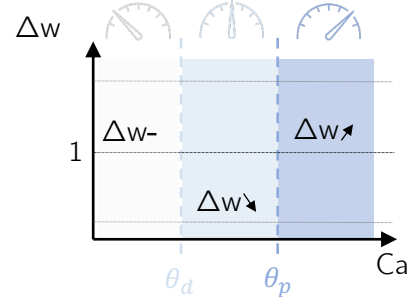


Figure 3.4: **Model 2:** Two thresholds-calcium dependency rule. The synaptic rule induces no changes for  $[Ca] < \theta_d$ , depression for  $[Ca] > \theta_d$  and  $[Ca] < \theta_p$ , and potentiation for  $[Ca] > \theta_p$ . Potentiation is faster than depression. Adapted from [Jacquerie et al., 2022].

Regarding calcium dynamics, while [Shouval et al., 2002] hypothesized that the dominant source of calcium influx to the postsynaptic cell is through NMDARs, [Graupner et al., 2016] have decided to implement the contribution of NMDARs (calcium influx mediated by a prespike, denoted by  $c_{pre}$ ) but also of VDCCs (calcium influx mediated by a postspike, denoted by  $c_{post}$ ). The differential equations derived are:

$$\begin{aligned} \dot{c}_{pre}(t) &= \frac{-c_{pre}}{\tau_{Ca}} + C_{pre} \sum_i \delta(t - t_{pre} - D) \\ \dot{c}_{post}(t) &= \frac{-c_{post}}{\tau_{Ca}} + C_{post} \sum_j \delta(t - t_{post}) \\ [Ca(t)] &= c_{pre}(t) + c_{post}(t) \end{aligned} \quad (3.7)$$

where  $C_{pre}$  (resp.  $C_{post}$ ) is the maximal calcium influx going into the postsynaptic spike from a presynaptic (resp. postsynaptic) spike,  $D$  is the slow rise time of the NMDAR-mediated calcium influx,  $t_{pre}$  (resp.  $t_{post}$ ) is the time at which a prespike (resp. postspike) occurs and  $\tau_{Ca}$  is the time-constant associated to the calcium decay in the neuron.

Mathematically, [Graupner et al., 2016] wrote the synaptic rule as follow:

$$\tau_w \dot{w} = \underbrace{\gamma_p(1-w)}_{\gamma_p^*} \Theta([Ca] - \theta_p) - \underbrace{\gamma_d w}_{\gamma_d^*} \Theta([Ca] - \theta_d) \quad (3.8)$$

where  $\tau_w$  is the time constant associated to synaptic change,  $\gamma_p$  (resp.  $\gamma_d$ ) is the potentiation (resp. depression) rate and  $\Theta([Ca] - \theta_p)$  means  $\Theta = 1$  if  $[Ca] > \theta_p$  otherwise  $\Theta = 0$ . This rule is seen as a *soft-bound* rule because the effective potentiation and depression rates ( $\gamma_p^*$  and  $\gamma_d^*$ ) are weight-dependent [Jacquerie et al., 2022]. In other words, it means that strong weights are more easily depressed than potentiated and weak weights have the opposite effect such that the extreme values are not reached. The parameters values can be found in Appendix section D.2.

Following [Shouval et al., 2002] Equation 3.1, an *hard-bound* equivalent definition of Equation 3.8 can also be constructed [Jacquerie et al., 2022] :

$$\tau_w \dot{w} = \frac{1}{2} \gamma_p \Theta([Ca] - \theta_p) - \frac{1}{2} \gamma_d \Theta([Ca] - \theta_d) \quad (3.9)$$

To avoid a physiologically impossible state where synaptic weights evolve linearly with time for a sustained level of calcium, it is important to bound this equation such that the weights can not exceed a maximal and minimal limit that are respectively set at 1 and 0 ( $w = 1$  if  $w \geq 1$  and  $w = 0$  if  $w \leq 0$ ).

### 3.3 Equivalence between the continuous-calcium dependency model and the two thresholds-calcium dependency model

#### 3.3.1 Construction of a model equivalent to model 2 written in the format of model 1

In their article, [Jacquerie et al., 2022] reshaped the rule of [Graupner et al., 2016] (**model 2**) into the standard form of a classical first-order differential equation formalism developed by [Shouval et al., 2002] (**model 1**) and therefore proved that, despite a different formulation, the behavior is equivalent. To do so, for each of the three calcium-dependent regions (low, intermediate, and high level of calcium) delimited by the depression and potentiation thresholds, they expressed a variable  $\tau_w^x$  and a variable  $\Omega^x$  (seen in **model 1**) in function of the variables  $\tau_w$ ,  $\gamma_p$  and  $\gamma_d$  (seen in **model 2**). Table 3.1 compares the different models and provides the parameters identification to reshape **model 2** into the formalism of **model 1** whose behavior is more straightforward to understand

(see Figure 3.5). All taken together, the evolution of synaptic strength in *soft-bound* model is described by the following global equation:

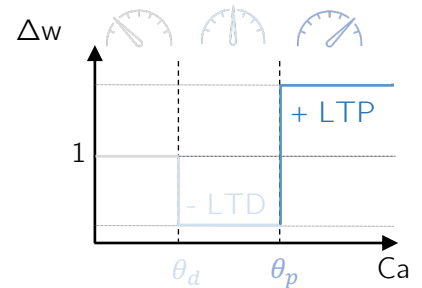


Figure 3.5: **Model 3:** Two thresholds-calcium dependency rule reshaped in a standard form of differential equation. Adapted from [Jacquerie et al., 2022].

$$\begin{aligned}
[Ca] < \theta_d & \tau_w^0 \dot{w} = \Omega^0 - w \\
[Ca] \in [\theta_d, \theta_p] & \tau_w^d \dot{w} = \Omega^d - w \\
[Ca] > \theta_p & \tau_w^p \dot{w} = \Omega^p - w
\end{aligned} \tag{3.10}$$

This model is named **model 3** in this thesis for clarity and is the one that is used in further analysis. The parameters values can be found in Appendix section D.3.

As for **model 1** and **model 2**, an *hard-bound* formalism can be derived. Starting from Equation 3.10, removing the weight dependency gives:

$$\begin{aligned}
[Ca] < \theta_d & \tau_w^0 \dot{w} = \Omega^0 \\
[Ca] \in [\theta_d, \theta_p] & \tau_w^d \dot{w} = \Omega^d \\
[Ca] > \theta_p & \tau_w^p \dot{w} = \Omega^p
\end{aligned} \tag{3.11}$$

To avoid a physiologically impossible state where synaptic weights evolve linearly with time for a sustained level of calcium, it is important to bound this equation such that the weights can not exceed a maximal and minimal limit that are respectively set at 1 and 0 ( $w = 1$  if  $w \geq 1$  and  $w = 0$  if  $w \leq 0$ ).

Table 3.2 summarizes how the removal of the dependency on the weight affects the previous parameters identification. Interestingly, Equation 3.10 can be transformed in a continuous sigmoid shape matching even more closely the implementation made in [Shouval et al., 2002]. This is done by fitting the frequency pairing protocol (see subsection 3.3.2) in a way that reproduces the continuous sigmoid shape and finds the different parameters of Equation 3.6 and Equation 3.4. This yields a continuous implementation of the evolution of the synaptic strength as done in **model 1** (section 3.1) and the parameters values are in Appendix section D.1.

Model 1	Calcium ranges	Model 2	Standard form	Equivalence
$\tau_w([Ca])\dot{w} = \Omega([Ca]) - w$	$[Ca] < \theta_d$	$\tau_w \dot{w} = 0$	$\dot{w} = \frac{1}{\tau_w^0}(\Omega^0 - w)$	$\tau_w^0 = 0, \Omega^0 = 0$
	$[Ca] \in [\theta_d, \theta_p]$	$\tau_w \dot{w} = -\gamma_d w$	$\dot{w} = \frac{1}{\tau_w^d}(\Omega^d - w)$	$\tau_w^d = \frac{\tau_w}{\gamma_d}, \Omega^d = 0$
	$[Ca] > \theta_p$	$\tau_w \dot{w} = \gamma_p(1 - w) - \gamma_d w$	$\dot{w} = \frac{1}{\tau_w^p}(\Omega^p - w)$	$\tau_w^p = \frac{\tau_w}{\gamma_d + \gamma_p}, \Omega^p = \frac{\gamma_p}{\gamma_d + \gamma_p}$

Table 3.1: Comparison of **model 1** and **model 2** equations and parameters equivalence for **model 3** in soft-bound weight dependency. Adapted from [Jacquerie et al., 2022]

Model 1	Calcium ranges	Model 2	Standard form	Equivalence
$\tau_w([Ca])\dot{w} = \Omega([Ca])$	$[Ca] < \theta_d$	$\tau_w \dot{w} = 0$	$\dot{w} = \frac{1}{\tau_w^0} \Omega^0$	$\tau_w^0 = 0, \Omega^0 = 0$
	$[Ca] \in [\theta_d, \theta_p]$	$\tau_w \dot{w} = -\frac{1}{2} \gamma_d$	$\dot{w} = \frac{1}{\tau_w^d} \Omega^d$	$\tau_w^d = \tau_w, \Omega^d = -\frac{1}{2} \gamma_d$
	$[Ca] > \theta_p$	$\tau_w \dot{w} = \frac{1}{2}(\gamma_p - \gamma_d)$	$\dot{w} = \frac{1}{\tau_w^p} \Omega^p$	$\tau_w^p = \tau_w, \Omega^p = \frac{1}{2}(\gamma_p - \gamma_d)$

Table 3.2: Comparison of **model 1** and **model 2** equations and parameters equivalence for **model 3** in hard-bound weight dependency. Adapted from [Jacquerie et al., 2022]

### 3.3.2 Similarities between the models

[Jacquerie et al., 2022] demonstrated the similarities between the continuous-calcium dependency rule (**model 1**), the two thresholds-calcium dependency rule (**model 2**), and the two thresholds-calcium dependency rule reshaped in a standard form of differential equation (**model 3**) by reproducing the experimental data of [Sjöström et al., 2001] as it is done in [Graupner et al., 2016].

This plasticity induction protocol consists of 75 consecutive pairs of presynaptic and postsynaptic spikes with a delay of  $\Delta t = t_{post} - t_{pre} = 10\text{ms}$  or  $-10\text{ms}$  for pairing frequencies  $f$  ranging from  $0.1\text{Hz}$  to  $50\text{Hz}$ . The variable  $t_{post}$  (resp.  $t_{pre}$ ) represents the spike time of the postsynaptic cell (resp. presynaptic cell) (see Figure 3.6) [Jacquerie et al., 2022].

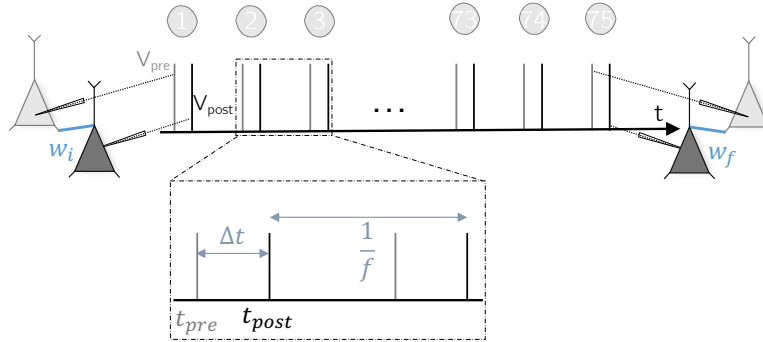


Figure 3.6: [Sjöström et al., 2001] plasticity induction protocol as it is done in [Graupner et al., 2016]. The pair of presynaptic (grey) and postsynaptic (black) is stimulated 75 times with a delay of  $\Delta t = t_{post} - t_{pre}$  between the prespike ( $V_{pre}$ ) and the postspike ( $V_{post}$ ) for different pairing frequencies  $f$ . The change in synaptic change after such protocol is computed as  $\Delta w = \frac{w_f}{w_i}$ .

The results obtained from such protocol is the frequency-response curve of synaptic plasticity :

- When the presynaptic neuron fires 10ms before the postsynaptic neuron ( $\Delta t = 10\text{ms}$ ), low pairing frequencies induce no changes in the synaptic strength while high pairing frequencies strengthen the synapse.
- When the presynaptic neuron fires 10ms after the postsynaptic neuron ( $\Delta t = -10\text{ms}$ ), low pairing frequencies induce depression in the synaptic strength while high pairing frequencies strengthen the synapse.

As it can be seen on Figure 3.7, all the models fit the experimental data provided by [Sjöström et al., 2001] confirming the validity of **model 2** during wakefulness and demonstrating the equivalence with **model 3**. By fitting wakefulness experimental data, this equivalence is very powerful because **model 2** is now translated into a formalism that is easier to interpret through the use of **model 3** while still conserving the definition of potentiation and depression thresholds.

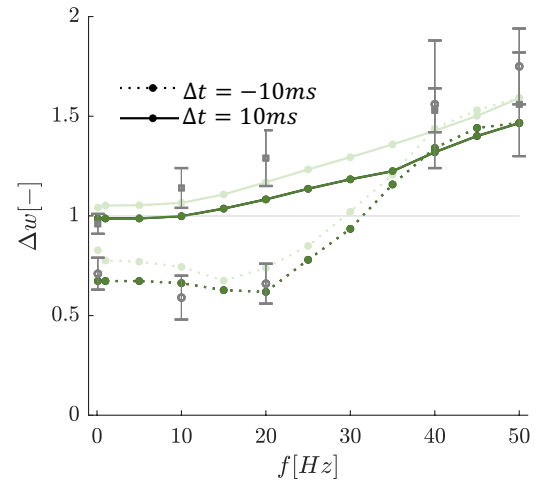


Figure 3.7: Frequency-response curve of synaptic plasticity. As shown in [Graupner et al., 2016], **model 2** (black) fit the experimental data of [Sjöström et al., 2001] (grey bars). The discrete (dark green) and continuous (light green) implementation of **model 3** also fit the experimental data.

### 3.4 Summary

## Calcium-based plasticity rules

**Model 1**

[Shouval et al., 2002]

$$\tau_w([Ca])\dot{w} = \Omega([Ca]) - w$$

**Model 2**

[Graupner et al., 2016]

$$\tau_w\dot{w} = \gamma_p(1-w)\Theta([Ca] - \theta_p) - \gamma_d w\Theta([Ca] - \theta_d)$$

Construction of a model equivalent to model 2 written in the format of model 1

[Jacquerie-Minne, 2022, in progress]

**Model 3**

$$[Ca] < \theta_d \quad \tau_w^0\dot{w} = \Omega^0 - w$$

$$[Ca] \in [\theta_d, \theta_p] \quad \tau_w^d\dot{w} = \Omega^d - w$$

$$[Ca] > \theta_p \quad \tau_w^p\dot{w} = \Omega^p - w$$

[Jacquerie-Minne, 2022, in progress]

Fitting model 3 on wakefulness experimental data

[Sjöström et al., 2001]

Fitting completed ✓

## Part II

# Neuromodulation of synaptic plasticity from a biological perspective

## Chapter 4

# Review of neuromodulators influence on synaptic plasticity and their activity during sleep

Through the diversity of their interactions, neuromodulators allow the modulation of many neuron-specific processes and they particularly play a role in the control of synaptic activity for many applications (*i.e.* addiction [Sun et al., 2005], neuropsychiatric disorders [Madadi Asl et al., 2018], reward circuit-related structure [Turlik et al., 2021], etc).

We wonder if, during sleep, neuromodulators could act as regulators of synaptic plasticity and affect the different cellular signaling cascades linked to it. Indeed, it is well-established that neuromodulators play a critical role in the transition from wake to sleep and therefore they could also be involved in the regulation of synaptic plasticity during sleep for memory consolidation. With this in mind, this chapter provides a global overview of the impact of a multitude of neuromodulators on cellular signaling cascades that are known to promote/inhibit LTP/LTD induction. For a multitude of neuromodulators regardless of the application and then focuses more specifically on their potential effect on memory consolidation during sleep. More specifically the role of acetylcholine, noradrenaline, serotonin, dopamine, histamine, and brain-derived neurotrophic factor are addressed.

Before focusing on a few particular neuromodulators, it is interesting to note that a general principle has been observed by some scientists: when a specific neuromodulator associates with a G protein-coupled receptor, if this protein is of subtype  $G_s$ , then potentiation is more likely to be induced, whereas if this protein is of subtype  $G_{i/o}$  or  $G_q$ , then it is depression which is more likely to be induced [Foncelle et al., 2018, Salgado et al., 2012, Nadim and Bucher, 2014]. The simultaneous activation of  $G_q$  and  $G_s$  coupled receptors also negates their respective effects. [Salgado et al., 2012, Huang et al., 2012]

### 4.1 Acetylcholine

#### Biological mechanisms promoting/inhibiting LTP induction

In the hippocampus, researchers developed *in vivo* LTP induction stimulation protocols based on weak (not inducing LTP in control condition) and strong high-frequency stimulation (inducing LTP in control condition) termed subthreshold stimulation and suprathreshold stimulation respectively. They

found that after the stimulation of the medial septum, a major source of ACh in the hippocampus, the subthreshold stimulation-induced LTP and that this facilitation is  $M_1$ -dependent. These results suggest that the pre-conditioning medial septum tetanus reduced the threshold for LTP induction in a narrow time window [Ovsepien et al., 2004].

Still in the hippocampus, an *in vitro* study showed that a low concentration of carbachol, an acetylcholine receptors agonist (*i.e.*, chemical that activates a receptor to produce a biological response), enhanced LTP mediated by  $M_1$  receptors underlying physiological modulation of LTP by ACh in the hippocampus [Shinoo, 2005]. However, in both studies, no biological phenomena were particularly highlighted and both stated that additional studies were necessary to clarify the mechanisms of synaptic potentiation. A few years later, it was shown that activation of  $M_1$  receptors induces LTP during a pairing protocol where suprathreshold summation of EPSPs is avoided. This induction is mediated by the fact that mAChRs enhance NMDAR activation in a voltage-dependent manner by inhibiting **small conductance calcium-activated potassium (SK) channels**. In this specific case, the activation of the Protein kinase C (PKC) signaling pathway by the  $M_1$  receptors activation is responsible for the inhibition of **SK channels** (Figure 4.1A) [Buchanan et al., 2010].

### Biological mechanisms promoting/inhibiting LTD induction

In the hippocampus, a study tried to uncover the cellular mechanisms behind the LTD induction invoked by  $M_1$  receptors activation. They found that, in response to  $M_1$  receptor activation, new proteins mediating AMPA receptor endocytosis were synthesized and this rapid synthesis was presumably dependent on the mammalian Target Of Rapamycin (mTOR) and Extracellular-signal-Regulated Kinase (ERK) signaling pathways. On top of this, they demonstrated that cholinergic and glutamatergic  $G_q$ -coupled receptors both activate a protein synthesis-dependent LTD mechanism. Interestingly, mGluRs and mAChRs are coupled to the same G-protein suggesting that activation of mAChRs use the same molecular mechanisms as mGluR-dependent LTD explained in subsection 2.4.2 (Figure 4.1B.1) [Choi et al., 2005, Volk et al., 2007].

Interestingly, similar AMPAR endocytosis has been reported in other hippocampal studies. In one of them, they suggested that the molecular mechanisms relied on a  $Ca^{2+}$ -independent signaling cascade. mAChR activation would interfere with a **glutamate receptor interacting protein (GRIP)** that forms a complex with the **liprin- $\alpha$**  protein and the **leukocyte common antigen-related receptor (LAR)**. This interference results in the dephosphorylation of AMPAR by LAR, initiating AMPAR en-

#### SK channels mediated synaptic plasticity

SK channels on a hippocampal postsynaptic neuron are known to oppose AMPAR activity by quickly repolarizing the cell after its depolarization by AMPAR such that  $Mg^{+2}$  are not released and NMDA receptor currents are inhibited [Ngo-Anh et al., 2005]. Studies have even shown that knockdown of SK channels facilitates the induction of LTP while a reverse effect is induced by overexpressing SK channels, which proves the importance of these ion channels in synaptic plasticity [Buchanan et al., 2010]. CaM proteins bound to **SK channels** and sense intracellular calcium levels to gate the opening of the channel, when SK-bound CaM is phosphorylated by kinase CK2, the  $Ca^{2+}$  sensitivity of **SK channel** is reduced [Allen et al., 2007].

#### GRIP-liprin- $\alpha$ -LAR complex

LAR is a membrane protein that is a member of the protein tyrosine phosphatase family. GRIP binds to the liprin- $\alpha$  family of proteins that interact with LAR receptor protein tyrosine phosphatases (LAR-RPTPs) and are implicated in synapse development. Interfering with the GRIP-liprin interaction is known to disrupt AMPAR trafficking in the neuron and induce LTD [Wyszynski et al., 2002].



docytosis (Figure 4.1B.2) [Dickinson et al., 2009].

Internalization of NMDAR is also expressed by  $M_1$ -dependent hippocampal LTD. In the hypothesis of the study, under normal conditions, hippocalcin, a neuronal calcium sensor protein, is bound to the postsynaptic density protein 95 (PSD-95), and the latter forms a complex with NMDAR. The activation of  $M_1$  receptors trigger the phosphoinositide pathway resulting in IP3-mediated  $Ca^{2+}$  release from intracellular stores. This increase in calcium is sensed by hippocalcin which in turn moves towards the plasma membrane, and by an unknown mechanism, the PSD-95 dissociates from the NMDAR enabling a transport molecule to bind to the NMDAR and trigger endocytosis (Figure 4.1B.3) [Jo et al., 2010].

In the cortex, [Seol et al., 2007] pointed out that receptors impacting intracellular PLC cascades, such as  $M_1$  receptors, trigger LTD by presumably impacting the phosphorylation status of AMPARs. The activation of PLC results therefore in the phosphorylation of the GluR1 AMPARs subunit at a specific site, tagging the synapse for LTD (Figure 4.1B.4). This is interesting because, in the hippocampus, the same signaling cascade involving PLC rather drives LTP induction (Figure 4.1A).

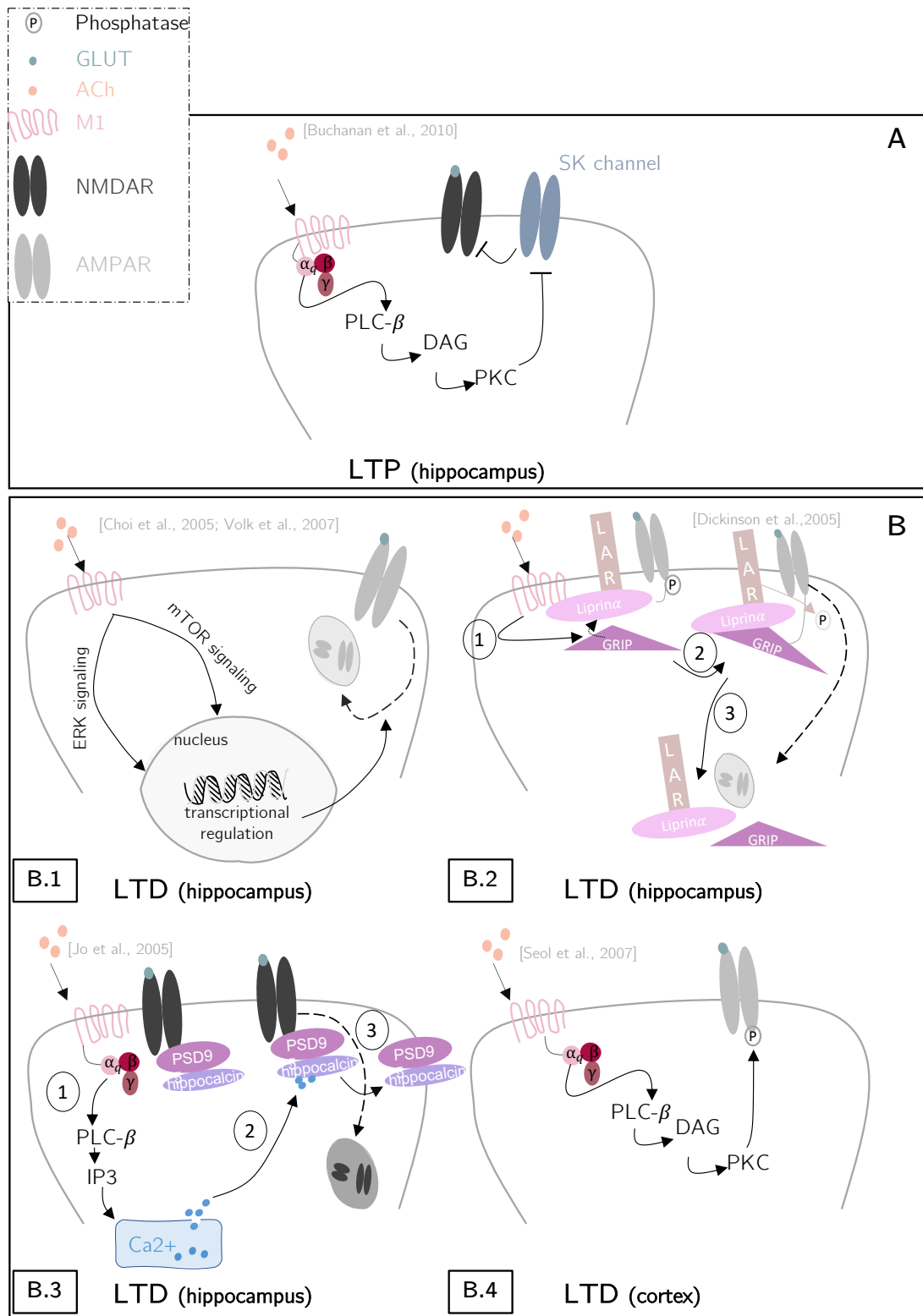


Figure 4.1: *Biological mechanisms promoting/inhibiting acetylcholine-dependent LTP/LTD induction.* **A.** Acetylcholine promotes LTP via  $M_1$  activation and is expressed by disinhibition of NMDARs via the inhibition of SK channel that otherwise inhibit NMDARs. **B.** Acetylcholine promotes LTD via  $M_1$  activation and is expressed by endocytosis of AMPARs (**B.1**;**B.2**) and NMDARs (**B.3**) and phosphorylation of AMPARs (**B.4**).

## During sleep

It is well established that wake and REM sleep are characterized by high levels of acetylcholine while during NREM sleep the levels remain low (Figure 4.2A) [Marrosu et al., 1995]. What is not yet fully understood is whether this neuromodulator has an effect on memory consolidation during these sleep phases and if so, what are the biological mechanisms underlying this.

It was previously shown that PKA signaling pathway and NMDAR activity are key players in memory consolidation [Reyes-Resina et al., 2021, Aton et al., 2009]. As PKA activation is affected by AC activation, this signaling pathway might be related to the receptors NMDA and the subsequent change in calcium concentration known to influence AC activity. Muscarinic acetylcholine receptors might also play a role in this phenomenon during REM sleep [Graves, 2001]. Indeed, although typically  $M_1$  and  $M_4$  receptors are coupled to  $G_q$  and  $G_s$  proteins respectively, it has been shown that activation of these receptors sometimes result in cAMP synthesis [Taussig et al., 1993]. In his review, [Graves, 2001] mentions three different explanations for this phenomenon (Figure 4.2B):

- The considered muscarinic receptor is a  $G_s$ -coupled protein receptor and therefore activates AC [Dittman et al., 1994].
- The considered muscarinic receptor is not necessarily coupled to a  $G_s$  protein but rather to either  $G_{i/o}$  or  $G_q$  protein and AC activation is mediated by the other subunits,  $\beta \gamma$  [Taussig et al., 1993].
- The considered muscarinic receptor is a  $G_q$ -coupled protein receptor and is, therefore, able to increase intracellular calcium from intracellular stores mediated by PLC activation [Choi et al., 1992].

Once activated, PKA could be responsible for the expression of genes involved in memory consolidation during sleep [Reyes-Resina et al., 2021, Graves, 2001]. These studies however do not precise if the expressed genes are either related to long-term potentiation or long-term depression.

Acetylcholine is also involved in the modulation of some cerebral rhythms that occur during sleep (Figure 4.2C) [Huerta and Lisman, 1995, Vandecasteele et al., 2014]. These rhythms in turn imply information encoding processes [Langille, 2019]. In the hippocampus, it was shown that cholinergic stimulation promotes hippocampal REM theta oscillations [Vandecasteele et al., 2014], whose peaks are thought to be involved in potentiation processes and troughs in forgetting processes [Langille, 2019]. On the contrary, the same stimulation is responsible for the suppression of Sharp-Wave Ripples (SWRs) [Vandecasteele et al., 2014] that are believed to be associated with the memory trace replay phenomenon [Atherton et al., 2015, Reyes-Resina et al., 2021, Langille, 2019]. These replays, according to the Active Systems Consolidation Hypothesis (ASCHY) (see chapter 6), tag synapses for further consolidation processes (and preservation of downscaling) [Diekelmann and Born, 2010]. However, in line with the Synaptic Homeostasis Hypothesis (SHY) (see chapter 6) [Tononi and Cirelli, 2006, Tononi and Cirelli, 2014], other studies suggest that ripples are involved in the down-regulation of synapses [Norimoto et al., 2018]. The role of brain oscillations on memory consolidation and the subsequent implication of acetylcholine in the latter remain, up to date, very unclear.

It is suspected that during wake activity some neurons are primed for further consolidation during sleep. This process would rely on transcriptional changes depending on the **cAMP-response element-binding protein (CREB)** to increase cell excitability [Lisman et al., 2018]. This priming process allows the re-activation of these neurons during sleep and facilitates re-induction of **Immediate Early Genes (IEGs)** expression during subsequent REM sleep, impacting the synaptic plasticity [Reyes-Resina et al., 2021]. Indeed, IEGs expression is known to be increased during wakefulness and studies also showed that during REM sleep phase, IEGs are expressed in some specific regions [Calais et al., 2015, Renouard et al., 2018, Reyes-Resina et al., 2021]. The IEGs expression during wakefulness and REM sleep may be related to the increase in acetylcholine levels in these two states.

**cAMP-response element-binding protein (CREB)**

CREB is a transcription factor. In this context, neuronal activity triggers intracellular signaling cascades resulting in the phosphorylation of CREB and activating subsequent gene expression [Delghandi et al., 2005].

**Immediate early genes (IEGs)**

IEGs are genes that are rapidly activated during neuronal activity without the need for de novo protein synthesis to activate them [Sheng and Greenberg, 1990, Okuno, 2011]. Among these, *arc*, *homer1a*, *c-fos*, or *egr1/zif268* are associated with synaptic plasticity [Gallo et al., 2018].

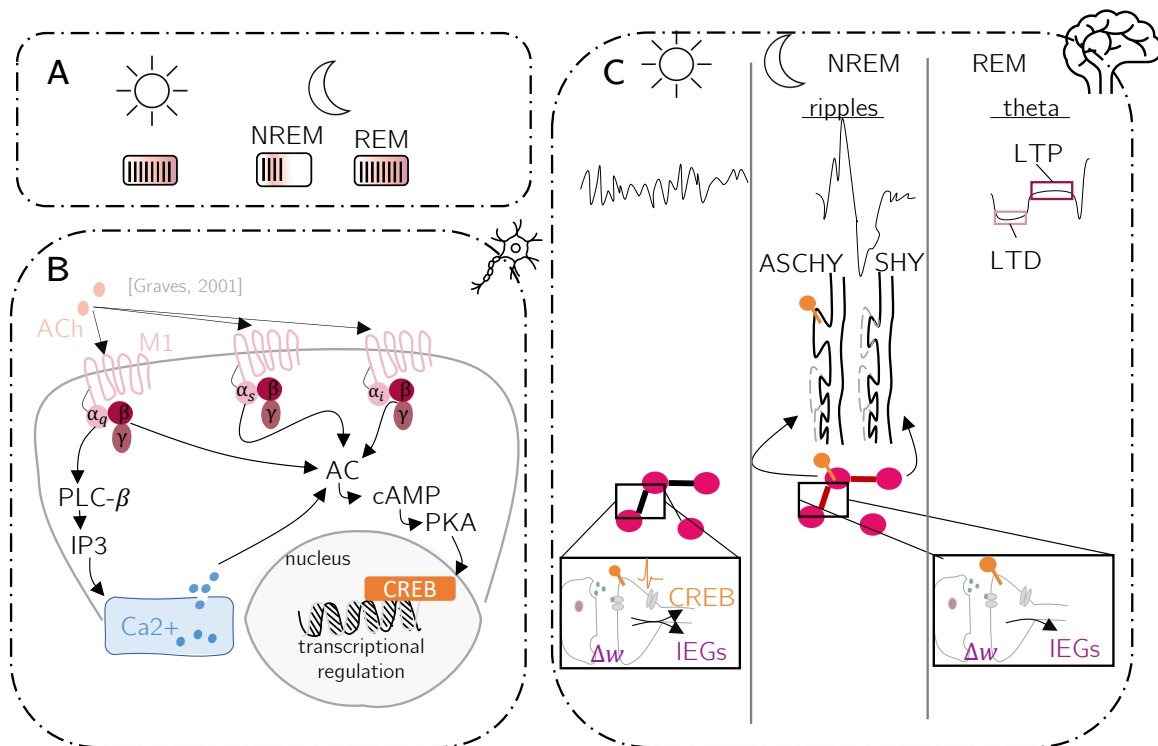


Figure 4.2: *Effects of acetylcholine during sleep.* **A.** Acetylcholine level is high during wakefulness and REM sleep and low during NREM. **B.**  $M_1$  activation triggers the cAMP/PKA pathway resulting in synaptic changes during sleep (the polarity is not specified by the paper). **C.** During wakefulness, neurons connect and change their connectivity ( $\Delta w$ ) by immediate early gene expression (IEGs, purple). There is also a change in excitability through CREB activation (orange). This tags synapses for further replay. Replays occur during NREM sleep ripples leading to possible different consolidation hypotheses (ASCHY in which synapses that are replayed are preserved from downscaling (orange pin) or SHY with global downscaling of synapses). Following the replay, in REM sleep, IEGs are expressed in specific synapses for consolidation. During REM, theta peaks facilitate LTP and theta troughs facilitate LTD.

## 4.2 Noradrenaline

### Biological mechanisms promoting/inhibiting LTP induction

The facilitation of LTP is mediated by the activation of  $\beta$  receptors that are coupled to protein  $G_s$  [Trevino and Kirkwood, 2008]. In the hippocampus, several cellular mechanisms come into play for this phenomenon, among these are found mechanisms that depend or not on the synthesis of protein. The induction of LTP is presumably mostly mediated by ERK and PKA signaling cascades [O'Dell et al., 2010]. Possible scenarios in which PKA activation is involved in LTP enhancement is one involving the reduced expression of SK channels on the cell surface (Figure 4.3A.1) [Ren et al., 2006]. Indeed, it has been shown on dorsal root ganglion neurons (in the spinal cord) that noradrenaline promotes CK2 phosphorylation of SK-associated CaM [Maingret et al., 2008], therefore inhibiting SK channels that otherwise act to hyperpolarize postsynaptic spines and inhibit NMDAR opening. This noradrenaline-mediated inhibition possibly promotes LTP induction and this process was already observed in the

hippocampus with acetylcholine (Figure 4.1A). Similar results are observed for other voltage-gated potassium channel subtypes such as Kv1.1, and Kv4.2 [Palacios-Filardo and Mellor, 2019, Liu et al., 2017]. Another possible mechanism is the phosphorylation of NMDAR and AMPAR (Figure 4.3A.2) [Lee, 2006]. ERK and mTOR pathways are mostly involved in complex translational upregulation (Figure 4.3A.3) [Kelleher et al., 2004].

In [Seol et al., 2007] they observed that the application of the noradrenaline agonist isoproterenol enables the induction of LTP for greater time delays between pre- and postsynaptic spiking in the cortex. They suggested that, under normal conditions, the appropriate calcium elevation necessary to induce LTP mediated by AC and/or PLC activation is only met when the postsynaptic spike coincides with the peak of NMDAR activation around 10ms. On the other hand, when considering the direct activation of AC by neuromodulators through G proteins, LTP would be induced for a longer duration as it would not require this specific calcium-mediated activation of AC signaling pathways (Figure 4.3A.4) [Seol et al., 2007].

### Biological mechanisms promoting/inhibiting LTD induction

The facilitation of LTD is mediated by the activation of  $\alpha_1$  receptors that are coupled to protein  $G_q$  [Trevino and Kirkwood, 2008]. When  $\alpha_1$  receptors are activated in the hippocampus, an adequate level

#### Hebbian plasticity

In 1949, the neuroscientist Donald Hebb developed a theory on synaptic plasticity called Hebbian plasticity. He stated in his book; "*When an axon of cell A is near enough to excite a cell B and repeatedly or persistently takes part in firing it, some growth process or metabolic change takes place in one or both cells such that A's efficiency, as one of the cells firing B, is increased*" [Hebb, 1949].

#### Spike-Timing Dependent Plasticity (STDP)

STDP is a process highlighting the synaptic strength changes according to various time lag  $\Delta t$  between the presynaptic and postsynaptic spikes. In the hippocampus, in line with Hebb's postulate, LTP is induced when the presynaptic cell fires before the postsynaptic cell, and LTD is induced when the postsynaptic spike occurs before the presynaptic spike, resulting in the classical Hebbian STDP curve. It is important to note that, depending on the brain area considered, this curve can be of different shapes (anti-Hebbian, neo-Hebbian, etc.) [Song et al., 2000].

of calcium is reached to promote LTD. This calcium increase is thought to come from the  $\alpha_1$  receptor-mediated enhancement of NMDAR currents and/or from  $\alpha_1$  receptor-mediated release of intracellular  $Ca^{2+}$  from internal stores (Figure 4.3B.1) [Scheiderer et al., 2004].

Moreover, depending on the level of noradrenaline, the neuromodulator binds to particular subtypes of adrenergic receptors with a varying affinity. While low levels of noradrenaline favor the activation of  $\alpha_1$  receptor, high levels co-activate  $\alpha_1$  receptor and  $\beta$  receptor [Salgado et al., 2012]. In their work, [Salgado et al., 2012] showed that in the cortex, low noradrenaline concentration enabled LTD via  $\alpha_1$  receptor activation while high noradrenaline concentration enabled the traditional **hebbian spike-timing dependent plasticity (STDP)** curve via the activation of both subtypes suggesting the existence of a synaptic plasticity push-pull mechanism (Figure 4.3B.2).

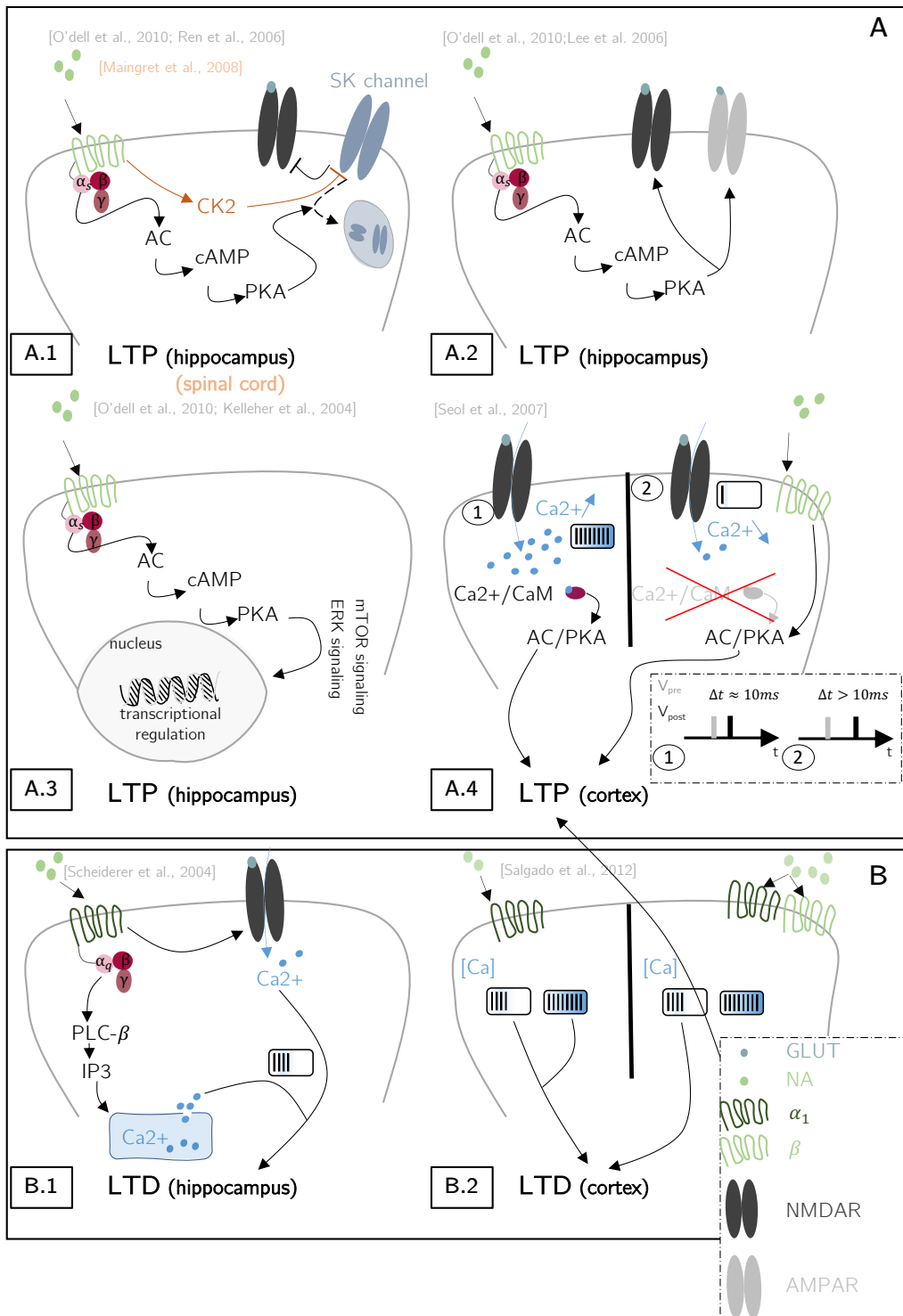


Figure 4.3: *Biological mechanisms promoting/inhibiting noradrenaline-dependent LTP/LTD induction.* **A.** Noradrenaline promotes LTP via  $\beta$  receptors and is expressed by desinhibition of NMDARs by SK channels due to their endocytosis (**A.1**), increase in NMDARs and AMPARs efficiency (**A.2**), transcriptional regulation of LTP-promoting proteins (**A.3**) and direct activation of PKA rather than NMDARs-mediated activation when the postsynaptic neuron spike more than 10ms after the presynaptic neuron (**A.4**). **B.** Noradrenaline promotes LTD via  $\alpha_1$  receptors activation and is expressed by increase in calcium concentration from NMDARs and internal stores to a level adequate for LTD (**B.1**). Low levels of noradrenaline promotes LTD via  $\alpha_1$  receptors activation over broad positive and negative delays (*i.e.* high and low levels of calcium) while co-activation of  $\alpha_1$  receptors and  $\beta$  receptors by high levels of NA promotes usual bidirectional plasticity (**B.2**).

## During sleep

Some hypotheses regarding memory consolidation suggest that IEGs drive plasticity through their expression patterns during the sleep-wake cycle [Reyes-Resina et al., 2021]. Among these, *homer1a* is expressed during waking activity and redistributed to the postsynaptic density upon sleep. At the synapse, *homer1a* binds to *mGluR<sub>1/5</sub>*, changes the conformity of these receptors, and activates a downstream cascade promoting AMPAR endocytosis and LTD. It has been demonstrated that noradrenaline plays a role in the process of targeting *homer1a* in the postsynaptic density (PSD) at the onset of sleep. A low level of NA increases *homer1a* PSD level, suggesting that *homer1a* transfer to the PSD is inhibited by a high level of noradrenaline during wake, preventing LTD, while a lower NA level during sleep allows *homer1a* redistribution to PSD and subsequent depression (Figure 4.4A) [Diering et al., 2017].

In 1981, some researchers postulated in a study that sleep was associated with a decline in noradrenaline levels [Aston-Jones and Bloom, 1981]. However, one study monitored that during NREM the average thalamic noradrenaline remained higher than during quiet wakefulness and this level fluctuates over 50s. Interestingly, it was also shown that sleep spindles cluster on a 50s timescale during NREM and that sleep-spindle variation across NREM requires noradrenergic signaling. While fluctuating according to the same time scale, noradrenaline level and sleep spindle clusters are anti-correlated (*i.e.*, the maxima of sleep spindle clusters occur around the minima of NA level) suggesting that noradrenaline coordinates sleep spindle clusters in a negative manner (Figure 4.4B) [Osorio-Forero et al., 2021].

Combining the results from [Osorio-Forero et al., 2021] with the observation made by [Langille, 2019] and [Diering et al., 2017] and the fact that SWRs are believed to be associated with the memory trace replay phenomenon is very interesting. Indeed, [Langille, 2019] postulated that while slow oscillations in the cortex facilitate forgetting of memories, coupling sleep spindles with slow oscillations and sharp waves ripples improve memory in the brain [Langille, 2019]. Therefore, during NREM, fluctuation of high levels of noradrenaline would generate sleep spindles that would couple to slow oscillations and SWRs in replayed neurons (*i.e.*, neurons that were highly activated during previous wakefulness) and this coupling enables an increase in synaptic strength in these network of neurons. In this case, LTD could be inhibited by the blockage of the translocation of *homer1a* from translation sites to the PSD due to high levels of noradrenaline. In the subsequent REM sleep, low levels of noradrenaline might drive global downscaling such that at the end of an NREM-REM cycle, strong synapses are preserved (Figure 4.4B).



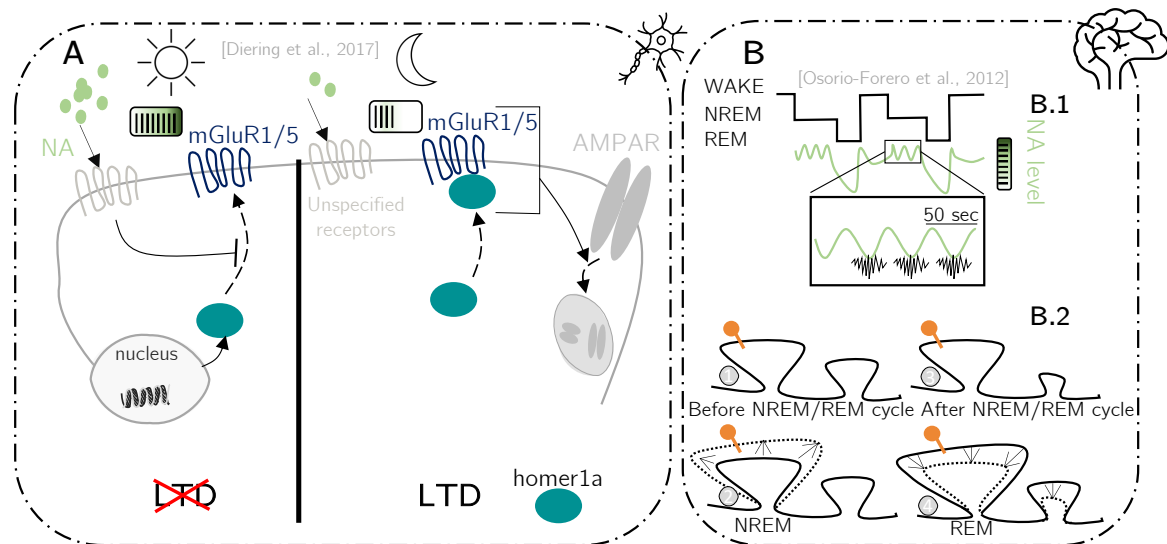


Figure 4.4: *Effects of noradrenaline during sleep.* **A.** Noradrenaline is high during wakefulness preventing homer1a (blue-green circle) (that has been expressed) to form a complex with mGluRs. Lower levels of NA during sleep enable homer1a to bind to mGluRs inducing AMPARs endocytosis and LTD. **B.** At the brain level, NA is higher during NREM than during quiet wakefulness and REM. Noradrenaline levels during NREM and sleep spindles clusters fluctuate over 50s in an anti-correlated manner (**B.1**). Combination of the results from [Osorio-Forero et al., 2021], [Langille, 2019] and [Diering et al., 2017] in a NREM-REM cycle: 1) synapses that were highly active during wakefulness are tagged for replay (orange pin). 2) During NREM, high levels of NA prevent LTD and associated sleep spindles and SWRs facilitate LTP in replayed tagged synapses. 3) During REM, low levels of noradrenaline promote global downscaling for all synapses. 4) This results in an unchanged tagged synapse after one NREM-REM cycle (**B.2**).

### 4.3 Serotonin

#### Biological mechanisms promoting/inhibiting LTP induction

In the hippocampus, serotonin inhibits LTP via different mechanisms:

- LTP is inhibited predominantly by exogenous application of serotonin activating  $5HT_4$  receptors (and to some extent by  $5HT_{1A}$  activation, which is a sub-type of  $5HT_A$  receptor). This modulation is dose-dependent in the range of micrograms (Figure 4.5A.2) [Kulla and Manahan-Vaughan, 2002].
- Using exogenous serotonin in the range of micrograms, [Corradetti et al., 1992] observed a blockage of hippocampal LTP by activation of  $5HT_{1A}$  and  $5HT_3$  receptors. They suggested that, by acting on  $5HT_3$ , serotonin reinforces the inhibition of pyramidal cells activity (hyperpolarization via  $5HT_{1A}$  activation) by increasing the activity of GABAergic interneurons, therefore, blocking LTP. This effect is dependent on the protocol used for LTP induction (Figure 4.5A.1) [Corradetti et al., 1992]. One year later, researchers found that 5HT modulation of LTP was frequency-dependent such that blockage of LTP was not induced by low-frequency stimulation. Moreover, they blocked GABAergic transmission to test the hypothesis of [Corradetti et al., 1992] but found that the inhibitory effect of 5HT was still present suggesting that this hypothesis was incorrect and that serotonin might rather act directly on pyramidal neuron synapses through  $5HT_{1A}$  activation (Figure 4.5A.2) [Villani and Johnston, 1993].

- Another study confirmed [Corradetti et al., 1992] observations and further showed that the inhibitory effect of serotonin on LTP was dose-dependent. They demonstrated that the biological mechanisms relied on the inhibition (even the suppression) of NMDA currents by serotonin (Figure 4.5A.2) [Staubli and Otaky, 1994].

Conversely to the above results, at excitatory hippocampal synapses, it was shown that endogenous serotonin leads to synaptic potentiation mediated by the activation of  $5HT_4$  (Figure 4.5A.2) [Teixeira et al., 2018]. [Mlinar et al., 2015] also demonstrated that when considering endogenous serotonin in the hippocampal region, LTP was not impaired at excitatory synapses. This study explained the discrepancy between inhibition or enhancement of LTP by the fact that endogenous 5HT is released at an appropriate concentration (*i.e.*, nanomolar) for  $5HT_{1B}$  receptors (sub-type of  $5HT_B$  receptor) activation while exogenous 5HT applied at high concentration (*i.e.*, micromolar) results in an unequal activation of  $5HT_{1A}$  receptors responsible for LTP inhibition [Mlinar et al., 2015]. In another study conducted in the hippocampus, researchers observed an increase in phosphorylated GSK3 $\beta$  after  $5HT_{1A}$  stimulation, resulting in the inactivation of GSK3 $\beta$  [Polter et al., 2012]. These results are interesting as inhibition of GSK3 $\beta$  results in the induction of LTP [Duda et al., 2020].

#### glycogen synthase kinase 3 $\beta$ (GSK3 $\beta$ )

GSK3 $\beta$  is a kinase regulated by the PI3K-Akt pathway. PI3K phosphorylates (and activates) Akt which in turn phosphorylates (and deactivates) GSK3 $\beta$  [Hermida et al., 2017]. GSK3 $\beta$  has a role in synaptic plasticity, its activated form promotes LTD and its non-active form promotes LTP [Duda et al., 2020]. Moreover, it has been shown that LTP inhibits LTD in the hippocampus via regulation of GSK3 $\beta$  [Peineau et al., 2007].

In the cortex, the same inhibitory effect of serotonin on LTP has been observed. Rats that underwent a depletion of 5HT showed an augmented magnitude of LTP compared to control conditions [Ohashi et al., 2003]. The molecular mechanisms behind this inhibition involve NMDA currents inhibition by  $5HT_{1A}$  receptors activation as this process was observed in other studies (Figure 4.5A.3) [Edagawa et al., 1999].

In other brain areas, LTP was induced upon serotonergic receptors activation. In the mammalian sympathetic ganglia, the activation of  $5HT_3$  receptors, which are known to induce a large  $Ca^{2+}$  influx upon activation, induces LTP by possibly triggering a signaling cascade dependent on calcium influx and CaMKII but independent of NMDAR (Figure 4.5A.4) [Alkadhi, 2021]. It has also been shown that 5HT is involved in long-term potentiation expressed by translational upregulation in the amygdala where stimulation of  $5HT_4$  receptors triggered PKA and MAPK pathways activation (Figure 4.5A.4) [Turner et al., 2007].

### Biological mechanisms promoting/inhibiting LTD induction

In the cortex, [Meunier et al., 2017a] observed opposite results in comparison to the study carried out by [Polter et al., 2012] in the hippocampus. By acting on  $5HT_{1A}$  receptors, serotonin activates GSK3 $\beta$  (via dephosphorylation) and therefore induces LTD resulting in AMPAR internalization [Meunier et al., 2017a, Hsiung et al., 2008]. Furthermore, still in the cortex, it has been shown that  $5HT_{1A}$  activation decreases the efficiency of AMPARs by inhibiting CaMKII activity. This decrease in CaMKII activity is regulated by the inhibition of AC/cAMP activity [Blitzer et al., 1998] triggered by  $5HT_{1A}$  activation [Perez-García and Meneses, 2008]. This could in turn regulates synaptic plasticity

by constraining the intracellular calcium level to the level required for LTD [Cai et al., 2002]. These results are consistent with a previous study showing a decrease in neuronal excitability as well as inhibition of sodium currents by triggering the PKC pathway following activation of  $5HT_{2A/C}$  receptors [Carr et al., 2002] (Figure 4.5B).

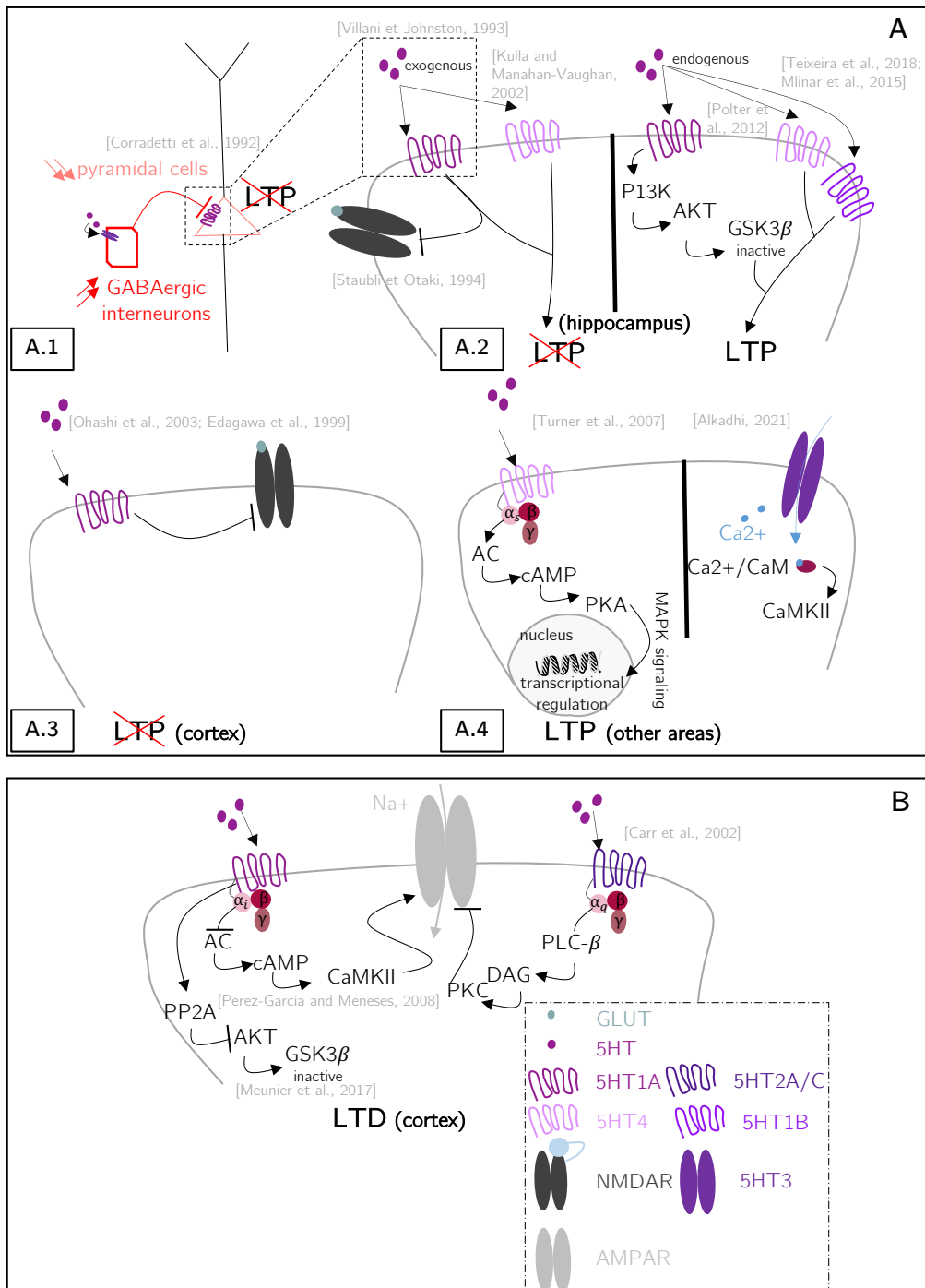


Figure 4.5: *Biological mechanisms promoting/inhibiting serotonin-dependent LTP/LTD induction.* **A.** Serotonin activates 5HT<sub>3</sub> receptors located on the membrane of GABAergic inhibitory neurons. Therefore, by stimulating GABAergic neurons that have inhibitory projections on pyramidal cells, 5HT inhibits indirectly LTP in pyramidal cells (**A.1**). Locally on pyramidal cells, exogenous serotonin inhibits LTP by acting on 5HT<sub>1A</sub> and/or 5HT<sub>4</sub> receptors and is expressed by NMDARs inhibition (**A.2 left; A.3**). Endogenous serotonin enhances LTP by acting on 5HT<sub>1A</sub>, 5HT<sub>4</sub> and/or 5HT<sub>1B</sub> expressed by, for example, transcriptional regulation (**A.2, right; A.4, left**). Serotonin activates 5HT<sub>3</sub> receptors located on the membrane of mammalian sympathetic ganglia neurons. **B.** Serotonin favors LTD expressed by AMPARs inhibition by acting on 5HT<sub>1A</sub> and 5HT<sub>2A/C</sub> receptors.

## During sleep

Levels of serotonin in the hippocampus follow a wake-sleep cycle where the maximal peak is reached during the active wake state and the lowest levels are during REM sleep (Figure 4.6A) [Park et al., 1999]. Due to the emerging evidence of 5HT role in synaptic plasticity, it is tempting to speculate its possible role in memory consolidation through this level fluctuation during sleep. For example,  $5HT_{1A}$  decreases AC activity [Bevilaqua et al., 1997] and a study suggested that the low level of serotonin during REM sleep in the hippocampal area is related to the disinhibition of AC activity and the subsequent activation of PKA involved in gene transcription mechanisms for synaptic plasticity changes [Meunier et al., 2017b] (Figure 4.6C). The serotonergic effects on learning and memory are wide-ranging and quite complex, making it difficult to study their impact during sleep.

Theta rhythm is a prominent characteristic of REM sleep and serotonin has been revealed to be a key player in the modulation of this rhythm (Figure 4.6B) via  $5HT_{2C}$  receptors (Figure 4.6C) [Sörman et al., 2011]. As explained above, the activation of this receptor promotes LTD induction such that serotonin might be involved in the general synaptic strength downscaling process occurring during NREM and/or REM sleep [Born and Feld, 2012].

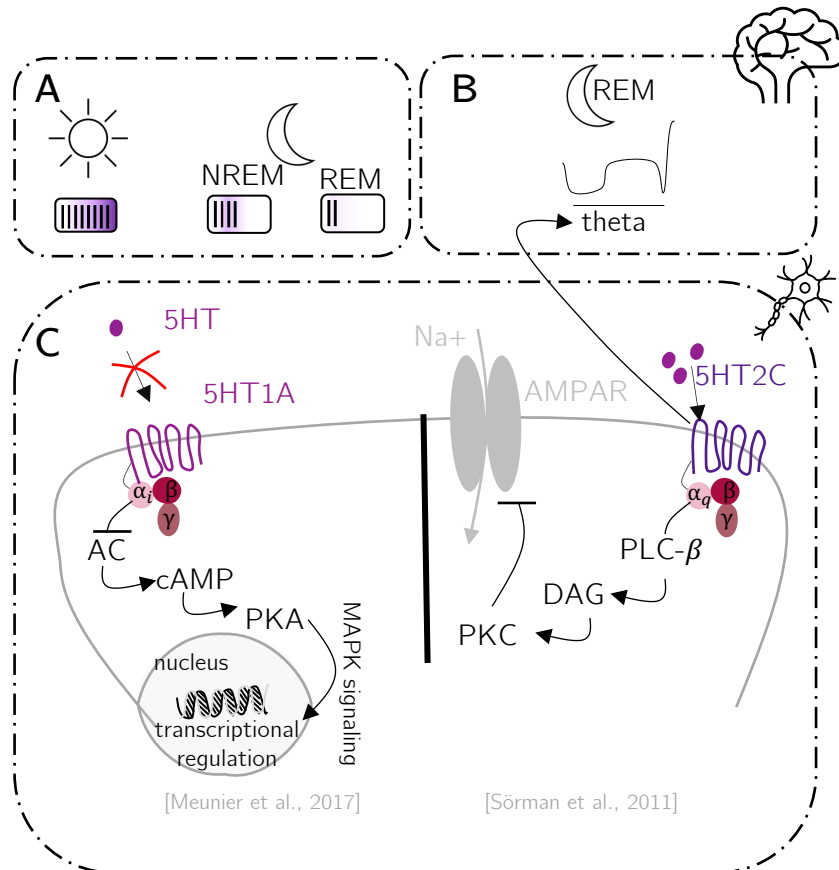


Figure 4.6: *Effects of serotonin during sleep.* **A.** Serotonin is high during wakefulness, lowers during NREM sleep, and reaches its minimum during REM sleep. **B.** At the brain level, REM hippocampal theta rhythms are modulated by serotonin acting on  $5HT_{2C}$  receptors. **C.** At the cellular level, due to low levels of NA during sleep,  $5HT_{1A}$  is not activated and therefore AC activity is disinhibited such that there is no transcriptional regulation and no LTP.  $5HT_{2C}$  receptors are thought to be involved in AMPARs inhibition and LTD facilitation during sleep.

## 4.4 Dopamine

### Biological mechanisms promoting/inhibiting LTP induction

By binding to  $D_1$ -like receptors, dopamine is thought to convert depression into potentiation by reducing the threshold for LTP induction in the hippocampus.  $D_1$  receptors are coupled to  $G_s$  proteins involved in the activation of adenylyl cyclase. This results in the activation of PKA signaling pathway reversing the dephosphorylation of AMPARs usually occurring in LTD-induction protocol. In LTP conditions,  $D_1$ R activation yields a stronger potentiation effect due to the stimulation of AC and subsequent enhancement activation of PKA signaling cascade that triggers AMPA receptors exocytosis (Figure 4.8A.1) [Brzosko et al., 2019]. The same results are shown in other studies where  $D_1$  activation facilitates LTP in an NMDAR-dependent manner. In this case, inhibition of NMDA currents by dopamine is observed. These results seem controversial knowing that NMDARs control calcium influx and that a medium level of calcium favors LTD while high levels favor LTP. However, dopamine likely acts on another signaling cascade mediated by NMDA receptors (because NMDAR currents are inhibited but NMDARs are necessary for the reversal of LTD to LTP) (Figure 4.8A.1) [Zhang et al., 2009].

In the cortex,  $D_1$  receptors activation also mediates the enhancement of synaptic potentiation. This phenomenon implies the facilitation of AMPA receptors exocytosis dependent on the PKA signaling pathway and requires that  $D_1$  receptors are stimulated after NMDA receptors stimulation [Sun et al., 2005]. Along the same lines,  $D_1$  receptor-mediated PKA activation mediates translational changes required for long-term synaptic changes (Figure 4.8A.2) [Huang et al., 2004]. Interestingly, [Otani et al., 2003] discovered that, in cortex slice conditions (*i.e.*, *in-vitro*), a tetani protocol induces LTD when dopamine is present in the cell medium. In this case, the LTD induction mechanism is NMDA receptor-independent and depends on mGluRs activation (Figure 4.8B.2) (the biological mechanism is described in the next section). However, they observed that if the medium is exposed to dopamine prior ( $\sim 30$ min) to this same dopamine-tetani coupling protocol (*i.e.* two dopamine bathing mediums), this induces LTP. These results suggest that some cellular processes changing the plasticity polarity are triggered by the first application of dopamine. The first application of dopamine would change the properties of the cell enabling LTP facilitation dependent on NMDARs and  $D_1$  receptor-mediated PKA activation (Figure 4.8B.1) [Otani et al., 2003]. See Figure 4.7 for visualization of the experiment.

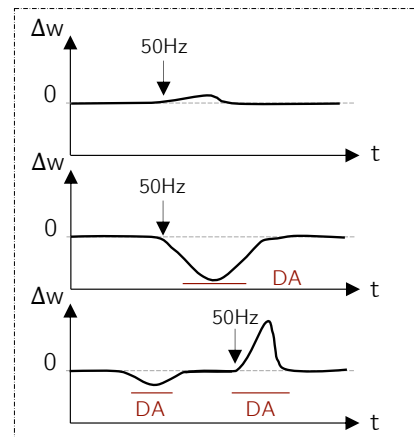


Figure 4.7: [Otani et al., 2003]' experiment: one dopamine bath followed by a 50Hz stimulation results in a negative change in synaptic plasticity ( $\Delta w < 0$ ) while two dopamine baths followed by a 50Hz stimulation results in a positive synaptic change ( $\Delta w > 0$ ).

### Biological mechanisms promoting/inhibiting LTD induction

Besides facilitating LTP,  $D_1$  receptor activation, under certain conditions, promotes LTD in the cortex. Once again, this facilitation is thought to be dependent on the PKA signaling pathway [Huang et al., 2004] and also on the co-activation of the mGluRs [Otani et al., 2003]. It is suggested

that mGluRs activation increases calcium from internal stores as well as activates PKC and MAPK signaling cascades while  $D_1$  receptors activate cAMP, PKA, and MAPK signaling (Figure 4.8B.2). In their work, [Meunier et al., 2017b] have found an alternative explanation for this  $D_1$ -mediated LTD induction. They observed an interaction between serotonin and dopamine to determine the polarity of the synaptic change. Mice lacking serotonin receptors exhibited a greater number of cells inducing LTD when activating  $D_1$  receptors compared to controlled mice. It could be that the co-activation of  $5HT_{1A}$  and  $D_1$  receptors generate enough calcium influx such that LTP is induced but  $D_1$  receptors activation rather results in calcium concentration adequate for LTD (Figure 4.8C.1) [Meunier et al., 2017b].

When dopamine binds to  $D_2$ -like receptors, LTD is preferentially induced. The molecular mechanisms behind this phenomenon are driven by multiple hypotheses. One of them is the activation of **glycogen synthase kinase 3 $\beta$**  (GSK3 $\beta$ ) by  $D_2$  receptors (Figure 4.8C.1) [Meunier et al., 2017b, Li et al., 2009]. Alternatively, activation of these dopamine  $G_{i/o}$ -coupled receptors (*i.e.*,  $D_2$ ,  $D_4$ ) in the cortex mediates the endocytosis of NMDAR by the inhibition of CaMKII by PP1 which is active due to the inhibition of cAMP/PKA signaling pathway (Figure 4.8C.2) [Meunier et al., 2017b, Wang et al., 2003]. However, results challenging this dependence on PKA inhibition have been reported. Indeed, findings indicating a diminishment of AMPA receptors at the membrane surface are reported but the injection of a PKA inhibitor did not replicate AMPA receptor endocytosis, suggesting that another mechanism is responsible for this phenomenon [Sun et al., 2005]. One of them could be the cooperation between the glutamate metabotropic receptors (mGluR) and  $D_2$  receptors which would result in the joint activation of MAPKs involved in new gene expression (Figure 4.8C.2) [Otani et al., 2003].

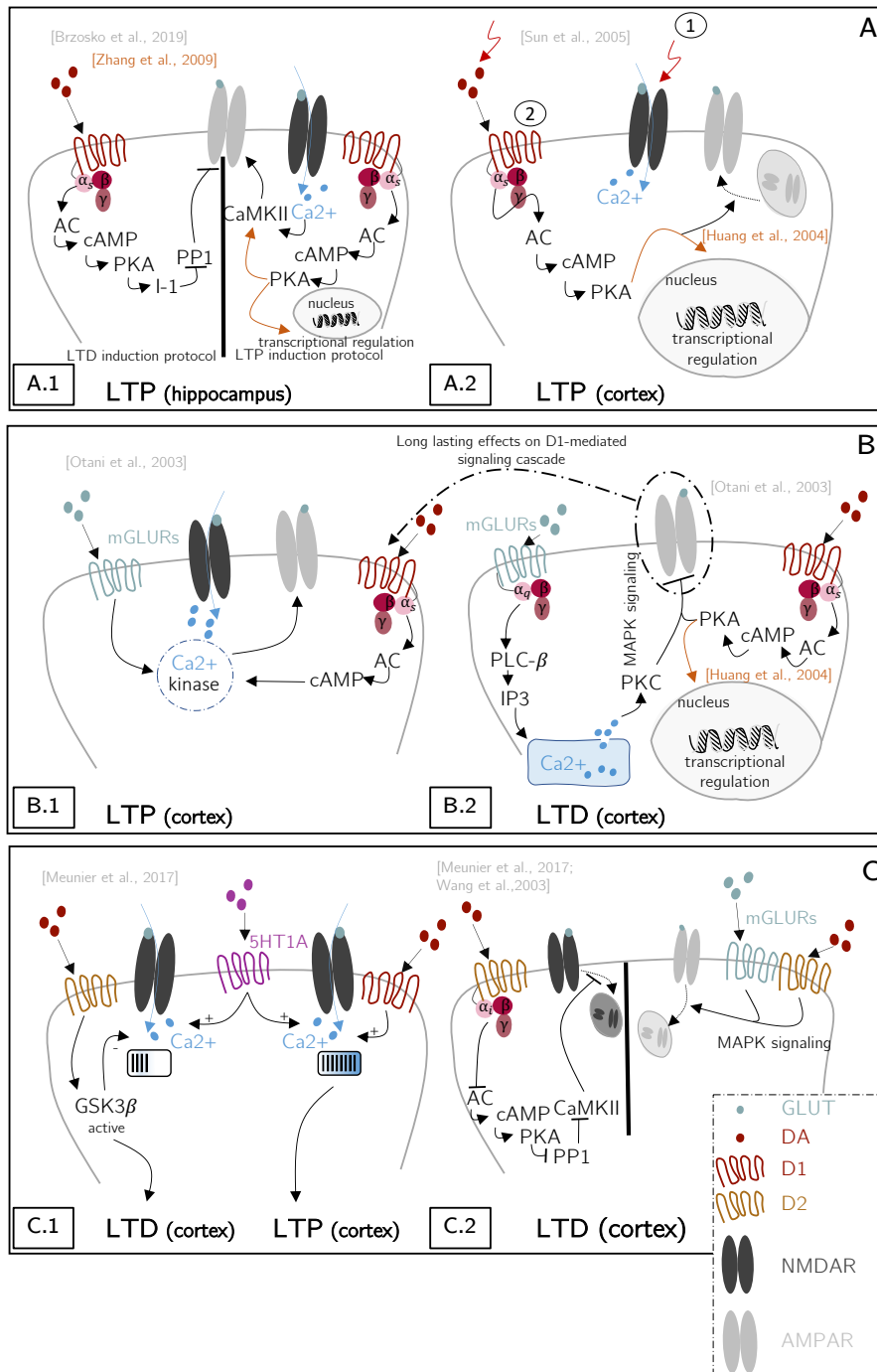


Figure 4.8: *Biological mechanisms promoting/inhibiting dopamine-dependent LTP/LTD induction.* **A.** Dopamine acting on  $D_1$  receptors mediates LTP expressed by desinhibition of AMPARs during a protocol usually triggering LTD without DA action. Co-activation of  $D_1$  receptors and NMDARs enhances LTP expressed by an increase in AMPARs efficiency (**A.1**), AMPARs exocytosis and transcriptional regulation (**A.2**). **B.** First application of DA mediates LTD by the co-activation of mGLURs and  $D_1$  receptors and is expressed by inhibition of AMPARs and transcriptional regulation (**B.2**). This also leads to long lasting effects on the  $D_1$ -mediated signaling cascade such that a second application of DA within 30min rather mediates LTP by the co-activation of mGLURs and  $D_1$  receptors. This is expressed by the enhancement of AMPARs (**B.1**). **C.** Co-activation of  $D_1$  receptors and  $5HT_{1A}$  receptors mediates LTP such that, without serotonin action,  $D_1$  receptors alone mediates LTD. Co-activation of  $D_2$  receptors and  $5HT_{1A}$  receptors mediates LTD. Serotonin favors LTD expressed by AMPARs inhibition by acting on  $5HT_{1A}$  and  $5HT_{2A/C}$  receptors (**C.1**). Activation of  $D_2$  receptors enables the endocytosis of NMDARs usually inhibited by CaMKII activity. Co-activation of mGluRs and  $D_2$  mediates LTD expressed by AMPARs endocytosis (**C.2**).



## During sleep

In the basal forebrain, a study was conducted regarding the effect of dopamine stimulation during wakefulness on synaptic plasticity during sleep in the presence of chronic stress [Radwan et al., 2019]. They suggested that the release of a high dose of DA during wakefulness resulted in the inhibition of adenosine 2A receptors ( $A_{2A}R$ ) during subsequent sleep (Figure 4.9B). However, the activation of this receptor is thought to induce SWS. Therefore, dopamine, by inhibiting  $A_{2A}R$ , suppresses SWS and disrupts the homeostatic downscaling suggested by SHY (Figure 4.9A) [Tononi and Cirelli, 2006, Tononi and Cirelli, 2014].

It has been shown that dopaminergic transmission has a contribution to REM sleep regulation [Lima, 2013, Trampus et al., 1991]. More specifically, blockage of  $D_2$  receptors reduces or even suppresses REM sleep [Lima, 2008]. One study, therefore, asked whether "*the effects of dopamine on learning could be mediated by REM sleep*" [França et al., 2015]. They found that  $D_2$  dopaminergic transmission blockage impairs hippocampal calcium signaling after training by possibly the disinhibition of AC activity. First, decreased level in phosphorylated CaMKII was observed 3h after training, zif-268 levels were reduced after 6h, and BDNF levels after 12h. This suggests that dopamine regulated a calcium-dependent signaling cascade and that this regulation connects sleep and learning (Figure 4.9B) [França et al., 2015].

Dopaminergic stimulation during spatial exploration and learning promotes SWRs in subsequent NREM sleep (Figure 4.9A) [McNamara et al., 2014, Moncada, 2017]. These SWRs, with other brain rhythms, are thought to play a role in the replay phenomenon and memory consolidation [Atherton et al., 2015, Reyes-Resina et al., 2021, Langille, 2019]. Therefore, it is suggested that the consolidation process of memories depends on dopamine such that this neuromodulator tags wake-activated cells for further reactivation in SWRs during sleep [Atherton et al., 2015, Seibt and Frank, 2019, Gerstner et al., 2018].

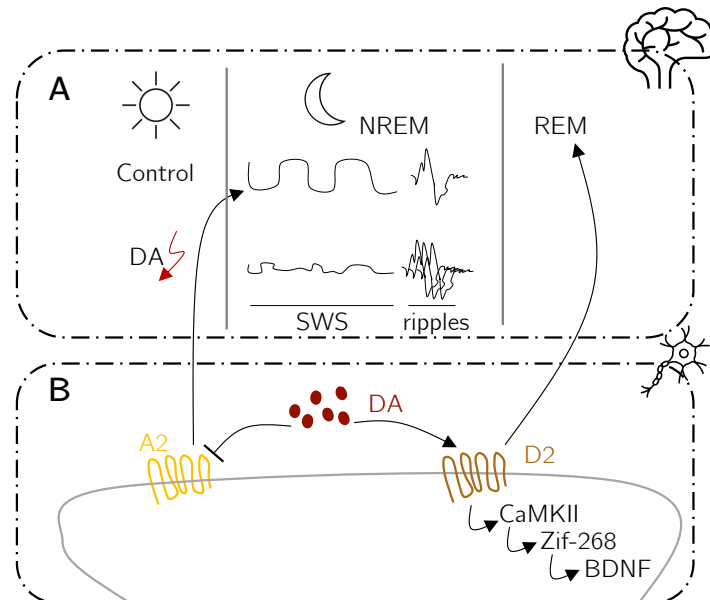


Figure 4.9: *Effects of dopamine during sleep.* **A.** At the brain level, dopamine stimulation during wakefulness leads to a decrease in slow waves sleep activity during NREM sleep and an increase in ripples. **B.** At the cellular level, slow waves sleep activity is reduced due to the inhibition of adenosine receptors  $A_2$  by dopamine.  $D_2$  activation is responsible for calcium-mediated signaling involving CaMKII, zif-268, and BDNF proteins responsible for the regulation of REM sleep.

## 4.5 Histamine

### Biological mechanisms promoting/inhibiting LTP induction

Memory performance is influenced by the activation of histamine  $H_1$  receptors [Chen et al., 1999]. In the hippocampus, various studies showed that mutated  $H_1$  receptors reduced LTP compared to normal conditions [Dai et al., 2007, Masuoka et al., 2019, Luo and Leung, 2010] and that histamine reduces the threshold for LTP induction of glutamatergic neurons [Gobetto et al., 2021]. Some researchers have therefore tried to understand the biological mechanisms behind this effect.

Some studies suggested that histamine  $H_1$  receptors activation influences the excitatory transmission by directly or indirectly modulating NMDAR activity in the hippocampus or in the cortex [Masuoka et al., 2008, Payne and Neuman, 1997, Rodriguez et al., 1997, Masuoka et al., 2019]:

- Histamine induces changes in the probability of glutamate release at the presynapse and therefore triggers a form of presynaptic long-term plasticity in the hippocampus (Figure 4.10A.1) [Rodriguez et al., 1997].
- Activation of  $H_1$  receptors at the membrane surface of astrocytes induces the release of D-serine which is a co-agonist of NMDARs. By binding to NMDARs, D-serine drives the facilitation of NMDAR-mediated excitatory postsynaptic currents and LTP in hippocampal CA1 neurons (Figure 4.10A.2) [Masuoka et al., 2019].
- In the cortex,  $H_1$  receptors activation facilitates the NMDA activity by possibly the activation of phospholipase C and action on the efficiency of NMDAR [Payne and Neuman, 1997].
- Histamine influences a binding site on NMDAR in a histamine receptor-independent manner such that cortical NDMA receptor currents are enhanced (Figure 4.10A.3) [Payne and Neuman, 1997].

In their work, [Dai et al., 2007] suggested that LTP facilitation by histamine receptors throughout the brain is somewhat mediated by the influence of the histaminergic neuron system on the cholinergic transmission, known to be involved in synaptic plasticity. While tuberomammillary nuclei (*i.e.*, region where HA is secreted) stimulation increased hippocampal cholinergic activity,  $H_3$  activation decreased the cholinergic tone in the cortex. In the amygdala, histaminergic compounds modulate cholinergic tone in a bimodal fashion (Figure 4.10C) [Passani and Blandina, 2004].

### Biological mechanisms promoting/inhibiting LTD induction

Fewer studies have been carried out to determine the possible effect of histamine on LTD. One of the few existing studies demonstrated that the application of histamine causes a pronounced and long-lasting depression in the striatum due to histamine  $H_3$  receptors activation. Data suggested that histamine depresses synaptic transmission by a presynaptic mechanism as the neuromodulator did not affect postsynaptic membrane properties of the neurons but still reduced EPSP amplitude such that histamine-mediated LTD occurred as a consequence of glutamate release inhibition (Figure 4.10B) [Doreulee et al., 2001]. The same decrease in cortico-striatal synaptic transmission was observed in other studies [Sergeeva et al., 2005] and thalamo-striatal synaptic transmission [Ellender et al., 2011].

In the dentate gyrus, which is part of the hippocampal formation, it has also been shown that histamine depresses synaptic transmission through activation of  $H_3$  by modulating the release of glutamate. Moreover, the results of the study indicated that the biological mechanisms behind this LTD do not rely on the signaling pathway activated by this  $G_{i/o}$ -coupled receptor [Brown and Reymann, 1996].

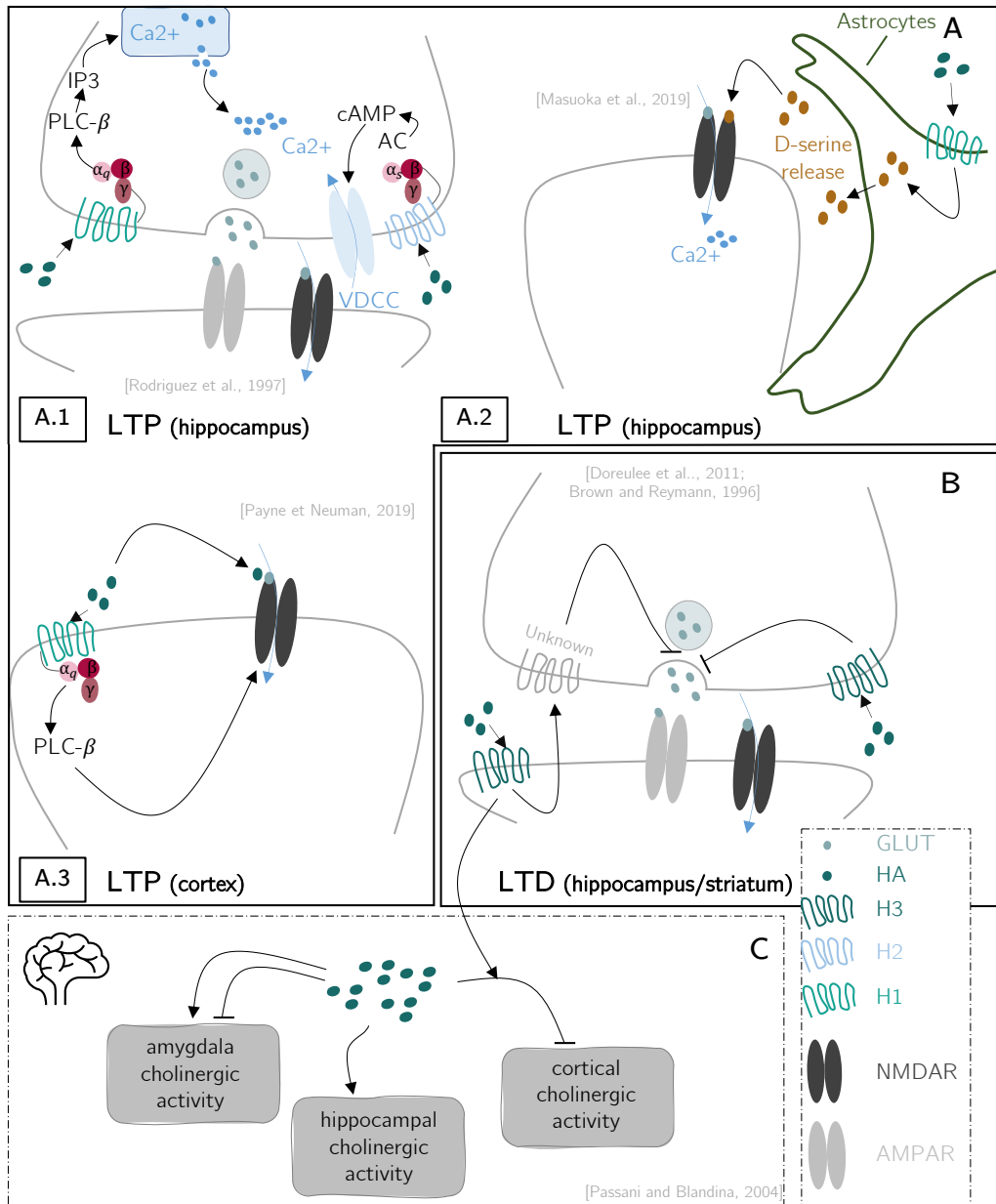


Figure 4.10: *Biological mechanisms promoting/inhibiting dopamine-dependent LTP/LTD induction.* **A.** Histamine leads to a presynaptic LTP induced presynaptically by acting on  $H_1$  and  $H_2$  receptors located on the presynaptic neuron (autocrine process) and this is expressed by the increase in neurotransmitters release (**A.1**). By acting on  $H_1$  located on astrocytes, histamine enhances the release of D-serine which, by binding to NMDARs, triggers LTP (**A.2**). Histamine drives LTP expressed by the enhancement of NMDARs activity either directly or indirectly by acting on  $H_1$  located on the postsynaptic neuron (**A.3**). **B.** Histamine leads to a presynaptic LTD induced presynaptically (resp. postsynaptically) by acting on  $H_3$  receptors located on the presynaptic neuron (resp. postsynaptic neuron) and this is expressed by inhibition of neurotransmitters release. **C.** At the brain level, histamine inhibits (resp. enhances) cortical (resp. hippocampal) cholinergic activity. Histamine modulates amygdala cholinergic activity in a bimodal fashion.

## During sleep

Histaminergic activity is high during wakefulness and almost inactive during sleep (Figure 4.11A) [Lin et al., 1988, Reiner and McGeer, 1987, Steininger et al., 1999, Takahashi et al., 2006]. Histamine is a wake-promoting substance and regulates the sleep-wake cycle [Lin et al., 2011]. However, little is known about its possible role in long-term memory processes during sleep.

In the hippocampus, blockage of histamine  $H_1$  receptors decreases hippocampal theta activity known to play a critical role in memory processes and this decrease is mediated by NMDA and AMPA receptors and  $H_1$  activation (Figure 4.11C) [Masuoka et al., 2008]. As hippocampal theta activity is a key feature of REM sleep, we suggest that histamine improves memory through the regulation of REM sleep.

Our literary research failed to provide detailed information on this topic. The only paper found is one that briefly discusses a theory suggesting that histamine indirectly controls memory consolidation processes during sleep by influencing acetylcholine release in the amygdala [Köhler et al., 2011]. Indeed, there is considerable scientific evidence supporting the theory that the amygdala plays an essential role in memory consolidation (Figure 4.11B) [McGaugh, 2002, Maren, 2001, LeDoux, 2000].

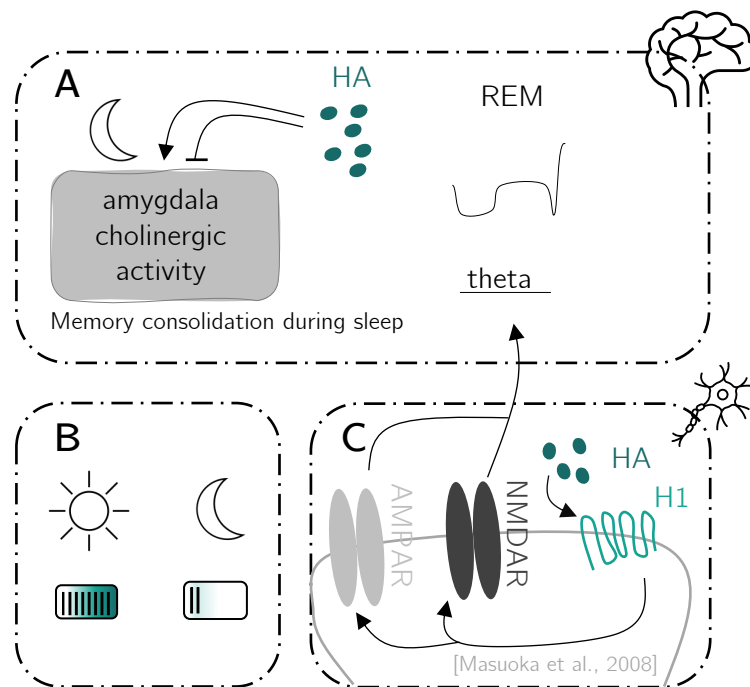


Figure 4.11: *Effects of histamine during sleep.* **A.** At the brain level, histamine is thought to regulate amygdala cholinergic activity in a bimodal fashion. This region is known to be a key player in memory consolidation during sleep and acetylcholine is also involved in LTP and LTD during sleep as seen previously. During REM sleep, histamine enhances hippocampal theta rhythms. **B.** Histamine is high during wakefulness and low during sleep. **C.** At the cellular level, theta rhythms are modulated by NMDARs and AMPARs which are enhanced by  $H_1$  activation.

## 4.6 Brain-Derived Neurotrophic Factor (BDNF)

### Biological mechanisms promoting/inhibiting LTP induction

A variety of studies outline how BDNF is involved in the facilitation of LTP in the cortex and hippocampus. Among them, some reveal discrepant mechanisms as a consequence of the different techniques used to induce LTP (See [Bramham and Messaoudi, 2005] for a further detailed review). It has been shown that BDNF can be released presynaptically and postsynaptically to modify synaptic plasticity [Zagrebelsky et al., 2020, Leal et al., 2017].

In the hippocampus, one of the BDNF-dependent presynaptic LTP mechanism that suggested involves both calcium influx from NMDARs and VDCC receptors. BDNF binds to TrkB receptors located on the membrane of the presynaptic neuron and triggers a signal enhancing the release of glutamate. Additionally, it binds to TrkB receptors located on the postsynaptic neuron and directly enhances NMDAR activity (Figure 4.13A.1) [Zakharenko et al., 2003]. In the cortex, it has been shown that cortical BDNF presynaptic release modifies the structure of neighboring dendrites. However, the study does not provide a molecular mechanism for this phenomenon (Figure 4.13A.3) [Horch and Katz, 2002].

For BDNF postsynaptic release, scientists revealed a signaling pathway responsible for LTP that involves the role of BDNF in the hippocampus. Activation of NMDARs and CaMKII leads to the release of BDNF from the postsynaptic neuron itself. In turn, by acting on its receptor TrkB, BDNF contributes to structural and functional changes (Figure 4.13A.2) [Harward et al., 2016]. Such a loop was already observed in previous studies investigating the maintenance of sensory neurons during development [Davies and Wright, 1995, Krüttgen et al., 1998]. Later on, [Bramham and Messaoudi, 2005] suggested "*The BDNF hypothesis of synaptic consolidation*" (Figure 4.13C) after an extensive analysis of multiple previous studies. In this hypothesis, NMDARs are activated upon stimulation and generate the postsynaptic release of BDNF. The subsequent activation of TrkB from BDNF release induces translation of CaMKII (that were stored in dendritic storage sites) as well as ERK-dependent CREB activation which in turn induces Arc gene expression in the soma. This Arc messenger ribonucleic acid (mRNA) is then targeted in dendritic local mRNA storage. Finally, BDNF acts as a synaptic tag by capturing Arc mRNA for further translation such that sustained synthesis of Arc drives synaptic consolidation [Bramham and Messaoudi, 2005, Seibt and Frank, 2019].

Interestingly, some results showed that, in the hippocampus, BDNF produces a vertical shift in the frequency-response curve of synaptic plasticity (described in subsection 3.3.2) such that depression was reduced with "low" tetanus (1Hz) usually triggering LTD and potentiation was increased with "mild" tetanus (30Hz) usually being suboptimal for LTP induction (Figure 4.12). Activation of the TrkB receptors and PLC protein by BDNF is thought to be the biological mechanism behind this enhancement of LTP [Ikegaya et al., 2002].

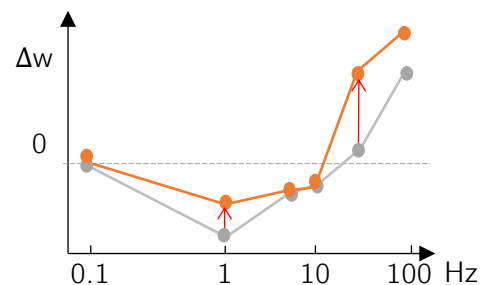


Figure 4.12: A vertical shift in the frequency-response curve of synaptic plasticity [Ikegaya et al., 2002]. Neurons are stimulated at 0.33, 1, 5, 10, 30, and 100Hz in control (grey) and BDNF (orange) conditions. Synaptic strength changes ( $\Delta w$ ) are recorded.

It has also been shown in other studies (which do not specify the source of BDNF release), that BDNF is implicated in AMPAR trafficking as well as AMPAR and NMDAR phosphorylation but the underlying mechanisms remain elusive in the cortex (Figure 4.13A.3) [Itami et al., 2003, Rutherford et al., 1998] and the hippocampus (Figure 4.13A.1) [Leal et al., 2017, Liao et al., 1999]. Meanwhile, another study investigated the role of cAMP as an effective regulator of BDNF-mediated synaptic plasticity in the hippocampus. They observed that cAMP was involved in the formation of spines (L-LTP) by acting on TrkB signaling but that cAMP was not affecting EPSPs (E-LTP) (Figure 4.13A.2) [Ji et al., 2005].

### **Biological mechanisms promoting/inhibiting LTD induction**

During neuronal development of the brainstem, it was shown that BDNF reduced (and even almost abolished) AMPAR currents via TrkB receptors activation in such a way that BDNF impairs synaptic transmission (Figure 4.13B) [Balkowiec et al., 2000].

Additionally, findings have shown that BDNF mostly facilitated LTD when it is in its precursor form, named BDNF pro-peptide or proBDNF. In this state, the binding of proBDNF requires a receptor complex formed by the p75 neurotrophin receptor (p75NTR) [Kojima and Mizui, 2017, Leal et al., 2017].

In the hippocampus, proBDNF was shown to act as a structural plasticity mediator. By an increase in the expression of p75NTR, proBDNF would take over BDNF-mediated LTP and LTD would rather be induced (Figure 4.13B) [Egashira et al., 2010]. Indeed, another study suggested that when TrkB receptors were blocked, pro-BDNF-p75NTR LTD was facilitated, whereas when p75NTR receptors were blocked, BDNF-TrkB LTP was facilitated. These results also support this dominance interaction between the two forms of BDNF-based plasticity [Sakuragi et al., 2013]. Moreover, [Mizui et al., 2015] found that, in the hippocampus, by acting on p75NTR, proBDNF induces AMPA receptors number decrease at the membrane and that this endocytosis requires the activation of NMDAR [Mizui et al., 2015]. This dependence on NMDAR had already been addressed by another study [Woo et al., 2005]. In addition to this molecular LTD marker, morphological and functional proBDNF-mediated LTD markers have also been observed such as reduced dendritic arborization and spine density, reduced hippocampal volume, and altered synaptic transmission. Some mechanisms by which proBDNF impairs hippocampal dendritic arborization, spine density, and synaptic transmission are discussed in the study but are beyond the scope of this review (Figure 4.13B) [Yang et al., 2014].

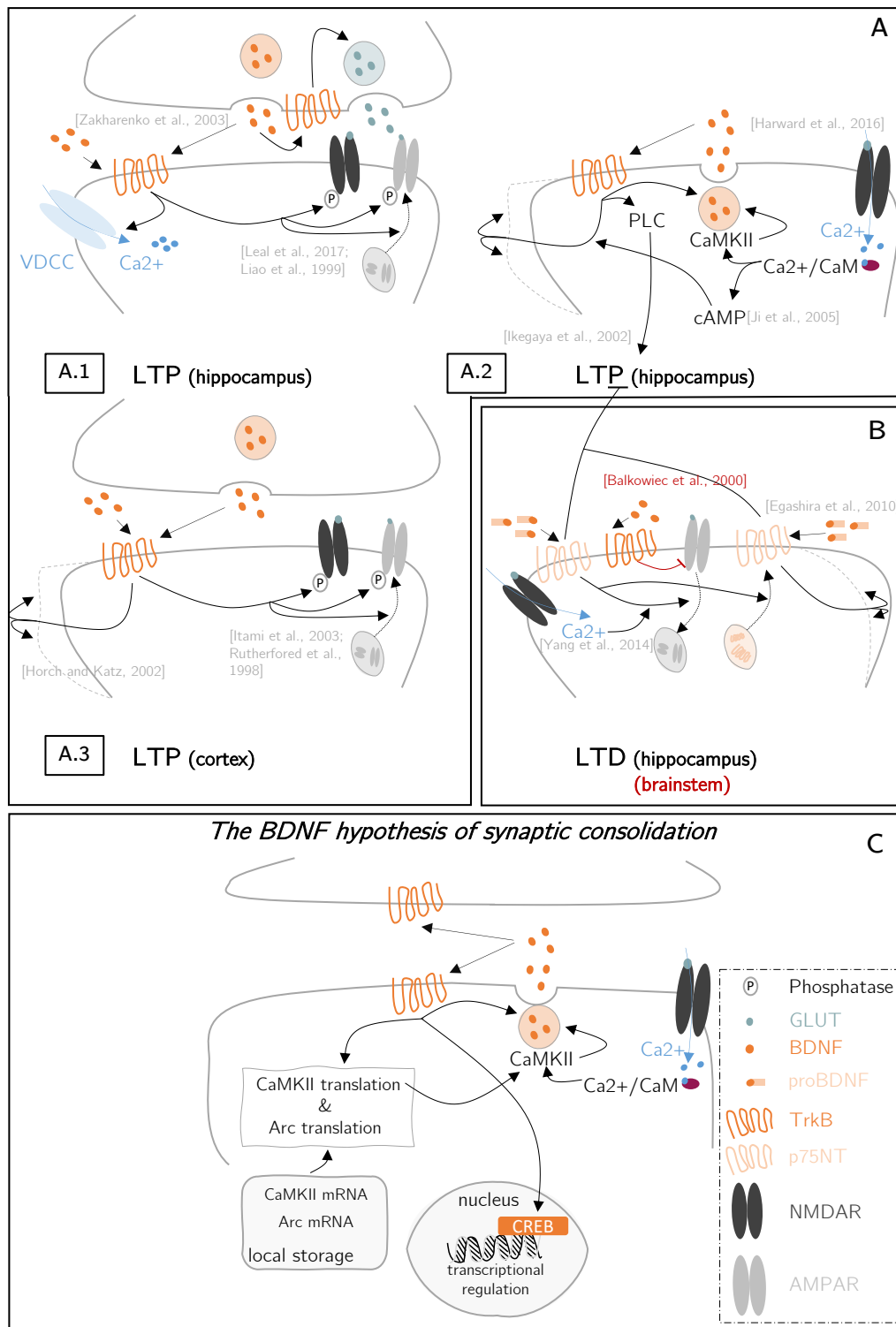


Figure 4.13: *Biological mechanisms promoting/inhibiting BDNF-dependent LTP/LTD induction.* **A.** When released presynaptically, BDNF drives LTP by acting on TrkB receptors located on the presynaptic neuron and enhances neurotransmitters release (autocrine presynaptic LTP) (**A.1**). By acting on TrkB receptors located on the postsynaptic neuron, histamine (regardless of the release source) drives LTP and enhances phosphorylation of NMDARs and AMPARs, exocytosis of AMPARs, (**A.1**; **A.3**) calcium influx from VDCC (**A.1**) and growth of dendritic spines (**A.3**). With the contribution of calcium influx from NMDARs, activation of postsynaptic TrkB receptors leads to BDNF release from the postsynaptic neuron itself and promotes LTP (**A.2**). **B.** With the contribution of calcium influx from NMDARs, activation of p75NTR by proBDNF leads to LTD expressed by the exocytosis of AMPARs. Activation of p75NTR leads to the endocytosis of more p75NTR such that proBDNF-mediated LTD takes the lead over BDNF-mediated LTP. TrkB activation in the brainstem drives LTD expressed by inhibition of AMPARs. **C.** According to the BDNF hypothesis of synaptic consolidation, TrkB receptor activation is responsible for the BDNF release from the postsynaptic neuron, for the transcriptional regulation of Arc, and translation of CaMKII and Arc from local dendritic storage.

## During sleep

It is challenging to determine a specific pattern characterizing BDNF levels throughout the day and night because fluctuations vary greatly between individuals [Cain et al., 2017]. However, one study was able to show an increase in BDNF mRNA throughout waking activity and a decrease of BDNF mRNA during sleep suggesting that the transcription occurs during wakefulness and translation during sleep [Faraguna et al., 2008, Cirelli and Tononi, 2000]. Another study showed that REM sleep was associated with the secretion of BDNF [Sei et al., 2000].

BDNF is a key player in learning capabilities. Indeed, many studies investigated the role of BDNF and levels of BDNF upon different learning tasks and some revealed that an increase in BDNF levels led to better learning abilities [Hall et al., 2000, Naimark et al., 2007, Klintsova et al., 2004, Sharma et al., 2021, Rattiner et al., 2005, Aarse et al., 2016]. Furthermore, [Gosselin et al., 2016] noticed that focus should be put on the polymorphism (*i.e.*, variant forms of a specific deoxyribonucleic acid (DNA) sequence that can occur among different individuals or populations) of BDNF. Indeed, while a longer period of sleep results in better learning for the BDNF Val66Val polymorphism, individuals carrying the BDNF Val66Met polymorphism show no change or even a decline in learning performance after a longer period of sleep. Along these lines, another study showed that slow-wave activities were higher in Val/Val compared to Val/Met genotype (Figure 4.14C) [Bachmann et al., 2012].

It is tempting to speculate on a memory consolidation mechanism according to the results shown by [Faraguna et al., 2008] and "*The BDNF hypothesis of synaptic consolidation*" which is proposed by [Bramham and Messaoudi, 2005]. During wakefulness, BDNF promotes synaptic potentiation by TrkB receptors activation and tags active synapses by capturing Arc mRNA for further translation (Figure 4.14B). Upon sleep, this tag would induce more slow-wave activity in neuronal networks that were already activated during the day (replay phenomenon) exempting them from synaptic downscaling (Figure 4.14A) [Bachmann et al., 2012].

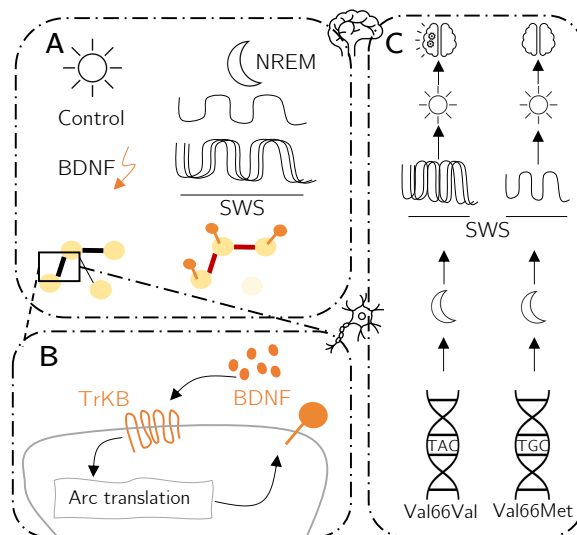


Figure 4.14: *BDNF during sleep*. **A**. At the brain level, BDNF stimulation during wakefulness increases slow waves sleep activity during NREM. **B**. At the cellular level, BDNF would tag activated synapses during wakefulness through Arc translation allowing replay of these neurons during following NREM sleep in turn enabling memory consolidation processes. **C**. BDNF Val66Val polymorphism increases slow waves activity and memory compared to BDNF Val66Met polymorphism.



## 4.7 Summary

Through our literature review, we demonstrated that the role of neuromodulators on synaptic plasticity is widely varied depending on the neuromodulator considered, the type of receptor it affects, the region of the brain, and the state of the neuron it interacts with. This makes a global conclusion of their actions quite difficult. Thus, it may be risky to further summarize this work, as it may cause readers to jump to conclusions.

Nevertheless, it is reasonable to conclude that they are capable of inhibiting and enhancing both LTD and LTP. This synaptic plasticity is expressed by changes in the probability of neurotransmitter release, efficacy and the number of AMPA/NMDA receptors on the membrane surface, and gene regulation. Moreover, some neuromodulators (acetylcholine, noradrenaline, BDNF) are also involved in the possible tagging process of specific synapses for their strengthening during sleep. Others (serotonin, dopamine, histamine, BDNF) are involved in the regulation of different sleep rhythms (slow-wave activity, spindles, ripples, theta rhythms), which in turn are considered to influence memory.

## Part III

# Computational Study

## Chapter 5

# Homeostatic reset: development of the analytical prediction

In their article, [Jacquerie et al., 2022] built a three-cells circuit able to switch from tonic to burst to represent a cortical network. A presynaptic neuron is connected to a postsynaptic neuron via excitatory AMPA connections and an inhibitory neuron is connected to the pre- and post- synaptic neurons through  $GABA_A$  and  $GABA_B$  connections (Figure 5.1A) (Appendix B and Appendix C). To mimic wakefulness cellular signatures, an external current is applied ( $I_{app}$ ) to the inhibitory cell such that the neuron exhibits a tonic activity, and pulse currents ( $I_{pre,post}$ ) are applied at a given frequency ( $f$ ) on both pre- and post- synaptic neurons with a certain delay between the prespike and the postspike ( $\Delta t$ ). To mimic sleep cellular signatures, the inhibitory cell is hyperpolarized by playing on the applied external current to reproduce the effect of neuromodulators in the neurobiology of sleep (subsection 2.3.2). The inhibitory cell switches from tonic to burst activity and pulls the other two cells into this rhythm as well (Figure 5.1B). The evolution of the synaptic strength is analyzed between the pre- and post-synaptic neurons using the synaptic plasticity rule described in subsection 3.3.1 (Figure 5.1C).

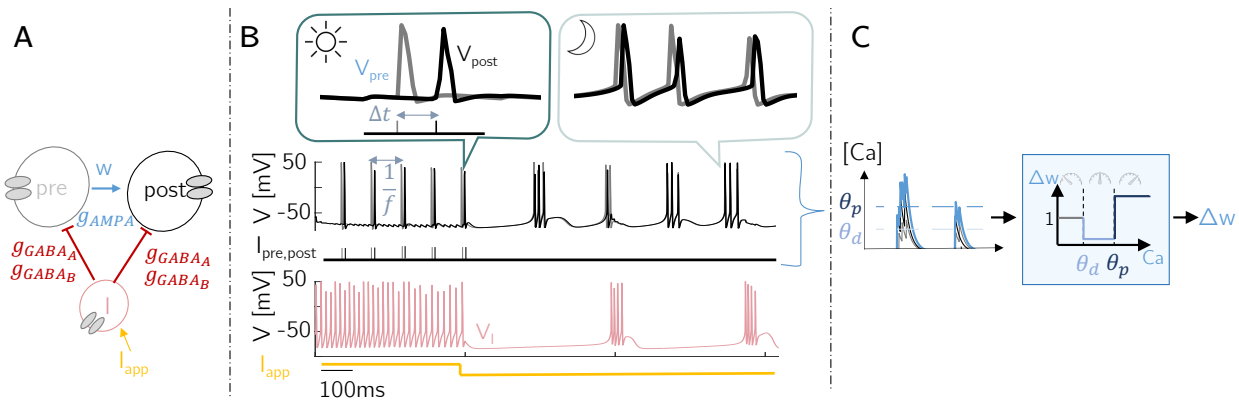


Figure 5.1: *Cortical network, neuron activity, and synaptic plasticity.* **A.** The presynaptic neuron (pre, grey) is connected to the postsynaptic neuron (post, black) via excitatory connections and the inhibitory neuron (I, pink) is connected to the pre- and post- synaptic neurons. **B.** During wakefulness, the inhibitory neuron fires at high frequency, and the pre- and post- synaptic neurons fire at a given frequency ( $f$ ) with a delay of  $\Delta t$ . During sleep, the inhibitory cell is hyperpolarized and pulls the network in a bursting activity. **C.** The evolution of the synaptic strength change ( $\Delta w$ ) is analyzed between the pre- and post- synaptic neurons according to the total calcium influx (dark blue trace) using the synaptic rule "model 3". Adapted from [Jacquerie et al., 2022].

During wakefulness, [Jacquerie et al., 2022] showed that this network was able to reproduce experimental data acquired in wakefulness by [Sjöström et al., 2001] regarding synaptic plasticity (as seen in subsection 3.3.2). However, when the network was switched to a bursting activity without any modification of the synaptic rule, they observed a phenomenon that they called the *homeostatic reset*. Meaning that, during the bursting activity, all synaptic weights  $w$  converge towards the same basal value whatever the initial weight at the beginning of the simulation (Figure 5.2).

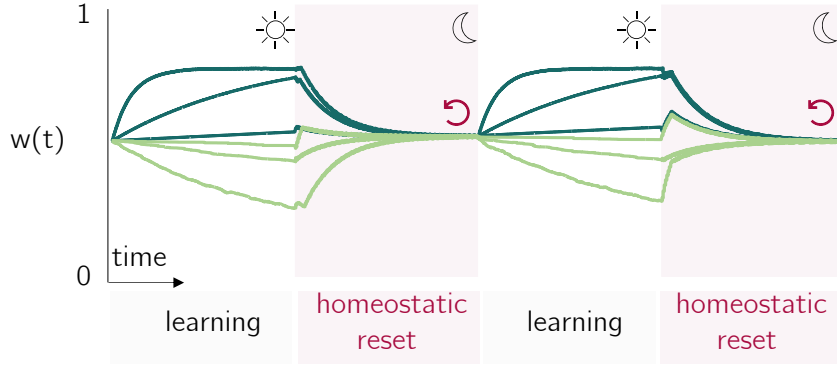


Figure 5.2: *Synaptic weight evolution during wake-sleep cycles.* During wakefulness, strongly (resp. weakly) correlated neurons (dark (resp. light) green) exhibit a strengthening (resp. weakening) of synaptic weight  $w$ . Upon sleep, all synaptic weights converge towards the same basal value whatever the initial weight at the beginning of the bursting activity associated with sleep. Adapted from [Jacquerie et al., 2022].

The goal of this chapter is to demonstrate analytically the intuitive explanation of this homeostatic reset given by [Jacquerie et al., 2022].

## 5.1 The explanation for *soft-based* models

Consider the calcium-based plasticity rule explained in subsection 3.3.1, the evolution of the synaptic strength is defined by a classical 1<sup>st</sup> ordinary differential equation  $\dot{w} = \frac{1}{\tau_w}(\Omega^x - w)$ . As already discussed in the section outlining the different calcium-based models, this mathematical expression describes the fact that  $w \rightarrow \Omega^x$  (see Equation 3.5). Thus, in the model that we consider,  $w$  tends towards  $\Omega^d$  when  $\theta_d < [\text{Ca}] < \theta_p$ , tends towards  $\Omega^p$  when  $[\text{Ca}] > \theta_p$  and remains the same when  $[\text{Ca}] < \theta_d$ . By wording the equation in this manner, [Jacquerie et al., 2022] could understand easily that when the calcium concentration is between the potentiation and depression thresholds, regardless of the initial strength of the synaptic weight,  $w$  converges to  $\Omega^d = 0$  and thus decreases. In the case where the calcium is above the potentiation threshold,  $w$  converges to  $\Omega^p = 0.8$ . Meaning that, if the initial strength of the synaptic weight is lower than  $\Omega^p$  (*i.e.*, 0.2) there is an increase of  $w$  but if the initial strength of the weight is higher (*i.e.*, 0.9), there is a decrease of  $w$ . Intuitively, this explains that, for a weak weight, [Jacquerie et al., 2022] observed potentiation while for a strong weight they observed depression. At the onset of the switch from tonic to burst, strong weights have a value  $w$  higher than  $\Omega^p$  leading to depression while weak weights have a value  $w$  lower than  $\Omega^p$  leading to potentiation in laps of time where the maximal calcium influx exceed the potentiation threshold (Figure 5.3B). After a long enough recording time, due to the calcium dynamics that maintain the same behavior throughout the bursting pattern, there is an equilibrium value  $w_{HR}$  between  $\Omega^d$  and  $\Omega^p$  towards which  $w$  stabilizes according to the fraction of time spent in depression ( $\alpha_d$ ) and the fraction of time spent in potentiation ( $\alpha_p$ ) (Figure 5.3A).

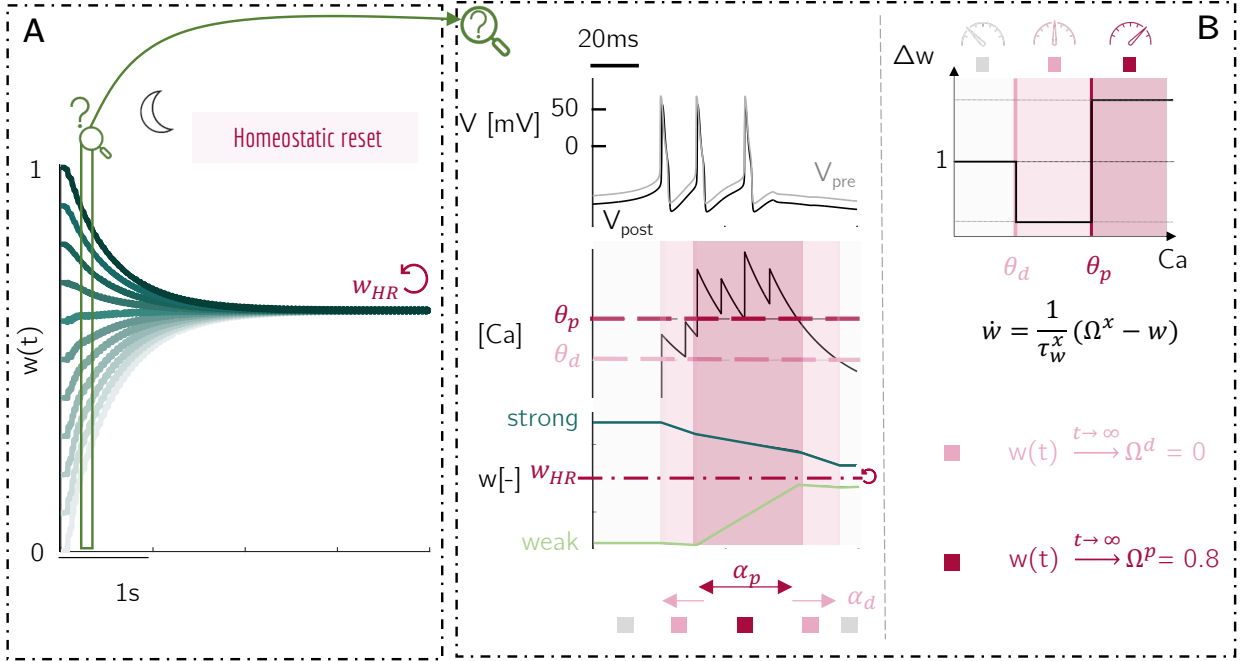


Figure 5.3: *Intuitive explanation of the homeostatic reset.* **A.** All weights converge towards  $w_{HR} \in [\Omega^d, \Omega^p]$ . **B.** The time evolution of weak (light green) and strong (dark green) synaptic weights is different despite the same total calcium trace. In the potentiation region (red), strong (resp. weak) weights decrease (resp. increase) due to their convergence towards  $\Omega^p = 0.8$ . The convergence towards  $\Omega^p$  is faster than the convergence towards  $\Omega^d$  (i.e.,  $\frac{1}{\tau_w^p} > \frac{1}{\tau_w^d}$ ). The equilibrium value  $w_{HR}$  depends on the fraction of time spent in depression ( $\alpha_d$ ) and the fraction of time spent in potentiation ( $\alpha_p$ ). Adapted from [Jacquerie et al., 2022].

### 5.1.1 Analytical demonstration of the convergence value

The convergence value of the synaptic strength depends on the bursting pattern and this value is approximated analytically.

First of all, the bursting pattern affects the fraction of time spent in the region where  $\theta_d < [Ca] < \theta_p$  which we denote  $\alpha_d$  and the fraction of time spent in the region where  $[Ca] > \theta_p$  denoted  $\alpha_p$ . Note that the time spent in the region where no change occurs is not taken into account.

Then, it must be remembered that the speed of convergence depends on the calcium concentration: it is faster for levels of calcium inducing potentiation than for levels of calcium inducing depression. Thus, for the same amount of time spent in depression and potentiation,  $w$  converges faster towards  $\Omega^p$  than towards  $\Omega^d$ . To take into account these discrepancies in convergence speed, it is necessary to normalize  $\alpha_d$  and  $\alpha_p$  and write instead  $\alpha_d^*$  and  $\alpha_p^*$  in our calculations:

$$\alpha_d^* = \frac{\alpha_d \tau_w^p}{\alpha_p \tau_w^d + \alpha_d \tau_w^p}$$

$$\alpha_p^* = \frac{\alpha_p \tau_w^d}{\alpha_p \tau_w^d + \alpha_d \tau_w^p}$$

Finally, to derive  $w_{HR}$ , the reasoning is to consider that the fraction of time spent in depression (resp. potentiation), is in fact the fraction of time where  $w$  does not converge towards  $\Omega^p$  (resp.  $\Omega^d$ ):

$$\begin{aligned}
w_{HR} &= \Omega^d - (\alpha_p^* \Omega^d) + \Omega^p - (\alpha_d^* \Omega^p) \\
&= \Omega^d \alpha_d^* + \Omega^p \alpha_p^* \\
&= \Omega^d \frac{\alpha_d \tau_w^p}{\alpha_p \tau_w^d + \alpha_d \tau_w^p} + \Omega^p \frac{\alpha_p \tau_w^d}{\alpha_p \tau_w^d + \alpha_d \tau_w^p}
\end{aligned} \tag{5.1}$$

It is important to note that Equation 5.1 is valid only after a recording time  $t_\infty$  long enough to reach the convergence of the network towards a steady-state value  $w_{HR}$ . Another strong assumption is that the spiking pattern is considered "regular", which means that for a simulation time greater than the necessary time to reach the stabilization towards  $w_{HR}$  ( $t > t_\infty$ ), the time spent in potentiation ( $\alpha_p$ ) and depression ( $\alpha_d$ ) regions remain unchanged.

### 5.1.2 Comparison of the equation obtained to compute the convergence value with the one given by [Graupner and Brunel, 2012]

In their articles [Graupner and Brunel, 2012, Graupner et al., 2016], the researchers defined the average value of  $w$  in the limit of a very long protocol (corresponding to our  $w_{HR}$ ) as follows:

$$\bar{w} = \frac{\Gamma_p}{\Gamma_p + \Gamma_d} \tag{5.2}$$

where  $\Gamma_p$  ( $\Gamma_d$ ) is the potentiation (depression) rate multiplied by the average time spent above the potentiation (depression) threshold, *i.e.*,  $\Gamma_p = \gamma_p \alpha_p$  ( $\Gamma_d = \gamma_d \alpha_d$ ).

Considering the demonstration that transforms Equation 3.8 into a classical first order ordinary differential equation (see section 3.2), we have the following equivalences:

$$\gamma_d = \frac{\tau_w}{\tau_w^d} \tag{5.3}$$

$$\gamma_p = \frac{\tau_w}{\tau_w^p} - \frac{\tau_w}{\tau_w^d} \tag{5.4}$$

However, when Equation 5.3 and Equation 5.4 are substituted in Equation 5.2, Equation 5.1 fails to be restored. To understand this discrepancy, it is important to realize that in [Graupner and Brunel, 2012], the average fraction of time spent above a given threshold is defined by

$$\alpha_x = \frac{1}{nT} \int_0^{nT} \Theta [c(t) - \theta_x] dt$$

where  $nT$  refers to the duration of the stimulation protocol ( $n$  presentations at interval  $T$ ;  $x = p, d$ ). This suggests that when considering Equation 3.8, the only contribution to potentiation is  $\gamma_p$  and the only contribution to depression is  $\gamma_d$  and thus Equation 3.8 should be rewritten as :

$$\tau_w \dot{w} = \gamma_p (1 - w) \mathbb{1} (Ca - \theta_p) - \gamma_d w \mathbb{1} (Ca - \theta_d) \mathbb{1} (Ca + \theta_p)$$

While  $\tau_w^0$ ,  $\Omega^0$ ,  $\tau_w^d$ , and  $\Omega^d$  remain unchanged, in potentiation conditions we get :

$$[Ca] > \theta_p : \begin{cases} \tau_w^p = \frac{\tau_w}{\gamma_p} \\ \Omega^p = 1 \end{cases} \tag{5.5}$$

such that when  $\gamma_d = \frac{\tau_w}{\tau_w^d}$  and  $\gamma_p = \frac{\tau_w}{\tau_w^p}$  are substitute to Equation 3.8:

$$\begin{aligned}\bar{w} &= 1 \times \frac{\alpha_p \frac{\tau_w}{\tau_w^p}}{\alpha_p \frac{\tau_w}{\tau_w^p} + \alpha_d \frac{\tau_w}{\tau_w^d}} \\ &= \underbrace{1}_{\Omega^p} \times \frac{\alpha_p \tau_w^d}{\alpha_p \tau_w^d + \alpha_d \tau_w^p}\end{aligned}$$

Equation 5.1 is finally recovered since, in **model 3**,  $\Omega^p = 1$  and  $\Omega^d = 0$ .

### 5.1.3 Numerical simulation against analytical prediction

First, the cortical network described in Figure 5.1A is simulated during wakefulness to confirm the validity of Equation 5.1. To do so, we reproduce known and real experimental data from [Sjöström et al., 2001] in order to verify the accuracy of the values given by Equation 5.1.

After this first validity check, the cortical network is switched into a burst activity in order to observe the homeostatic reset. Equation 5.1 is then used to see if it is able to correctly predict this convergence value.

#### Validity of the equation predicting the convergence value during wakefulness

The numerical simulation consists in reproducing the experimental data of [Sjöström et al., 2001] as it is done in [Graupner et al., 2016] (see subsection 3.3.2). Analytically, Equation 5.1 is used to predict the synaptic weight change obtained at the end of the 75 pulses for each of the different frequencies ranging from 0.1 to 50Hz. Setting the initial weight  $w_i$  at 0.5, the synaptic weight change is computed by  $\Delta w = \frac{w_f}{w_i}$  where  $w_f$  is either the value obtained after the simulation or the value given by the analytical prediction. The corresponding values are given on Table 5.1 and are presented graphically on Figure 5.4A .

Pairing frequency [Hz]	0.1	10	20	30	40	50
<b><math>\Delta t = 10\text{ms}</math></b>						
Numerical simulation	0.9872	0.9984	1.0828	1.1835	1.3196	1.4657
Analytical prediction	0.9798	0.9989	1.1302	1.2482	1.3974	1.5580
<b><math>\Delta t = -10\text{ms}</math></b>						
Numerical simulation	0.6733	0.6628	0.6188	0.9351	1.3404	1.466
Analytical prediction	0	0	0.1397	0.9031	1.4142	1.5583

Table 5.1: Synaptic change  $\Delta w = \frac{w_f}{w_i}$  obtained after the numerical simulation according to the protocol described in subsection 3.3.2 for frequencies  $f = 0.1, 10, 20, 30, 40$  and 50Hz. The values from the analytical prediction are given by Equation 5.1. Values highlighted in red represent a mismatch between the values obtained after the numerical simulation and the values predicted by Equation 5.1.

Equation 5.1 is able to predict quite closely the synaptic weight change after the protocol except for  $\Delta t = -10\text{ms}$  with pairing frequencies  $f = 0.1, 10$  and 20Hz. A more detailed analysis of the cortical circuit behavior shows that, for low frequencies  $f = 0.1$  and 10Hz, a postsynaptic spike followed by a presynaptic spike within 10 ms results in a calcium trace that never exceeds the potentiation threshold  $\theta_p$  (Figure 5.4B). Therefore,  $\alpha_p$  (*i.e.*, the time spent in the potentiation region) is put to zero and due to the fact that the parameter  $\Omega^d$  is set at 0 in the model,  $w_{HR}$  equals 0 by Equation 5.1.

To understand the discrepancy between the values obtained after the numerical simulation and the values given by the analytical prediction it must be remembered that Equation 5.1 predicts the steady-state value, meaning that it predicts the value towards which the synaptic strength converges after a long enough<sup>1</sup> recording time for a regular spiking pattern. Thus, at the end of the 75 pulse train, the numerical simulation does not (*yet*) reach a synaptic weight of zero whereas the analytical formula predicts that, if this pulse train were to continue, the synaptic weight would be equal to zero after a given time ( $t_\infty$ ). This behavior is proven to be correct in a numerical simulation where the pairing protocol is applied on 750 pulses (Figure 5.4A, green curve). Regarding the slight differences between the numerical simulation and analytical prediction values for the other frequencies, the same explanation holds true: the simulation time is not long enough to reach the exact final convergence value.

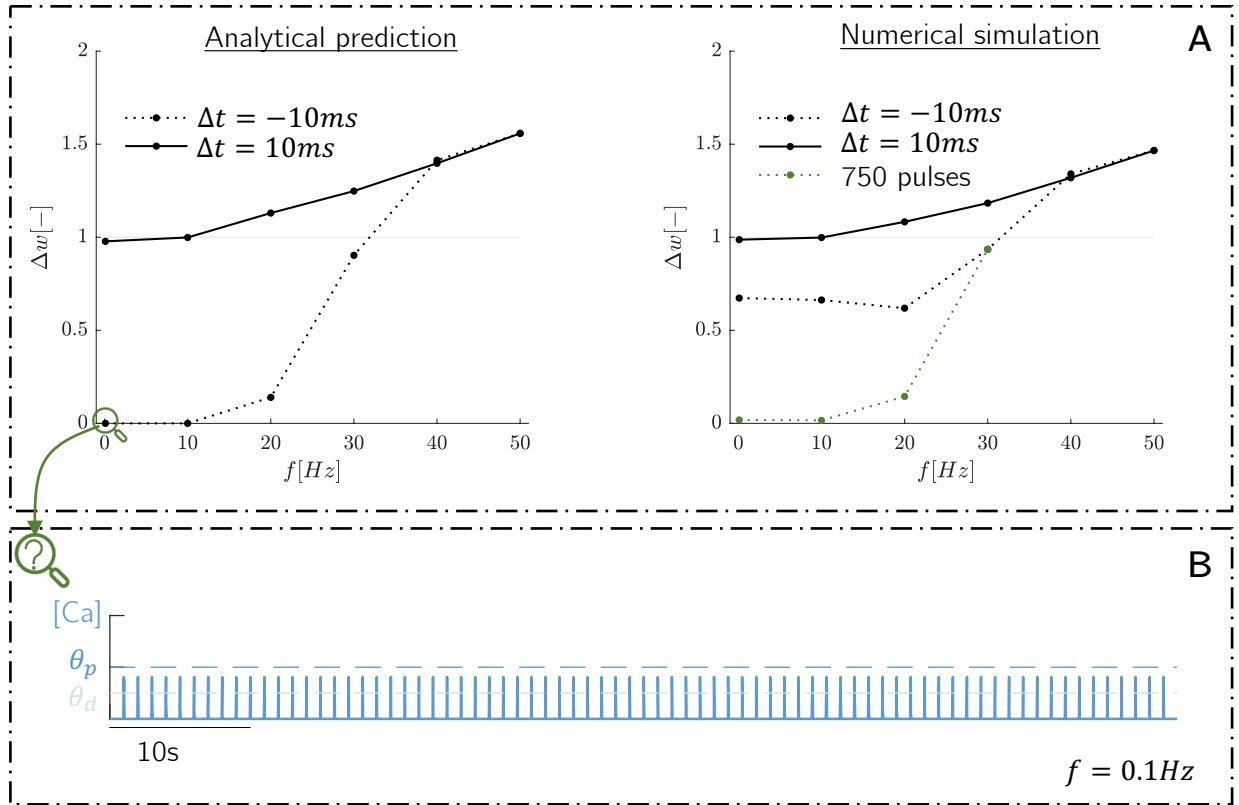


Figure 5.4: *Validity of Equation 5.1 during wakefulness by reproducing [Sjöström et al., 2001] as it is done in [Graupner et al., 2016]. A.* Frequency-response curve of synaptic plasticity according to data obtained after analytical prediction (left) and numerical simulation (right). Data obtained for the numerical simulation with 750 pulses (instead of 75) is depicted in green. **B.** Total calcium trace resulting from the 75 pulses at a frequency of  $f = 0.1\text{Hz}$ .

#### 5.1.4 Validity of the equation predicting the convergence value during sleep

To test and validate Equation 5.1 during sleep and to provide an analytical solution of the homeostatic reset, the cortical network is switched into a bursting activity by hyperpolarizing the inhibitory cell. More specifically, several circuits are hyperpolarized by different currents  $I_{app}$  (Figure 5.5A). Each of these currents generate a slightly different bursting pattern (all of them are shown in Appendix section C.2) and therefore a different convergence value, enabling to test the robustness of Equation 5.1 given some variability (Figure 5.5B). An initial synaptic weight  $w_0 \in [0, 1]$  is assigned at the beginning of

<sup>1</sup>this recording time depends on the spiking pattern and thus on the pairing frequency



the simulation, referring to the activity underwent during the day. Thus, different values are considered for each simulation to mimic various memory levels at the onset of sleep (strong activity  $w_0 \approx 1$ , weak activity  $w_0 \approx 0$ ). In line with the observation made by [Jacquerie et al., 2022], during the bursting activity, all synaptic weights converge towards the same basal value  $w_{HR}$  whatever the initial weight. This homeostatic reset phenomenon is depicted on Figure 5.5C.

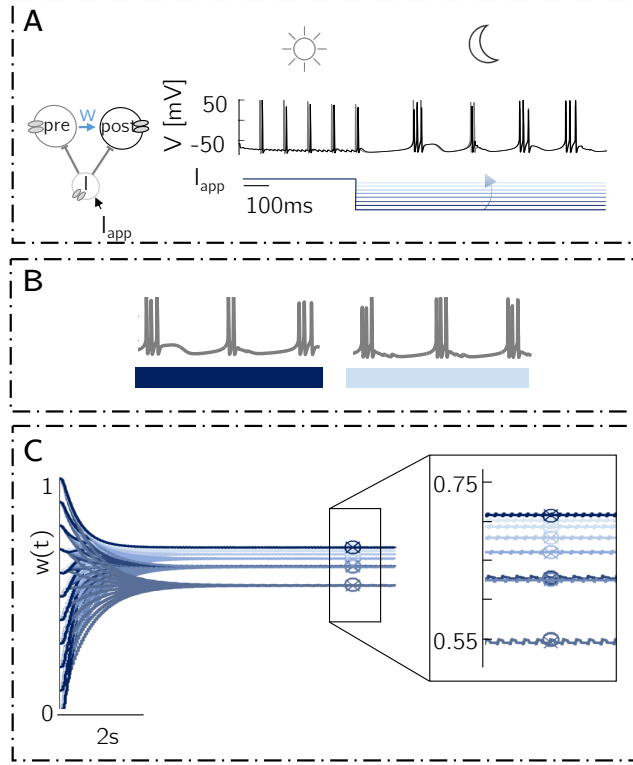


Figure 5.5: *Validity of Equation 5.1 during sleep.* **A.** Different external currents ( $I_{app}$ ) are applied to the inhibitory cell to switch the model in bursting activity **B.** Applying  $I_{app}=-4.7[\frac{nA}{cm^2}]$  (dark blue) generates a different bursting pattern to the pre- post- synaptic cells than applying  $I_{app}=-4.1[\frac{nA}{cm^2}]$  (light blue). **C.** During sleep, there is the homeostatic reset such that all weights converge towards the same steady-state value  $w_{HR}$  and Equation 5.1 can predict this value. The values computed by the numerical simulation are represented by crosses while the values predicted are represented by circles. Adapted from [Jacquerie et al., 2022].

Table 5.2 summarizes the values  $w_{HR}$  obtained after the numerical simulation and the values predicted by Equation 5.1 for different applied currents. The analytical prediction corresponds closely to the numerical simulation due to the fact that the circuit is simulated for a sufficiently long time ( $t \approx t_{\infty}$ ). It can be noticed that the values are not exactly the same because the simulation time has not exactly reached the required time  $t_{\infty}$  for the convergence towards the steady-state value.

$I_{app} [\frac{nA}{cm^2}]$	-4.7	-4.6	-4.5	-4.4	-4.4	-4.2	-4.1	-4.0
Numerical simulation	0.6268	0.5449	0.6246	0.6585	0.6787	0.6929	0.6998	0.7077
Analytical prediction	0.6273	0.5481	0.6252	0.6603	0.6789	0.6929	0.7007	0.7069

Table 5.2: Convergence values  $w_{HR}$  obtained after the numerical simulation during sleep for various cortical circuits to which an external current  $I_{app} = -4.7, -4.6, -4.5, -4.4, -4.3, -4.2, -4.1, -4.0[\frac{nA}{cm^2}]$  is applied. The values from the analytical prediction are given by Equation 5.1.

## 5.2 The explanation for *hard-bounds* models

The same demonstration is carried out considering now the *hard-bounds* version of this model explained in subsection 3.3.1 by Equation 3.11. In this setting, during sleep and the corresponding bursting activity, it is no longer towards an intermediate value within  $[\Omega^d, \Omega^p]$  to which all weights converge. In this case, the weights converge towards the upper limit defined by the model itself as  $w = 1$  (Figure 5.6A). As a reminder, this upper limit is set to avoid an unlimited increase in weight. This phenomenon is therefore called *saturation*: all weights converge towards the same limit whatever the value of the initial weight at the beginning of the simulation [Jacquerie et al., 2022]. According to the format of the Equation 3.11, this first-order differential equation does not have a zero-order term. Therefore its resolution gives the equation of a simple line with a specific slope  $\lambda_p$  (resp.  $\lambda_d$ ) determining the speed towards which the upper (resp. lower) limit is reached for a sustained level of calcium  $[Ca] > \theta_p$  (resp.  $\theta_d < [Ca] < \theta_p$ ) (Figure 5.6B).

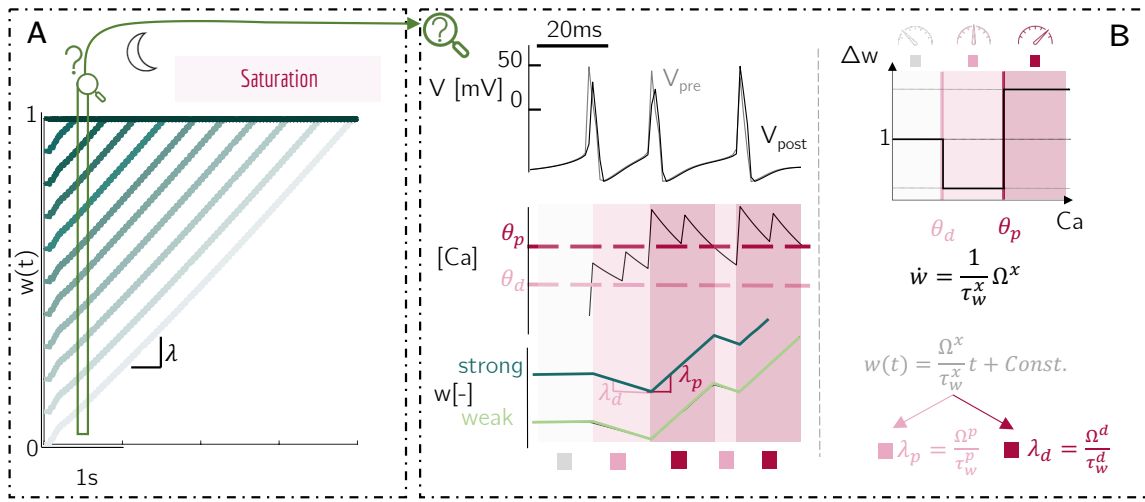


Figure 5.6: *Intuitive explanation of the saturation (hard-bounds)*. **A**. All weights converge towards the upper limit of the model at a certain speed (slope  $\lambda$ ). **B**. The time evolution of weak (light green) and strong (dark green) synaptic weights. In the depression (resp. potentiation) region (pink, resp. red), strong and weak weights decrease (resp. increase) with a slope of  $\lambda_d$  (resp.  $\lambda_p$ ).

### 5.2.1 Analytical demonstration of the slope value

The slope value depends on the bursting pattern which affects the fraction of time spent in the depression ( $\alpha_d$ ) and potentiation ( $\alpha_p$ ) regions. This slope value  $\lambda$  can be approximated analytically. Solving Equation 3.11 leads to the following linear equation:

$$\begin{aligned}
 [Ca] < \theta_d \quad w &= \frac{\Omega^0}{\tau_w^0} t + Const. \\
 [Ca] \in [\theta_d, \theta_p] \quad w &= \frac{\Omega^d}{\tau_w^d} t + Const. \\
 [Ca] > \theta_p \quad w &= \frac{\Omega^p}{\tau_w^p} t + Const.
 \end{aligned} \tag{5.6}$$

To avoid a physiologically impossible state where synaptic weights evolve linearly with time for a sustained level of calcium, it is important to bound this equation such that the weights can not exceed a maximal and minimal limit that are respectively set at 1 and 0 ( $w = 1$  if  $w \geq 1$  and  $w = 0$  if  $w \leq 0$ ).

According to Equation 5.6, when  $[Ca] > \theta_p$  (resp.  $\theta_d < [Ca] < \theta_p$ ), the synaptic weights increase linearly towards 1 (resp. decrease linearly towards 0) with a potentiation (resp. depression) slope of  $\lambda_p = \frac{\Omega^p}{\tau_w}$  (resp.  $\lambda_d = \frac{\Omega^d}{\tau_w}$ ). Therefore, the intermediate slope  $\lambda$  determining the saturation speed is the sum of the depression slope and potentiation slope each weighted by the fraction of time spent in their corresponding regions  $\alpha_d$  and  $\alpha_p$  :

$$\lambda = \alpha_p \frac{\Omega^p}{\tau_w} + \alpha_d \frac{\Omega^d}{\tau_w} \quad (5.7)$$

## 5.2.2 Numerical simulation against analytical prediction

The same validation procedure is applied as for the homeostatic reset demonstration: the cortical network is simulated during wakefulness to verify the accuracy of the values given by Equation 5.7. It is then switched to bursting activity to observe the saturation phenomenon and compute the convergence speed towards  $w = 1$ .

### Validity of the equation predicting the convergence value during wakefulness

The same process explained in section 5.1.3 is applied for the *hard-bounds* model to validate Equation 5.7 during wakefulness. As shown on Figure 5.7 and Table 5.3 the analytical prediction matches perfectly the numerical simulation. To predict the  $w_f$  at the end of the simulation the following line equation is used:

$$w_f = \lambda * (t_f - t_0) + w_0$$

where  $\lambda$  is computed from Equation 5.7 and depends on the activity pattern (mediated by various frequencies),  $t_0 = 0$  corresponds to the initial time,  $w_0 = 0.5$  corresponds to the initial weight and  $t_f$  is the final time of the simulation. Moreover, the final weight can not exceed a maximal and minimal limit that are respectively set at 1 and 0 ( $w_f = 1$  if  $w_f \geq 1$  and  $w_f = 0$  if  $w_f \leq 0$ ). Conversely to Equation 5.1, Equation 5.7 can be used at any time  $t$  because the speed of the synaptic change (the slope  $\lambda$ ) is derived from Equation 5.6 being the direct solution of the differential equation Equation 5.6.

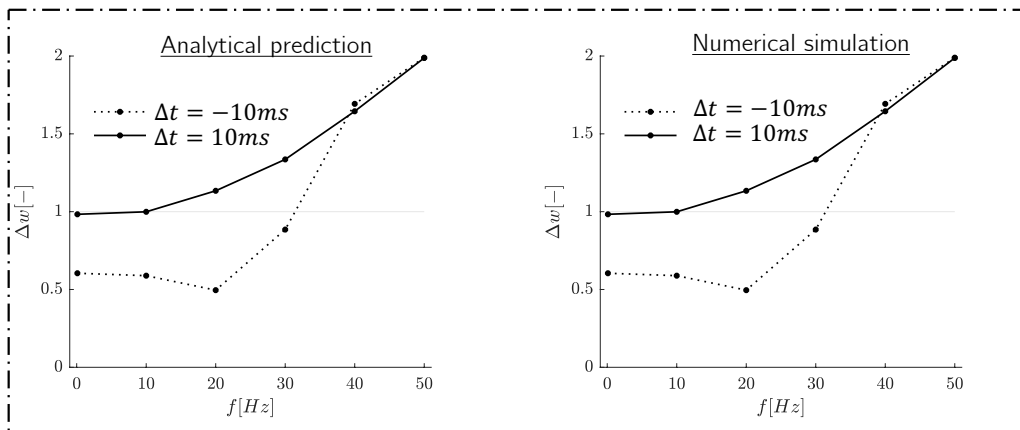


Figure 5.7: *Validity of Equation 5.7 (hard-bounds) during wakefulness by reproducing [Sjöström et al., 2001] as it is done in [Graupner et al., 2016].* Frequency-response curve of synaptic plasticity according to data obtained after analytical prediction and numerical simulation.

Pairing frequency [Hz]	0.1	10	20	30	40	50
<b><math>\Delta t = 10\text{ms}</math></b>						
Numerical simulation	0.9832	0.9992	1.1341	1.3358	1.6450	1.9877
Analytical prediction	0.9832	0.9992	1.1341	1.3358	1.6450	1.9877
<b><math>\Delta t = -10\text{ms}</math></b>						
Numerical simulation	0.6044	0.5887	0.4956	0.8850	1.6928	1.9893
Analytical prediction	0.6044	0.5887	0.4956	0.8850	1.6928	1.9893

Table 5.3: Synaptic change  $\Delta w = \frac{w_f}{w_i}$  obtained after the numerical simulation according to protocol described in subsection 3.3.2 for frequencies  $f = 0.1, 10, 20, 30, 40$  and  $50\text{Hz}$ . The values from the analytical prediction are given by Equation 5.7.

### Validity of the equation predicting the convergence value during sleep

The same process explained in subsection 5.1.4 is applied for the *hard-bounds* model to validate Equation 5.7 during sleep. In this protocol, even though the fraction of time spent in the potentiation region by calcium is close to (or sometimes even much lower than) the fraction of time spent in the depression region (see Table 5.4), the saturation value corresponds to the upper limit (*i.e.*,  $w = 1$ ) and not the lower limit (*i.e.*,  $w = 0$ ) because the speed of convergence given by  $\Omega^p$  is higher than the one given by  $\Omega^d$ . This leads to a global linear change of synaptic weight with an intermediate slope  $\lambda$  that lies in a range bounded by the depression slope  $\lambda_d$  and the potentiation slope  $\lambda_p$  ( $\lambda \in [\lambda_d, \lambda_p]$ ) but that is closer to  $\lambda_p$  than  $\lambda_d$ .

As it can be seen on Figure 5.8, Equation 5.7 is able to predict the speed of convergence (*i.e.*, the slope  $\lambda$ ) towards the upper limit. The values from Table 5.5 are slightly different for the numerical simulation and the analytical prediction due to data points chosen to compute the slope from the numerical simulation.

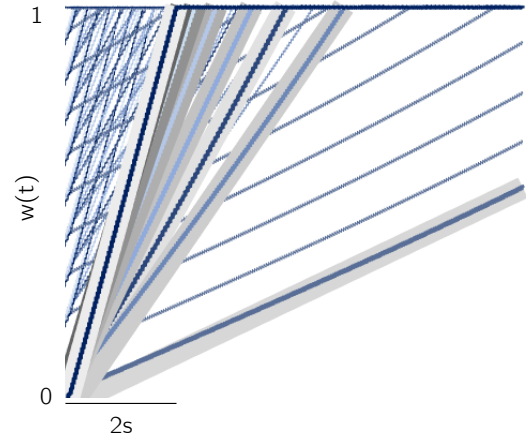


Figure 5.8: *Validity of Equation 5.7 (hard-bounds) during sleep.* During sleep, there is the saturation phenomenon such that all weights converge towards the upper limit and Equation 5.7 can predict this value. The slopes computed by the numerical simulation are represented in shades of blue while the values predicted are represented by shades of grey.

$I_{app} [\frac{nA}{cm^2}]$	-4.7	-4.6	-4.5	-4.4	-4.4	-4.2	-4.1	-4.0
Depression	0.1749	0.1895	0.1396	0.1343	0.1295	0.1251	0.1242	0.1231
Potentiation	0.1124	0.0724	0.0898	0.1084	0.1233	0.1363	0.1468	0.1560

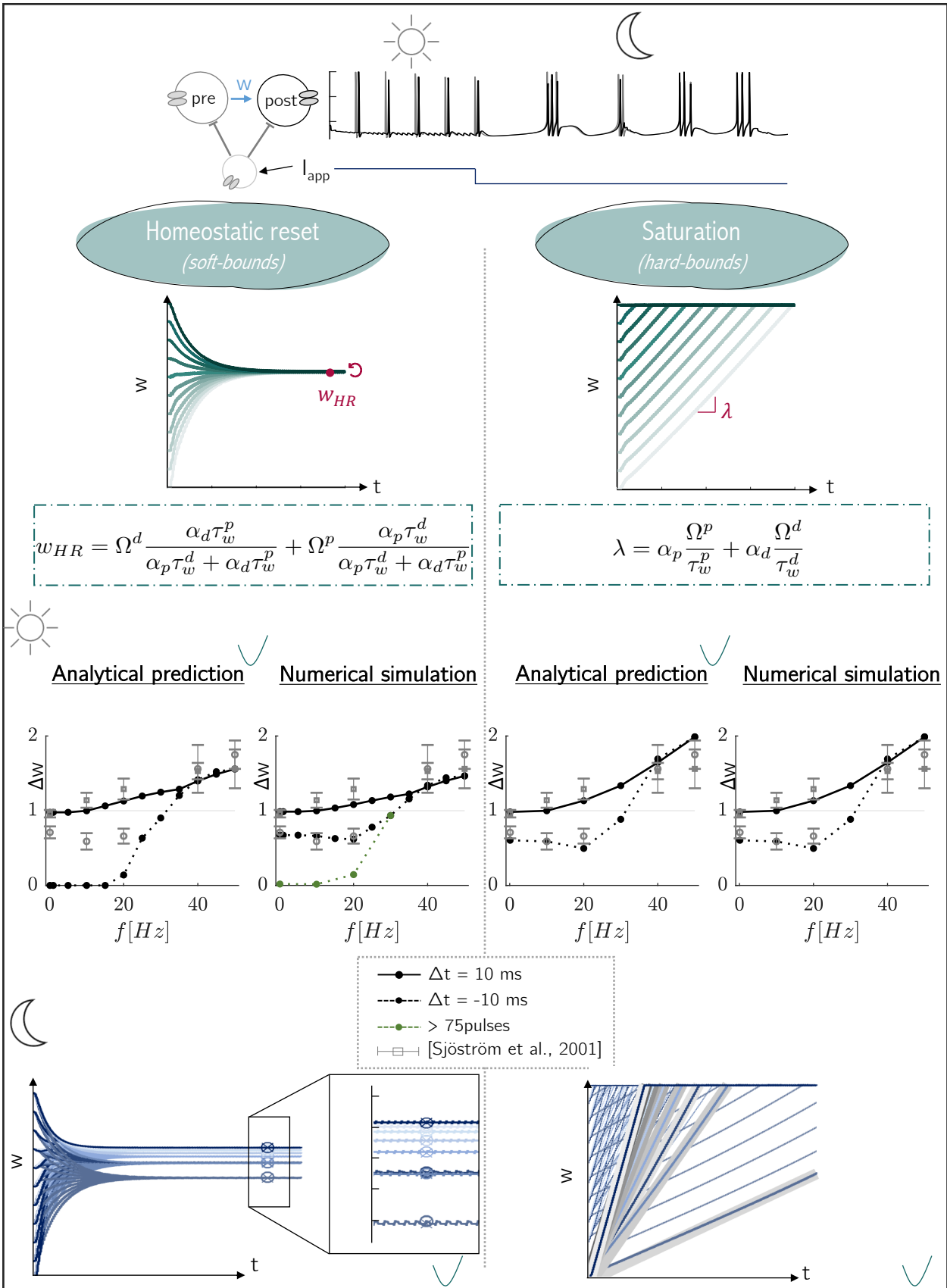
Table 5.4: Fraction of time spent in the depression ( $\alpha_d$ ) and potentiation ( $\alpha_p$ ) regions for various cortical circuits to which an external current  $I_{app} = -4.7, -4.6, -4.5, -4.4, -4.3, -4.2, -4.1, -4.0 [\frac{nA}{cm^2}]$  is applied (note that these values are also valid for *soft-bounds* model).

$I_{app} [\frac{nA}{cm^2}]$	-4.7	-4.6	-4.5	-4.4	-4.4	-4.2	-4.1	-4.0
Numerical simulation	2.64e-5	6.07e-6	2.04e-5	2.88e-5	3.54e-5	4.10e-5	4.66e-5	5.08e-5
Analytical prediction	2.64e-5	6.89e-6	2.11e-5	3.00e-5	3.72e-5	4.35e-5	4.83e-5	5.25e-5

Table 5.5: Slope values ( $\lambda$ ) obtained after the numerical simulation during sleep for various cortical circuits to which an external current  $I_{app} = -4.7, -4.6, -4.5, -4.4, -4.3, -4.2, -4.1, -4.0[\frac{nA}{cm^2}]$  is applied. The values from the analytical prediction are given by Equation 5.7.

### 5.3 Summary

## Analytical prediction of the homeostatic reset



## Chapter 6

# Homeostatic reset disabling: neuromodulation of calcium-based synaptic rules during sleep in *bursting* mode

The homeostatic reset described and demonstrated analytically in the previous section is not compatible with memory consolidation during sleep. Indeed, such a phenomenon means that strong synapses coding for important memories reset towards the same value as weak synapses coding for unnecessary information and any knowledge are memorized equally. However, human experience proves that the content of the morning lecture is more likely to be memorized than the color of the t-shirt worn by a stranger in the subway.

This section describes the various approaches that are taken in attempt to demonstrate that neuromodulation of calcium-based synaptic rule enables to bypass the homeostatic reset. There exist a whole range of different hypotheses regarding how memories are consolidated during sleep. So far, none of them is thought to be the ultimate one, suggesting cooperation between them overnight. Let's first review the most common beliefs on memory consolidation during sleep [Reyes-Resina et al., 2021] :

- *Synaptic homeostasis hypothesis (SHY)* : In this hypothesis, it is believed that sleep benefits the brain through global synaptic downscaling allowing storage of important information and reduction of noisy information. During the day preceding sleep, important items of information are encoded in highly potentiated synapses while noisy items information correspond are encoded in weakly triggered synapses. During sleep, all synapses are downscaled, decreasing the signal-to-noise ratio as a result of the depotentiation of synapses that overloaded during the former period of wakefulness. Although very interesting, this study focuses more on explaining the necessity of sleep rather than on the mechanisms underlying memory consolidation (Figure 6.1A) [Tononi and Cirelli, 2006, Tononi and Cirelli, 2014].
- *Sequential hypothesis*: This hypothesis focuses more on the processes of memory encoding overnight and argues that the succession of NREM and REM sleep stages is the key element for memory consolidation. While NREM is responsible for selective synapses weakening, REM sleep promotes the integration of remaining memories with those that already exist [Giuditta et al., 1995, Giuditta, 2014].
- *Active systems consolidation hypothesis*: Going a step further, this hypothesis brings together the two previous hypotheses by additionally stating that brain oscillations during NREM (*i.e.* slow oscillations, spindles, and ripples) enable re-activation (serving as a tagging process) of previously activated synapses as well as redistribution of memory from hippocampal to neocortical site. REM induces expression of IEGs related to plasticity in tagged synapses for stabilizing memories in the cortex (Figure 6.1B) [Diekelmann and Born, 2010, Born and Feld, 2012, Feld and Born, 2017, Klinzing et al., 2019].

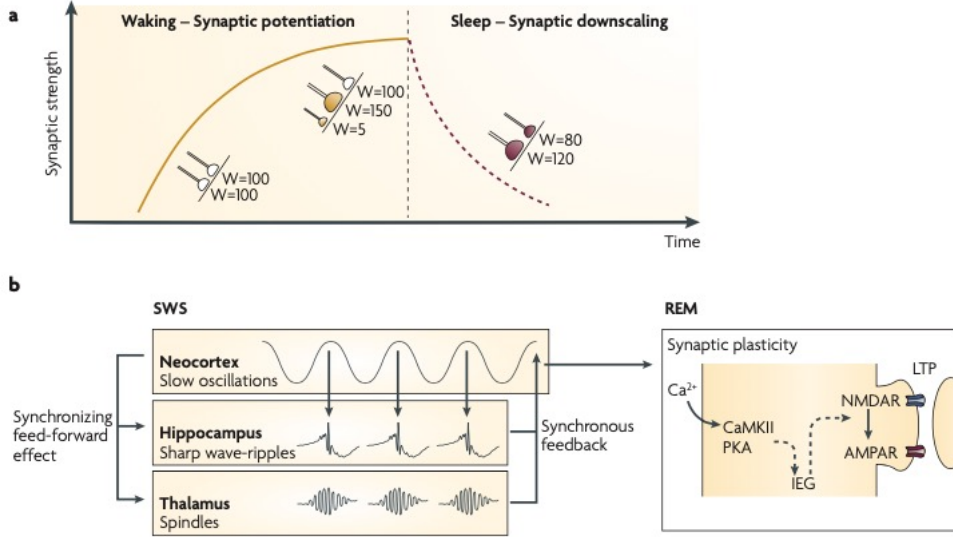


Figure 6.1: *Synaptic homeostasis (SHY) and active system consolidation*. **A.** The synaptic homeostasis hypothesis proposes that during wakefulness there is a net increase in synaptic strength  $w$  through the creation of new synapses or growth of existing dendrite spines that are being activated. During SWS, all synapses are downscaled to improve the signal-to-noise ratio. **B.** The active system consolidation model proposes that during wakefulness there is the encoding of information in the neocortex and the hippocampus. During sleep, there is a re-activation process of synapses activated during wakefulness. This process involves sharp-wave ripples and spindles. This supports the hippocampus-to-neocortex transfer of information and predisposes the synapses for further consolidation process during REM sleep. Taken from [Diekelmann and Born, 2010]

## 6.1 Hand-tuned calcium-based synaptic rules

To explore which neuromodulation mechanisms of synaptic plasticity rules lead to behavior consistent and compatible with memory consolidation, we follow a bottom-up approach.

The parameters  $\theta$ ,  $\Omega$ ,  $\tau$ , and  $C_{pre/post}$  are manually changed to get the expected results (*i.e.* potentiation/-maintenance of strong weights and depression of low weights) and, for each of them, we discuss the biological relevance of such a change. The same cortical circuit composed of three cells is used and eight different external currents  $I_{app}$  in  $[-4.7 -4.0]$  are applied to hyperpolarize the inhibitory cell to test the robustness of the neuromodulated model over distinct bursting patterns. The synaptic rule that is modified is the *soft-bounds* version of **model 3** because it allows a much simpler interpretation of the observed results and behaviors.

### 6.1.1 Modification of potentiation threshold $\theta_p$

During sleep, neuromodulators modulate the synaptic plasticity such that less or more calcium in the postsynaptic cell is necessary to trigger potentiation. Indeed, as seen in the literature review (chapter 4), acetylcholine, noradrenaline, histamine, and dopamine can trigger LTP although the stimulation is "subthreshold" (*i.e.*, not inducing LTP in the control condition) suggesting that, possibly, in the presence of these neuromodulators, less calcium influx from NMDARs and VDCCs is needed for potentiation. As suggested by [Seol et al., 2007], at least for noradrenaline and dopamine, this could result from the direct activation of PKA by the binding of neuromodulator to their respective  $G_s$ -coupled receptors  $\beta$  and  $D_1$ .

Using **model 3**, this is expressed by the modification of the parameter  $\theta_p$ . Initially set at 2, we simulate the cortical network with  $\theta_p = 3$  and then with  $\theta_p = 1.5$ . As seen on Figure 6.2, increasing (A) or decreasing (B)  $\theta_p$  does not enable to remove the homeostatic reset. Instead, when the potentiation threshold is increased (resp. decreased), the value towards which all weights converge is lower (resp. higher) than in the control condition. This makes sense because increasing (resp. decreasing)  $\theta_p$  drives the calcium influx resulting from the bursting



pattern (that has not changed) to be more (resp. less) often in the depression region than before, such that  $\alpha_d$  is increased (resp. decreased) and the value  $w_{HR}$  predicted by Equation 5.1 is therefore lowered (resp. increased).

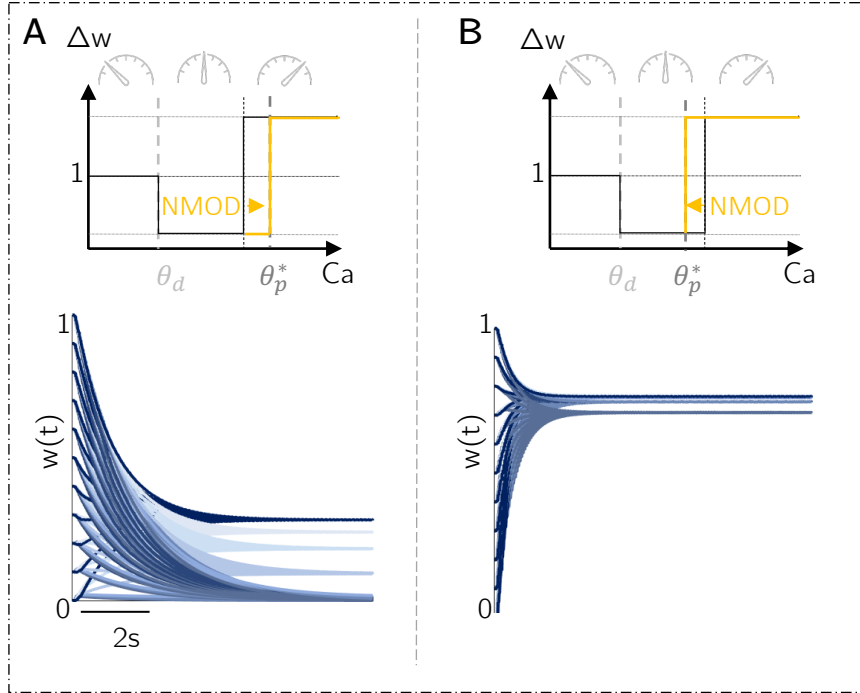


Figure 6.2: *Neuromodulation of potentiation threshold  $\theta_p$*  **A.** Neuromodulators act on the synaptic rule such that  $\theta_p$  is increased to 3. The homeostatic reset is still observed with a lower convergence value. **B.** Neuromodulators act on the synaptic rule such that  $\theta_p$  is decreased to 1.5. The homeostatic reset is still observed with a higher convergence value.

### 6.1.2 Modification of the potentiation level $\Omega^p$ to make it weight-dependent

To obtain results compatible with memory consolidation, a possibility is to impose a bimodal behavior by creating two groups of synapses undergoing different synaptic rules: strong synapses experiencing maintenance of synaptic weights and weak synapses experiencing downscaling. This possibility is in line with the tagging hypothesis discussed in the review: BDNF tags activated synapses during wakefulness through Arc translation allowing replay of these neurons during following NREM sleep and preserving these connections from the global downscaling suggested by SHY. The mechanism by which a replay preserves synaptic downscaling may involve the presence of noradrenaline and its inhibitory effect on LTD.

As already discussed, according to the shape of the *soft-bound* model equations  $\Omega^x$  corresponds to the value towards which  $w$  converges. This parameter is calcium-dependent and is equal to  $\Omega^p$  when the calcium concentration is such that the potentiation threshold  $\theta_p$  is exceeded ( $[Ca] > \theta_p$ ). Hence, it is interesting to define this parameter as weight-dependent such that for strong connections, the convergence value should be high whereas for weak ones it should be low. Such a change means that, in weak synapses, LTP is inhibited by neuromodulators whereas in strong synapses it is enhanced. Serotonin can act as an LTP inhibitor by inhibiting NMDARs current and all reviewed neuromodulators are involved in some form of LTP improvement.

One implementation is the following:

$$\Omega^p = \begin{cases} 1 & \text{if } w > 0.75 \\ 0 & \text{if } w \leq 0.75 \end{cases} \quad (6.1)$$

Note that  $w_{crit}$  is set at 0.75 with no specific justification and this choice does not impact the overall conclusion.

Results depicted on Figure 6.3A show an (*almost*) bimodal distribution of convergence weights according to the synaptic strength. However, two remarks can be made:

- This approach is an all-or-none operation meaning that the limit between strong and weak synapses is set at a fixed value and the convergence towards rather  $\Omega^p = 1$  if the synapse is strong (*i.e.*,  $w > 0.75$ ) or  $\Omega^p = 0.1$  if the synapse is weak (*i.e.*,  $w < 0.75$ ) is "non-continuous" (Figure 6.3A.1). The physiological justification for this strict limit is difficult to make, as it seems unlikely that cellular mechanisms within the brain have this "discrete" behavior.
- Moreover, this implementation is not robust to variability. Indeed, for one of the applied currents (red box), the bursting pattern gives a homeostatic reset value slightly under the critical weight set at  $w_{crit}=0.75$ . This causes strong weights to drop drastically at the homeostatic reset value from what is initially a low weight although the initial weight is high. To overcome this problem, it is possible to speculate that the brain can remember the initial state of the synapse at the onset of sleep such that, instead of being dependent on  $w$ ,  $\Omega^p$  is dependent on  $w_i$  (*i.e.*  $\Omega^p(w_i)$ ). The results are shown on Figure 6.3A.2.

It is interesting to note that using Equation 5.1, it is possible to predict the value towards which the weights converge by modifying adequately  $\Omega^p$  in the equation. However, the simulation are still very important. Indeed, even if we have already computed the time spent in potentiation ( $\alpha_p$ ) and depression ( $\alpha_d$ ) (see Table 5.4) by one "control" simulation, it is essential to highlight that the membrane potential of the postsynaptic cell is dependent on the  $w$  via the excitatory AMPA connection (see section C.1). Therefore, this slight change in the membrane potential drives (or not) the calcium influx into different region of plasticity (no change, depression or potentiation) thus changing  $\alpha_p$  and  $\alpha_d$  computed in the control condition. In this sense, Equation 5.1 is powerful for gaining insight into the behavior of our experiment, but a validity check must still be performed to ensure this outcome.

A more physiologically plausible approach is to consider a continuous evolution of  $\Omega^p(w)$  along a sigmoid function:

$$\Omega^p(w) = a_0 + m_2 \frac{\exp(b_2([Ca] - a_2))}{1 + \exp(b_2([Ca] - a_2))} \quad (6.2)$$

where  $a_0=0$  and  $m_2=1$  such that the converging value is 0 for weak weights and 1 for strong weights,  $b_2=40$  and  $a_2=0.75$  such that the concavity change occurs around  $w_{crit} = 0.75$  with a medium slope (Figure 6.3B).

This approach enables a smoother classification of "strong" and "weak" synapses and therefore a better physiological relevance. However, the issue regarding the fragility to the variability of the applied current is still prevalent (Figure 6.3B, red box) but this problem is handled by making  $\Omega^p$  depend on  $w_i$ , as explained just above.

Obtaining a behavior such as the one we get in our results for both non-continuous and continuous implementation is not simple and very sensitive to the choice of parameters. For example, setting the convergence value for weak weight above zero ( $\Omega^p(w) > 0$  if  $w \leq 0.75$  /  $a_0 > 0$ ) leads to incoherent results where synapses that had no neuronal connection at the onset of the night ( $w_0 = 0$ ) are somewhat strengthened during sleep ( $w_{HR} > w_0$ ), which is in our opinion meaningless in a real world. This inconsistency is because the converging value is bounded by  $[\Omega^d(w) \Omega^p(w)]$  from Equation 5.1. Therefore, fragility persists in both approaches.

An alternative to get a more robust implementation is to make both  $\Omega^d$  and  $\Omega^p$  evolve following sigmoid functions. This way  $\Omega^d$  and  $\Omega^p$  are high for strong weights, restraining the convergence value between high bounds and they are low for lower weights, allowing depression in this case. Our implementation is the following:

$$\Omega^p(w) = a_0^p + m_2^p \frac{\exp(b_2^p([Ca] - a_2^p))}{1 + \exp(b_2^p([Ca] - a_2^p))} \quad (6.3)$$

$$\Omega^d(w) = a_0^d + m_2^d \frac{\exp(b_2^d([Ca] - a_2^d))}{1 + \exp(b_2^d([Ca] - a_2^d))} \quad (6.4)$$

where  $a_0^p=a_0^d=0$ ,  $m_2^p=0.9$ ,  $m_2^d=0.8$  such that the converging value is 0 for weak weights and is bounded between  $[0.8 \ 0.9]$  for strong weights,  $b_2^p=b_2^d=40$ ,  $a_2^p=0.7$  and  $a_2^d=0.4$  such that there is a progressive decrease for weak weights and the critical weight to preserve strong synapses is around 0.7 (Figure 6.3C).

This method allows better control of the bounds of the convergence value for small weights and large weights resulting in a more robust approach to the problem. However, it is necessary to modify both  $\Omega^p$  and  $\Omega^d$  in

such a way that, for synaptic weights between 0.4 and 0.6, the convergence value in the depression region ( $\Omega^d=0.8$ ) is higher than that in the potentiation region ( $\Omega^p=0$ ). The well-established basic principle where a medium concentration of calcium leads to depression and a high concentration leads to potentiation is reversed for these weights. This hypothesis is an avenue to be explored experimentally but is, to our knowledge, not yet biologically justifiable.

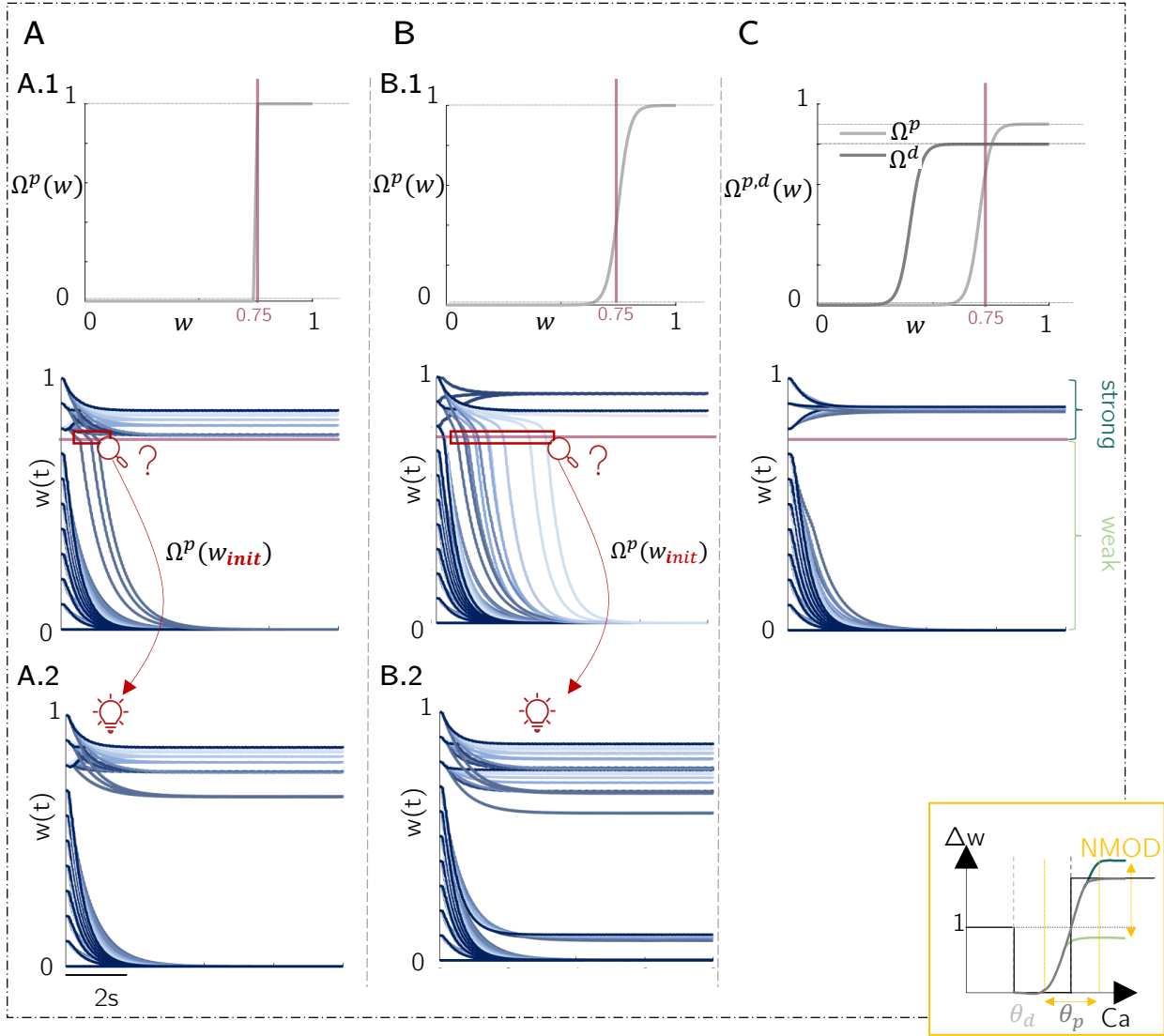


Figure 6.3: *Neuromodulation of the potentiation level  $\Omega^p$* . Neuromodulators can tag strong synapses (dark green) vs. weak synapses (light green) such that their convergence value in potentiation  $\Omega^p$  is different. Several currents  $I_{app}$  are applied to the inhibitory cell of the cortical network to test the robustness of the neuromodulated rule. **A.** Strict delimitation between weak and strong synapses where  $\Omega^p(w)$  follows Equation 6.1 and  $w_{crit}$  (separation value between strong and weak weights) is set at 0.75. The expected evolution of the weights is not robust to variability (red loop) (**A.1**) and, to overcome this, it is necessary to make  $\Omega^p$  dependent on  $w_i$  (**A.2**). **B.** Smooth delimitation between weak and strong synapses where  $\Omega^p(w)$  follows Equation 6.2 and  $w_{crit}$  is set at 0.75. The expected evolution of the weights is not robust to variability (red loop) (**B.1**) and, to overcome this, it is necessary to make  $\Omega^p$  dependent on  $w_i$  (**B.2**). **C.**  $\Omega^p(w)$  and  $\Omega^d(w)$  both evolve following sigmoid functions Equation 6.3 and Equation 6.4 allowing better control of the bounds of the convergence value for weak and strong synapses respectively and  $w_{crit}$  is set around 0.75.

### 6.1.3 Modification of the convergence speed in depression $1/\tau_d$ to make it weight-dependent

We have seen that the speed of convergence is calcium-dependent and is faster for potentiation than depression. It is interesting to see what happens if we impose that the speed of convergence for depression,  $1/\tau_d$ , is additionally weight-dependent such that weak synapses depress faster than strong ones. Considering ASCHY [Born and Feld, 2012], this change is in agreement with a global downscaling of the synapses while still maintaining previously stimulated synapses with relatively strong connections. However, to our knowledge, there is no biological study demonstrating a time-scale difference during sleep between strongly connected and weakly connected synapses since such an experiment is difficult to conduct. Nevertheless, it is still interesting to analyze the behavior of the computational simulation implemented by the following equation:

$$\tau_d = \begin{cases} 100 \times 3780.24 & \text{if } w > 0.75 \\ 3780.24 & \text{if } w \leq 0.75 \end{cases} \quad (6.5)$$

where 3780.24ms is the value of the parameter  $\tau_d$  in the unmodified model. By changing the rule in this way, it is expected that for the same amount of time spent in the depression region, large weights have a lower LTD effect compared to small weights. Mathematically, this is expressed by changing the relative time spent in depression and potentiation ( $\alpha_d^*$  and  $\alpha_p^*$ ).

Once again, this approach defines a strict limit between strong and weak synapses which is artificial but the results are consistent with what we are looking for (Figure 6.4A). However, it is very important to note that :

- For a longer duration of simulation the initial strong weights progressively decrease until they reach the critical weight  $w_{crit} = 0.75$ . At this point, the rate of decay is more important. This means that whatever the initial synaptic strength, all information are forgotten after a very long night of sleep, which is not the case in reality.
- The convergence speed is 100 times slower for high weights than low weights which is probably not physiologically relevant. This value is chosen because it is the one giving the expected behavior for our simulation time (4s), a lower  $\tau_d(w)$  leading to cross  $w_{crit}$  earlier in the simulation.

The two mentioned items highlight the fragility of the neuromodulated rule concerning the different settings that are chosen for the simulation (*i.e.*  $\tau_d$ , simulation time, etc.). Therefore, this implementation gives the expected behavior but is sensitive, artificial, and not realistic as it was built to fit exactly our simulation.

As it was done for weight-dependent  $\Omega^P$ , a continuous form can be considered for  $\tau_d$  through the use of the sigmoid function:

$$\tau_d(w) = a_0 + m_2 \frac{\exp(b_2 ([Ca] - a_2))}{1 + \exp(b_2 ([Ca] - a_2))} \quad (6.6)$$

where  $a_0=3780.24$ ms (*i.e.*, the original  $\tau_d$ ) and  $m_2=20 \times 3780.24$ ms such that the converging speed value is unchanged for weak weights and 20 times slower for strong weights,  $b_2=80$  and  $a_2=0.75$  such that the concavity change occurs around  $w_{crit} = 0.75$  with a steep slope.

This continuous experiment does not seem either to be the right track to take:

- Figure 6.2B shows incoherent results where synapses that had no neuronal connection at the onset of the night ( $w_0 = 0$ ) are somewhat strengthened during sleep ( $w_{HR} > w_0$ ), which is in our opinion meaningless in a real world.
- Moreover, the value of  $m_2$  is chosen on purpose to show the fragility of  $\tau_d$ -neuromodulated rules discussed here above: as it is seen on Figure 6.2B, choosing  $\tau_d$  for strong synapses lower than  $100 \times 3780.24$ ms causes some weights to drop drastically (a phenomenon already discussed in subsection 6.1.2).
- Finally, even though it is a continuous change, the steepness of the slope<sup>1</sup> is such that the speed is changed almost in a discrete manner between weak and strong synapses, questioning the biological relevance.

---

<sup>1</sup>making the slope flatter failed also to produce the desired results

Note that for both configurations the potentiation threshold is respectively increased to  $\theta_p = 4$  and  $\theta_p = 2.7$  to provide a behavior where only depression is possible. Without this change, we get the strengthening of some weak synapses and a drastic drop of strong weight for some specific bursting patterns. The biological relevance of this modification was discussed earlier in subsection 6.1.1.

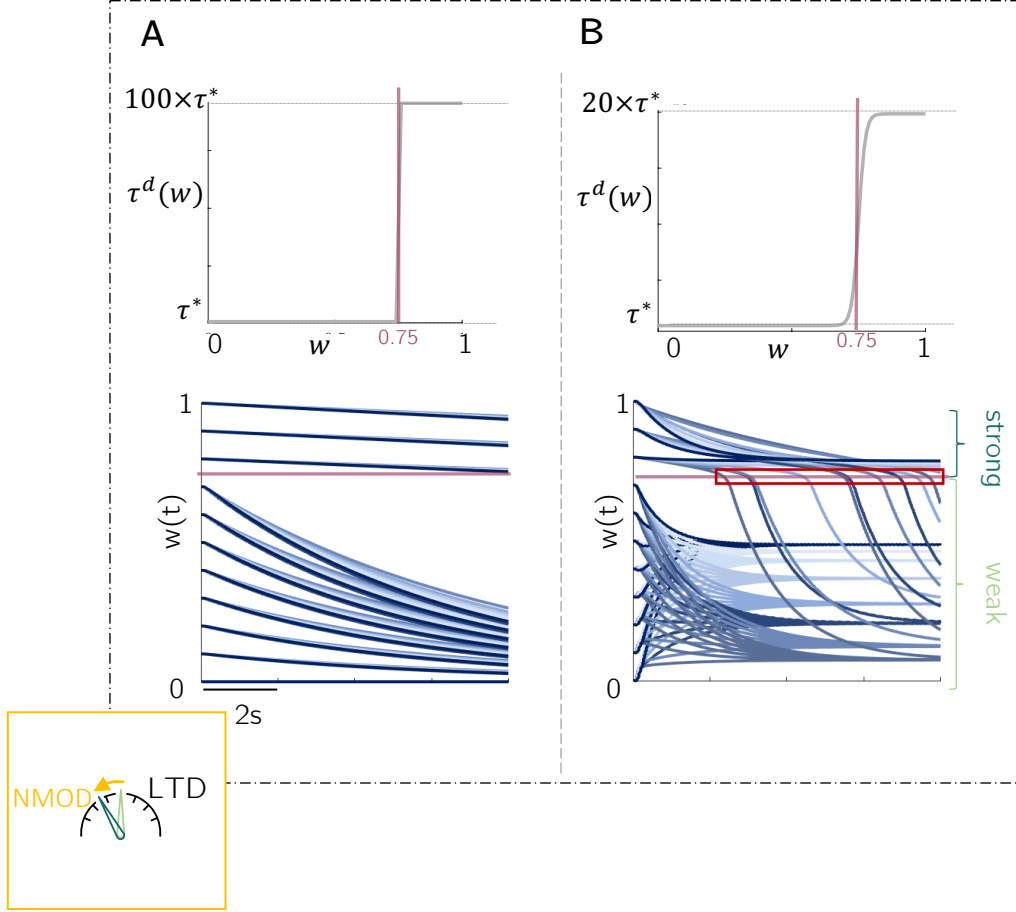


Figure 6.4: *Neuromodulation of convergence speed in depression*  $\frac{1}{\tau_d}$ . Neuromodulators can tag strong synapses (dark green) vs. weak synapses (light green) such that their convergence speed in depression  $\frac{1}{\tau_d}$  is different. Several currents  $I_{app}$  are applied to the inhibitory cell of the cortical network to test the robustness of the neuromodulated rule. **A.** Strict delimitation between weak and strong synapses where  $\tau_d$  follows Equation 6.5 and  $w_{crit}$  (separation value between strong and weak weights) is set at 0.75. **B.** Smooth delimitation between weak and strong synapses where  $\tau_d$  follows Equation 6.6. The expected evolution of the weights is not robust to variability (red) and leads to some incoherent behavior with the strengthening of non-existing neuronal connections and drastic drop of high weights.  $\tau^*$  is the value of the parameter  $\tau_d$  in the unmodified model.

#### 6.1.4 Modification of the maximal calcium influx to make it weight-dependent

In the considered model, the dominant source of calcium influx to the postsynaptic cell is through NMDARs and VDCCs represented by the parameters  $C_{pre}=0.84410$  and  $C_{post}=1.62138$  respectively. It is interesting to consider that during the night, the calcium dynamics are not the same for synapses that have been strongly activated during the day as for those which have been poorly triggered. This change is in line with a recent work that adapted **model 2** such that the coupling between postsynaptic calcium influx and synaptic weight is taken into account [Deperrois and Graupner, 2020].

To obtain results matching the expected behavior, we suggest lowering the pre- and postsynaptic-induced influx of calcium in such a way that for strong synapses the total amount of calcium [Ca] stays in the region

where no change occurs ( $[Ca] < \theta_d$ ) and for weak synapses the depression region is reached ( $\theta_d < [Ca] < \theta_p$ ) but not the potentiation region.

$$C_{pre} \text{ and } C_{post} = \begin{cases} 0.1 \text{ and } 0.3 & \text{if } w > 0.75 \\ 0.3 \text{ and } 0.7 & \text{if } w \leq 0.75 \end{cases} \quad (6.7)$$

The results are consistent with the *active systems consolidation hypothesis* theory [Born and Feld, 2012] where strong synapses are maintained at a high value while weak synapses are depressed. In this specific case, strongly connected synapses are tagged in such a way that the postsynaptic neuron undergoes less calcium influx leading to conservation of the strong weights (via no synaptic change) while the weak weights undergo depression (Figure 6.5). However, this idea is opposed to the recent findings of [Niethard et al., 2021]. In their study, they showed that spindle-active excitatory cortical cells increased their calcium activity during NREM sleep, whereas spindle-inactive cells decreased calcium activity. This suggests that neurons that have been previously activated (considered as active-spindle neurons) are spared from global down-regulation by an unknown mechanism increasing calcium influx (and not decreasing it) [Niethard et al., 2021].

Moreover, the delimitation between weak and strong synapses is once again strict and artificial. Making  $C_{pre}(w)$  and  $C_{post}(w)$  evolve as sigmoid functions makes the neuromodulated rule more physiologically plausible. However, this alternative has not been explored further as it was already well-investigated and discussed in the previous  $\Omega^p$ - and  $\tau_d$ - neuromodulated rules.

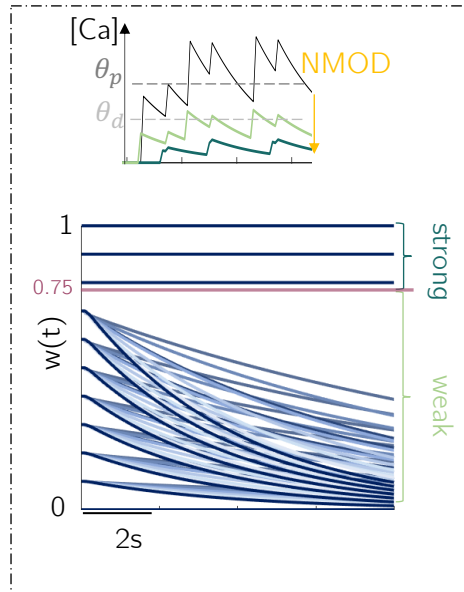


Figure 6.5: *Neuromodulation of maximal calcium influx.* Neuromodulators can tag strong synapses (dark green) vs. weak synapses (light green) such that their calcium influx after stimulation is different. Several currents  $I_{app}$  are applied to the inhibitory cell of the cortical network to test the robustness of the neuromodulated rule. There is a strict delimitation between weak and strong synapses where  $\tau_d$  follows Equation 6.7 and  $w_{crit}$  (separation value between strong and weak weights) is set at 0.75.

## 6.2 Implementation of [González-Rueda et al., 2018] phenomenological Up state-mediated plasticity rule in calcium-based plasticity rules

In this section we suggest that neuromodulators could act on the shape of the curve resulting from the STDP protocol. As a reminder, the STDP is a process highlighting the synaptic strength changes according to various time lag  $\Delta t$  between the presynaptic and postsynaptic spikes. In the hippocampus, LTP is induced when the presynaptic cell fires slightly before the postsynaptic cell, and LTD is induced when the postsynaptic spike occurs slightly before the presynaptic spike, resulting in the classical STDP curve (Figure 6.6B.1). Computationally, this curve is reproduced following a pairing protocol consisting in 60 pair pulses of the presynaptic and postsynaptic neurons at a fixed frequency of 1 Hz for various time lags  $\Delta t$  between the presynaptic and postsynaptic spikes [Bi and Poo, 1998].

Based on SHY [Tononi and Cirelli, 2006], [González-Rueda et al., 2018] consider that the same synaptic rule can not explain both net synaptic potentiation during the day and net synaptic depression during sleep. Therefore, according to their experimental results, they implemented an Up state-mediated plasticity rule where *presynaptic spikes alone lead to synaptic depression whereas a pair of pre- postsynaptic spikes within 10ms leads to no change in synaptic weight* (Figure 6.6B.2) [González-Rueda et al., 2018]. To derive this rule, they based themselves on experimental data that they obtained following a pairing protocol during UP-states of anesthetized mice at 3 distinct delays between pre- post- spikes ( $\Delta t = -10, 10$  and  $50\text{ms}$ , 3 grey crosses on Figure 6.6B.1).

The implementation of this phenomenological rule into a calcium rule is a promising avenue to explore. Indeed, during a burst, the presynaptic and postsynaptic neurons are spiking relatively closely. Thus, having no change in a narrow window could strongly influence the evolution of synaptic strength during bursts and result in a rule which is consistent with memory consolidation during sleep.

### 6.2.1 Translation of the Up state-mediated plasticity rule into a calcium-based plasticity rule

The procedure described below is undertaken to translate [González-Rueda et al., 2018] rule in such a way that the STDP curve is reproduced by a *hard-bounds* calcium-based plasticity rule.

- *One presynaptic spike:* As one presynaptic spike leads to depression, the parameter  $C_{pre}$  must be higher

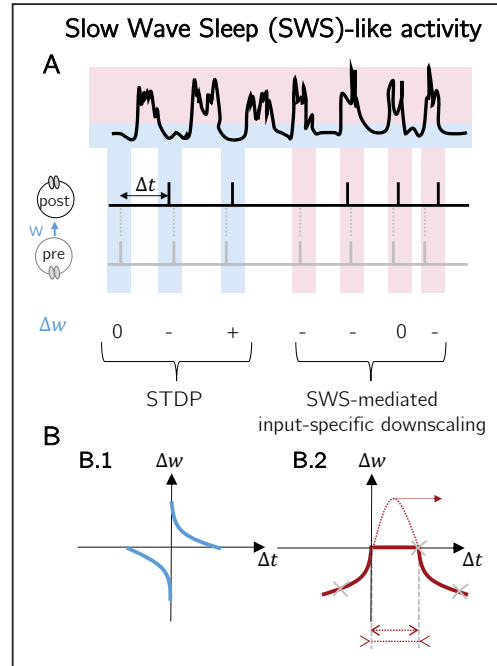


Figure 6.6: Adapted graphical abstract of [González-Rueda et al., 2018]. **A.** During DOWN states of SWS (blue), the classical STDP synaptic rule is used while during UP states of SWS (pink), the rule is modified such that when a postsynaptic spike follows a presynaptic spike within 10ms there is no change, otherwise there is LTD. **B.** Scheme of the classical hebbian STDP curve (**B.1**) and the STDP curve obtained with [González-Rueda et al., 2018] in sleep. We suggest to modify this curve (dotted arrays) maintaining the 3 experimental points (grey crosses)(**B.2**).

than the depression threshold ( $\theta_d$ ) but lower than the potentiation one ( $\theta_p$ ) such that the calcium influx arising from a single presynaptic spike leads to a calcium concentration necessary to be in the depression region (Figure 6.7A). Moreover, as the calcium concentration is additive following a spike train, the potentiation threshold is increased so that a burst does not lead (or very little) to potentiation.

- *One postsynaptic spike:* [González-Rueda et al., 2018] rule is built in such a way that one postsynaptic spike does not change the synaptic strength. Accordingly, the parameter  $C_{post}$  must be lower than the depression threshold (Figure 6.7B).
- *One postsynaptic spike followed by one presynaptic spike:* When there is a postsynaptic spike followed by a presynaptic spike it leads to depression. The maximum influx of calcium that can arise from this configuration is when the two spikes are occurring almost simultaneously such that the maximal calcium concentration is the sum of the calcium influx from the prespike ( $C_{pre}$ ) and the calcium influx from the postspike after a delay of  $D$  ( $C_{post}e^{-0.045 \times D}$ ). As a reminder,  $D$  is the slow rise time of the NMDAR-mediated [Graupner and Brunel, 2012] and Equation 3.7 is solved such that  $c_{post}(t) = C_{post}e^{\frac{-c_{post}}{\tau C_a} \times t}$ . Therefore, this maximal calcium concentration ( $C_{pre} + C_{post}e^{-0.045 \times D}$ ) should be higher than the depression threshold but lower than the potentiation one (Figure 6.7C).
- *One presynaptic spike is followed by one postsynaptic spike more than 10ms after:* When there is a presynaptic spike followed by a postsynaptic spike after 10ms it should
  - lead to depression if the spikes are close enough (but at least 10ms apart)
  - not change the synaptic strength otherwise.

If we decide to round  $D$  at 10ms (instead of 9.53709ms), the maximum influx of calcium arises when the presynaptic neuron spikes exactly 10ms before the postsynaptic spike such that  $C_{pre}$  and  $C_{post}$  sum up. The accumulation of  $C_{pre}$  and  $C_{post}$  should therefore be higher than the depression threshold but lower than the potentiation one (Figure 6.7D.1).

- *One presynaptic spike is followed by a postsynaptic spike within 10ms:* Finally, when the presynaptic spike is followed by a postsynaptic spike within 10ms no change should occur. To implement this configuration, it is considered that a postsynaptic spike prevents any NMDAR-mediated calcium influx induced less than 10ms beforehand by a presynaptic spike such that  $C_{pre}$  is set to zero. One actor in this phenomenon could be serotonin. Indeed, in chapter 4 it was highlighted that, when applied in the range of micromolar, serotonin acts as an inhibitor of LTP by inhibiting NMDARs current. This hypothesis is an avenue to be explored experimentally during sleep but is, to our knowledge, not yet biologically justifiable (Figure 6.7D.2).

All taken together, algorithm 1 is proposed where  $\tau_x = 1\text{ms}$ ,  $C_{pre} = 1.1$ ,  $C_{post} = 0.7$ ,  $t_{post}$  (resp.  $t_{pre}$ ) is the spiking time of the postsynaptic (resp. presynaptic) neuron,  $\delta()$  is Dirac's delta function and  $\Theta()$  is the indicator function. Following the phenomenological implementation of [González-Rueda et al., 2018] (detailed in Appendix section D.4), a postsynaptic trace decaying linearly ( $x$ ) is introduced to take into account the 10 ms window in which no change occurs.

---

**Algorithm 1:** [González-Rueda et al., 2018] translated in calcium-based synaptic rule

---

```

if  $t=t_{post}$  then
  |  $x = 10$ 
else
  |  $\tau_x \dot{x} = -1$ 
end
 $\dot{c}_{post} = -\frac{c_{post}}{\tau C_{a_{pre}}} + C_{post} \sum_{post} \delta(t - t_{post})$ 
 $\dot{c}_{pre} = -\frac{c_{pre}}{\tau C_{a_{post}}} + C_{pre} \times \Theta(-x(t)) \sum_{pre} \delta(t - t_{pre} - D)$ 
 $s.t \Theta(-x) = 0$  if  $x > 0$  and  $\Theta(-x) = 1$  if  $x \leq 0$ 

```

---



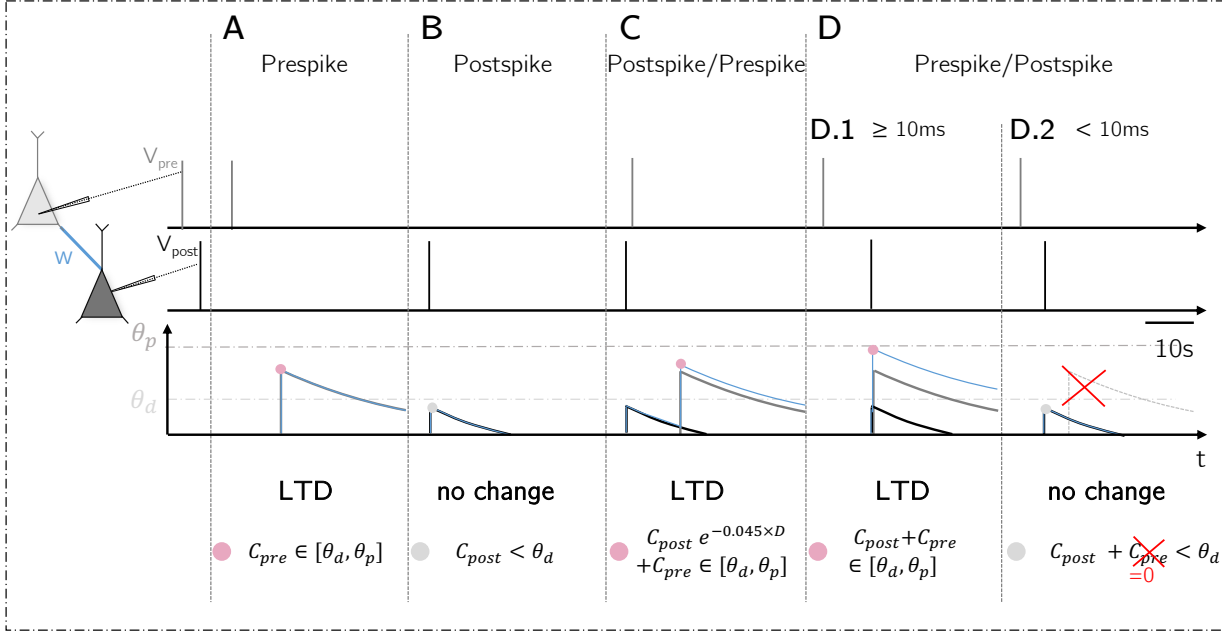


Figure 6.7: [González-Rueda et al., 2018] synaptic rule translated in an hard-bounds calcium-based plasticity rule. A presynaptic (grey) and postsynaptic (black) neuron fire and the spiking pattern favors either LTD (pink dot) or no change (grey dot) as function of the resulting total calcium trace (blue). **A.** Only a prespike favors LTD. **B.** Only a postspike favors no change. **C.** A postspike is followed by a prespike favors LTD. **D.** A prespike is followed by a postspike either favors LTD when the postspike occurs more than 10ms after ( $\Delta t \geq 10\text{ms}$ ) (**D.1**) or favors no change when the postspike occurs within 10ms ( $\Delta t < 10\text{ms}$ ) (**D.2**). In the latter case,  $C_{pre}$  is set at zero to limit the influx of calcium resulting from the presynaptic spike.

## 6.2.2 Evolution of synaptic weights during sleep using algorithm 1

To verify that the algorithm operates as required, we check if the protocol described above corresponds to the STDP curve hypothesized by the algorithm of [González-Rueda et al., 2018] (*i.e.*, the red curve on Figure 6.6). To do so, the STDP protocol consisting of 60 pair pulses of the presynaptic and postsynaptic neurons for various time lag  $\Delta t$  is reproduced computationally at the frequency of 1Hz. It is important to note that this protocol mimics a tonic activity seen in wakefulness behavior and not a bursting activity seen in sleep whose frequency is much higher. However, the reproduction of this protocol allows a first check on the validity of the algorithm 1 that translates the phenomenological synaptic model into a calcium-based model.

As it can be seen on Figure 6.8A.1, the main requirements of the model defined by [González-Rueda et al., 2018] are full-filled: if a presynaptic spike is followed by a postsynaptic spike within 10ms, no synaptic change occurs otherwise the synapses are depressed. Upon completion of this verification, the system is switched into a bursting activity to see how the synaptic strength evolves during the night under this protocol according to their initial weight  $w_0$ . Various external current  $I_{app}$  are applied to the inhibitory cell of the cortical network to test the robustness of the model on various bursting patterns (detailed evolution of synaptic strength for each current are given in Appendix section E.1).

As it can be seen on the leftmost plot on Figure 6.8A.2, a consistent result is obtained for an applied current of  $I_{app} = -4.7[\frac{nA}{cm^2}]$ , *i.e.* the large weights are preserved while the small weights are depressed. However, as soon as current variability is added ( $I_{app2,3}$ ), the results are no longer what is expected and we can observe two distinct behaviors: all weights are either depressed or maintained depending on the applied current  $I_{app}$ . These results highlight the fact that setting  $C_{pre} = 0$  when there is a pair of pre- postsynaptic spikes within 10ms is strict and fragile. Indeed, as soon as the burst pattern slightly changes so that the peaks are no longer within 10 ms but perhaps a little longer, the rule no longer works.

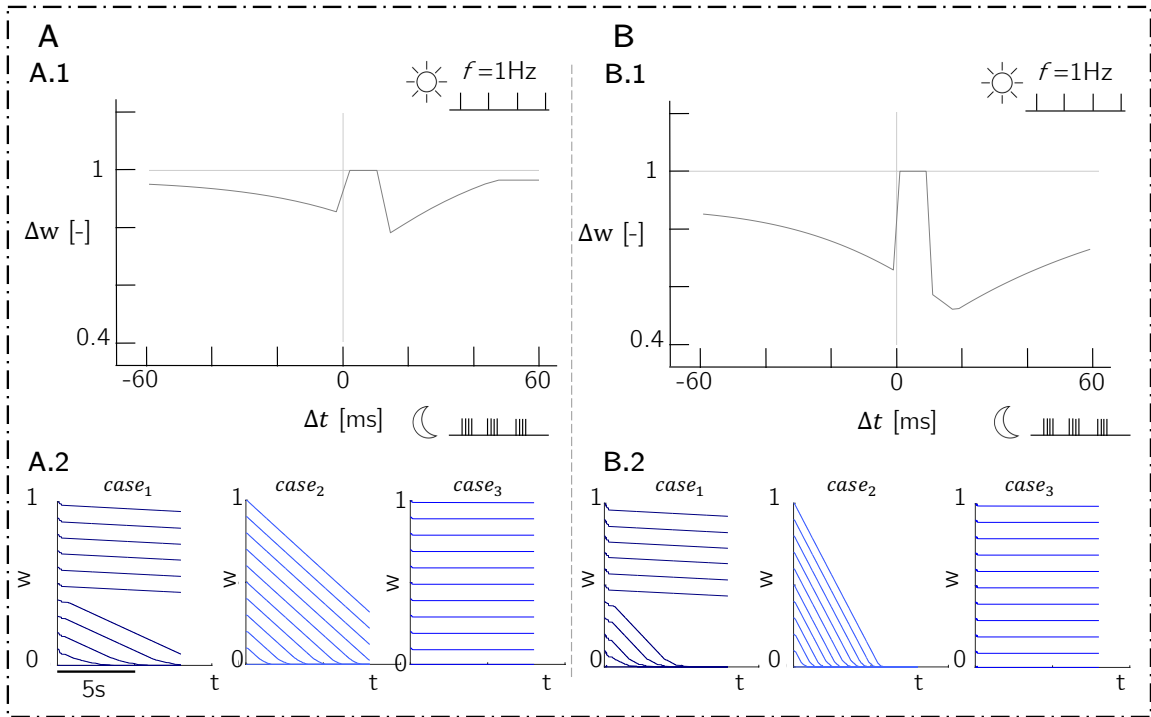


Figure 6.8: [González-Rueda et al., 2018] phenomenological plasticity rule translated into a calcium-based plasticity rule **A**. algorithm 1 correctness is checked by reproducing the STDP protocol at 1Hz (representative of wake-like tonic activity) and the curve matches the expected behavior (**A.1**). Then, the circuit is switched in a bursting activity for various applied current  $I_{app}$ . For  $I_{app} = -4.7[\frac{nA}{cm^2}]$  (case 1) the results are consistent with memory consolidation but for other currents it is not, there is either global depression (case 2, for four  $I_{app}$ ) or global maintenance (case 3, for three  $I_{app}$ ) (**A.2**). **B**. The algorithm is revised to correspond more closely to the STDP experimental data of [González-Rueda et al., 2018] (**B.1**). When switching to a bursting activity, the results are unchanged (**B.2**).

Although the STDP curve represented in Figure 6.8A.1 agrees with the computational algorithm built by [González-Rueda et al., 2018], it should be noted that the synaptic change when the time lag  $\Delta t = 50$ ms does not match with the synaptic change recorded by the experimental protocol realized in the paper (see Figure 6.9). Indeed, the synaptic change induced when  $\Delta t = 50$ ms should be close to the one induced when  $\Delta t = -10$ ms. To impose this constraint we suggest modifying the decay of calcium induced presynaptically in such a way that the total amount of calcium arising from a pair of neurons spiking -10ms apart (post-pre  $\Delta t = -10$ ms) is the same as one arising from a pair of neurons spiking 50ms apart (pre-post  $\Delta t = 50$ ms). To satisfy this constraint Equation 6.8 is derived.

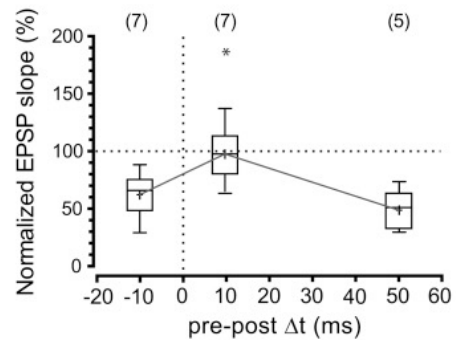


Figure 6.9: STDP experiment during the UP state of SWS: "LTD is prevented by postsynaptic spikes following presynaptic stimulation within 10 ms, while LTD is still present if the pre-post time window is widened to 50 ms" [González-Rueda et al., 2018].

$$C_{post}e^{-\frac{1}{\tau_{Ca_{post}}}\times 20} + C_{pre} = C_{pre}e^{\frac{1}{\tau_{Ca_{pre}}}\times 40} + C_{post} \quad (6.8)$$

where  $C_{post}$ ,  $C_{pre}$  are kept at 0.7 and 1.1 respectively,  $\tau_{Ca_{post}}$  is kept at  $\tau_{Ca} = 22.27ms$  and  $\tau_{Ca_{pre}}$  is found to be equal at 84.35ms by solving this equation.

The resulting STDP curve (Figure 6.8B.1) provides a better fit on the experimental data. As desired, there is more depression of synaptic weights for  $\Delta t=50ms$ . We obtain such a behavior because a presynaptic spike drives the calcium in the depression region ( $C_{pre} 1.1 > \theta_d$ ) and we have modified  $\tau_{Ca_{pre}}$  such that the calcium induced presynaptically decays slower and thus stays longer in the depression region. However, such an implementation implies that the calcium influx induced by a pre-spike is not pumped out of the postsynaptic neuron at the same rate as the calcium influx induced by a post-spike, a phenomenon challenging to prove experimentally.

When switching to a bursting activity, the results remain unchanged compared to the previous STDP curve (Figure 6.8B.2). Thus, the rule developed by [González-Rueda et al., 2018] is not adapted for the calcium-based plasticity model although it is for their neuronal network. The reliability of their achievement to validate this Up state-mediated plasticity during sleep is discussed based on two facts:

- [González-Rueda et al., 2018] used a leaky integrate-and-fire neuron model unable to generate a realistic bursting activity and their neurons fire independently following a Poisson process. However, there exists no biological evidence suggesting that neuronal firing follows a Poisson distribution during SWS. In addition, by using such a stochastic process, the researchers may have artificially increased the probability of postsynaptic firing within a 10ms duration interval for large weights to validate their theory with an artificial computational model.
- [González-Rueda et al., 2018] experimental model is conducted on anesthetized mice and not on sleeping mice, questioning the relevance of such data for the current study.

The last point that need to be addressed regarding these results is *why do we obtain the expected behavior for  $I_{app} = -4.7[\frac{nA}{cm^2}]$  but not for other currents?* As we can see on Figure 6.10, for weak weights (A) the bursting pattern is slightly different than for strong weights (B): the last pair of spikes of one burst is delayed within 10ms for strong weights but not for weak weights. This very slight difference results in a bimodal behavior because, for strong weights, the calcium influx induced presynaptically ( $C_{pre}$ ) is set to 0 because  $\Delta t \in [0, 10]ms$  (case depicted on Figure 6.7D.2) whereas for weak weights it remains at its maximal value (grey curve) (case depicted on Figure 6.7D.1). Therefore, for the latter case, the total calcium influx lies further in the depression region than for strong weights. Although we obtain consistent results, we can already see the fragility of this implementation. Indeed, in strong synapses, the total calcium influx is very close to the depression threshold  $\theta_d$ . A slight change would lead the system to a region of depression and give completely different results.

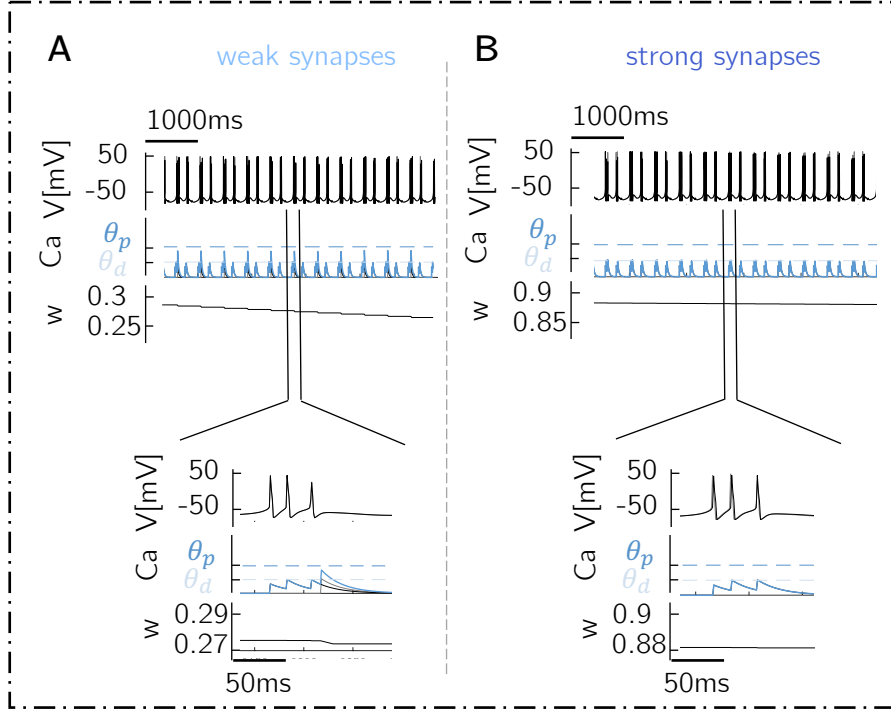


Figure 6.10: *Maintenance of connections for strong synapses and depression for weak synapses for  $I_{app} = -4.7[\frac{nA}{cm^2}]$*  **A.** The bursting pattern for weak synapses is such that the total calcium influx (blue curve) lies in the depression region. This is due to the fact that the last presynaptic spike of the burst is followed by a postsynaptic spike slightly after 10ms such that  $C_{pre}$  (grey curve) is not set at 0 resulting in a total amount of calcium  $\in [\theta_d, \theta_p]$ . **B.** The bursting pattern for weak synapses is such that the total calcium influx (blue curve) lies below the depression region, in the no-change region. This is because the last presynaptic spike of the burst is followed by a postsynaptic spike within 10ms such that  $C_{pre}$  (grey curve) is set at 0 resulting in a total amount of calcium  $\leq \theta_d$ .

### 6.2.3 Change of the original 3-points STDP curve

During their experimental procedure, the researchers used only three different time lags ( $\Delta t = -10, 10, \text{ and } 50\text{ms}$ ) to analyze the change in synaptic strength via the normalized EPSP slope. They subsequently interpreted these results to suggest a behavior where depression occurs all the time except when the prespike is followed by a postspike within 10ms. However, a myriad of other behaviors can take place and still be consistent with these 3 experimental data. Since the Up state-mediated plasticity rule proposed by [González-Rueda et al., 2018] did not recover the desired behavior during sleep, this justifies our suggestion to slightly modify the rules into a different STDP curve that still fits the three experimental data.

#### Extension or retraction of the *no-change* 10ms window

The first idea is to extend the time lag  $\Delta t$  between a prespike and a postspike which leads to no synaptic change. To this end, presynaptic spikes alone still result in synaptic depression, a pair of pre- post- spikes within 10 ms still results in no change in synaptic weight, and now in addition a pair of post- pre- spikes within 5 ms results in no change in synaptic weight as well (Figure 6.11B.1). To implement this, the indicator function  $\Theta()$  defined in algorithm 1 is modified:

$$\dot{c}_{pre} = -\frac{c_{pre}}{\tau C a_{post}} + C_{pre} \times \Theta(-x(t) - 5) \sum_{pre} \delta(t - t_{pre} - D)$$

such that  $\Theta(-x - 5) = 0$  if  $x > -5$  and  $\Theta(-x - 5) = 1$  if  $w \leq -5$ .

The results are not consistent with the memory consolidation hypothesis during sleep (Figure 6.11B.2). For different currents and initial weights, we obtain a similar behavior with the overall maintenance of the weights

and sometimes a slight depression, suggesting that most of the spike pairs are delayed within  $\Delta t \in [-5, 10]$ ms. It must be noted that the window cannot be extended to a longer positive time lag due to biological irrelevance. Indeed, if we expect a postspike to block presynaptic calcium influx 20 ms after the postspike, the neuron would have to block the calcium influx even before the postspike occurred. However, the neuron cannot predict that such an event will occur. This is only possible for time lags up to 10 ms due to the delay between the presynaptic calcium influx and the pre-spike ( $D=10$ ms). Therefore, to extend the *no-change* window to a longer positive time lag, we would need to modify the parameter  $D$  as well.

Alternatively, it is possible to shorten the region in which no synaptic change should occur. Therefore, instead of being between 0 and 10 ms, it could be between 5 and 10 ms (Figure 6.11A.1). Once again, the indicator function  $\Theta()$  defined in algorithm 1 must be modified. In this specific case the evolution of calcium influx induced presynaptically follows :

$$c_{pre} = -\frac{C_{pre}}{\tau C_{a_{post}}} + C_{pre} \times [\Theta(-x(t) + 5) + \Theta(x(t) - 10)] \sum_{pre} \delta(t - t_{pre} - D)$$

such that  $\Theta(-x+5) + \Theta(x-10) = 0$  if  $x \in [5, 10[$  and  $\Theta(-x+5) + \Theta(x-10) = 1$  otherwise. However, shortening the *no-change* window does not lead to better results than elongating it. It can be seen on Figure 6.11A.2, that all weights follow the same behavior (either a global depression of the initial weights or the maintenance of the initial weights) but there is no maintenance of strong synapses and depression of weak synapses.

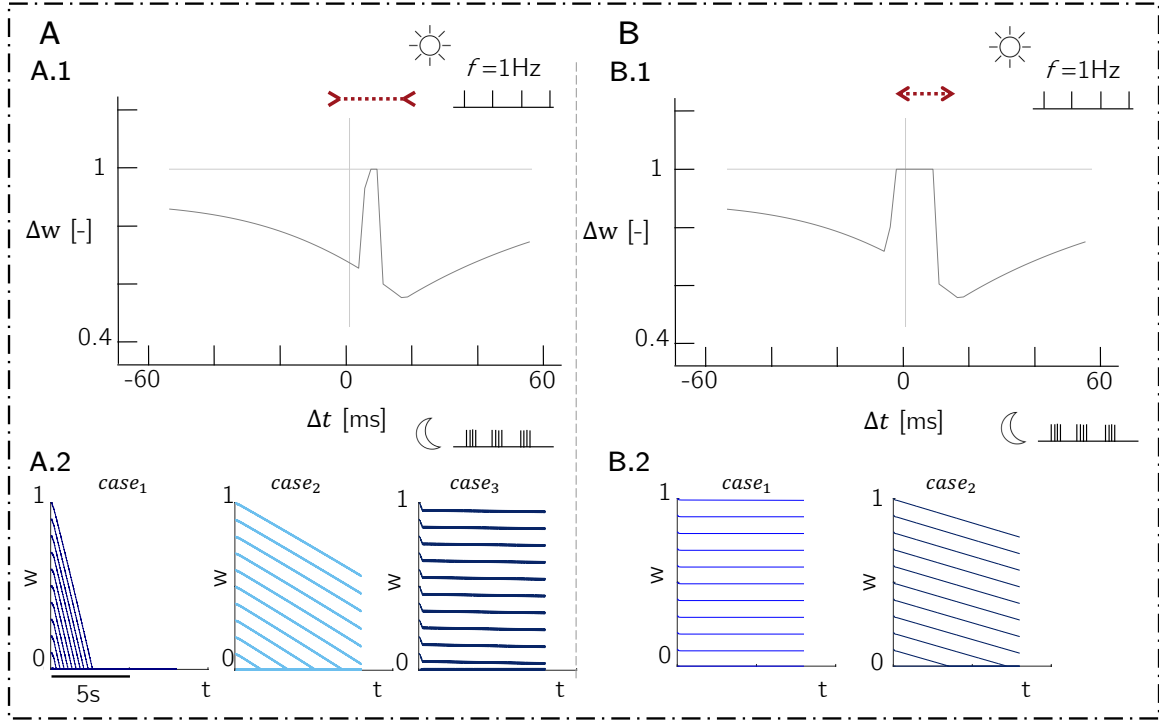


Figure 6.11: *Modification of the length of the no change 10ms window.* **A.** The *no change* window is shortened such that a prespike is followed by a postspike between 5 to 10ms induces no change in synaptic plasticity and all other spiking configurations induce LTD. The STDP curve from the protocol at 1Hz is shown (**A.1**). When switching to a bursting activity, the synaptic weights undergo a very steep global depression (case 1, for four  $I_{app}$ ), a less steep global depression (case 2, for three  $I_{app}$ ) or global maintenance (case 3, for one  $I_{app}$ ) according to the bursting pattern. This is not consistent with memory consolidation during sleep (**A.2**) **B.** The *no change* window is extended such that a prespike is followed by a postspike and a postspike is followed by a prespike within 10ms induce no change in synaptic plasticity and all other spiking configurations induce LTD. The STDP curve from the protocol at 1Hz is shown (**B.1**). When switching to a bursting activity, the synaptic weights undergo a global maintenance (case 1, for four  $I_{app}$ ) or global depression (case 2, for four  $I_{app}$ ) according to the bursting pattern. This is not consistent with memory consolidation during sleep (**B.2**)

## Modification of the *no change* window into a *potentiation* window.<sup>2</sup>

There is no indication that potentiation could not occur when the presynaptic spike is followed by a postsynaptic spike within 10ms. Therefore, we suggest to change the rule saying that "*no change should occur when a prespike is followed by a postspike within 10ms*" into the new rule "*potentiation should occur when a prespike is followed by a postspike within 10ms*" (Figure 6.12A.1). To do this we assume that there is an additional calcium presynaptic supply  $C_{add}=2.7$  instead of imposing  $C_{pre}$  at zero as in algorithm 1. This is once again implemented by modifying the rule  $\Theta()$  such that the indicator function  $\Theta()$  defined in algorithm 1 mediates if  $C_{add}$  is added to the induced calcium  $C_{pre}$  when a presynaptic spike occurs.

$$c_{pre} = -\frac{C_{pre}}{\tau C_{a_{post}}} + \sum_{pre} \delta(t - t_{pre} - D) [C_{pre} + C_{add} \times \Theta(x(t))]$$

such that  $\Theta(x) = 0$  if  $x > 0$  and  $\Theta(x) = 1$  if  $w \leq 0$ .

However, when attempting this configuration, we inevitably experience a saturation phenomenon for all initial weights and currents, which is once again not the desired behavior (Figure 6.12A.2). The saturation speed is governed by the value chosen for  $C_{add}$  and by the bursting pattern. The larger  $C_{add}$  is, the more it leads the neurons in the potentiated zone for a longer time, thus increasing the saturation speed towards  $w=1$  according to Equation 5.7.

As another option, potentiation could take place when the time lag falls within the interval  $\Delta t \in [10, 20]$  (Figure 6.12B.1). To do this, we must now assume that the additional calcium influx is induced postsynaptically and no more presynaptically as the time lags are greater than the delay between the prespike and the presynaptic calcium ( $\Delta t > D$ ). Therefore, algorithm 1 is changed such that  $C_{pre}$  is not imposed at zero and there is an additional postsynaptic calcium influx  $C_{add}=2.7$  when the presynaptic spike is followed by a postsynaptic spike 10ms to 20ms after. To this end, algorithm 2 is proposed.

---

### Algorithm 2: Modification of algorithm 1 to potentiate for $\Delta t \in [10, 20]$ ms

---

**if**  $t=t_{pre}$  **then**

|  $x = 10$

**else**

|  $\tau_x \dot{x} = -1$

**end**

$$c_{post} = -\frac{C_{post}}{\tau C_{a_{pre}}} + \sum_{post} \delta(t - t_{post}) [C_{post} + C_{add} \times [\Theta(x(t) + 10) + \Theta(-x(t))]]$$

$$c_{pre} = -\frac{C_{pre}}{\tau C_{a_{post}}} + C_{pre} \sum_{pre} \delta(t - t_{pre} - D)$$

*s.t*  $\Theta(x + 10) + \Theta(-x) = 1$  if  $x \in ] - 10, 0]$  and  $\Theta(x + 10) + \Theta(-x) = 0$  otherwise

---

The results of (Figure 6.12B.2) show that not all the currents give rise to depression of the initial weights. Some currents lead to depression, one to relative maintenance of initial weights, and others to rapid saturation towards  $w=1$ . This suggests that the different applied currents generate bursting patterns with a variable probability of having a prespike is followed by a postspike in the 10 to 20ms after. Once again for the same current, the initial weights follow a similar pattern, which is not consistent with the memory consolidation hypothesis during sleep.

---

<sup>2</sup>Note that for these experiments  $C_{post}$  is set at 1.37 and no longer at 0.7 and  $\tau C_{a_{pre}} = 29.7712$ ms to satisfy Equation 6.8

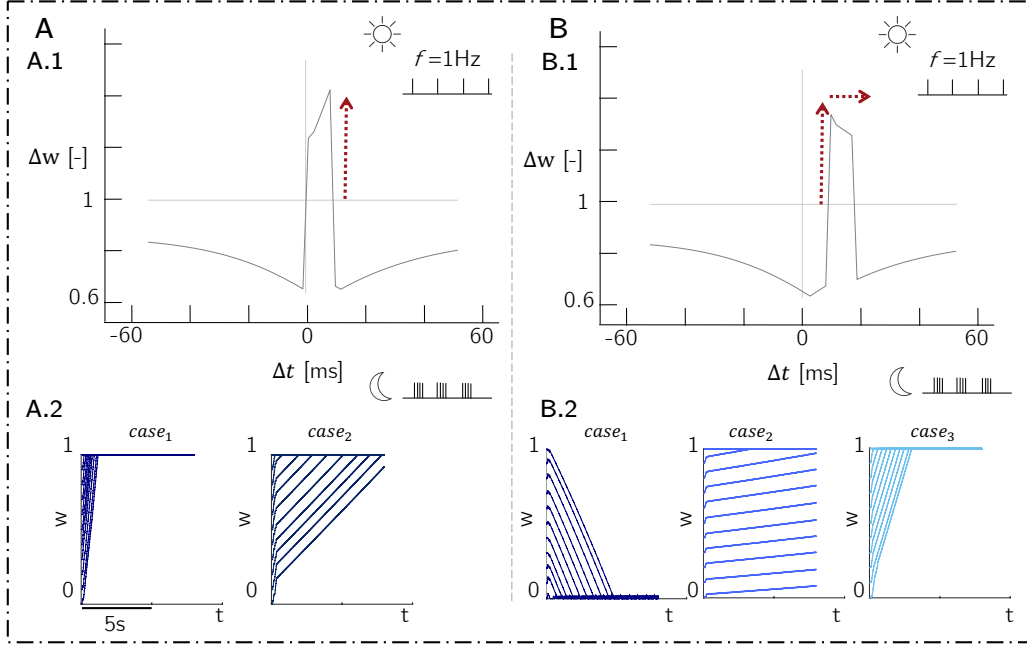


Figure 6.12: *Modification of the no change 10ms window in a potentiation 10ms window* **A**. The synaptic rule is changed such that when a prespike is followed by a postspike within 10ms it induces LTP and all other spiking configurations induce LTD. The STDP curve from the protocol at 1Hz is shown (**A.1**). When switching to a bursting activity, the synaptic weights undergo a global potentiation (either very steep as in case 1 for seven  $I_{app}$  or less steep as in case 2 for one  $I_{app}$ ) whatever the bursting pattern. This is not consistent with memory consolidation during sleep (**A.2**) **B**. The potentiation window is shifted such that a prespike is followed by a postspike 10ms to 20ms after inducing LTP and all other spiking configurations induce LTD. The STDP curve from the protocol at 1Hz is shown (**B.1**). When switching to a bursting activity, the synaptic weights undergo a global depression (case 1, for five  $I_{app}$ ), global maintenance (case 2, for one  $I_{app}$ ), or global potentiation (case 3, for two  $I_{app}$ ) according to the bursting pattern. This is not consistent with memory consolidation during sleep (**B.2**)

### Translation [González-Rueda et al., 2018] phenomenological plasticity rule into a calcium-based plasticity rule by changes in parameterization only

Imposing that no synaptic change occurs for a time lag  $\Delta t \in [0, 10]$ ms by setting  $C_{pre}$  to zero is artificial because, up to our knowledge, there is no biological evidence supporting that a postsynaptic spike prevents any NMDAR-mediated calcium influx induced less than 10ms beforehand by a presynaptic spike. Therefore, we prefer to take a new approach and try to keep the calcium rule as implemented in *model 3*. In this implementation we only play with the parameter values.

The parameters are tuned such that, at  $\Delta t = 10$ ms, the potentiation effect on the synaptic strength counterbalances the depression effect on the latter (Figure 6.13B.1). At  $\Delta t = 10$ ms, because the delay  $D$  between the prespike and the presynaptic-mediated calcium influx into the post-neuron is set to exactly 10ms, the total calcium supply is maximal because  $C_{pre}$  and  $C_{post}$  sum up. Therefore,  $C_{post}$  is set at 1.37 such that when a prespike is followed by a postspike exactly 10ms after, this results in a calcium influx that is slightly in the potentiation area and is able to counterbalanced depression. Subsequently, according to Equation 6.8,  $\tau_{Ca_{pre}}$  is set to 29.7712ms. Moreover,  $\theta_p$  is set back to its initial value 2.009289 defined in *model 3* such that, at  $\Delta t = 10$ ms,  $C_{total} = C_{pre} + C_{post} = 2.47 > \theta_p$ .

As it can be seen on Figure 6.13B.1, at  $\Delta t = 10$ ms and a pairing frequency of 1Hz, this rule enables the balancing between LTP and LTD resulting in a net unchanged synaptic strength. This rule is less artificial as we do not impose any strict conditions but is very sensitive to the choice of parameter values. Indeed, it was very challenging to determine the adequate value for  $C_{post}$  such that the time spent in potentiation coun-

terbalances the time spent in depression. Moreover, this less artificial implementation is limited because it is difficult to play with the shape of the resulting STDP curve obtained at 1Hz. Indeed, for pairing frequencies of 1Hz, all other time lags inevitably lead to depression as the total calcium influx is maximal for  $\Delta t=10\text{ms}$  and this maximal value is set to counterbalance depression but not to take the lead over depression (Figure 6.13A.1).

When switching to a bursting activity (Figure 6.13A.2), saturation towards  $w=1$  is observed for all initial weights and all currents. At first sight, these results seem confusing because the STDP curve obtained following the 1Hz protocol does not drive the network into potentiation at any time lags. However, it is important to remember that, in the bursting activity, the spiking activity does not consist of a pair of pre-post neurons spiking at 1Hz as in the STDP protocol but it is rather a succession of pre-post spikes train followed by a period of silence. Therefore, the pairing frequency is increased and the calcium does not have time to fall back to its "pre-stimulation" value. Accordingly, the resulting calcium influx into the postsynaptic cell from one burst reaches the potentiating area for a longer time (Figure 6.13B.2). At high frequency, potentiation thus takes the lead over depression instead of counterbalancing it and makes this rule is not adequate for bursting activity.

This confirms our preference for using calcium-based models to model synaptic plasticity in the present work. Indeed, in order to provide explanations for certain phenomena, some papers (such as [González-Rueda et al., 2018]) use STDP modeling which relies on the fit of parameters on the experimental data given by the STDP protocol. However, this STDP protocol consists of pairs of spike pulses at 1 Hz and thus does not match the rather irregular activity of a real neuron. This is a major limitation for these models because it can lead to results that do not conform to reality, as we can see here when we translate a phenomenological model into a calcium-based rule that is instead based on known and well-accepted physiological behaviors.



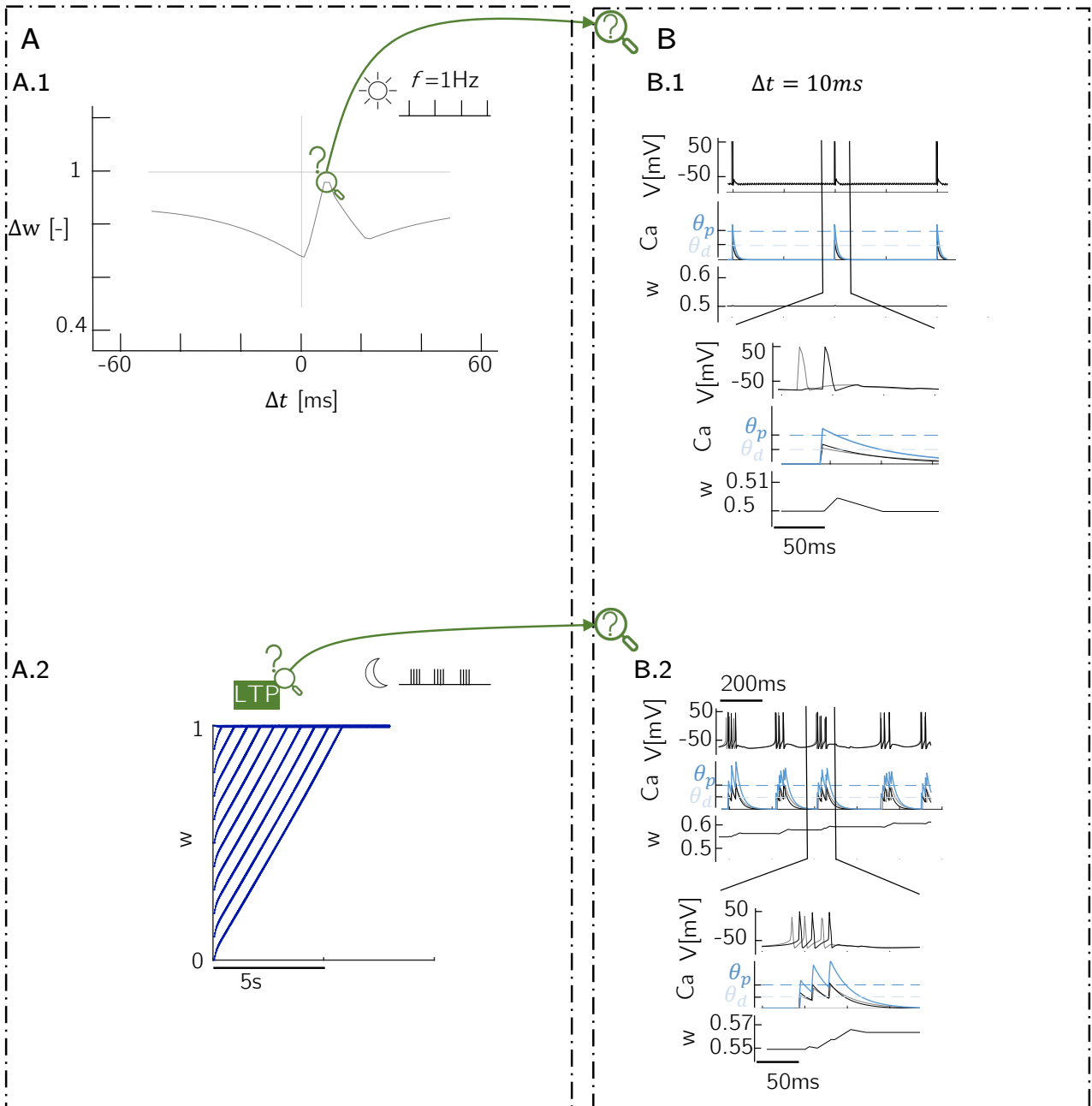


Figure 6.13: Translation of [González-Rueda et al., 2018] phenomenological plasticity rule in a calcium-based plasticity rule by changes in parameterization only **A**. The calcium-based rule **model 3** is no more fundamentally modified as it was done to implement algorithm 1. Instead, the parameters are tuned such that there is no synaptic change at  $\Delta t = 10$ ms and depression otherwise. The STDP curve from the protocol at 1Hz is shown (**A.1**). When switching to a bursting activity, the synaptic weights undergo a global potentiation which is, at first sight, confusing according to the shape of the STDP curve obtained at 1Hz as it contains no potentiating area (**A.2**). **B**. Explanation of this inconsistency between STDP curve at 1Hz and high frequency burst during sleep. For a pairing frequency of 1Hz, a presynaptic spike followed by a postsynaptic spike 10ms later ( $\Delta t = 10$ ms) drives the total calcium influx in the region of potentiation for the time necessary to counteract the passage into the depression region resulting from the calcium decay (**B.1**). During sleep, the calcium influx into the postsynaptic cell resulting from one burst reaches the potentiating area for a time that is long enough such that potentiation takes the lead over depression and this counterbalancing effect that was seen at 1Hz no longer exists (**B.2**).

### 6.3 Summary and conclusion

Firstly, in order to bypass the homeostatic reset phenomenon where all synaptic weights converge towards the same basal value whatever the initial weights, we hand-tuned **model 3**. By speculating that the replay phenomenon classifies the synapses into "strong" and "weak" synapses, we applied different plasticity rules to each group and observed the desired behavior. Such neuromodulation of calcium-based plasticity rules enabled a bimodal behavior that is consistent with memory consolidation, that is maintenance of strong synaptic weights and depression of weak synaptic weights.

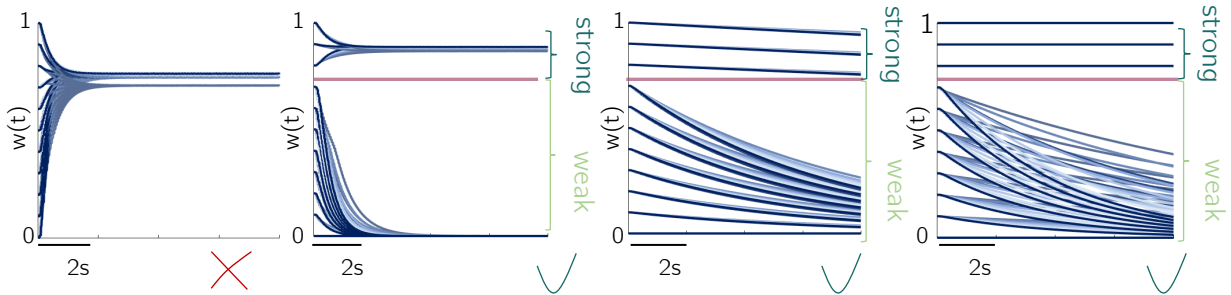
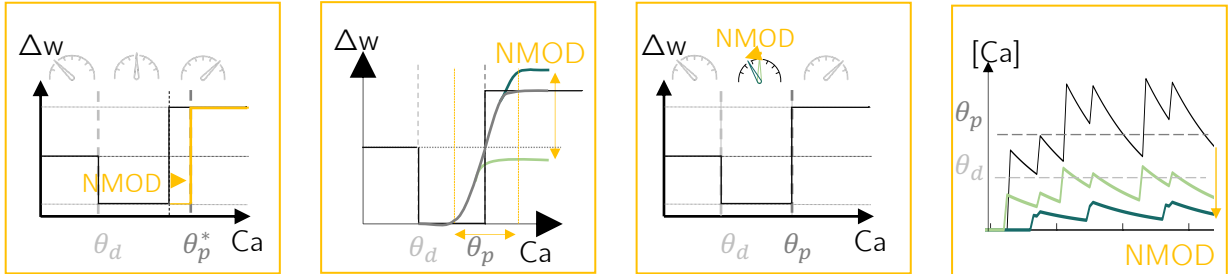
- By decreasing the level of potentiation  $\Omega^p$  for weak weights, we were able to imitate the inhibition of LTP for poor synapses.
- By decreasing the convergence speed in depression  $1/\tau_d$  for strong weights, we were able to imitate a slower depression effect for important information.
- By decreasing the presynaptic and postsynaptic maximal calcium influx  $C_{pre}$  and  $C_{post}$  to a level which lower than the depression threshold  $\theta_d$  for strong weights, we were able to imitate the removal of any form of synaptic plasticity for important information.

These neuromodulated rules were proven to be artificial and fragile, questioning the relevance of this approach. However, these changes were, to some extent, supported by biological facts while others were not or were even controversial. In this sense, it would be of great interest to obtain further experimental evidence of these behaviors during sleep.

Secondly, we translated [González-Rueda et al., 2018] phenomenological Up state-mediated plasticity rule into a calcium-based plasticity rule which enables a simulation closer to the behavior of real neurons in the nervous system. We obtained results consistent with memory consolidation but these results were not robust to variability. As the rule proposed by [González-Rueda et al., 2018] is based on only three experimental points, we also suggested to modify it while preserving these three points. None of these modifications succeeded in obtaining results consistent with memory consolidation during sleep.

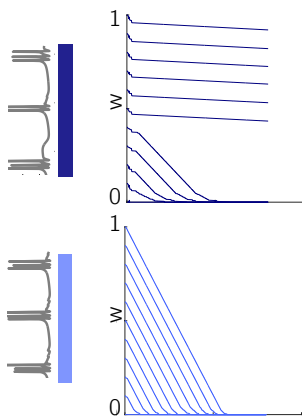
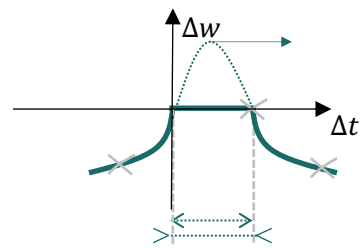
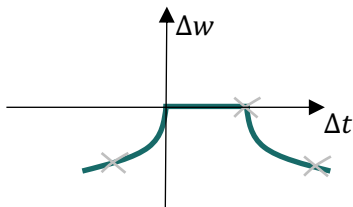
# Neuromodulation of calcium-based synaptic rules during sleep

Hand-tuning of calcium-based rules



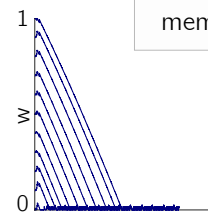
[González-Rueda et al., 2018] in calcium-based rule

✗ Experimental data



✓ Consistent with memory consolidation

✗ Not robust to variability



✗ Not consistent with memory consolidation

## Part IV

# Conclusion and Perspectives

# Chapter 7

## Conclusion and Perspectives

### 7.1 Thesis summary

When we sleep, our brain undergoes an intense period of reconstructing to process and store new important memory content and wash away noisy information. By speculating the role of neuromodulators during sleep, perhaps we can get the chance to understand better how memory consolidation occurs during sleep. To this end, we attempted to address the following key points:

- *What are the well-established notions regarding neuronal processes and the contributions of neuronal synapses in information transmission and memory? (CHAPTER 2) How can this synaptic plasticity be modeled based on experimental data? (CHAPTER 3)*

By fitting wakefulness experimental data provided by [Sjöström et al., 2001], we explained that it is possible to derive a calcium-based plasticity rule from the models proposed by [Shouval et al., 2002, Graupner et al., 2016] which is equivalent but more powerful as it is translated into a formalism that is easier to interpret.

- *How do neuromodulators affect synaptic plasticity in distinct brain regions, and more specifically in the hippocampus and cortex? Do they affect the mechanisms of synaptic plasticity during sleep? (CHAPTER 4)*

Through our literature review, we demonstrated that the role of neuromodulators on synaptic plasticity is widely varied depending on the neuromodulator considered, the type of receptor it affects, the region of the brain, and the state of the neurons. This makes a global conclusion of their actions quite difficult. Nevertheless, it is reasonable to conclude from the literature review that they are capable of inhibiting and enhancing both LTD and LTP. This synaptic plasticity is expressed by changes in the probability of neurotransmitter release, efficacy and the number of AMPA/NMDA receptors on the membrane surface, and gene regulation. Moreover, some neuromodulators (acetylcholine, noradrenaline, BDNF) are also involved in the tagging process of specific synapses for their strengthening during sleep. Others (serotonin, dopamine, histamine, BDNF) are involved in the regulation of different sleep rhythms (slow-wave activity, spindles, ripples, theta rhythms), which in turn are considered to influence memory.

- *What is the homeostatic reset associated with modeling of plasticity during sleep? How can this phenomenon, which is inconsistent with memory consolidation, be demonstrated analytically? (CHAPTER 5) Can the role of neuromodulators on synaptic plasticity be used to modify these plasticity models and overcome this homeostatic reset? (CHAPTER 6)*

As shown by [Jacquerie et al., 2022], when a synaptic rule parameterized to fit wakefulness experimental data is switched into a bursting activity that takes place during sleep, all synaptic weights converge towards the same basal value whatever the initial weights. This so-called homeostatic reset is inconsistent with memory consolidation as it would mean that strong synapses coding for important memories would reset towards the same value as weak synapses coding for unnecessary information and any knowledge would be memorized equally. However, human experience proves that the content of the morning lecture is more likely to be memorized than the color of the t-shirt worn by a stranger in the subway. It was

intuitively demonstrated that "the origin of the homeostatic reset lies in the model structure, not its parameterization" [Jacquiere et al., 2022] and we were able to quantify this phenomenon by deriving an analytical prediction of the convergence value. We further showed that this equation was able to correctly predict the behavior of the model during wakefulness and sleep.

Next, the synaptic rule has been modified to bypass the homeostatic reset phenomenon. We tuned the threshold of potentiation ( $\theta_p$ ), level of potentiation ( $\Omega^p$ ), the convergence speed in depression ( $1/\tau_d$ ), and the maximal calcium influx  $C_{pre}$  and  $C_{post}$  to observe the maintenance of strong weights and the depression of weak weights. Each of these changes were coupled with biological facts supporting or contradicting the relevance of such a change. Although the results obtained were artificial and fragile, we have succeeded in obtaining the expected bimodal behavior. Finally, we were able to translate the interesting phenomenological rule proposed by [González-Rueda et al., 2018] into a biological rule and obtained results coherent with memory consolidation during sleep. However, these results were not robust to variability. As the rule proposed by [González-Rueda et al., 2018] is based on only three experimental points, we also suggested modifying it while preserving these three points. None of these modifications succeeded in obtaining results consistent with memory consolidation during sleep.

## 7.2 Perspectives

### 7.2.1 Presence of variability in cortical network

So far, the circuit is composed of an identical presynaptic and postsynaptic neuron (i.e., they have the same maximal intrinsic conductances) and the inhibitory neuron has the same external current applied throughout the whole bursting pattern. To simulate a neuronal circuit that reflects *in-vivo* conditions as closely as possible, we decide to add variability in these two properties (i.e., neuronal variability and bursting variability).

#### Neuronal variability

As it can be seen on Figure 7.1, simulating a heterogeneous cortical network does not remove the homeostatic reset phenomenon. The heterogeneity rather changes the bursting pattern of each cell and subsequently the resulting calcium influx from the latter. Therefore, the time spent in potentiation ( $\alpha_p$ ) and depression ( $\alpha_d$ ) is increased or decreased and the convergence value, as predicted by Equation 5.1, is different for each network.

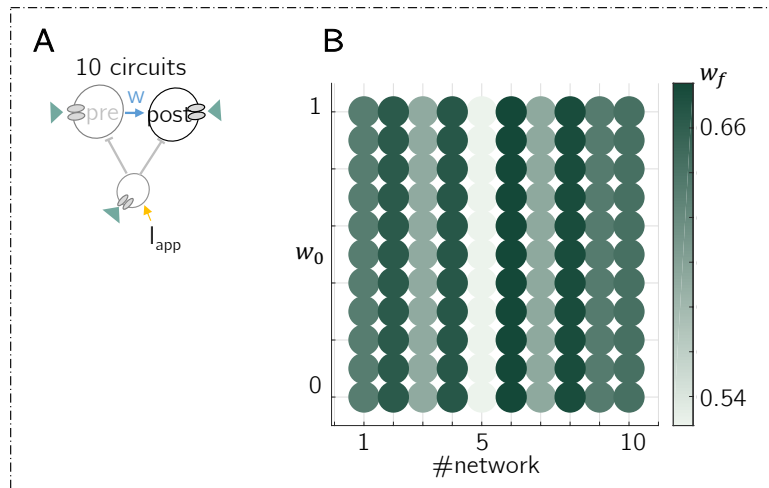


Figure 7.1: *The homeostatic reset phenomenon remains even in the presence of neuronal variability.* **A.** 10 cortical circuits composed of three heterogeneous cells are simulated during bursting activity. **B.** The evolution of synaptic weights initially set at  $w_0$  ranging from 0 (i.e., weak connections) to 1 (i.e. strong connections) is analyzed. To make the cells heterogeneous, the maximal conductance values are varied within an interval of 10%. As it can be seen, for every circuit, all weights converge towards the same final value  $w_f \in [0.54, 0.66]$  depending on the considered circuit.

It is important to note that the transition from tonic to burst activity when an external current is applied to the inhibitory cell must be checked. Indeed, playing with the maximum conductances can cause a cortical network that is no longer able to generate this switch and it is, therefore, important to perform this verification step.

### Bursting variability

Throughout the night, it is unlikely that the neurons exhibit a regular burst of activity such as the one that can be observed when the same external current  $I_{app}$  is applied to the inhibitory cell during the whole sleep simulation (see burst pattern in Appendix section C.2). Thus, for the same sleeping simulation,  $I_{app}$  is no longer a constant but rather a sinusoidal function which has as period  $\rho$  (Figure 7.2A), a minimum value of  $I_{app} = -4.4[\frac{nA}{cm^2}]$  and a maximal value of  $I_{app} = -4.0[\frac{nA}{cm^2}]$ . The cortical network is simulated for 3 distinct periods  $\rho = 1, 4, \text{ and } 7.5s$ . We observe that the homeostatic reset remains for each of them (Figure 7.2B). The only difference with the previous results is that instead of converging towards a single value as it was the case when the applied current  $I_{app}$  was fixed throughout the whole simulation, the convergence value fluctuates with a period of  $\rho$ . Actually, the maximal value is the  $w_{HR}$  obtained when the network is simulated with a fixed  $I_{app} = -4.4[\frac{nA}{cm^2}]$  while the minimal value is the  $w_{HR}$  obtained with a fixed  $I_{app} = -4.0[\frac{nA}{cm^2}]$ . This makes sense as the applied current is a sinusoidal ranging from  $-4.4[\frac{nA}{cm^2}]$  to  $-4.0[\frac{nA}{cm^2}]$  with a period of  $\rho$ .

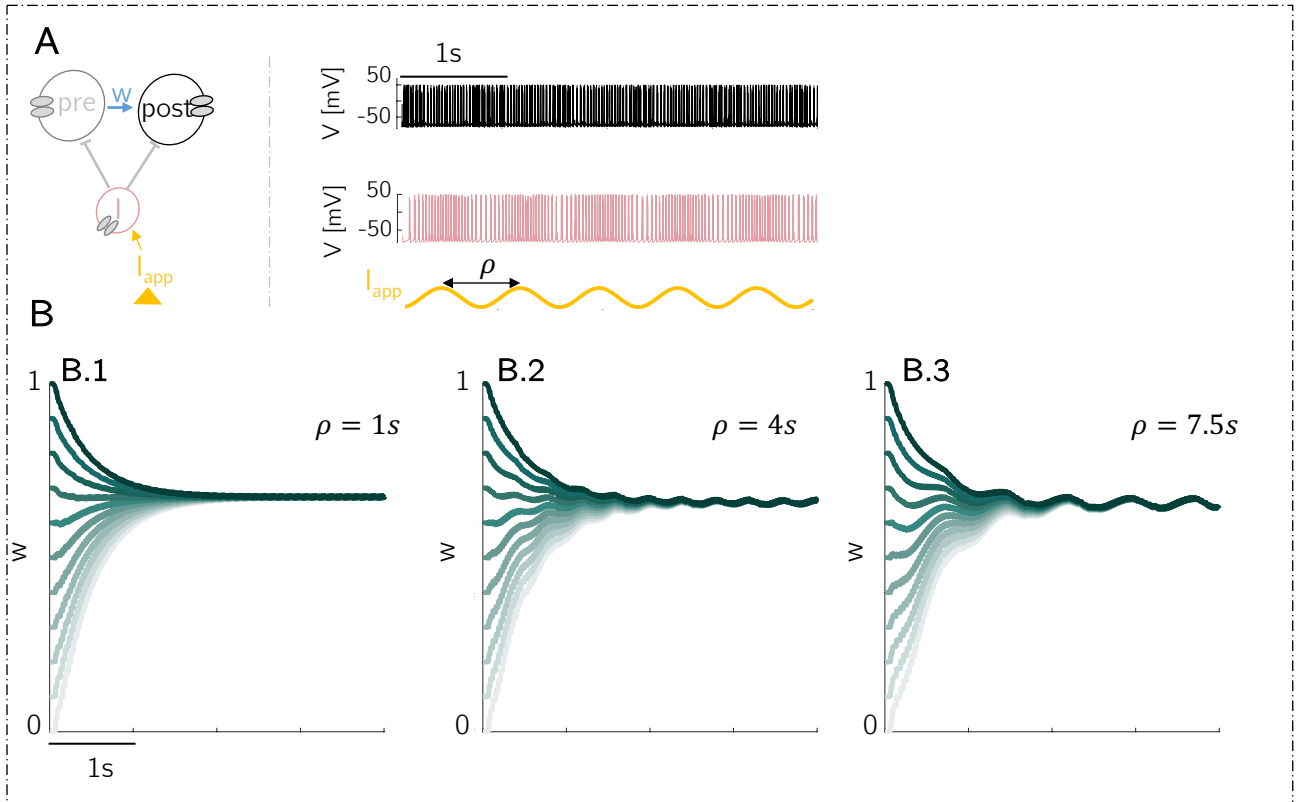


Figure 7.2: *The homeostatic reset phenomenon remains even in the presence of bursting variability.* **A.**  $I_{app}$  is no longer a constant but a sinusoidal function which has as period  $\rho$  with a minimal value of  $I_{app} = -4.4[\frac{nA}{cm^2}]$  and a maximal value of  $I_{app} = -4.0[\frac{nA}{cm^2}]$ . This enables an irregular bursting pattern throughout one night which is closer to *in-vivo* conditions. **B.** The cortical network is simulated for 3 distinct period  $\rho = 1, 4 \text{ and } 7.5s$ . All weights converge towards the same value, the latter fluctuating over a period of  $\rho$  between the minimum value corresponding to the reset value  $w_{HR}$  obtained when  $I_{app}$  is fixed at  $4.0[\frac{nA}{cm^2}]$  and the maximal value corresponding to the reset value  $w_{HR}$  obtained when  $I_{app}$  is fixed at  $-4.7[\frac{nA}{cm^2}]$ .

The above results suggest that the homeostatic reset is a resilient phenomenon and that it is difficult to disentangle from it. Despite all sorts of variabilities added to the circuit to make it more similar, all weights converge towards the same value due to the plasticity rule structure.

## 7.2.2 Taking advantage of the homeostatic reset: the AMPAfication

### Introductory scenario: representational drift in a larger neuronal network undergoing neuromodulated plasticity rules

Various studies have shown that when mice follow a spatial trajectory, place cells (*i.e.*, cells in the hippocampus that spike at a specific location in an environment) activate sequentially in the brain [Atherton et al., 2015, Leutgeb et al., 2005]. More recently, studies have observed that, in addition, the sequence of cells coding for this same trajectory changes over time when the mouse is again confronted with this environment. This process is referred to as "representational drift" by [Rule et al., 2019]. Let's consider the following scenario depicted on Figure 7.3: suppose there is, somewhere in the brain, a network of four neurons respectively named  $neuron_1$ ,  $neuron_2$ ,  $neuron_3$ , and  $neuron_4$  that are coding for the spatial trajectory represented by the sequence of colors red-brown-orange (Figure 7.3A.1). This network has twelve synapses because we consider bipartite synapses and we consider bi-directional communication between two cells (*i.e.*,  $neuron_i$  can be the presynaptic cell of  $neuron_j$  on day 1 while on day 2  $neuron_i$  can be the postsynaptic cell of  $neuron_j$ ). On day 1, a mouse is placed in this environment and learns the specific trajectory. At this moment, the group of four neurons encodes this information by spiking sequentially in the order  $neuron_4 \rightarrow neuron_1 \rightarrow neuron_3 \rightarrow neuron_2$  (Figure 7.3A.2). Then the mouse goes to sleep and we assume that during sleep, the plasticity rule is such that strong synapses are exempted from downscaling. On day 2, the same environment is presented to the mouse. This time, the same group of four neurons encode this same information but in a different sequence lets say  $neuron_2 \rightarrow neuron_4 \rightarrow neuron_3 \rightarrow neuron_1$ . This way, some synapses go from being highly active on day 1 but silent on day 2 although the same task is performed [Prsa et al., 2017]. As these synapses are silent, no synaptic plasticity (nor LTP or LTD) takes place over them. Once again, the mouse goes to sleep and strong synapses are exempted from downscaling. The same wake/sleep cycle is repeated until each synapse has been activated during the day via a representational drift (Figure 7.3B.1).

To implement this scenario, we built a larger heterogeneous network composed of one inhibitory cell and four other neurons. Within these cells, pairs of presynaptic and postsynaptic neurons are manually created to correspond to the scenario and these pairs are strongly correlated during tonic activity. To make them fire sequentially, the first neuron follows a Poisson point process at a rate of 25ms, and the following neurons undergo the same activity sequentially with a delay that itself follows a Gaussian distribution around a mean of 10ms (Figure 7.3A.2). Upon sleep, synapses undergo the neuromodulated rule defined in the previous chapter by Equation 6.7 so that strong weights are maintained and weak weights are depressed. The critical weight is modified and set at  $w_{crit} = 0.6$ .

On Figure 7.3B.2, we can see the evolution of the synaptic weights of each synapse in the network following the scenario described above. At the end of the simulation, the neuronal network is saturated because all synaptic weights have almost reached their maximal value. Therefore, it is impossible to encode novel information, which makes no sense. Thus, using a neuromodulated rule that seems consistent with memory consolidation over one night is actually not a good solution when multiple wake/sleep cycles are considered in combination with the "representational drift". But then, *what should the rule do?*



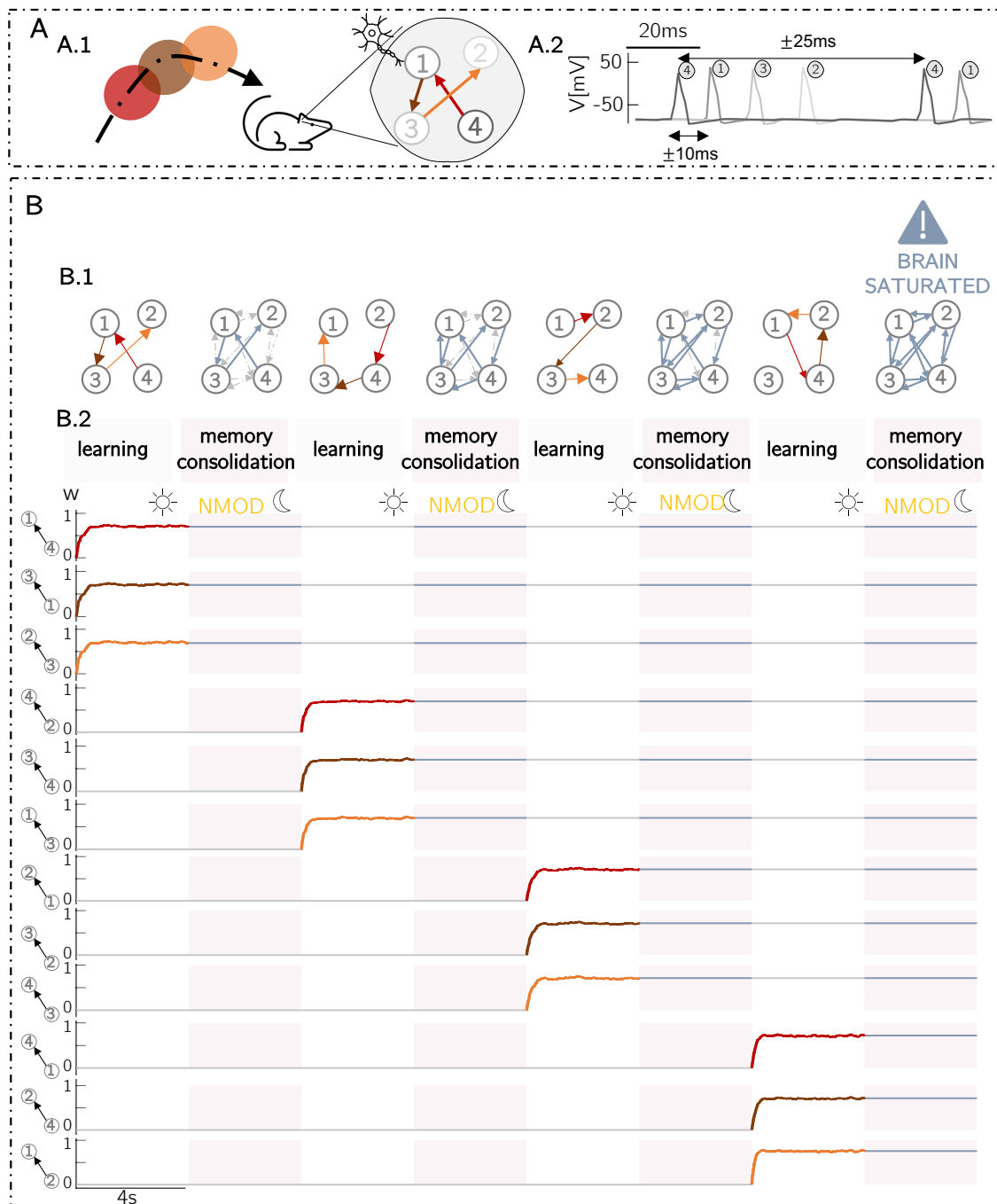


Figure 7.3: *Inconsistency with memory consolidation across wake/sleep cycles: scenario of representational drift and neuromodulation of plasticity during sleep* **A.** A mouse follows a spatial trajectory represented by colored circles (**A.1**). During this task, at the cellular level, cells are sequentially coding for this trajectory. In this case, cell number 4 fires, then cell number 1, cell number 3, and finally cell number 2. The order of the sequence is represented by the respective order of colors (**A.2**). Each day, the mouse must learn the same trajectory. **B.** Across various wake/sleep cycles, different combinations of cells are activated when the mouse follows the same spatial trajectory on different days (mimicking a representational drift) (**B.1**). During wakefulness, connectivity strengthens between activated neurons and during sleep, each of these synapses are consolidated following a neuromodulated calcium-based plasticity rule (**B.2**). After a certain number of wake/sleep cycles, every synapse is consolidated and there is no memory left for novel information. The brain is saturated.

## AMPAfication: concept

As explained above, using neuromodulated calcium-based rules during sleep brings the system to saturation when we consider a larger neuronal network undergoing representational drift over several wake/sleep cycles. This is inconsistent with memory consolidation. However, fitting a calcium-based rule on wakefulness data and using it during sleep leads to the homeostatic reset phenomenon, which is also not consistent with memory consolidation.

One alternative is to take advantage of the homeostatic reset and consider that, during sleep, the early phase of plasticity (represented by the parameter  $w$  in our computational model) is transformed into a more persistent late phase of plasticity when new proteins and ribonucleic acid messengers (mRNAs) are synthesized to support the maintenance of plastic changes by, for example, increasing the number of available AMPA receptors at the membrane surface [Bliss and Cooke, 2011] (represented by the AMPA conductance  $g_{AMPA}$  in our computational model). Thus, during bursting activity, there would be a shift from short-term connectivity strength expressed by  $w$  to a longer-term strength expressed by  $\bar{g}_{AMPA}$  such that the strength between the presynaptic and postsynaptic neuron is unchanged (because  $\bar{g}_{pre,post} = \bar{g}_{AMPA}w$  see Equation C.1). This process can be referred to as "AMPAfication" and a schematic representation of the latter is depicted on Figure 7.4.

Adding an equation to write the evolution of  $\bar{g}_{AMPA}$  over time would allow us to have an additional degree of freedom in our model without the need for neuromodulation of the rule which has been shown to be fragile. Although this value also has a maximum value, this variable represents structural changes. Therefore, the limits are physical as opposed to the limits observed with  $w$  and the saturated brain explained above as an introduction. Thus, given these strengths, this implementation is an opportunity to be explored.

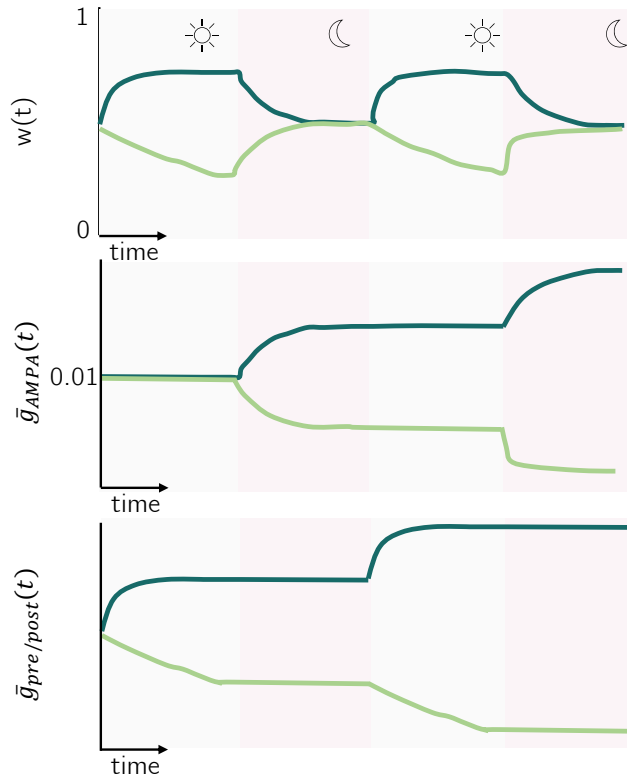


Figure 7.4: *Schematic representation of the AMPAfication.* During wakefulness,  $w$  representing early-phase of synaptic plasticity increases for correlated synapses (dark green) and decreases for uncorrelated synapses (light green) while  $\bar{g}_{AMPA}$  representing late-phase of synaptic plasticity does not change. During sleep,  $w$  for weak and strong synapses converge towards the same basal value due to the homeostatic reset. Conversely,  $\bar{g}_{AMPA}$  increases (resp. decreases) to balance the homeostatic reset of  $w$  for strong (resp. weak) weights such that  $\bar{g}_{pre,post} = \bar{g}_{AMPA}w$  representing the strength between the presynaptic and postsynaptic neuron is unchanged.

Part V

Appendix

# Appendix A

## Elements of neurophysiology

### A.1 Thalamocortical neurons: EEG and cellular signatures

The bursting activity during slow waves sleep (Figure A.1) can be explained by the properties of a calcium-mediated low-threshold current [McCormick and Bal, 1997, Deleuze et al., 2012]. These current are generated by T-type calcium channels which have activation and inactivation gates. Similarly to sodium channel gates, the activation gate of the T-type calcium channels opens with depolarization (*i.e.* increasing membrane potential) while the inactivation gate closes with depolarization. The difference yields in the gates kinetics: while the time scale of sodium activation is around 0.1ms and that of sodium inactivation is around 10ms, the time scale of calcium activation is in turn slower (around 5ms) and that of inactivation much slower (100ms) (see Figure A.2 ) [Steriade et al., 1993].

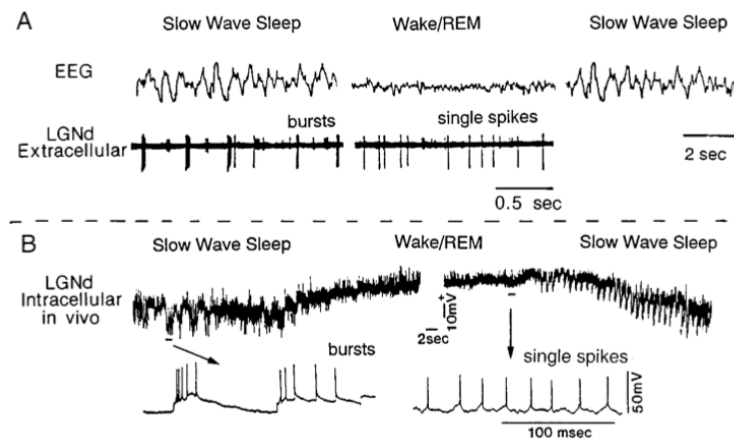


Figure A.1: Electroencephalogram (EEG), extracellular and intracellular in vivo recordings of the lateral geniculate relay neurons (LGNd). During periods of slow-wave sleep, the EEG exhibits synchronous slow waves, and LGNd relay neurons discharge in bursts of action potentials (A). In contrast, during waking LGNd neurons fire in tonic mode (A). Intracellular recordings in vivo during these transitions indicate that they are accomplished by depolarization of the membrane by 10–20 [mV] (B). [McCormick and Bal, 1997]

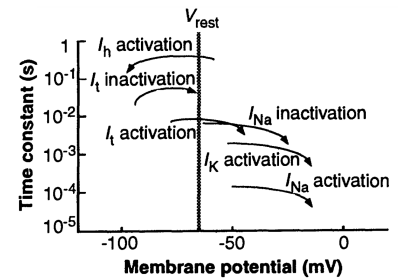


Figure A.2: Timescales of activation and inactivation gates of main voltage-dependent ionic currents in thalamocortical cells. Activation (resp. inactivation) starts on the left side of the arc and are fully activated (resp. inactivated) on the right side except of  $I_n$  which is the other way around. [Steriade et al., 1993]

### A.2 Others sleep concepts

Other important "sleep concepts" are sleep pressure after prolonged wakefulness (sleep deprivation) and circadian rhythm.

- Sleep pressure is thought to be due to a chemical called adenosine, which is elevated at the end of the day (and keeps increasing during prolonged wakefulness) and returns to normal after sleeping [Siegel, 2009]. Caffeine acts as an adenosine receptor antagonist (*i.e.*, a chemical that deactivates a receptor to produce a biological response) to maintain wakefulness [Boutrel and Koob, 2004].
- Circadian rhythm is essentially mediated by melatonin. It was shown in 1938 by the researchers Kleitman and Richardson [Kleitman, 1939] that our biological rhythm is approximately 24h but not precisely 24h. Later, it was shown that it is thanks to the light day and its inhibitory effect on the hormone melatonin, that we can regulate our circadian rhythm [Lockley et al., 1997]. The suprachiasmatic nucleus regulating melatonin secretion by the pineal gland is, therefore, the conductor of the sleep/wake cycle [Benarroch, 2008].

# Appendix B

## Neurons models description

### B.1 Conductance-based modeling

[Hodgkin and Huxley, 1952] compared the neuron membrane with an electric circuit model where the phospholipid bilayer is modeled as a capacitor and the quantity of open channels is assimilated to a variable conductance for each particular ion the channel is selective to. The Nernst potential (*i.e.* the membrane potential for which the electrical and osmotic forces cancel each other out for a specific ion) is modeled as a battery. This analogy is represented on Figure B.1.

Ion channels are responsible for the transfer of ions into and out of the cell. When considering the electrical behavior of neurons, we are mainly interested in the distribution of sodium ( $Na^+$ ) and potassium ( $K^+$ ) ions around the membrane. These ions being by definition charged, there is a potential difference between the inside and the outside of the cell. This potential is called membrane potential  $V_m$ .

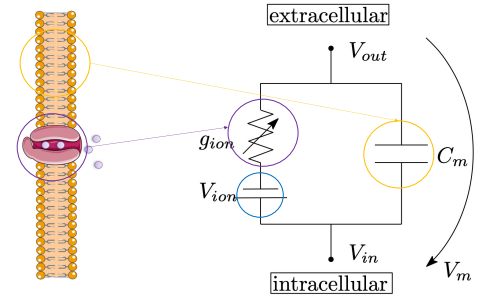


Figure B.1: Neuron membrane as an electric circuit model - phospholipid bilayer as a capacitor (orange circle), channels as conductance (purple circle) and Nernst potential as battery (blue circle) ([Bear et al., 2016])

Via Kirchhoff's law and Ohm's law, it is possible to derive the general Equation B.1 for the variation of the membrane potential  $V_m$  when considering multiple ions.

$$C_m \frac{dV_m}{dt} = - \sum_{ion} I_{ion} + I_{app} \quad (B.1)$$

where  $I_{app}$  is the applied current,  $C_m$  the membrane capacitance and  $I_{ion}$  the voltage-dependent ionic currents.

For each considered ion, Hodgkin and Huxley assumed that a maximum conductance  $\bar{g}_{ion}$  may be reached when all channels are open and that each channel has activation (and/or inactivation) gates regulating their opening. This resulted into the general following expression for ionic currents:

$$I_{ion} = \bar{g}_{ion} m_{ion}^{p_{ion}}(V_m) h_{ion}^{q_{ion}}(V_m) (V_m - V_{ion}) \quad (B.2)$$

where  $m_{ion}$  represents activation gate variable,  $h_{ion}$  represents inactivation gate variable for each ion and  $V_{ion}$  is the Nernst potential of the ion. In Hodgkin and Huxley experiment, they performed a curve fitting of the curves obtained experimentally to find the parameters  $p_{ion}$  and  $q_{ion}$  that best match the experimental data.

Finally, to complete the system, we can write the general form of the equation describing the variations of the fraction of open channels with time using the mass action law:

$$\frac{dm_{ion}}{dt} = \frac{(m_{ion,\infty}(V_m) - m_{ion})}{\tau_{m_{ion}}(V_m)}$$

$$\frac{dh_{ion}}{dt} = \frac{(h_{ion,\infty}(V_m) - h_{ion})}{\tau_{h_{ion}}(V_m)}$$

where  $m_{ion,\infty}$  and  $h_{ion,\infty}$  are the steady-state values of the activation and inactivation variables, and  $\tau_{m_{ion}}$  and  $\tau_{h_{ion}}$  are their respective voltage-dependent time constants.

As previously said, Hodgkin and Huxley model focuses mostly on sodium, which have one activation and one inactivation channel, and potassium which have one activation channel. The complete model is therefore composed of four equations that can served as a basis in other neurons modeling:

$$C_m \dot{V}_m = -\bar{g}_{Na} m_{Na}^3 h_{Na} (V_m - V_{Na}) - \bar{g}_K m_K^4 (V_m - V_K) - \bar{g}_{leak} (V_m - V_{leak}) + I_{app}$$

$$\dot{m}_{Na} = \frac{m_{Na,\infty} - m_{Na}}{\tau_{m_{Na}}}$$

$$\dot{h}_{Na} = \frac{h_{Na,\infty} - h_{Na}}{\tau_{h_{Na}}}$$

$$\dot{m}_K = \frac{m_{K,\infty} - m_K}{\tau_{m_K}}$$

## B.2 [Drion et al., 2018]

In [Drion et al., 2018] model, a single-compartment Hodgkin-Huxley model was used for the neuron model. It is composed of leak current  $I_{leak}$ , a transient sodium current  $I_{Na}$ , a delayed-rectifier potassium current  $I_{K,D}$ , a T-type calcium current  $I_{Ca_n,T}$ , a calcium-activated potassium current  $I_{K,Ca_n}$  and a hyperpolarization activated cation current  $I_H$ . According to Equation B.1, the variation of the membrane potential is

$$C_m \dot{V}_m = -I_{leak} - I_{Na} - I_{K,D} - I_{Ca_n,T} - I_{K,Ca_n} - I_H + I_{app}$$

The complete model is the following :

$$C_m \dot{V}_m = -\bar{g}_{Na} m_{Na}^3 h_{Na} (V_m - V_{Na}) - \bar{g}_{K,D} m_{K,D}^4 (V_m - V_K)$$

$$- \bar{g}_{Ca_n,T} m_{Ca_n,T}^3 h_{Ca_n,T} (V_m - V_{Ca_n}) - \bar{g}_{K,Ca_n} m_{K,Ca_n,\infty}([Ca_n]) (V_m - V_{Ca_n})$$

$$- \bar{g}_H m_H (V_m - V_H) - \bar{g}_{leak} (V_m - V_{leak}) + I_{app}$$

$$\dot{m}_x = \frac{m_{x,\infty}(V_m) - m_x}{\tau_{m,x}(V_m)} \quad \text{for } x = Na; K,D; Ca_n,T; K,Ca_n; H$$

$$\dot{h}_x = \frac{h_{x,\infty}(V_m) - h_x}{\tau_{h,x}(V_m)} \quad \text{for } x = Na; Ca_n,T$$

where  $m$  represents activation variables and  $h$  represents inactivation variables. For more details about parameter values and model configuration please refer to Table B.1 and Table B.2.

Calcium dynamics present in the activation of the calcium-activated potassium current  $m_{K,Ca_n,\infty}([Ca_n]) = (\frac{[Ca_n]}{[Ca_n] + K_D})^2$  follows the equation  $[Ca_n] = -k_1 I_{Ca_n,T} - k_2 [Ca_n]$  where the rate parameters  $k_1$  and  $k_2$  are 0.1 and 0.01 respectively and  $K_D = 170$ . Finally, the membrane capacitor  $C_m$  is  $1 [\frac{F}{cm^2}]$

	$m_{x,\infty}(V_m) = h_{x,\infty}(V_m) = \frac{1}{1+\exp(\frac{V-V_{half}}{V_{slope}})}$		$\tau_{m,x}(V_m) = \tau_{h,x}(V_m) = \frac{A-B}{1+\exp(\frac{V-D}{E})}$			
	$V_{half}$	$V_{slope}$	<b>A</b>	<b>B</b>	<b>D</b>	<b>E</b>
$m_{Na}$	-35.5	-5.29	1.32	1.26	-120	-25
$h_{Na}$	-48.9	5.18	$\tau_{h,Na}(V_m) = \frac{0.67}{1+\exp(\frac{V+62.9}{-10})} \times (1.5 + \frac{1}{1+\exp(\frac{V+34.9}{3.6})})$			
$m_{Kd}$	-12.3	-11.8	7.2	6.4	-28.3	-19.2
$m_{Ca_nT}$	-67.1	-7.2	21.7	21.3	-68.1	-20.5
$h_{Ca_nT}$	-80.1	5.5	410	179.6	-55	-16.9
$m_H$	-80	6	272	-1149	-42.2	-8.73

Table B.1: Parameter values for steady-state channel gating curves and time-constant curves for the different ion channels present in the model neuron in [Drion et al., 2018]

$x$	$V_x$ [mV]	$\bar{g}_x [\frac{mS}{cm^2}]$
$Na$	50	170
$K$	-85	/
$K,D$	/	40
$Ca_n$	120	/
$Ca_n,T$	/	0.55
$K,Ca_n$	/	4
$H$	-20	0.01
$leak$	-59	0.055

Table B.2: Parameters values used in simulations for the the Nerst potential of each considered ion  $V_{ion}$  and maximal conductance  $\bar{g}_{ion}$  values present in the model neuron in [Drion et al., 2018].



# Appendix C

## Cortical network

### C.1 Connection between cells

#### Excitatory (AMPA) and inhibitory (GABA) connections

$$\begin{aligned}I_{AMPA} &= \bar{g}_{AMPA}s_{AMPA}(V - 0) \\I_{GABA_A} &= \bar{g}_{GABA_A}s_{GABA_A}(V - V_{Cl}) \\I_{GABA_B} &= \bar{g}_{GABA_B}s_{GABA_B}(V - V_K)\end{aligned}$$

where  $V_{Cl}=-70[\text{mV}]$ ,  $V_K=-85[\text{mV}]$ ,  $\bar{g}_{AMPA}$ ,  $\bar{g}_{GABA_A}$ ,  $\bar{g}_{GABA_B}$  are the receptors conductance, and  $s_{AMPA}$ ,  $s_{GABA_A}$ ,  $s_{GABA_B}$  are variables whose dynamics depends on the presynaptic membrane potential  $V_{Pre}$ :

$$\begin{aligned}s_{AMPA} \dot{} &= 1.1\tau_m(V_{Pre})(1 - s_{AMPA}) - 0.19s_{AMPA} \\s_{GABA_A} \dot{} &= 0.53\tau_m(V_{Pre})(1 - s_{GABA_A}) - 0.19s_{GABA_A} \\s_{GABA_B} \dot{} &= 0.016\tau_m(V_{Pre})(1 - s_{GABA_B}) - 0.0047s_{AMPA}\end{aligned}$$

For both excitatory and inhibitory connections  $\tau_m(V_{Pre})$  is defined by:

$$\tau_m(V_{Pre}) = \frac{1}{1 + \exp\left(-\frac{V_{Pre}-2}{5}\right)}$$

#### Plasticity implementation

In the cortical circuit implemented, the plasticity occurs between the presynaptic cell and the postsynaptic cell by changing the AMPA receptors conductance connecting the two neurons:  $\bar{g}_{AMPA}$  is multiplied by the synaptic weight  $w$  that follows one of the synaptic rules (**model 1, 2 or 3**).

$$\bar{g}_{pre,post} = \bar{g}_{AMPA}w \tag{C.1}$$

## C.2 Burst pattern

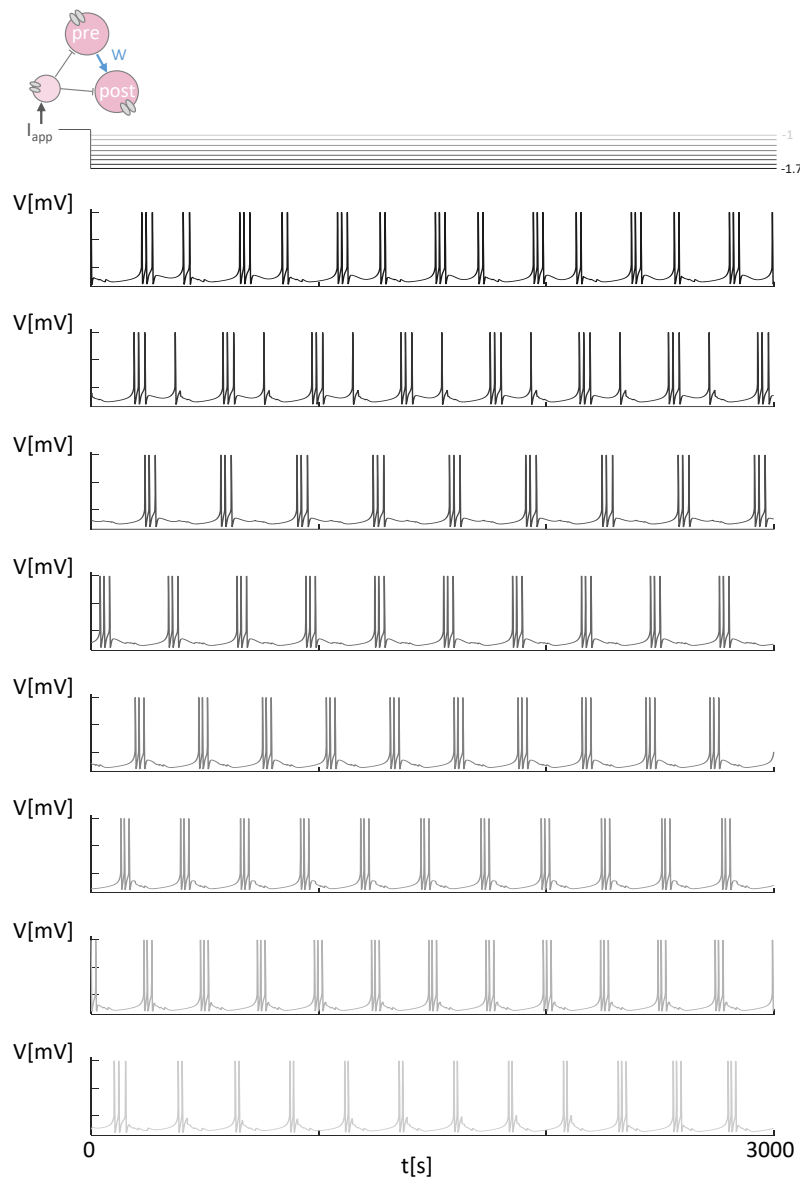


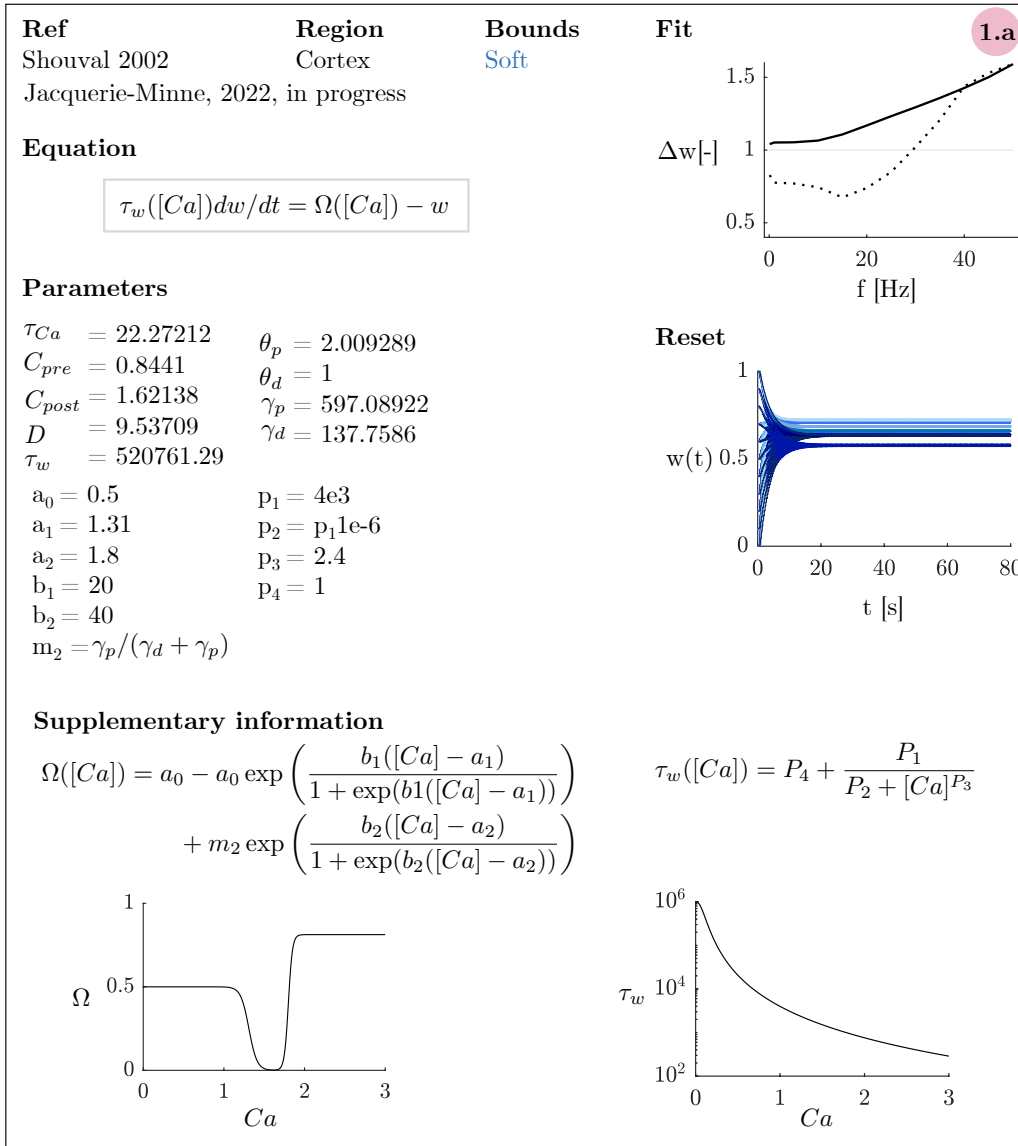
Figure C.1: Time-evolution of the membrane voltage of the presynaptic and postsynaptic cells for different hyperpolarizing currents applied to the inhibitory cell ( $I_{app} \in (-4.7 -4.0)[\frac{nA}{cm^2}]$ ). The various current are represented by different shades of grey. Taken from [Jacquerie et al., 2022] with permission.

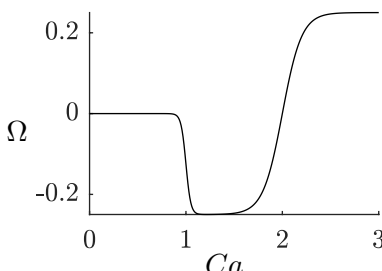
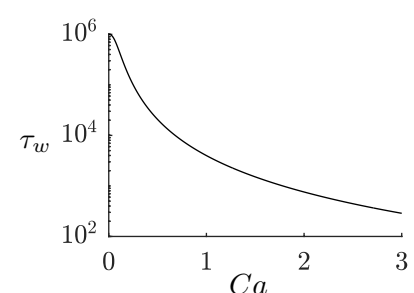
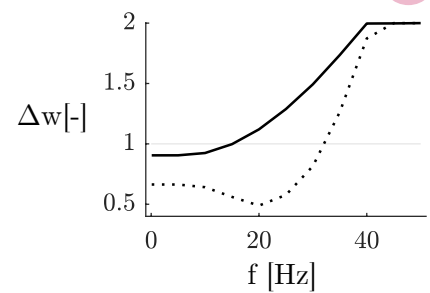
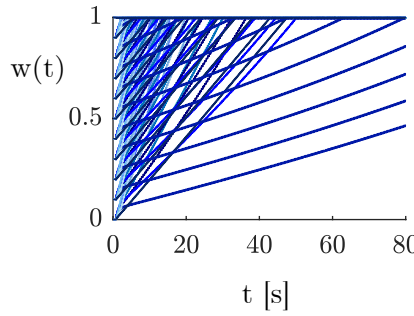
# Appendix D

## Synaptic plasticity models description

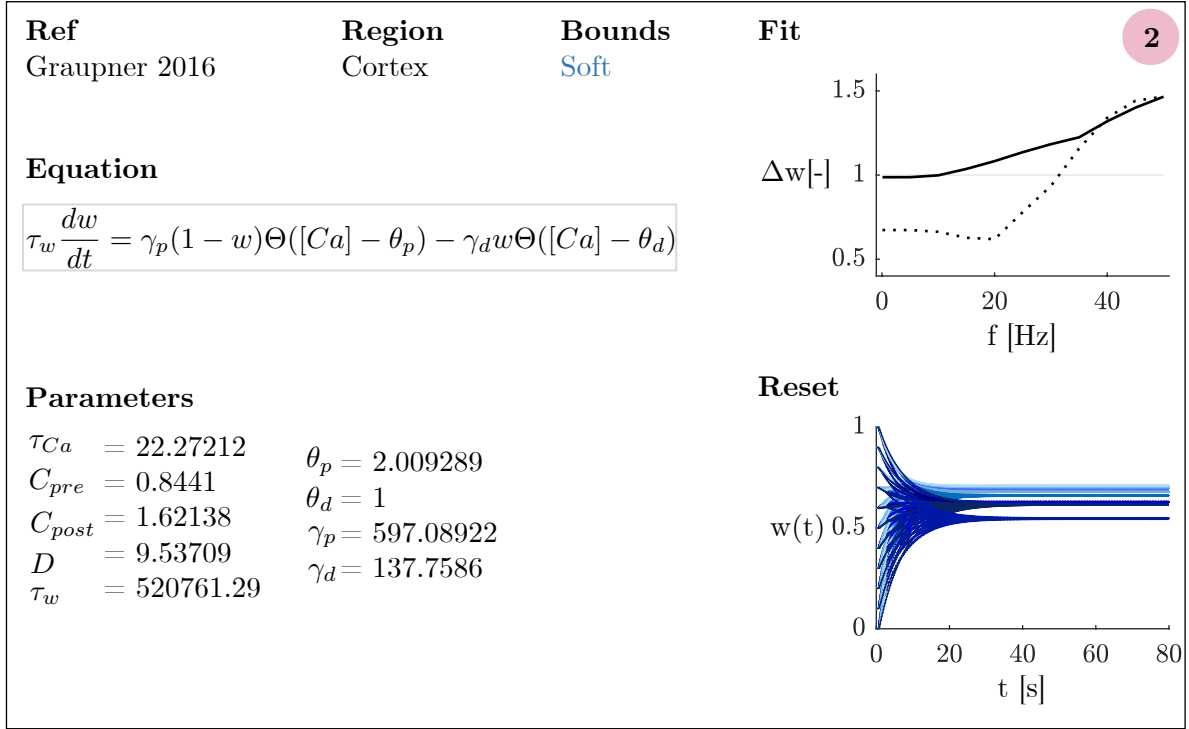
All the following summary sheets are taken from [Jacquerie et al., 2022] with permission.

### D.1 Model 1: soft-bounds and hard-bounds parameters

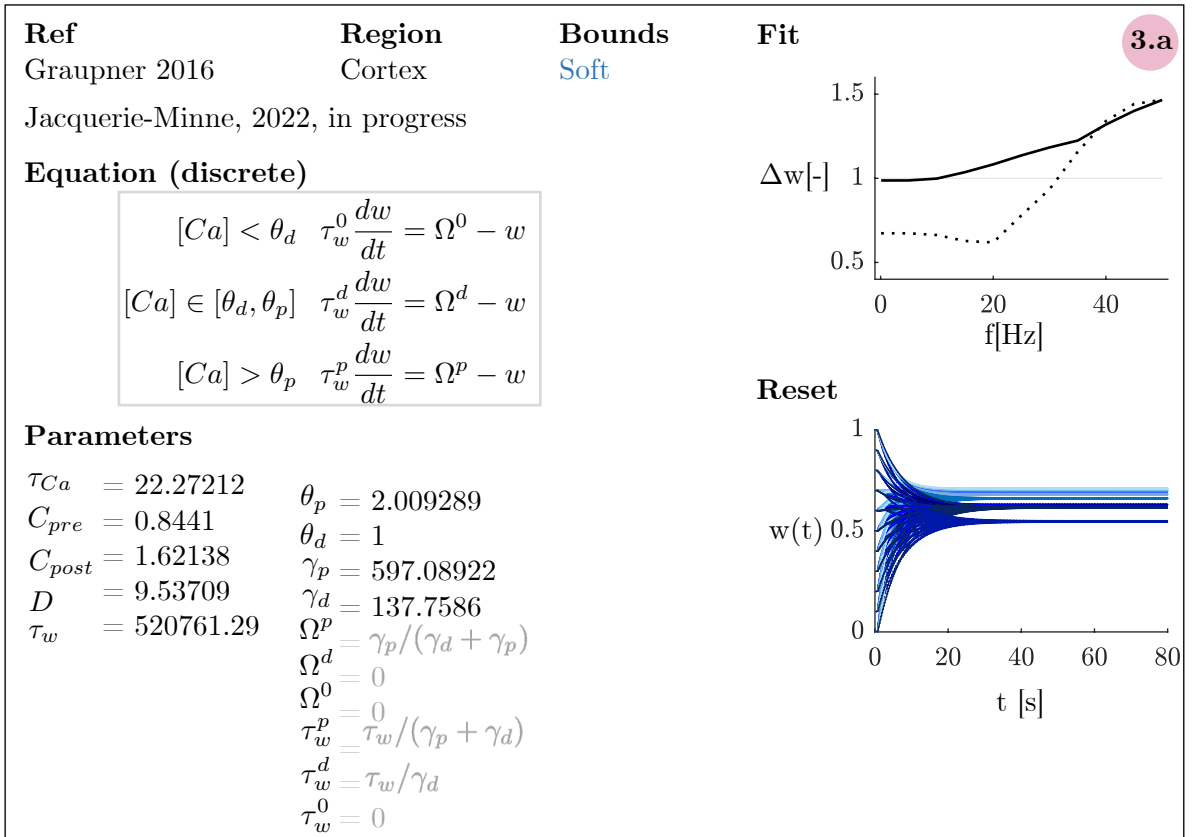


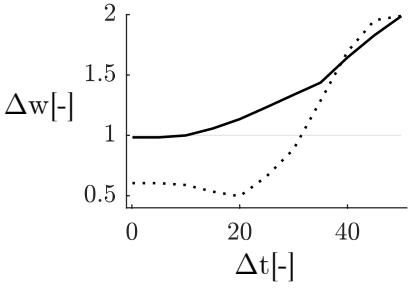
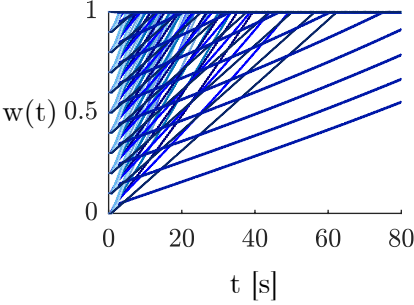
Ref	Region	Bounds	Fit
Shouval 2002 Jacquerie-Minne, 2022, in progress	Cortex	Hard	<span style="background-color: #e91e63; color: white; border-radius: 50%; padding: 2px;">1.b</span>
<b>Equation</b>			
$\tau_w([Ca])dw/dt = \Omega([Ca])$			
<b>Parameters</b>			
$\tau_{Ca} = 22.27212$	$\theta_p = 2.009289$		
$C_{pre} = 0.8441$	$\theta_d = 1$		
$C_{post} = 1.62138$	$\gamma_p = 597.08922$		
$D = 9.53709$	$\gamma_d = 137.7586$		
$\tau_w = 520761.29$			
$m_1 = 0.25$	$p_1 = 4e3$		
$a_1 = 1$	$p_2 = p_1 1e-6$		
$a_2 = 2$	$p_3 = 2.4$		
$b_1 = 40$	$p_4 = 1$		
$b_2 = 10$			
$m_2 = 0.5$			
<b>Supplementary information</b>			
$\Omega([Ca]) = m_2 \exp(b_2([Ca] - a_2)) / (1 + \exp(b_2([Ca] - a_2))) - m_1 \exp(b_1([Ca] - a_1)) / (1 + \exp(b_1([Ca] - a_1)))$ $\tau_w([Ca]) = P_4 + \frac{P_1}{P_2 + [Ca]^{P_3}}$			
			
<b>Fit</b>			
			
<b>Reset</b>			
			

## D.2 Model 2: soft-bounds parameters



## D.3 Model 3: soft-bounds and hard-bounds parameters



Ref	Region	Bounds	Fit
Graupner 2016 Jacquerie-Minne, 2022, in progress	Cortex	Hard	
<b>Equation</b>			
$[Ca] < \theta_d \quad \tau_w^0 \frac{dw}{dt} = \Omega^0$ $[Ca] \in [\theta_d, \theta_p] \quad \tau_w^d \frac{dw}{dt} = \Omega^d$ $[Ca] > \theta_p \quad \tau_w^p \frac{dw}{dt} = \Omega^p$			
<b>Parameters</b>			
$\tau_{Ca}$ = 22.27212	$\theta_p$ = 2.009289		
$C_{pre}$ = 0.8441	$\theta_d$ = 1		
$C_{post}$ = 1.62138	$\gamma_p$ = 597.08922		
$D$ = 9.53709	$\gamma_d$ = 137.7586		
$\tau_w$ = 520761.29	$\Omega^p = 0.5(\gamma_p - \gamma_d)$		
$\tau_w^p$ = $\tau_w$	$\Omega^d = -0.5\gamma_d$		
$\tau_w^d$ = $\tau_w$	$\Omega^0 = 0$		
$\tau_w^0$ = 0			
<b>Reset</b>			
			

## D.4 Up state-mediated plasticity rule from [González-Rueda et al., 2018]

Based on SHY [Tononi and Cirelli, 2006], [González-Rueda et al., 2018] consider that the same synaptic rule can not explain both net synaptic potentiation during the day and net synaptic depression during sleep. Therefore, according to their experimental results, they implemented an Up state-mediated plasticity rule where *presynaptic spikes alone lead to synaptic depression whereas a pair of pre- postsynaptic spikes within 10ms leads to no change in synaptic weight*[González-Rueda et al., 2018].

$$x_j \rightarrow 10 \text{ if presynaptic neuron } j \text{ fires}$$

$$\tau \frac{dx_j}{dt} = -1 \quad \text{otherwise,}$$

where  $\tau = 1[ms]$  and the weight is updated following:

$$w_j(t) \rightarrow w_j(t) - A \quad \text{if } t = t^{\text{pre}}$$

$$w_j(t) \rightarrow w_j(t) + A \times \Theta(x_j(t)) \quad \text{if } t = t^{\text{post}}$$

$\Theta(x) = 1$  if  $x > 0$  and  $\Theta(x) = 0$  otherwise.

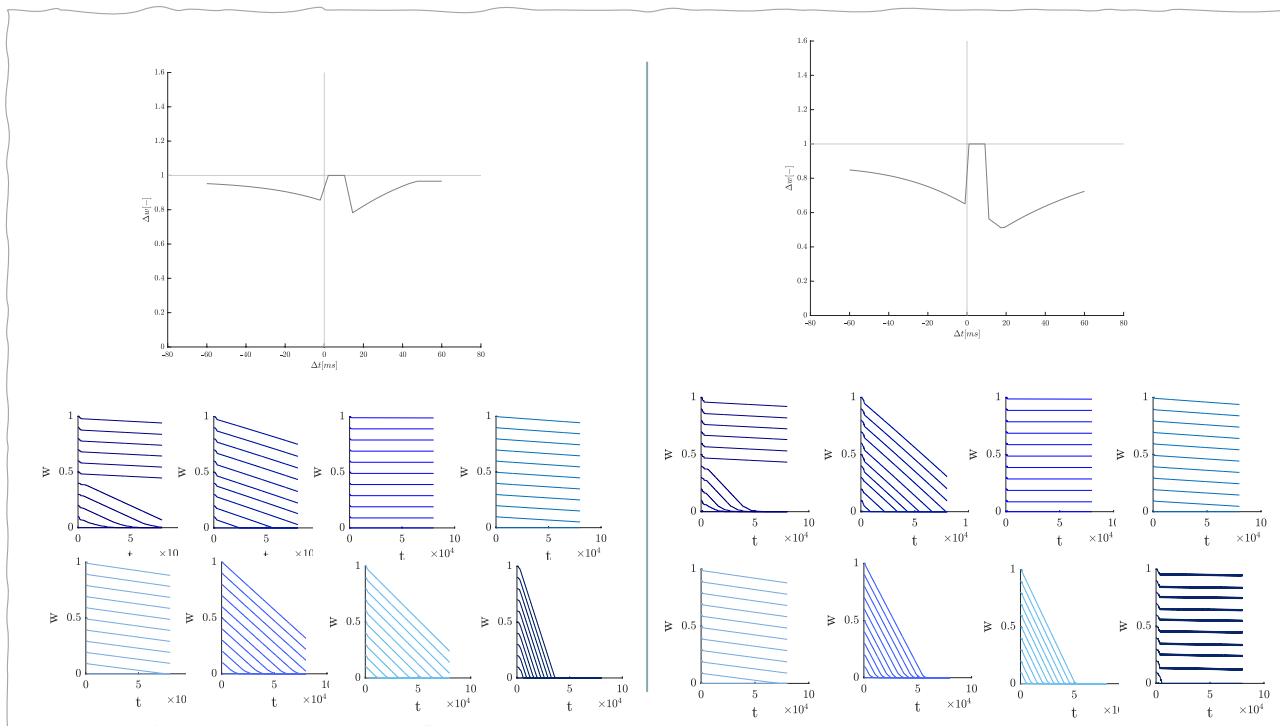
# Appendix E

## Supplementary results

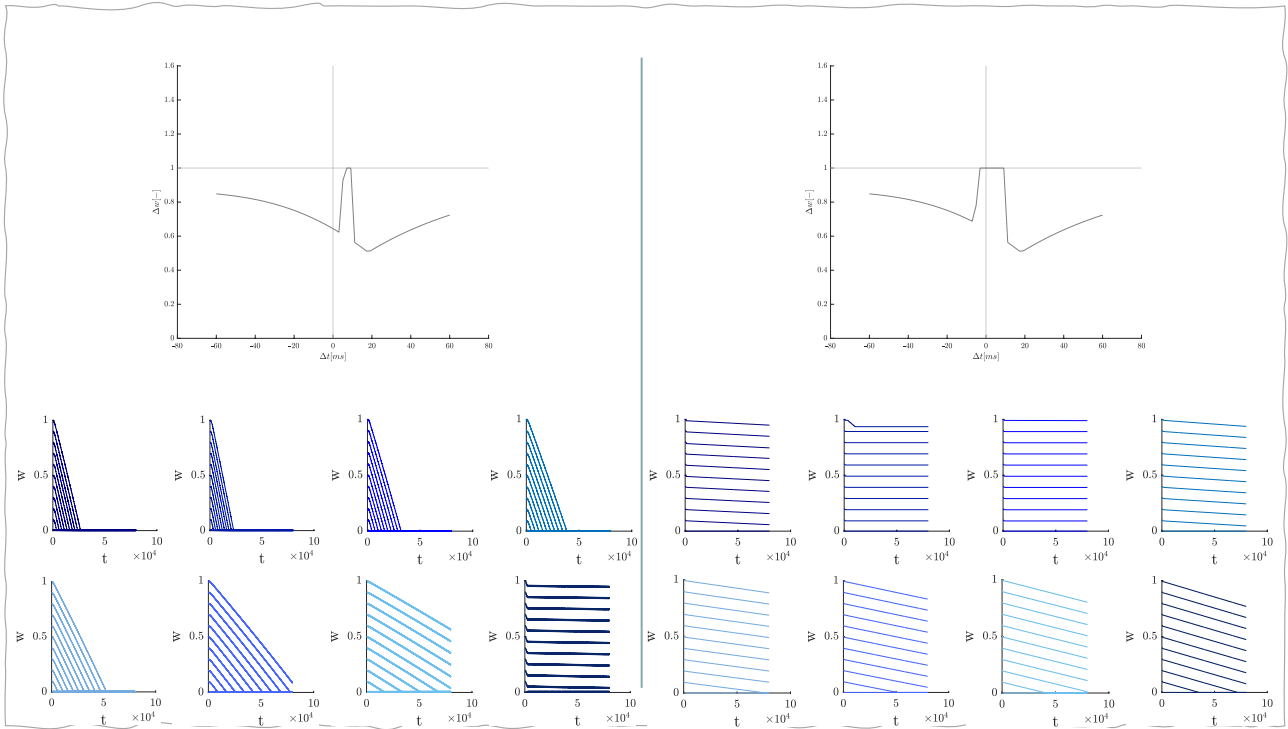
### E.1 [González-Rueda et al., 2018] into calcium-based rule: change of the original 3-points STDP curve

In this appendix you may find the evolution of the weights for each of the applied current  $I_{app} = -4.7, -4.6, -4.5, -4.4$  (first row in this order),  $-4.3, -4.2, -4.1, -4.0 \frac{nA}{cm^2}$  (second row in this order) for every modification we made on the STDP curve of [González-Rueda et al., 2018] Up-state mediated plasticity rule

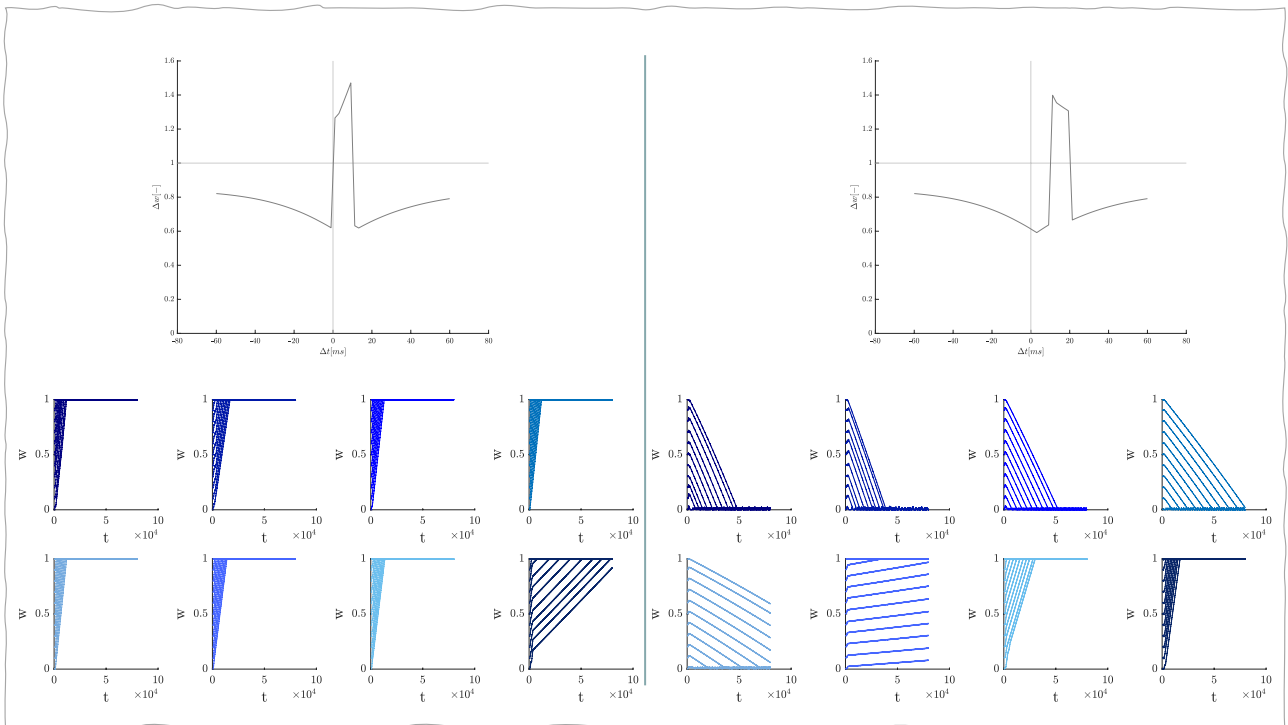
#### E.1.1 Original STDP curve



### E.1.2 Extension or retraction of the *no-change* 10ms window

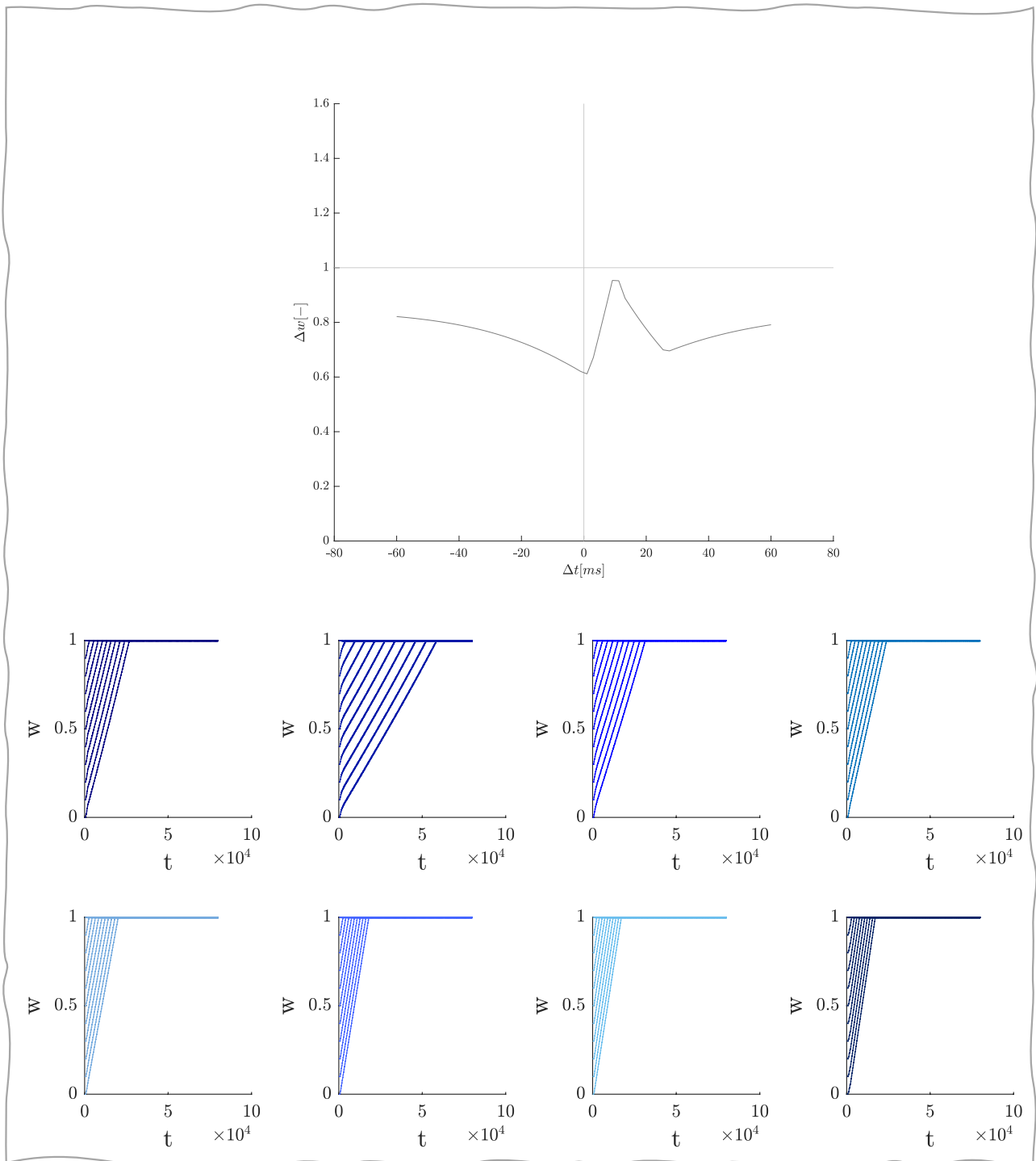


### E.1.3 Modification of the *no-change* window into a potentiation window





**E.1.4 Translation of [González-Rueda et al., 2018] phenomenological plasticity rule in a calcium-based plasticity rule by changes in parameterization only**



# Bibliography

- [Aarse et al., 2016] Aarse, J., Herlitz, S., and Manahan-Vaughan, D. (2016). The requirement of BDNF for hippocampal synaptic plasticity is experience-dependent. *Hippocampus*, 26(6):739–751. \_eprint: <https://onlinelibrary.wiley.com/doi/pdf/10.1002/hipo.22555>.
- [Acheson et al., 1995] Acheson, A., Conover, J. C., Fandl, J. P., DeChiara, T. M., Russell, M., Thadani, A., Squinto, S. P., Yancopoulos, G. D., and Lindsay, R. M. (1995). A BDNF autocrine loop in adult sensory neurons prevents cell death. *Nature*, 374(6521):450–453.
- [Aizpurua-Olaizola et al., 2017] Aizpurua-Olaizola, O., Elezgarai, I., Rico-Barrio, I., Zarandona, I., Etxebarria, N., and Usobiaga, A. (2017). Targeting the endocannabinoid system: future therapeutic strategies. *Drug Discovery Today*, 22(1):105–110.
- [Alkadhi, 2021] Alkadhi, K. A. (2021). NMDA receptor-independent LTP in mammalian nervous system. *Progress in Neurobiology*, 200:101986.
- [Allen et al., 2007] Allen, D., Fakler, B., Maylie, J., and Adelman, J. P. (2007). Organization and Regulation of Small Conductance Ca<sup>2+</sup>-activated K<sup>+</sup> Channel Multiprotein Complexes. *Journal of Neuroscience*, 27(9):2369–2376.
- [Aston-Jones and Bloom, 1981] Aston-Jones, G. and Bloom, F. E. (1981). Activity of norepinephrine-containing locus coeruleus neurons in behaving rats anticipates fluctuations in the sleep-waking cycle. *Journal of Neuroscience*, 1(8):876–886. Publisher: Society for Neuroscience Section: Articles.
- [Atherton et al., 2015] Atherton, L. A., Dupret, D., and Mellor, J. R. (2015). Memory trace replay: the shaping of memory consolidation by neuromodulation. *Trends in Neurosciences*, 38(9):560–570.
- [Aton et al., 2009] Aton, S. J., Seibt, J., Dumoulin, M., Jha, S. K., Steinmetz, N., Coleman, T., Naidoo, N., and Frank, M. G. (2009). Mechanisms of Sleep-Dependent Consolidation of Cortical Plasticity. *Neuron*, 61(3):454–466.
- [Bachmann et al., 2012] Bachmann, V., Klein, C., Bodenmann, S., Schäfer, N., Berger, W., Brugger, P., and Landolt, H.-P. (2012). The BDNF Val66Met polymorphism modulates sleep intensity: EEG frequency- and state-specificity. *Sleep*, 35(3):335–344.
- [Balkowiec et al., 2000] Balkowiec, A., Kunze, D. L., and Katz, D. M. (2000). Brain-Derived Neurotrophic Factor Acutely Inhibits AMPA-Mediated Currents in Developing Sensory Relay Neurons. *The Journal of Neuroscience*, 20(5):1904–1911.
- [Barde et al., 1982] Barde, Y. A., Edgar, D., and Thoenen, H. (1982). Purification of a new neurotrophic factor from mammalian brain. *The EMBO journal*, 1(5):549–553.
- [Bear et al., 2016] Bear, M. F., Connors, B. W., and Paradiso, M. A. (2016). *Neuroscience: exploring the brain*. Philadelphia. Issue: International Edition.
- [Benarroch, 2008] Benarroch, E. E. (2008). Suprachiasmatic nucleus and melatonin: Reciprocal interactions and clinical correlations. *Neurology*, 71(8):594–598.
- [Berry, 2012] Berry, R. B. (2012). Neurobiology of Sleep. *Fundamentals of Sleep Medicine*, pages 91–100.

- [Bevilaqua et al., 1997] Bevilaqua, L., Ardenghi, P., Schröder, N., Bromberg, E., Schmitz, P. K., Schaeffer, E., Quevedo, J., Bianchin, M., Walz, R., Medina, J. H., and Izquierdo, I. (1997). Drugs acting upon the cyclic adenosine monophosphate/ protein kinase A signalling pathway modulate memory consolidation when given late after training into rat hippocampus but not amygdala. *Behavioural Pharmacology*, 8(4):331–338.
- [Bi and Poo, 1998] Bi, G.-q. and Poo, M.-m. (1998). Synaptic modifications in cultured hippocampal neurons: Dependence on spike timing, synaptic strength, and postsynaptic cell type. *The Journal of Neuroscience*, 18(24):10464–10472.
- [Binder and Scharfman, 2004] Binder, D. K. and Scharfman, H. E. (2004). Brain-derived neurotrophic factor - mini Review. *Growth Factors*, 22(3):123–131.
- [Bliss and Cooke, 2011] Bliss, T. V. and Cooke, S. F. (2011). Long-term potentiation and long-term depression: a clinical perspective. *Clinics*, 66:3–17.
- [Blitzer et al., 1998] Blitzer, R. D., Connor, J. H., Brown, G. P., Wong, T., Shenolikar, S., Iyengar, R., and Landau, E. M. (1998). Gating of CaMKII by cAMP-Regulated Protein Phosphatase Activity During LTP. *Science*, 280(5371):1940–1943.
- [Born and Feld, 2012] Born, J. and Feld, G. (2012). Sleep to Upscale, Sleep to Downscale: Balancing Homeostasis and Plasticity. *Neuron*, 75(6):933–935.
- [Boutrel and Koob, 2004] Boutrel, B. and Koob, G. F. (2004). What Keeps Us Awake: the Neuropharmacology of Stimulants and Wakefulness Promoting Medications. *Sleep*, 27(6):1181–1194.
- [Bramham and Messaoudi, 2005] Bramham, C. R. and Messaoudi, E. (2005). Bdnf function in adult synaptic plasticity: The synaptic consolidation hypothesis. *Progress in Neurobiology*, 76(2):99–125.
- [Brown and Reymann, 1996] Brown, R. E. and Reymann, K. G. (1996). Histamine H3 receptor-mediated depression of synaptic transmission in the dentate gyrus of the rat in vitro. *The Journal of Physiology*, 496(1):175–184.
- [Brzosko et al., 2019] Brzosko, Z., Mierau, S. B., and Paulsen, O. (2019). Neuromodulation of Spike-Timing-Dependent Plasticity: Past, Present, and Future. *Neuron*, 103(4):563–581. Publisher: Elsevier Inc.
- [Buchanan et al., 2010] Buchanan, K. A., Petrovic, M. M., Chamberlain, S. E., Marrion, N. V., and Mellor, J. R. (2010). Facilitation of Long-Term Potentiation by Muscarinic M1 Receptors Is Mediated by Inhibition of SK Channels. *Neuron*, 68(5):948–963.
- [Cabelli et al., 1995] Cabelli, R. J., Hohn, A., and Shatz, C. J. (1995). Inhibition of Ocular Dominance Column Formation by Infusion of NT-4/5 or BDNF. *Science*, 267(5204):1662–1666. Publisher: American Association for the Advancement of Science.
- [Cai et al., 2002] Cai, X., Gu, Z., Zhong, P., Ren, Y., and Yan, Z. (2002). Serotonin 5-HT<sub>1A</sub> Receptors Regulate AMPA Receptor Channels through Inhibiting Ca<sup>2+</sup>/Calmodulin-dependent Kinase II in Prefrontal Cortical Pyramidal Neurons. *Journal of Biological Chemistry*, 277(39):36553–36562.
- [Cain et al., 2017] Cain, S. W., Chang, A.-M., Vlasac, I., Tare, A., Anderson, C., Czeisler, C. A., and Saxena, R. (2017). Circadian Rhythms in Plasma Brain-derived Neurotrophic Factor Differ in Men and Women. *Journal of Biological Rhythms*, 32(1):75–82.
- [Calais et al., 2015] Calais, J. B., Ojopi, E. B., Morya, E., Sameshima, K., and Ribeiro, S. (2015). Experience-dependent upregulation of multiple plasticity factors in the hippocampus during early REM sleep. *Neurobiology of Learning and Memory*, 122:19–27.
- [Caputi et al., 2013] Caputi, A., Melzer, S., Michael, M., and Monyer, H. (2013). The long and short of GABAergic neurons. *Current Opinion in Neurobiology*, 23(2):179–186.
- [Carr et al., 2002] Carr, D. B., Cooper, D. C., Ulrich, S. L., Spruston, N., and Surmeier, D. J. (2002). Serotonin Receptor Activation Inhibits Sodium Current and Dendritic Excitability in Prefrontal Cortex via a Protein Kinase C-Dependent Mechanism. *The Journal of Neuroscience*, 22(16):6846–6855.

- [Chebib and Johnston, 1999] Chebib, M. and Johnston, G. A. R. (1999). THE 'ABC' OF GABA RECEPTORS: A BRIEF REVIEW. *Clinical and Experimental Pharmacology and Physiology*, 26(11):937–940.
- [Chen et al., 1999] Chen, Z., Zhao, Q., Sugimoto, Y., Fujii, Y., and Kamei, C. (1999). Effects of histamine on MK-801-induced memory deficits in radial maze performance in rats. *Brain Research*, 839(1):186–189.
- [Choi et al., 1992] Choi, E. J., Wong, S. T., Hinds, T. R., and Storm, D. R. (1992). Calcium and muscarinic agonist stimulation of type I adenylylcyclase in whole cells. *The Journal of Biological Chemistry*, 267(18):12440–12442.
- [Choi et al., 2005] Choi, S.-Y., Chang, J., Jiang, B., Seol, G.-H., Min, S.-S., Han, J.-S., Shin, H.-S., Gallagher, M., and Kirkwood, A. (2005). Multiple receptors coupled to phospholipase C gate long-term depression in visual cortex. *The Journal of Neuroscience: The Official Journal of the Society for Neuroscience*, 25(49):11433–11443.
- [Cirelli and Tononi, 2000] Cirelli, C. and Tononi, G. (2000). Differential Expression of Plasticity-Related Genes in Waking and Sleep and Their Regulation by the Noradrenergic System. *The Journal of Neuroscience*, 20(24):9187–9194.
- [Citri and Malenka, 2008] Citri, A. and Malenka, R. C. (2008). Synaptic Plasticity: Multiple Forms, Functions, and Mechanisms. *Neuropsychopharmacology*, 33(1):18–41.
- [Corradetti et al., 1992] Corradetti, R., Ballerini, L., Pugliese, A. M., and Pepeu, G. (1992). Serotonin blocks the long-term potentiation induced by primed burst stimulation in the CA1 region of rat hippocampal slices. *Neuroscience*, 46(3):511–518.
- [Dai et al., 2007] Dai, H., Kaneko, K., Kato, H., Fujii, S., Jing, Y., Xu, A., Sakurai, E., Kato, M., Okamura, N., Kuramasu, A., and Yanai, K. (2007). Selective cognitive dysfunction in mice lacking histamine H1 and H2 receptors. *Neuroscience Research*, 57(2):306–313.
- [Davies and Wright, 1995] Davies, A. M. and Wright, E. M. (1995). Neurotrophic Factors: Neurotrophin autocrine loops. *Current Biology*, 5(7):723–726.
- [De Petrocellis and Di Marzo, 2009] De Petrocellis, L. and Di Marzo, V. (2009). An introduction to the endocannabinoid system: from the early to the latest concepts. *Best Practice & Research Clinical Endocrinology & Metabolism*, 23(1):1–15.
- [Deleuze et al., 2012] Deleuze, C., David, F., Behuret, S., Sadoc, G., Shin, H.-S., Uebele, V. N., Renger, J. J., Lambert, R. C., Leresche, N., and Bal, T. (2012). T-type calcium channels consolidate tonic action potential output of thalamic neurons to neocortex. *Journal of Neuroscience*, 32(35):12228–12236.
- [Delghandi et al., 2005] Delghandi, M. P., Johannessen, M., and Moens, U. (2005). The cAMP signalling pathway activates CREB through PKA, p38 and MSK1 in NIH 3T3 cells. *Cellular Signalling*, 17(11):1343–1351.
- [Della Sala, 2021] Della Sala, S. (2021). *Encyclopedia of behavioral neuroscience*. OCLC: 1288341504.
- [Deperrois and Graupner, 2020] Deperrois, N. and Graupner, M. (2020). Short-term depression and long-term plasticity together tune sensitive range of synaptic plasticity. *PLoS Computational Biology*, 16(9):1–25.
- [Derkach et al., 1999] Derkach, V., Barria, A., and Soderling, T. R. (1999).  $\text{Ca}^{2+}$ /calmodulin-kinase II enhances channel conductance of  $\alpha$ -amino-3-hydroxy-5-methyl-4-isoxazolepropionate type glutamate receptors. *Proceedings of the National Academy of Sciences*, 96(6):3269–3274.
- [Dickinson et al., 2009] Dickinson, B. A., Jo, J., Seok, H., Son, G. H., Whitcomb, D. J., Davies, C. H., Sheng, M., Collingridge, G. L., and Cho, K. (2009). A novel mechanism of hippocampal LTD involving muscarinic receptor-triggered interactions between AMPARs, GRIP and liprin-. *Molecular Brain*, 2(1):18.
- [Diekelmann and Born, 2010] Diekelmann, S. and Born, J. (2010). The memory function of sleep. *Nature Reviews Neuroscience*, 11(2):114–126.

- [Diering et al., 2017] Diering, G. H., Nirujogi, R. S., Roth, R. H., Worley, P. F., Pandey, A., and Huganir, R. L. (2017). Homer1a drives homeostatic scaling-down of excitatory synapses during sleep. *Science*, 355(6324):511–515.
- [Dittman et al., 1994] Dittman, A. H., Weber, J. P., Hinds, T. R., Choi, E. J., Migeon, J. C., Nathanson, N. M., and Storm, D. R. (1994). A novel mechanism for coupling of m4 muscarinic acetylcholine receptors to calmodulin-sensitive adenylyl cyclases: crossover from G protein-coupled inhibition to stimulation. *Biochemistry*, 33(4):943–951.
- [Doreulee et al., 2001] Doreulee, N., Yanovsky, Y., Flaggmeyer, I., Stevens, D. R., Haas, H. L., and Brown, R. E. (2001). Histamine H3 receptors depress synaptic transmission in the corticostriatal pathway. *Neuropharmacology*, 40(1):106–113.
- [Drion et al., 2018] Drion, G., Dethier, J., Franci, A., and Sepulchre, R. (2018). Switchable slow cellular conductances determine robustness and tunability of network states. *PLOS Computational Biology*, 14:e1006125.
- [Duda et al., 2020] Duda, P., Hajka, D., Wójcicka, O., Rakus, D., and Gizak, A. (2020). GSK3: A Master Player in Depressive Disorder Pathogenesis and Treatment Responsiveness. *Cells*, 9(3):727.
- [Edagawa et al., 1999] Edagawa, Y., Saito, H., and Abe, K. (1999). Stimulation of the 5-HT1A receptor selectively suppresses NMDA receptor-mediated synaptic excitation in the rat visual cortex. *Brain Research*, 827(1):225–228.
- [Egashira et al., 2010] Egashira, Y., Tanaka, T., Soni, P., Sakuragi, S., Tominaga-Yoshino, K., and Ogura, A. (2010). Involvement of the p75NTR signaling pathway in persistent synaptic suppression coupled with synapse elimination following repeated long-term depression induction. *Journal of Neuroscience Research*, 88(16):3433–3446. [\\_eprint: https://onlinelibrary.wiley.com/doi/pdf/10.1002/jnr.22505](https://onlinelibrary.wiley.com/doi/pdf/10.1002/jnr.22505).
- [Ellender et al., 2011] Ellender, T. J., Huerta-Ocampo, I., Deisseroth, K., Capogna, M., and Bolam, J. P. (2011). Differential Modulation of Excitatory and Inhibitory Striatal Synaptic Transmission by Histamine. *Journal of Neuroscience*, 31(43):15340–15351.
- [Fraguna et al., 2008] Fraguna, U., Vyazovskiy, V. V., Nelson, A. B., Tononi, G., and Cirelli, C. (2008). A Causal Role for Brain-Derived Neurotrophic Factor in the Homeostatic Regulation of Sleep. *Journal of Neuroscience*, 28(15):4088–4095. Publisher: Society for Neuroscience Section: Articles.
- [Feld and Born, 2017] Feld, G. B. and Born, J. (2017). Sculpting memory during sleep: concurrent consolidation and forgetting. *Current Opinion in Neurobiology*.
- [Fernandez and Luthi, 2019] Fernandez, L. M. and Luthi, A. (2019). Sleep spindles: Mechanisms and functions. *Physiological Reviews*, 100:805–868.
- [Fernández-Ruiz et al., 1999] Fernández-Ruiz, J., Berrendero, F., Hernández, M., Romero, J., and Ramos, J. (1999). Role of endocannabinoids in brain development. *Life Sciences*, 65(6-7):725–736.
- [Foncelle et al., 2018] Foncelle, A., Mendes, A., Jędrzejewska-Szmek, J., Valtcheva, S., Berry, H., Blackwell, K. T., and Venance, L. (2018). Modulation of spike-timing dependent plasticity: Towards the inclusion of a third factor in computational models. *Frontiers in Computational Neuroscience*, 12(July):1–21.
- [França et al., 2015] França, A., Lobão-Soares, B., Murtatori, L., Nascimento, G., Winne, J., Pereira, C., Jeronimo, S., and Ribeiro, S. (2015). D2 dopamine receptor regulation of learning, sleep and plasticity. *European Neuropsychopharmacology*, 25(4):493–504.
- [Gage et al., 1997] Gage, A. T., Reyes, M., and Stanton, P. K. (1997). Nitric-oxide-guanylyl-cyclase-dependent and -independent components of multiple forms of long-term synaptic depression. *Hippocampus*, 7(3):286–295.
- [Gallo et al., 2018] Gallo, F. T., Kathe, C., Morici, J. F., Medina, J. H., and Weisstaub, N. V. (2018). Immediate Early Genes, Memory and Psychiatric Disorders: Focus on c-Fos, Egr1 and Arc. *Frontiers in Behavioral Neuroscience*, 12:79.
- [Gasbarri and Pompili, 2014] Gasbarri, A. and Pompili, A. (2014). The Role of GABA in Memory Processes. In *Identification of Neural Markers Accompanying Memory*, pages 47–62. Elsevier.

- [Gerstner et al., 2018] Gerstner, W., Lehmann, M., Liakoni, V., Corneil, D., and Brea, J. (2018). Eligibility traces and plasticity on behavioral time scales: Experimental support of neohebbian three-factor learning rules. *Frontiers in Neural Circuits*, 12(July):1–16.
- [Giuditta, 2014] Giuditta, A. (2014). Sleep memory processing: the sequential hypothesis. *Frontiers in Systems Neuroscience*, 8.
- [Giuditta et al., 1995] Giuditta, A., Ambrosini, M. V., Montagnese, P., Mandile, P., Cotugno, M., Zucconi, G. G., and Vescia, S. (1995). The sequential hypothesis of the function of sleep. *Behavioural Brain Research*, 69(1-2):157–166.
- [Gobetto et al., 2021] Gobetto, M. N., González-Inchauspe, C., and Uchitel, O. D. (2021). Histamine and Corticosterone Modulate Acid Sensing Ion Channels (ASICs) Dependent Long-term Potentiation at the Mouse Anterior Cingulate Cortex. *Neuroscience*, 460:145–160.
- [González-Rueda et al., 2018] González-Rueda, A., Pedrosa, V., Feord, R. C., Clopath, C., and Paulsen, O. (2018). Activity-Dependent Downscaling of Subthreshold Synaptic Inputs during Slow-Wave-Sleep-like Activity In Vivo. *Neuron*, 97(6):1244–1252.e5.
- [Gosselin et al., 2016] Gosselin, N., Beaumont, L. D., Gagnon, K., Baril, A.-A., Mongrain, V., Blais, H., Montplaisir, J., Gagnon, J.-F., Pelleieux, S., Poirier, J., and Carrier, J. (2016). BDNF Val66Met Polymorphism Interacts with Sleep Consolidation to Predict Ability to Create New Declarative Memories. *Journal of Neuroscience*, 36(32):8390–8398. Publisher: Society for Neuroscience Section: Articles.
- [Graupner, 2017] Graupner, M. (2017). Synaptic Plasticity : Spike-timing dependent plasticity ( STDP )  
Synaptic Plasticity : Spike-timing dependent plasticity ( STDP ).
- [Graupner and Brunel, 2012] Graupner, M. and Brunel, N. (2012). Calcium-based plasticity model explains sensitivity of synaptic changes to spike pattern, rate, and dendritic location. *Proceedings of the National Academy of Sciences of the United States of America*, 109(10):3991–3996.
- [Graupner et al., 2016] Graupner, M., Wallisch, P., and Ostojic, S. (2016). Natural Firing Patterns Imply Low Sensitivity of Synaptic Plasticity to Spike Timing Compared with Firing Rate. *The Journal of Neuroscience*, 36(44):11238–11258.
- [Graves, 2001] Graves, L. (2001). Sleep and memory: a molecular perspective. *Trends in Neurosciences*, 24(4):237–243.
- [Gu, 2002] Gu, Q. (2002). Neuromodulatory transmitter systems in the cortex and their role in cortical plasticity. *Neuroscience*, 111(4):815–835.
- [Hall et al., 2000] Hall, J., Thomas, K. L., and Everitt, B. J. (2000). Rapid and selective induction of BDNF expression in the hippocampus during contextual learning. *Nature neuroscience*, 3(6):533–535.
- [Harward et al., 2016] Harward, S. C., Hedrick, N. G., Hall, C. E., Parra-Bueno, P., Milner, T. A., Pan, E., Laviv, T., Hempstead, B. L., Yasuda, R., and McNamara, J. O. (2016). Autocrine BDNF–TrkB signalling within a single dendritic spine. *Nature*, 538(7623):99–103.
- [Hebb, 1949] Hebb, D. O. (1949). *The organization of behavior : a neuropsychological theory*. A Wiley book in clinical psychology. John Wiley, New York, NY.
- [Heidelberger et al., 2014] Heidelberger, R., Shouval, H., Zucker, R. S., and Byrne, J. H. (2014). Synaptic Plasticity. In *From Molecules to Networks: An Introduction to Cellular and Molecular Neuroscience: Third Edition*, pages 533–561. Elsevier Inc.
- [Hermida et al., 2017] Hermida, M. A., Dinesh Kumar, J., and Leslie, N. R. (2017). GSK3 and its interactions with the PI3K/AKT/mTOR signalling network. *Advances in Biological Regulation*, 65:5–15.
- [Hodgkin and Huxley, 1952] Hodgkin, A. L. and Huxley, A. F. (1952). A quantitative description of membrane current and its application to conduction and excitation in nerve. *The Journal of Physiology*, 117(4):500–544.
- [Horch and Katz, 2002] Horch, H. W. and Katz, L. C. (2002). BDNF release from single cells elicits local dendritic growth in nearby neurons. *Nature Neuroscience*, 5(11):1177–1184.

- [Hoyle, 1985] Hoyle, G. (1985). Neurotransmitters, Neuromodulators, and Neurohormones. In Gilles, R. and Balthazart, J., editors, *Neurobiology*, pages 264–279. Springer Berlin Heidelberg, Berlin, Heidelberg. Series Title: Proceedings in Life Sciences.
- [Hsiung et al., 2008] Hsiung, S.-c., Tin, A., Tamir, H., Franke, T. F., and Liu, K.-p. (2008). Inhibition of 5-HT<sub>1A</sub> receptor-dependent cell survival by cAMP/protein kinase A: Role of protein phosphatase 2A and Bax. *Journal of Neuroscience Research*, 86(10):2326–2338. \_eprint: <https://onlinelibrary.wiley.com/doi/pdf/10.1002/jnr.21676>.
- [Huang and Reichardt, 2001] Huang, E. J. and Reichardt, L. F. (2001). Neurotrophins: roles in neuronal development and function. *Annual Review of Neuroscience*, 24:677–736.
- [Huang, 1997] Huang, E. P. (1997). Synaptic plasticity: A role for nitric oxide in LTP. *Current Biology*, 7(3):R141–R143.
- [Huang et al., 2012] Huang, S., Treviño, M., He, K., Ardiles, A., de Pasquale, R., Guo, Y., Palacios, A., Haganir, R., and Kirkwood, A. (2012). Pull-Push Neuromodulation of LTP and LTD Enables Bidirectional Experience-Induced Synaptic Scaling in Visual Cortex. *Neuron*, 73(3):497–510.
- [Huang et al., 2004] Huang, Y.-Y., Simpson, E., Kellendonk, C., and Kandel, E. R. (2004). Genetic evidence for the bidirectional modulation of synaptic plasticity in the prefrontal cortex by D1 receptors. *Proceedings of the National Academy of Sciences*, 101(9):3236–3241.
- [Huerta and Lisman, 1995] Huerta, P. T. and Lisman, J. E. (1995). Bidirectional synaptic plasticity induced by a single burst during cholinergic theta oscillation in CA1 in vitro. *Neuron*, 15(5):1053–1063.
- [Huguenard and McCormick, 2007] Huguenard, J. R. and McCormick, D. A. (2007). Thalamic synchrony and dynamic regulation of global forebrain oscillations. *Trends in Neurosciences*, 30(7):350–356.
- [Iannotti et al., 2016] Iannotti, F. A., Di Marzo, V., and Petrosino, S. (2016). Endocannabinoids and endocannabinoid-related mediators: Targets, metabolism and role in neurological disorders. *Progress in Lipid Research*, 62:107–128.
- [Ikegaya et al., 2002] Ikegaya, Y., Ishizaka, Y., and Matsuki, N. (2002). BDNF attenuates hippocampal LTD via activation of phospholipase C: implications for a vertical shift in the frequency-response curve of synaptic plasticity: BDNF attenuates CA1 LTD. *European Journal of Neuroscience*, 16(1):145–148.
- [Itami et al., 2003] Itami, C., Kimura, F., Kohno, T., Matsuoka, M., Ichikawa, M., Tsumoto, T., and Nakamura, S. (2003). Brain-derived neurotrophic factor-dependent unmasking of "silent" synapses in the developing mouse barrel cortex. *Proceedings of the National Academy of Sciences of the United States of America*, 100(22):13069–13074.
- [Jacquerie et al., 2022] Jacquerie, K., Minne, C., and Drion, G. (2022). Synaptic plasticity, neuronal excitability and neuromodulation: are they compatible from a computational approach? page Unpublished Manuscript.
- [Jan et al., 2009] Jan, J. E., Reiter, R. J., Wasdell, M. B., and Bax, M. (2009). The role of the thalamus in sleep, pineal melatonin production, and circadian rhythm sleep disorders. *Journal of Pineal Research*, 46(1):1–7.
- [Jankowsky and Patterson, 2001] Jankowsky, J. and Patterson, P. (2001). The role of cytokines and growth factors in seizures and their sequelae. *Progress in Neurobiology*.
- [Ji et al., 2005] Ji, Y., Pang, P. T., Feng, L., and Lu, B. (2005). Cyclic AMP controls BDNF-induced TrkB phosphorylation and dendritic spine formation in mature hippocampal neurons. *Nature Neuroscience*, 8(2):164–172. Number: 2 Publisher: Nature Publishing Group.
- [Jo et al., 2010] Jo, J., Son, G. H., Winters, B. L., Kim, M. J., Whitcomb, D. J., Dickinson, B. A., Lee, Y.-B., Futai, K., Amici, M., Sheng, M., Collingridge, G. L., and Cho, K. (2010). Muscarinic receptors induce LTD of NMDAR EPSCs via a mechanism involving hippocalcin, AP2 and PSD-95. *Nature Neuroscience*, 13(10):1216–1224.
- [Kelleher et al., 2004] Kelleher, R. J., Govindarajan, A., and Tonegawa, S. (2004). Translational Regulatory Mechanisms in Persistent Forms of Synaptic Plasticity. *Neuron*, 44(1):59–73.

- [Kleitman, 1939] Kleitman, N. (1939). Sleep And Wakefulness As Alternating Phases in the Cycle of Existence. *Chigaco*, 20(1):60–61.
- [Klintsova et al., 2004] Klintsova, A. Y., Dickson, E., Yoshida, R., and Greenough, W. T. (2004). Altered expression of BDNF and its high-affinity receptor TrkB in response to complex motor learning and moderate exercise. *Brain research*, 1028(1):92–104.
- [Klinzing et al., 2019] Klinzing, J. G., Niethard, N., and Born, J. (2019). Mechanisms of systems memory consolidation during sleep. *Nature Neuroscience*, 22(October). Publisher: Springer US.
- [Kojima and Mizui, 2017] Kojima, M. and Mizui, T. (2017). BDNF Propeptide. In *Vitamins and Hormones*, volume 104, pages 19–28. Elsevier.
- [Krüttgen et al., 1998] Krüttgen, A., Möller, J. C., Heymach, J. V., and Shooter, E. M. (1998). Neurotrophins induce release of neurotrophins by the regulated secretory pathway. *Proceedings of the National Academy of Sciences*, 95(16):9614–9619. Publisher: Proceedings of the National Academy of Sciences.
- [Kulla and Manahan-Vaughan, 2002] Kulla, A. and Manahan-Vaughan, D. (2002). Modulation by serotonin 5-HT(4) receptors of long-term potentiation and depotentiation in the dentate gyrus of freely moving rats. *Cerebral Cortex (New York, N.Y.: 1991)*, 12(2):150–162.
- [Köhler et al., 2011] Köhler, C. A., da Silva, W. C., Benetti, F., and Bonini, J. S. (2011). Histaminergic Mechanisms for Modulation of Memory Systems. *Neural Plasticity*, 2011:1–16.
- [Langille, 2019] Langille, J. J. (2019). Remembering to Forget: A Dual Role for Sleep Oscillations in Memory Consolidation and Forgetting. *Frontiers in Cellular Neuroscience*, 13:71.
- [Leal et al., 2017] Leal, G., Bramham, C., and Duarte, C. (2017). BDNF and Hippocampal Synaptic Plasticity. In *Vitamins and Hormones*, volume 104, pages 153–195. Elsevier.
- [LeDoux, 2000] LeDoux, J. E. (2000). Emotion Circuits in the Brain. *Annual Review of Neuroscience*, 23(1):155–184.
- [Lee, 2006] Lee, H.-K. (2006). Synaptic plasticity and phosphorylation. *Pharmacology Therapeutics*, 112(3):810–832.
- [Leutgeb et al., 2005] Leutgeb, S., Leutgeb, J. K., Barnes, C. A., Moser, E. I., McNaughton, B. L., and Moser, M.-B. (2005). Independent codes for spatial and episodic memory in hippocampal neuronal ensembles. *Science*, 309(5734):619–623.
- [Li et al., 2009] Li, Y.-C., Xi, D., Roman, J., Huang, Y.-Q., and Gao, W.-J. (2009). Activation of Glycogen Synthase Kinase-3 Is Required for Hyperdopamine and D2 Receptor-Mediated Inhibition of Synaptic NMDA Receptor Function in the Rat Prefrontal Cortex. *Journal of Neuroscience*, 29(49):15551–15563.
- [Liao et al., 1999] Liao, D., Zhang, X., O’Brien, R., Ehlers, M. D., and Huganir, R. L. (1999). Regulation of morphological postsynaptic silent synapses in developing hippocampal neurons. *Nature Neuroscience*, 2(1):37–43.
- [Lima, 2008] Lima, M. (2008). Blockage of dopaminergic D2 receptors produces decrease of REM but not of slow wave sleep in rats after REM sleep deprivation. *Behavioural Brain Research*, 188(2):406–411.
- [Lima, 2013] Lima, M. M. (2013). Sleep disturbances in Parkinson’s disease: The contribution of dopamine in REM sleep regulation. *Sleep Medicine Reviews*, 17(5):367–375.
- [Lin et al., 1988] Lin, J.-S., Sakai, K., and Jouvet, M. (1988). Evidence for histaminergic arousal mechanisms in the hypothalamus of cat. *Neuropharmacology*, 27(2):111–122.
- [Lin et al., 2011] Lin, J.-S., Sergeeva, O. A., and Haas, H. L. (2011). Histamine H<sub>3</sub> Receptors and Sleep-Wake Regulation. *Journal of Pharmacology and Experimental Therapeutics*, 336(1):17–23.
- [Lisman et al., 2018] Lisman, J., Cooper, K., Sehgal, M., and Silva, A. J. (2018). Memory formation depends on both synapse-specific modifications of synaptic strength and cell-specific increases in excitability. *Nature Neuroscience*, 21(3):309–314.



- [Liu et al., 2017] Liu, Y., Cui, L., Schwarz, M. K., Dong, Y., and Schlüter, O. M. (2017). Adrenergic Gate Release for Spike Timing-Dependent Synaptic Potentiation. *Neuron*, 93(2):394–408.
- [Lockley et al., 1997] Lockley, S. W., Skene, D. J., Arendt, J., Tabandeh, H., Bird, A. C., and DeFrance, R. (1997). Relationship between Melatonin Rhythms and Visual Loss in the Blind <sup>1</sup>. *The Journal of Clinical Endocrinology & Metabolism*, 82(11):3763–3770.
- [Luo and Leung, 2010] Luo, T. and Leung, L. S. (2010). Endogenous histamine facilitates long-term potentiation in the hippocampus during walking. *The Journal of Neuroscience: The Official Journal of the Society for Neuroscience*, 30(23):7845–7852.
- [Madadi Asl et al., 2018] Madadi Asl, M., Vahabie, A.-H., and Valizadeh, A. (2018). Dopaminergic Modulation of Synaptic Plasticity, Its Role in Neuropsychiatric Disorders, and Its Computational Modeling. *Basic and Clinical Neuroscience Journal*.
- [Maingret et al., 2008] Maingret, F., Coste, B., Hao, J., Giamarchi, A., Allen, D., Crest, M., Litchfield, D. W., Adelman, J. P., and Delmas, P. (2008). Neurotransmitter Modulation of Small-Conductance Ca<sup>2+</sup>-Activated K<sup>+</sup> Channels by Regulation of Ca<sup>2+</sup> Gating. *Neuron*, 59(3):439–449.
- [Malcangio and Lessmann, 2003] Malcangio, M. and Lessmann, V. (2003). A common thread for pain and memory synapses? Brain-derived neurotrophic factor and trkB receptors. *Trends in Pharmacological Sciences*, 24(3):116–121.
- [Maren, 2001] Maren, S. (2001). Neurobiology of Pavlovian Fear Conditioning. *Annual Review of Neuroscience*, 24(1):897–931.
- [Marrosu et al., 1995] Marrosu, F., Portas, C., Mascia, M. S., Casu, M. A., Fà, M., Giagheddu, M., Imperato, A., and Gessa, G. L. (1995). Microdialysis measurement of cortical and hippocampal acetylcholine release during sleep-wake cycle in freely moving cats. *Brain Research*, 671(2):329–332.
- [Masuoka et al., 2019] Masuoka, T., Ikeda, R., and Konishi, S. (2019). Persistent activation of histamine H1 receptors in the hippocampal CA1 region enhances NMDA receptor-mediated synaptic excitation and long-term potentiation in astrocyte- and D-serine-dependent manner. *Neuropharmacology*, 151:64–73.
- [Masuoka et al., 2008] Masuoka, T., Saito, S., and Kamei, C. (2008). Participation of hippocampal ionotropic glutamate receptors in histamine H1 antagonist-induced memory deficit in rats. *Psychopharmacology*, 197(1):107–114.
- [McCormick and Bal, 1997] McCormick, D. A. and Bal, T. (1997). Sleep and arousal: Thalamocortical mechanisms. *Annual Review of Neuroscience*, 20(1):185–215. PMID: 9056712.
- [McGaugh, 2002] McGaugh, J. (2002). Amygdala Modulation of Memory Consolidation: Interaction with Other Brain Systems. *Neurobiology of Learning and Memory*, 78(3):539–552.
- [McNamara et al., 2014] McNamara, C. G., Tejero-Cantero, , Trouche, S., Campo-Urriza, N., and Dupret, D. (2014). Dopaminergic neurons promote hippocampal reactivation and spatial memory persistence. *Nature Neuroscience*, 17(12):1658–1660.
- [Meunier et al., 2017a] Meunier, C. N. J., Cancela, J. M., and Fossier, P. (2017a). Lack of GSK3 activation and modulation of synaptic plasticity by dopamine in 5-HT<sub>1A</sub>-receptor KO mice. *Neuropharmacology*, 113:124–136.
- [Meunier et al., 2017b] Meunier, C. N. J., Chameau, P., and Fossier, P. M. (2017b). Modulation of Synaptic Plasticity in the Cortex Needs to Understand All the Players. *Frontiers in Synaptic Neuroscience*, 9.
- [Mizui et al., 2015] Mizui, T., Ishikawa, Y., Kumanogoh, H., Lume, M., Matsumoto, T., Hara, T., Yamawaki, S., Takahashi, M., Shiosaka, S., Itami, C., Uegaki, K., Saarma, M., and Kojima, M. (2015). BDNF pro-peptide actions facilitate hippocampal LTD and are altered by the common BDNF polymorphism Val66Met. *Proceedings of the National Academy of Sciences*.
- [Mlinar et al., 2015] Mlinar, B., Stocca, G., and Corradetti, R. (2015). Endogenous serotonin facilitates hippocampal long-term potentiation at CA3/CA1 synapses. *Journal of Neural Transmission*, 122(2):177–185.

- [Moncada, 2017] Moncada, D. (2017). Evidence of VTA and LC control of protein synthesis required for the behavioral tagging process. *Neurobiology of Learning and Memory*, 138:226–237.
- [Mulkey et al., 1994] Mulkey, R. M., Endo, S., Shenolikar, S., and Malenka, R. C. (1994). Involvement of a calcineurin/ inhibitor-1 phosphatase cascade in hippocampal long-term depression. *Nature*, 369(6480):486–488.
- [Nadim and Bucher, 2014] Nadim, F. and Bucher, D. (2014). Neuromodulation of neurons and synapses. *Current Opinion in Neurobiology*, 29:48–56.
- [Naimark et al., 2007] Naimark, A., Barkai, E., Matar, M. A., Kaplan, Z., Kozlovsky, N., and Cohen, H. (2007). Upregulation of Neurotrophic Factors Selectively in Frontal Cortex in Response to Olfactory Discrimination Learning. *Neural Plasticity*, 2007:13427.
- [Ngo-Anh et al., 2005] Ngo-Anh, T. J., Bloodgood, B. L., Lin, M., Sabatini, B. L., Maylie, J., and Adelman, J. P. (2005). SK channels and NMDA receptors form a Ca<sup>2+</sup>-mediated feedback loop in dendritic spines. *Nature Neuroscience*, 8(5):642–649.
- [Niethard et al., 2021] Niethard, N., Brodt, S., and Born, J. (2021). Cell-Type-Specific Dynamics of Calcium Activity in Cortical Circuits over the Course of Slow-Wave Sleep and Rapid Eye Movement Sleep. *The Journal of Neuroscience*, 41(19):4212–4222.
- [Norimoto et al., 2018] Norimoto, H., Makino, K., Gao, M., Shikano, Y., Okamoto, K., Ishikawa, T., Sasaki, T., Hioki, H., Fujisawa, S., and Ikegaya, Y. (2018). Hippocampal ripples down-regulate synapses. *Science*, 359(6383):1524–1527. Publisher: American Association for the Advancement of Science.
- [O’Dell et al., 2010] O’Dell, T. J., Connor, S. A., Gelinias, J. N., and Nguyen, P. V. (2010). Viagra for your synapses: Enhancement of hippocampal long-term potentiation by activation of beta-adrenergic receptors. *Cellular Signalling*, 22(5):728–736.
- [Ofek et al., 2011] Ofek, O., Attar-Namdar, M., Kram, V., Dvir-Ginzberg, M., Mechoulam, R., Zimmer, A., Frenkel, B., Shohami, E., and Bab, I. (2011). CB2 cannabinoid receptor targets mitogenic Gi protein-cyclin D1 axis in osteoblasts. *Journal of Bone and Mineral Research*, 26(2):308–316.
- [Ohashi et al., 2003] Ohashi, S., Matsumoto, M., Togashi, H., Ueno, K.-i., and Yoshioka, M. (2003). The serotonergic modulation of synaptic plasticity in the rat hippocampo-medial prefrontal cortex pathway. *Neuroscience Letters*, 342(3):179–182.
- [Ohno-Shosaku et al., 2005] Ohno-Shosaku, T., Hashimoto-dani, Y., Maejima, T., and Kano, M. (2005). Calcium signaling and synaptic modulation: Regulation of endocannabinoid-mediated synaptic modulation by calcium. *Cell Calcium*, 38(3-4):369–374.
- [Okuno, 2011] Okuno, H. (2011). Regulation and function of immediate-early genes in the brain: Beyond neuronal activity markers. *Neuroscience Research*, 69(3):175–186.
- [Osorio-Forero et al., 2021] Osorio-Forero, A., Cardis, R., Vantomme, G., Guillaume-Gentil, A., Katsioudi, G., Devenoges, C., Fernandez, L. M., and Lüthi, A. (2021). Noradrenergic circuit control of non-REM sleep substates. *Current Biology*, 31(22):5009–5023.e7.
- [Otani et al., 2003] Otani, S., Daniel, H., Roisin, M.-P., and Crepel, F. (2003). Dopaminergic modulation of long-term synaptic plasticity in rat prefrontal neurons. *Cerebral Cortex (New York, N.Y.: 1991)*, 13(11):1251–1256.
- [Ovsepian et al., 2004] Ovsepian, S. V., Anwyl, R., and Rowan, M. J. (2004). Endogenous acetylcholine lowers the threshold for long-term potentiation induction in the CA1 area through muscarinic receptor activation: in vivo study. *European Journal of Neuroscience*, 20(5):1267–1275.
- [Palacios-Filardo and Mellor, 2019] Palacios-Filardo, J. and Mellor, J. R. (2019). Neuromodulation of hippocampal long-term synaptic plasticity. *Current Opinion in Neurobiology*, 54:37–43.
- [Park et al., 1999] Park, S. P., Lopez-Rodriguez, F., Wilson, C. L., Maidment, N., Matsumoto, Y., and Engel, J. (1999). In vivo microdialysis measures of extracellular serotonin in the rat hippocampus during sleep–wakefulness. *Brain Research*, 833(2):291–296.

- [Passani and Blandina, 2004] Passani, M. and Blandina, P. (2004). The Neuronal Histaminergic System in Cognition. *Current Medicinal Chemistry-Central Nervous System Agents*, 4(1):17–26.
- [Payne and Neuman, 1997] Payne, G. W. and Neuman, R. S. (1997). Effects of hypomagnesemia on histamine H1 receptor-mediated facilitation of NMDA responses. *British Journal of Pharmacology*, 121(2):199–204.   
\_eprint: <https://onlinelibrary.wiley.com/doi/pdf/10.1038/sj.bjp.0701123>.
- [Peineau et al., 2007] Peineau, S., Taghibiglou, C., Bradley, C., Wong, T. P., Liu, L., Lu, J., Lo, E., Wu, D., Saule, E., Bouschet, T., Matthews, P., Isaac, J. T., Bortolotto, Z., Wang, Y. T., and Collingridge, G. L. (2007). LTP Inhibits LTD in the Hippocampus via Regulation of GSK3. *Neuron*, 53(5):703–717.
- [Pencea et al., 2001] Pencea, V., Bingaman, K. D., Wiegand, S. J., and Luskin, M. B. (2001). Infusion of Brain-Derived Neurotrophic Factor into the Lateral Ventricle of the Adult Rat Leads to New Neurons in the Parenchyma of the Striatum, Septum, Thalamus, and Hypothalamus. *The Journal of Neuroscience*, 21(17):6706–6717.
- [Peng et al., 2011] Peng, S., Zhang, Y., Zhang, J., Wang, H., and Ren, B. (2011). Glutamate receptors and signal transduction in learning and memory. *Molecular Biology Reports*, 38(1):453–460.
- [Perez-García and Meneses, 2008] Perez-García, G. and Meneses, A. (2008). Ex vivo study of 5-HT1A and 5-HT7 receptor agonists and antagonists on cAMP accumulation during memory formation and amnesia. *Behavioural Brain Research*, 195(1):139–146.
- [Piscitelli, 2015] Piscitelli, F. (2015). Endocannabinoidomics: “Omics” Approaches Applied to Endocannabinoids and Endocannabinoid-Like Mediators. In *The Endocannabinoidome*, pages 137–152. Elsevier.
- [Polter et al., 2012] Polter, A. M., Yang, S., Jope, R. S., and Li, X. (2012). Functional significance of glycogen synthase kinase-3 regulation by serotonin. *Cellular Signalling*, 24(1):265–271.
- [Prsa et al., 2017] Prsa, M., Galiñanes, G. L., and Huber, D. (2017). Rapid integration of artificial sensory feedback during operant conditioning of motor cortex neurons. *Neuron*, 93(4):929–939.e6.
- [Purves, 2004] Purves, D. (2004). Neuroscience, 3rd Edition. Technical report.
- [Radwan et al., 2019] Radwan, B., Liu, H., and Chaudhury, D. (2019). The role of dopamine in mood disorders and the associated changes in circadian rhythms and sleep-wake cycle. *Brain Research*, 1713:42–51.
- [Rattiner et al., 2005] Rattiner, L. M., Davis, M., and Ressler, K. J. (2005). Brain-Derived Neurotrophic Factor in Amygdala-Dependent Learning. *The Neuroscientist*, 11(4):323–333. Publisher: SAGE Publications Inc STM.
- [Reiner and McGeer, 1987] Reiner, P. B. and McGeer, E. G. (1987). Electrophysiological properties of cortically projecting histamine neurons of the rat hypothalamus. *Neuroscience Letters*, 73(1):43–47.
- [Ren et al., 2006] Ren, Y., Barnwell, L. F., Alexander, J. C., Lubin, F. D., Adelman, J. P., Pfaffinger, P. J., Schrader, L. A., and Anderson, A. E. (2006). Regulation of Surface Localization of the Small Conductance Ca<sup>2+</sup>-activated Potassium Channel, Sk2, through Direct Phosphorylation by cAMP-dependent Protein Kinase. *Journal of Biological Chemistry*, 281(17):11769–11779.
- [Renouard et al., 2018] Renouard, L., Bridi, M. C. D., Coleman, T., Arckens, L., and Frank, M. G. (2018). Anatomical correlates of rapid eye movement sleep-dependent plasticity in the developing cortex. *Sleep*, 41(10).
- [Reyes-Resina et al., 2021] Reyes-Resina, I., Samer, S., Kreutz, M. R., and Oelschlegel, A. M. (2021). Molecular Mechanisms of Memory Consolidation That Operate During Sleep. *Frontiers in Molecular Neuroscience*, 14:767384.
- [Rodriguez et al., 1997] Rodriguez, F., Lluch, M., Dot, J., Blanco, I., and Rodriguez-Alvarez, J. (1997). Histamine modulation of glutamate release from hippocampal synaptosomes. *European Journal of Pharmacology*, 323(2-3):283–286.
- [Rule et al., 2019] Rule, M. E., O’Leary, T., and Harvey, C. D. (2019). Causes and consequences of representational drift. *Current Opinion in Neurobiology*, 58:141–147.

- [Rutherford et al., 1998] Rutherford, L. C., Nelson, S. B., and Turrigiano, G. G. (1998). BDNF has opposite effects on the quantal amplitude of pyramidal neuron and interneuron excitatory synapses. *Neuron*, 21(3):521–530.
- [Sakuragi et al., 2013] Sakuragi, S., Tominaga-Yoshino, K., and Ogura, A. (2013). Involvement of TrkB- and p75NTR-signaling pathways in two contrasting forms of long-lasting synaptic plasticity. *Scientific reports*.
- [Salgado et al., 2012] Salgado, H., Köhr, G., and Treviño, M. (2012). Noradrenergic ‘Tone’ Determines Dichotomous Control of Cortical Spike-Timing-Dependent Plasticity. *Scientific Reports*, 2(1):417.
- [Saper et al., 2010] Saper, C. B., Fuller, P. M., Pedersen, N. P., Lu, J., and Scammell, T. E. (2010). Sleep State Switching. *Neuron*, 68(6):1023–1042.
- [Scheiderer et al., 2004] Scheiderer, C. L., Dobrunz, L. E., and McMahan, L. L. (2004). Novel Form of Long-Term Synaptic Depression in Rat Hippocampus Induced By Activation of 1 Adrenergic Receptors. *Journal of Neurophysiology*, 91(2):1071–1077.
- [Schinder and Poo, 2000] Schinder, A. F. and Poo, M. (2000). The neurotrophin hypothesis for synaptic plasticity. *Trends in Neurosciences*.
- [Segal, 2005] Segal, M. (2005). Dendritic spines and long-term plasticity. *Nature Reviews Neuroscience*, 6(4):277–284.
- [Sei et al., 2000] Sei, H., Saitoh, D., Yamamoto, K., Morita, K., and Morita, Y. (2000). Differential effect of short-term REM sleep deprivation on NGF and BDNF protein levels in the rat brain. *Brain Research*, 877(2):387–390.
- [Seibt and Frank, 2019] Seibt, J. and Frank, M. G. (2019). Primed to sleep: The dynamics of synaptic plasticity across brain states. *Frontiers in Systems Neuroscience*, 13(February):1–19.
- [Seol et al., 2007] Seol, G. H., Ziburkus, J., Huang, S., Song, L., Kim, I. T., Takamiya, K., Huganir, R. L., Lee, H.-K., and Kirkwood, A. (2007). Neuromodulators Control the Polarity of Spike-Timing-Dependent Synaptic Plasticity. *Neuron*, 55(6):919–929.
- [Sergeeva et al., 2005] Sergeeva, O., Schulz, D., Doreulee, N., Ponomarenko, A., Selbach, O., Borsch, E., Kircheis, G., Huston, J., Häussinger, D., and Haas, H. (2005). Deficits in cortico-striatal synaptic plasticity and behavioral habituation in rats with portacaval anastomosis. *Neuroscience*, 134(4):1091–1098.
- [Sharma et al., 2021] Sharma, R., Sahota, P., and Thakkar, M. M. (2021). Short-term sleep deprivation immediately after contextual conditioning inhibits BDNF signaling and disrupts memory consolidation in predator odor trauma mice model of PTSD. *Brain Research*, 1750:147155.
- [Sheng and Greenberg, 1990] Sheng, M. and Greenberg, M. E. (1990). The regulation and function of c-fos and other immediate early genes in the nervous system. *Neuron*, 4(4):477–485.
- [Shinoe, 2005] Shinoe, T. (2005). Modulation of Synaptic Plasticity by Physiological Activation of M1 Muscarinic Acetylcholine Receptors in the Mouse Hippocampus. *Journal of Neuroscience*, 25(48):11194–11200.
- [Shouval et al., 2002] Shouval, H. Z., Bear, M. F., and Cooper, L. N. (2002). A unified model of NMDA receptor-dependent bidirectional synaptic plasticity. *Proceedings of the National Academy of Sciences of the United States of America*, 99(16):10831–10836.
- [Siegel, 2009] Siegel, J. M. (2009). The Neurobiology of Sleep. *Seminars in Neurology*, 29(04):277–296. Publisher: © Thieme Medical Publishers.
- [Sjöström et al., 2001] Sjöström, P. J., Turrigiano, G. G., and Nelson, S. B. (2001). Rate, timing, and cooperativity jointly determine cortical synaptic plasticity. *Neuron*, 32(6):1149–1164.
- [Song et al., 2000] Song, S., Miller, K. D., and Abbott, L. F. (2000). Competitive hebbian learning through spike-timing-dependent synaptic plasticity. *Nature Neuroscience*, 3(9):919–926.

- [Stanton et al., 2003] Stanton, P. K., Winterer, J., Bailey, C. P., Kyrozis, A., Raginov, I., Laube, G., Veh, R. W., Nguyen, C. Q., and Müller, W. (2003). Long-Term Depression of Presynaptic Release from the Readily Releasable Vesicle Pool Induced by NMDA Receptor-Dependent Retrograde Nitric Oxide. *The Journal of Neuroscience*, 23(13):5936–5944.
- [Staubli and Otaky, 1994] Staubli, U. and Otaky, N. (1994). Serotonin controls the magnitude of LTP induced by theta bursts via an action on NMDA-receptor-mediated responses. *Brain Research*, 643(1):10–16.
- [Steininger et al., 1999] Steininger, T. L., Alam, M., Gong, H., Szymusiak, R., and McGinty, D. (1999). Sleep-waking discharge of neurons in the posterior lateral hypothalamus of the albino rat. *Brain Research*, 840(1-2):138–147.
- [Steriade et al., 1993] Steriade, M., McCormick, D. A., and Sejnowski, T. J. (1993). Thalamocortical oscillations in the sleeping and aroused brain. *Science*, 262(5134):679–685.
- [Sun et al., 2005] Sun, X., Zhao, Y., and Wolf, M. E. (2005). Dopamine receptor stimulation modulates AMPA receptor synaptic insertion in prefrontal cortex neurons. *The Journal of Neuroscience: The Official Journal of the Society for Neuroscience*, 25(32):7342–7351.
- [Sörman et al., 2011] Sörman, E., Wang, D., Hajos, M., and Kocsis, B. (2011). Control of hippocampal theta rhythm by serotonin: Role of 5-HT<sub>2c</sub> receptors. *Neuropharmacology*, 61(3):489–494.
- [Takahashi et al., 2006] Takahashi, K., Lin, J.-S., and Sakai, K. (2006). Neuronal Activity of Histaminergic Tuberomammillary Neurons During Wake-Sleep States in the Mouse. *Journal of Neuroscience*, 26(40):10292–10298.
- [Taussig et al., 1993] Taussig, R., Quarmby, L., and Gilman, A. (1993). Regulation of purified type I and type II adenylyl cyclases by G protein beta gamma subunits. *Journal of Biological Chemistry*, 268(1):9–12.
- [Teixeira et al., 2018] Teixeira, C. M., Rosen, Z. B., Suri, D., Sun, Q., Hersh, M., Sargin, D., Dincheva, I., Morgan, A. A., Spivack, S., Krok, A. C., Hirschfeld-Stoler, T., Lambe, E. K., Siegelbaum, S. A., and Ansorge, M. S. (2018). Hippocampal 5-HT Input Regulates Memory Formation and Schaffer Collateral Excitation. *Neuron*, 98(5):992–1004.e4.
- [The Nature Reviews Drug Discovery GPCR Questionnaire Participants. and Ellis, 2004] The Nature Reviews Drug Discovery GPCR Questionnaire Participants. and Ellis, C. (2004). The state of GPCR research in 2004. *Nature Reviews Drug Discovery*, 3(7):577–626.
- [Tononi and Cirelli, 2006] Tononi, G. and Cirelli, C. (2006). Sleep function and synaptic homeostasis. *Sleep Medicine Reviews*.
- [Tononi and Cirelli, 2014] Tononi, G. and Cirelli, C. (2014). Sleep and the Price of Plasticity: From Synaptic and Cellular Homeostasis to Memory Consolidation and Integration. *Neuron*, 81(1):12–34. Publisher: Elsevier Inc.
- [Trampus et al., 1991] Trampus, M., Ferri, N., Monopoli, A., and Ongini, E. (1991). The dopamine D1 receptor is involved in the regulation of REM sleep in the rat. *European Journal of Pharmacology*, 194(2-3):189–194.
- [Trevino and Kirkwood, 2008] Trevino, M. and Kirkwood, A. (2008). Alpha-1 and beta adrenergic receptors facilitate and suppress ltp and ltd in a mutually exclusive manner. In *Program No. 335. 16. Neuroscience Meeting Planner. Washington (DC): Society for Neuroscience*.
- [Turlik et al., 2021] Turlik, J., Wąsikiewicz, E., Domaradzka, A., Chrostek, G., Gniadzik, W., Domagalski, M., and Duda, P. (2021). GSK3 Activity in Reward Circuit Functioning and Addiction. *NeuroSci*, 2(4):443–466.
- [Turner et al., 2007] Turner, J. H., Garnovskaya, M. N., and Raymond, J. R. (2007). Serotonin 5-HT<sub>1A</sub> receptor stimulates c-Jun N-terminal kinase and induces apoptosis in Chinese hamster ovary fibroblasts. *Biochimica et Biophysica Acta (BBA) - Molecular Cell Research*, 1773(3):391–399.
- [Valentinova and Mameli, 2016] Valentinova, K. and Mameli, M. (2016). mGluR-LTD at Excitatory and Inhibitory Synapses in the Lateral Habenula Tunes Neuronal Output. *Cell Reports*, 16(9):2298–2307.

- [Vandecasteele et al., 2014] Vandecasteele, M., Varga, V., Berényi, A., Papp, E., Barthó, P., Venance, L., Freund, T. F., and Buzsáki, G. (2014). Optogenetic activation of septal cholinergic neurons suppresses sharp wave ripples and enhances theta oscillations in the hippocampus. *Proceedings of the National Academy of Sciences*, 111(37):13535–13540. Publisher: Proceedings of the National Academy of Sciences.
- [Villani and Johnston, 1993] Villani, F. and Johnston, D. (1993). Serotonin inhibits induction of long-term potentiation at commissural synapses in hippocampus. *Brain Research*, 606(2):304–308.
- [Volk et al., 2007] Volk, L. J., Pfeiffer, B. E., Gibson, J. R., and Huber, K. M. (2007). Multiple Gq-Coupled Receptors Converge on a Common Protein Synthesis-Dependent Long-Term Depression That Is Affected in Fragile X Syndrome Mental Retardation. *Journal of Neuroscience*, 27(43):11624–11634.
- [Wang et al., 2003] Wang, X., Zhong, P., Gu, Z., and Yan, Z. (2003). Regulation of NMDA Receptors by Dopamine D<sub>4</sub> Signaling in Prefrontal Cortex. *The Journal of Neuroscience*, 23(30):9852–9861.
- [Watson et al., 2011] Watson, C. J., Lydic, R., and Baghdoyan, H. A. (2011). Sleep duration varies as a function of glutamate and GABA in rat pontine reticular formation. *Journal of Neurochemistry*, 118(4):571–580. \_eprint: <https://onlinelibrary.wiley.com/doi/pdf/10.1111/j.1471-4159.2011.07350.x>.
- [Willard and Koochekpour, 2013] Willard, S. S. and Koochekpour, S. (2013). Glutamate, Glutamate Receptors, and Downstream Signaling Pathways. *International Journal of Biological Sciences*, 9(9):948–959.
- [Williams and Herrup, 1988] Williams, R. W. and Herrup, K. (1988). The Control of Neuron Number. *Annual Review of Neuroscience*, 11(1):423–453. \_eprint: <https://doi.org/10.1146/annurev.ne.11.030188.002231>.
- [Woo et al., 2005] Woo, N. H., Teng, H. K., Siao, C.-J., Chiaruttini, C., Pang, P. T., Milner, T. A., Hempstead, B. L., and Lu, B. (2005). Activation of p75NTR by proBDNF facilitates hippocampal long-term depression. *Nature Neuroscience*, 8(8):1069–1077. Number: 8 Publisher: Nature Publishing Group.
- [Wyszynski et al., 2002] Wyszynski, M., Kim, E., Dunah, A. W., Passafaro, M., Valtschanoff, J. G., Serra-Pagès, C., Streuli, M., Weinberg, R. J., and Sheng, M. (2002). Interaction between GRIP and Liprin-/SYD2 Is Required for AMPA Receptor Targeting. *Neuron*, 34(1):39–52. Publisher: Elsevier.
- [Yamada and Nabeshima, 2003] Yamada, K. and Nabeshima, T. (2003). Brain-derived neurotrophic factor/TrkB signaling in memory processes. *Journal of pharmacological sciences*.
- [Yang et al., 2014] Yang, J., Harte-Hargrove, L. C., Siao, C.-J., Marinic, T., Clarke, R., Ma, Q., Jing, D., LaFrancois, J. J., Bath, K. G., Mark, W., Ballon, D., Lee, F. S., Scharfman, H. E., and Hempstead, B. L. (2014). proBDNF Negatively Regulates Neuronal Remodeling, Synaptic Transmission, and Synaptic Plasticity in Hippocampus. *Cell Reports*, 7(3):796–806.
- [Yang et al., 1999] Yang, S.-N., Tang, Y.-G., and Zucker, R. S. (1999). Selective Induction of LTP and LTD by Postsynaptic [Ca<sup>2+</sup>]<sub>i</sub> Elevation. *Journal of Neurophysiology*, 81(2):781–787.
- [Yang and Calakos, 2013] Yang, Y. and Calakos, N. (2013). Presynaptic long-term plasticity. *Frontiers in Synaptic Neuroscience*, 5.
- [Zagha and McCormick, 2014] Zagha, E. and McCormick, D. A. (2014). Neural control of brain state. *Current Opinion in Neurobiology*, 29(1):178–186.
- [Zagrebelsky et al., 2020] Zagrebelsky, M., Tacke, C., and Korte, M. (2020). BDNF signaling during the lifetime of dendritic spines. *Cell and Tissue Research*, 382(1):185–199.
- [Zakharenko et al., 2003] Zakharenko, S. S., Patterson, S. L., Dragatsis, I., Zeitlin, S. O., Siegelbaum, S. A., Kandel, E. R., and Morozov, A. (2003). Presynaptic BDNF Required for a Presynaptic but Not Postsynaptic Component of LTP at Hippocampal CA1-CA3 Synapses. *Neuron*, 39(6):975–990.
- [Zhang et al., 2009] Zhang, J.-C., Lau, P.-M., and Bi, G.-Q. (2009). Gain in sensitivity and loss in temporal contrast of STDP by dopaminergic modulation at hippocampal synapses. *Proceedings of the National Academy of Sciences*, 106(31):13028–13033.